Università Politecnica delle Marche
Scuola di Dottorato di Ricerca in Scienze dell'Ingegneria
Corso di Dottorato in Ingegneria Industriale

Technology Evolution of Natural Gas systems from Renewable Energy Sources: CNG and LNG

Evoluzione dei Sistemi Energetici per il Gas Naturale da Fonte Rinnovabile: CNG e LNG

Ph.D. Dissertation of:
Marco Spitoni

Supervisor:
Prof. Comodi Gabriele

Co – Supervisor
Prof. Alessia Arteconi

Co – Supervisor:
Prof. Carlo Maria Bartolini

Ph.D. Course coordinator:
Prof. F. Mandorli

XVI Edition - new series

ABSTRACT

At present, there is an increasing focus on environmental issues and air pollution. Emissions are mainly related to electricity and heat generation sector, accounting for about 42% of total emissions. With about 24% of total CO_2 emissions from fuel combustion, transport sector represents a major item in air pollution. The emission trend for this sector is constantly increasing. Provisions declare an increase of 50% by 2030 and 80% by 2050. In order to reduce this trend and meet the target for the Green House Gas (GHG) emissions, international institutions and national governments have established several regulation policies. Such policies are varying from a region to another, but the common adopted scheme is based on the mechanism of incentive / penalty. For the transport sector, such policies are focused on the biofuels production and utilization. Historically, the most common used biofuels were bioethanol and biodiesel. During the years, several incentive schemes caused some issues associated with the production of these biofuels, such as the rise of food prices, the intensive land utilization and so on. Thus, other regulations are ongoing in order to produce biofuels in a more sustainable way. On the other hand, biogas production encountered a weak development if compared to that of those biofuels. However, it is growing quickly and at present several countries are adopting specific incentives for this biofuel. This is also because of the biogas potential to be used as vehicle fuel. In fact, after been purified, it is almost pure methane, which is a clean source of energy. In Italy, a specific incentive scheme designed for biomethane exists. If the produced biomethane is used for the transport sector, the incentive is higher and biomethane becomes really interesting, since it can be used as Compressed or Liquefied Biogas (CBG – LBG). However, at present, the base incentive is still not available and some estimation were proposed to evaluate its minimum value.

In the first Chapter, a brief introduction regarding the environmental issues associated with the GHG emissions is presented. Emissions are divided on the base of producing region and sector. Biofuels policies are shortly presented as well as the role of natural gas and biogas.

In the second Chapter, a review over the governmental policies adopted worldwide is presented. Critical aspects and provisions are also discussed. The biogas fuel is analyzed as well as biomethane. Their potential as vehicle fuels and achievable production is presented for the European region and the Chinese regions. Considering the Italian incentive scheme, a feasibility analysis for the LBG production is also carried out. The main objective was to evaluate the minimum incentive in order to make the LBG production economically possible. Some cases were analyzed to explore its potentiality. Depending on the biomass composition and business model, the minimum value of the base incentive was estimated to vary from 0.10 € Sm^3 to 0.42 € Sm^3.

In the third Chapter, the Compressed Natural Gas (CNG) refueling technology is presented and investigated. The possibility of combining biogas plant production and upgrading with CNG refueling stations allows the production of the Compressed BioGas (CBG). In order to evaluate the potential of an alternative refueling station, a comparison was proposed with a traditional buffer station. Results show that the alternative station presents lower required

power and a higher compression efficiency. On the other hand, the overall performances of the station are too low and a further detailed sizing of the station would be required.
In the fourth Chapter, the Liquefied Natural Gas (LBG) technology is briefly presented. Considering the biogas fuel, the possibility to achieve Liquefied BioGas (LBG) is investigated. Taking into account the state-of-the-art technology for the LBG production, a particular cryogenic separation technology is proposed to achieve carbon dioxide removal and LBG production. The process presented a specific energy consumption ranging from 1.284 kWh kg^{-1} to 1.982 kWh kg^{-1}. A further optimization of the plant to investigate the carbon dioxide liquefaction to be sold as by-products was also conducted. Results show a specific energy consumption of 1.093 kWh kg^{-1}. Finally, the possibility to achieve carbon dioxide and hydrogen sulfide was investigated. The ternary mixture was analyzed to find operative parameters of the plant. A final specific energy consumption of 1.526 kW kg^{-1} was found. However, in this case, carbon dioxide cannot be recovered because of the hydrogen sulfide.
In the last Chapter, conclusions of the thesis are reported, with potential future works.

List of Figures

List of Tables

Contents

1. INTRODUCTION

In this thesis, a brief introduction regarding climate changes and global warming issues related with air pollution due to human activities is presented. Pollutant emissions will be divided into main sectors. Major item of the thesis is on the reduction in emissions related with the transport sector, in particular road transport sector. This is essentially linked with light-duty and heavy-duty vehicles utilization. One of the hottest key point regarding transportation is to achieve CO_2 emissions reduction during fuel combustion with engine efficiencies and autonomy as high as for traditional fuels. In this work, Natural Gas (NG) was selected as the best vehicle fuel that can better substitute oil and diesel in the short-medium term. In particular, biogas and biomethane potential in transport sector is considered and investigated. To reduce GHG emissions from the transport sector, many aspects must be considered. Therefore, biofuels have to be cleaner than fossil fuels. However, technologies and plants necessary to produce such biofuels must be competitive. High energy efficiency, low operative costs as well as low environmental impact of processes involved in biofuels production and utilization are mandatory targets. Related technologies are presented in order to better understand how this renewable source can be used as a feedstock for NG vehicles. Therefore, Compressed Natural Gas (CNG) and Liquefied Natural Gas (LNG) technologies are also investigated. Related state of the art is presented for both of them. Conventional CNG and LNG technologies are investigated considering biogas instead of NG. In order to better understand energy efficiency potential in standard CNG refueling stations, a novel patented scheme is presented and discussed in detailed. Since the refueling process suffers for vehicle vessels temperature increase and high compression power installed, those are considered as key factor in the present analysis. Vehicle refueling time was considered as a critical parameter too, able to drive final user's opinion toward NG vehicles. The stations were completely modeled by means of a quasi-steady analysis, thus final performance comparisons were possible. Regarding LNG using biogas, the main issues to overcome are those related with biogas cleaning procedure and specific energy consumption during liquefaction. At present several technologies are able to efficiently purify biogas. However, further purification would be necessary in order to liquefy it. Moreover, liquefaction technology is well known to be high energy intensive process, only feasible for the medium-large scale. By the way, in order to allow biogas diffusion and utilization as vehicle fuel, LNG techniques development is a critical aspect. In this thesis, cryogenic separation process is proposed as a possible solution. Two different plants are presented, investigated and finally compared with standard processes for LBG production.

1.1. The Environmental Background

At present, more than 7 billion of human being are living on earth while about 200 years ago this number was less than one billion. From 1900 to 2000 human population had grown from 1.5 to 6.1 billion, also due to the increased average in life expectancy. Moreover, in recent years, highly densely populated countries, such as India and China, have been growing considerably, thus increasing their energy and resources requirements (Roser et al., 2017). As a consequence, in the last decades, interests related with energy consumption, energy efficiency and environmental issues have become more and more important. One of the major items in the scientific research is to maximize energy efficiency, reducing resources waste. To the purpose of containing global warming and prevent environmental disasters, managing with air pollution due to human activities is of paramount importance. Carbon Dioxide (CO_2) concentration in the atmosphere is generally taken as the main indicator of air pollution level. Such gas, as well as other gases, are known as Green House Gas (GHG), able to negatively influence global air temperature.

Table 1.1. GHG potential for CO_2, CH_4 and N_2O compounds (IPCC, 2013).

Name of GHG	**Global Warming Potential estimates over last 100 years**		
	Second Report	**Fourth Report**	**Fifth Report**
Carbon Dioxide (CO_2)	1	1	1
Methane (CH_4)	21	25	28
Nitrous Oxygen (N_2O)	310	298	265

Atmosphere CO_2 concentration level measured in 2016 was of 403 parts per million, almost 44% higher than those estimated for the mid-1800s, with an increasing rate of 2 ppm per year, related with the last decade (IEA, 2017). By the way, human activities are also responsible for other GHG emissions than CO_2, namely methane (CH_4) and nitrous oxygen (N_2O). Those compounds are even more dangerous than simple CO_2, as reported in Table 1.1. Other substances, such as Chlorofluorocarbons (CFC) and Hydrofluorocarbon (HFC), are not reported. However, those

kinds of compounds have a GHG potential ranging from 50 to 23500 times greater than CO_2 (IPCC, 2013). Among every sector responsible for the GHG production, the use of energy represents the largest source of emissions. Agriculture is mainly responsible for the production of CH4 and N2O, industrial sector not involved in energy production, is mainly responsible for fluorinated gases and N2O.

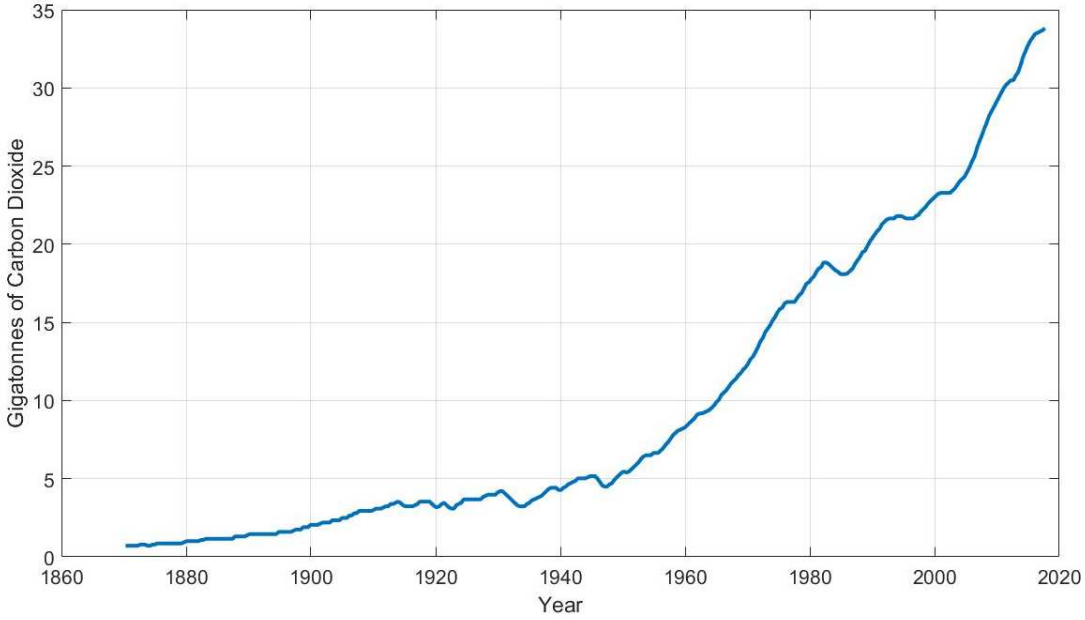

Figure 1.1. GHG emissions trend over the last 150 years (IEA, 2017)

Regarding the energy sector, CO2 due to fuel combustion are responsible for the total GHG emissions. Energy sector accounts for the largest share of global GHG emissions, representing about 58% of global emissions. This percentage is strictly related with worldwide economic growth and development. Global energy demand as measured by total primary energy supply increased by almost 150% between 1971 and 2015, still mainly relying on fossil fuels. Although the share in energy production by means of non-fossil sources had strongly grown (almost 30% from 1971 to 2015), the fossil fuel share in energy production on the same period is nearly the same. This is mainly related with the growth in energy demand during the last 150 years and especially from 1950. Figure 1.1 shows the consequences of energy demand as well as fossil fuels utilization.

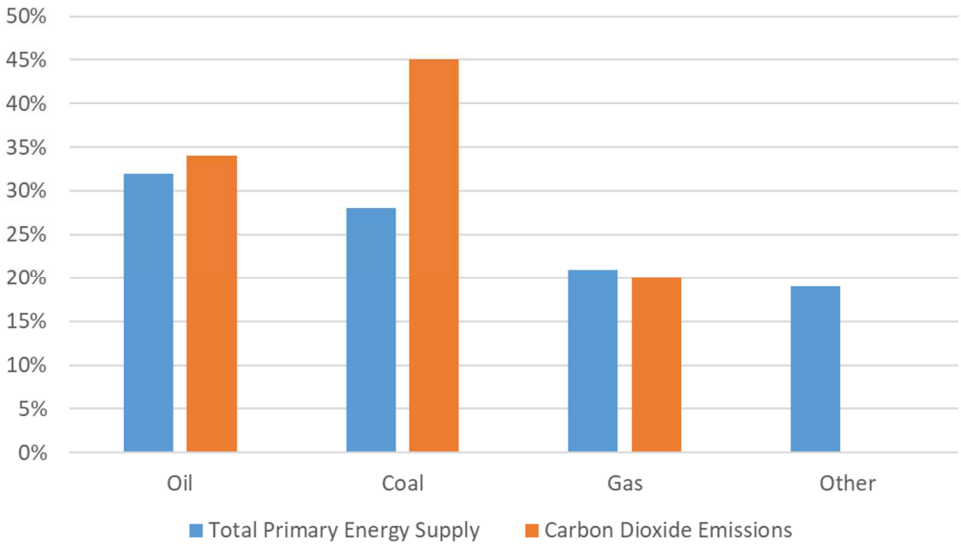

Figure 1.2. Combustion fuel share in GHG emissions and energy supply (IEA, 2017)

Coal accounts for 45% of the global CO2 emissions due to its heavy carbon content per unit of energy released. Comparing it to natural gas emissions, coal is almost twice as emission intensive. From the late 1980s until the early 2000s, coal and oil were each responsible for approximately 40% of global CO2 emissions, with emissions from oil

generally exceeding those from coal by a few percentage points. However, recent trends show that coal share has grown from 39% to 45% since 2002. On the other hand, oil share has decreased from 40% to 35%. In the same period, natural gas (NG) emission share was nearly unchanged at 20%. Figure 1.2 shows the 2015 situation in total primary energy supply and CO_2 production by fuel type.

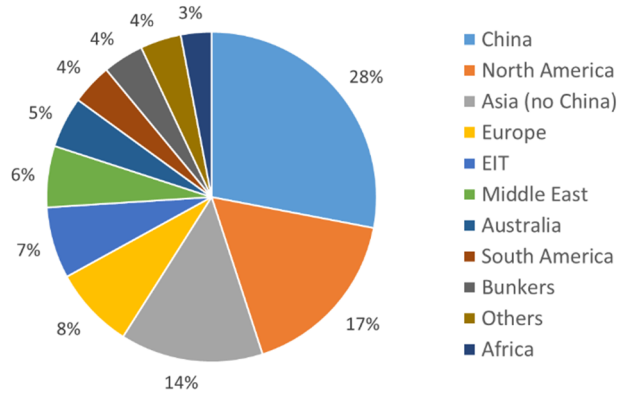

Figure 1.3. GHG emissions share per region (IEA, 2017)

Focusing on GHG emissions classified per geographic area, in 2015 non-Annex I countries were representing 58% of global CO2 emissions. Annex-I countries accounted for 38% while remaining 4% were related with international aviation and marine bunkers. With 28% of global share, China produced by far the greater part of GHG emissions. North America were responsible for 17% of CO_2 emissions, Asian countries (excluding China) represented 14%, while Europe and Economies in Transition part of Annex-I accounted for 15%. Finally, with an average share of about 4% of produced CO_2, Middle East countries, Australia, South America, Africa and others accounted for almost 25% of global emissions. Figure 1.3 gives some insight about regional share. As it can be seen, Asia (including China) and North America accounted for more than 50% of global CO_2 emissions. In 2015, those countries produced something like 19 $GtCO_2$.

1.2. Emissions by sector

In order to better understand how to manage with GHG emissions reduction, it is useful to divide them into specific application area. Pollutant emissions can be categorized in the following sectors:

- Electricity and heat production sector;
- Transport sector;
- Industrial sector;
- Residential sector;
- Services sector;
- Other sectors.

Other sector includes, but are not limited to, fishing and agriculture. Figure 1.4 shows the individual impact of each of those sectors.

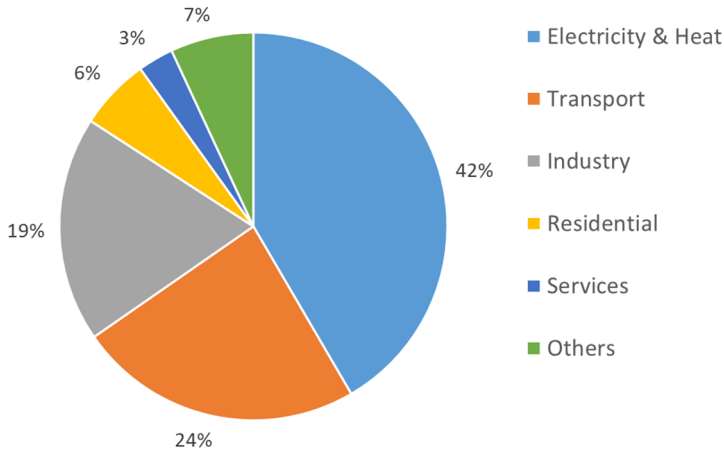

Figure 1.4. GHG emissions share per sector (IEA, 2017)

As it can be seen, two sectors produced two-thirds of global CO2 emissions from fuel combustion in 2015, namely electricity and heat generation and transport sector. The former represents the largest one, with a share of 42%, while the latter is responsible for 24%. Although renewable energy sources utilization is constantly growing, still electricity and heat sector are strongly coal dependent (IEA, 2017). This is the case of countries such as China, India and South Africa. Nevertheless, the share of coal in electricity and heat production sector have considerably grown from 65% to 72% between 1990 and 2015. On the other hand, in recent years this trend changed in favor of NG utilization. This is mainly the case of electricity production in regions such as North America and Europe. In Europe, Italy and United Kingdom are strongly decreasing their share in electricity production by means of fossil fuels by 20% and 7% respectively, between 2000 and 2015. On the other hand, other regions are experiencing an opposite trend, especially in Australia and Japan. However, Japanese situation strongly depend on the Fukushima Daiichi accident, in 2011 (IEA, 2017). Generally, increased emissions due to electricity production means an increased output. This is the case of emerging economies grown in a very short time, such as China and India, in which the growth rate forces the massive use of fossil fuel as primary source, especially coal. By the way, in China, improvements in energy efficiency as well as renewable energy sources utilization have sensibly reduced produced emissions per output unit. Regarding emissions from transport sector, an important growth of about 68% was registered from 1990 to 2015. Road transport accounts for the greater part of those emissions, with an increasing share of almost 60% in 1990 to more than 75% in 2015. It is forecasted that energy use and GHG emissions in this sector will continue to increase by 50% by 2030 and more than 80% by 2050. The Intergovernmental Panel on Climate Change (IPCC) advices that global GHG emissions must be reduced by at least 50% by 2050 (IEA, 2009).

1.3. The Waste Management

As for energy efficiency and environmental impact reduction issues, waste management had gained more and more importance in scientific research. The strong growing population rate combined with economic development and resources utilization have been dramatically increasing waste generation. As a consequence, development of new technologies for waste management is strictly required. The Waste Framework Directive (2008/98/EC) defined priorities and best practices for the waste management, in order to minimize its associated environmental. Continuous efforts are spent to improve the framework by means of new laws. Considering waste production and the necessity of efficient waste management in a context of globally increasing energy demand, the Waste-to-Energy procedure seems to be the best solution. The process allows double advantages, by producing energy from waste sources. New technologies to achieve this kind of renewable energy production are constantly developing. Around 19 % of the global energy consumption in 2008 came from renewable energy resources (Demirel, 2012). This kind of energy is far cleaner than fossil fuels and moreover it is sustainable over long term, while the former are finite and more pollutant (Dincer, 1998). Climate changes and global warming issues can be reduced by means of fossil fuels replacement with renewable energies utilization (IPCC, 2012). For those reasons, many researchers as well as companies all over the world are focusing on renewable energies, energy and plants efficiency and in GHG emissions reduction.

1.4. Biofuels Policies Introduction

In 2015, the Paris Agreement extended environmental obligation in climate mitigation to every country. The Agreement became effective in 4 November 2016 and up to now 170 Parties have ratified of 197 Parties to the Convention. Since that date, rules and guidelines for emissions were established. The first target in GHG emissions reduction were set under the Kyoto Protocol's first period (2008-12). The target required industrialized countries to achieve domestic emissions reduction of 5% relative to 1990 over this period. 38 Parties have also decided to take part to a second commitment period running from 2013 to 2020. Countries comply with their targets by reducing emissions from fossil fuel combustion, reducing emission in other sectors or through use of the flexible mechanisms consisting on earning emission credits by reducing emissions in developing countries and EIT. Kyoto Protocol has made CO2 a tradable commodity, and has been a key driver for the development of national emissions trading schemes. However, the smaller pool of countries with targets in the Kyoto Protocol's second commitment period (only 80 by August 2017), coupled with a large surplus of project credits carried forward from the first period, have led to low prices and project developers exiting the market. Therefore, Kyoto Protocol seemed to be limited in its potential regarding GHG emissions. United States was not into Protocol's jurisdiction while developing countries did not deal with emissions targets. The second commitment period targets imply action on less than 13% of global CO2 emissions in 2014. However, developed and developing countries submitted voluntary emission reduction target for 2020 under the Copenhagen Accord and Cancún Agreements. Participating Parties were responsible for over 80% of global emissions. Annex-I and non-Annex I countries established diverse targets regarding GHG emissions reduction. The former submitted absolute emissions reduction targets while the former submitted appropriate actions related with national policies. This is the case of China and India in which reduction targets are on a CO2/GDP basis. Table 1.2 reports information regarding the ten largest CO_2 emitters.

Table 1.2. GHG emissions of the ten larger emitters, during 1990, 2005, 2015, and further furcated emissions in 2020

Country	1990	2005	2015	2020 GHG targets
	$MtCO_2$ emitted			
China	2109	5399	9084	CO_2 emissions per unit of GDP by 40-45% below 2005
United States	4802	5702	4998	CO_2 emissions 17% below 2005
European Union	4028	3921	3201	CO_2 emissions 20% below 1990
India	530	1080	2066	CO_2 emissions per unit of GDP by 20-25% below 2005
Russian federation	2163	1482	1469	CO_2 emissions 15-25% below 1990
Japan	1042	1178	1142	CO_2 emissions 3.8 below 2005
Korea	232	458	585	None
Iran	171	418	552	None
Canada	420	541	549	CO_2 emissions 17% below 2005
Saudi Arabia	151	298	531	None

As it can be seen, reduction targets based on CO_2 emissions per unit of GDP do not reflect an effective overall CO_2 emission reduction. Although the ambition of these pledges is insufficient to limit temperature rise to 2°C above pre-industrial levels, the breadth of participation in mitigation commitments marked a significant improvement on the coverage of the Kyoto Protocol, and laid the groundwork for the Paris Agreement. In order to reduce GHG emissions related with fuel combustions, biofuels represent a possible solution. However, production of such fuels is unprofitable, thus incentives are necessary to develop their feasibility. Such incentives regard tax exemptions, subsides as well as penalties (Rajagopal and Zilberman, 2007). Up to now, main motivation in biofuels production was related with agriculture and energy policies in order to substitute oil, reducing fossil fuels importations. In recent years, another driving force regards reduction in CO_2 emissions level in the transport sector. Considering biofuels policies, volumetric production targets for biofuels failed in containing costs, avoiding environmental damage or even to achieve GHG emission reductions. Policies related with carbon content for fuels, combined by certification, seems to be the best choice. Those schemes have been developed in several countries, such as California, the Netherlands, Germany, Switzerland, the United Kingdom and the European Commission. However, by promoting incentives in biofuel production, high selectivity should be required in eligible producers and processes. Although certification could be used to modify farming and biomass harvesting methods in order to limit the environmental impact, it cannot control any displacement of existing farming activities induced by an expansion of biofuel production. As a consequence, biofuel production will significantly influence land-use and food production and market. Thus, other measures are required to protect valued natural and semi-natural ecosystems. Moreover, another consequence of incomplete regulations and incentives tools affect biofuels performance in terms of GHG emissions reduction. Biofuels production have been growing considerably in the last 20 years. Ethanol and

biodiesel production increased from 16.9 to 72 and from 0.8 to 14.7 billion liters respectively between 2000 and 2009 (Figure 1.5). This is mainly due to governmental policies and incentives. It is the case of US in which financial incentives for biofuel producers allowed United States to become the largest ethanol producer in the world. Regarding European Union, policies consist in mandatory blending levels. During 2007, OECD members invested about 15 billion US dollars in incentive policies related to biofuels production (OECD, 2007; OECD/ITF, 2008). On the other hand, those policies present several socio-economic and environmental critical consequences. This is due to the fact that biofuels manufacturers are strongly using food crops as their feedstock, such as sugarcane and sugar-beet and so on (Larson, 2008). In 2006, 20% of the total US corn supply was reallocated to fuel ethanol production (EIA, 2007). As a consequence, a sensible increment in food prices was registered between 2003 and 2008 (Mitchell, 2008; UNCTAD, 2008; Schmidhuber, 2007; Johnson, 2007; Mercer-Blackmanetal., 2007). From 2008 to 2010, food-price index changed considerably (OECD/FAO, 2009). In January 2010 the indexes for cereal grains, oils, and sugar prices were, respectively, 70%, 69% and 276% higher than in the 2002–2004 period. Moreover, among the increasing rate in food prices, energy several studies assessed that LCA related with biofuels production have a negative net contribution in reducing GHG emissions (Macedo et al., 2004; Pimentel and Patzek, 2005; Farreletal., 2006; Crutzenetal., 2007). Although LCA studies may diverge on to each other (OECD, 2008), ethanol produced by means of corns showed the most negative LCA profile. Therefore, develop biofuels production and related incentives in order to cost-effectively reduce air pollution is challenging.

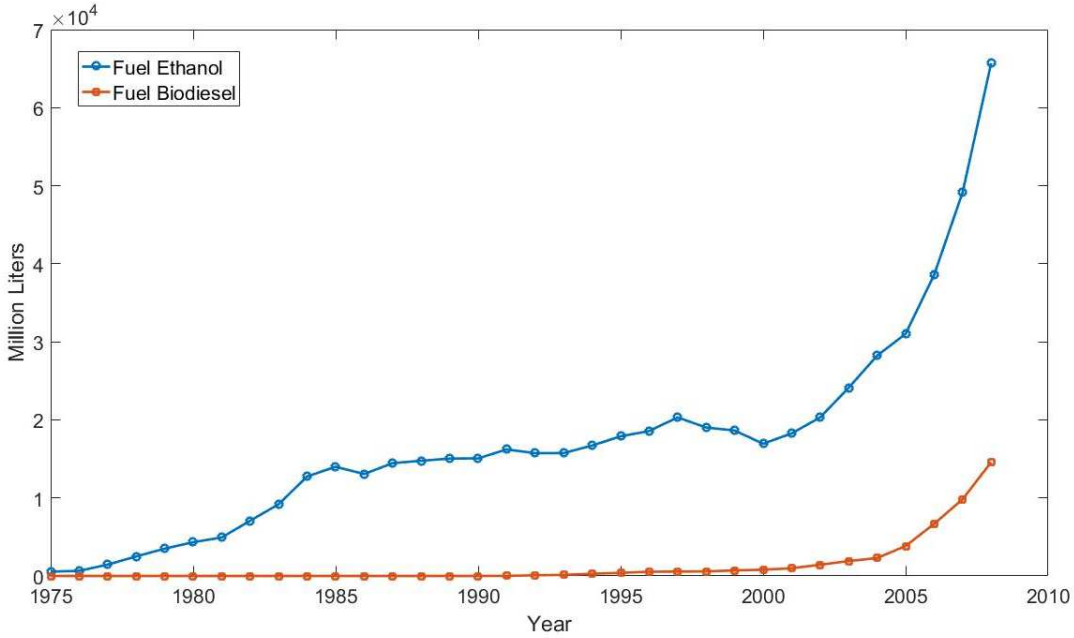

Figure 1.5. Biofuels production over the last 40 years; comparison between ethanol and biodiesel profiles (Sorda, 2010)

1.5. Natural Gas and Biogas Considerations

In order to reduce the environmental impact and GHG emissions some measures must be applied. Regarding transport sector the key point is to lower the carbon emissions during combustion. This could be achieved by introducing more efficient engines or other kind of new cars (such as electrical or hybrid vehicles) or introducing new fuels, to make the combustion cleaner. In this context, alternative fuels have assumed more and more importance and natural gas (NG) is considered the alternative fuel that, in the short-medium term, can best substitute conventional fuels (EC, 2001a), because it is readily available at a competitive price and it employs technologies already in widespread use (Hekkert *et al.* 2005). Yeh states that NG advantages over traditional fuels are as follows (Yeh, 2007): (i) environmental benefits, (ii) availability (iii) reduced dependency on imported oil. Regarding the utilization as vehicle fuel, NG vehicle autonomy must be comparable to that of standard vehicles. CNG is the compressed form of NG. One or more pressurized vessels allow enough stored energy density with an acceptable weight for light-duty vehicles. On the other hand, this possibility is not possible for heavy-duty vehicles. This is mainly due to the fact that the total weight to allow the required autonomy will be too high. For this reason, LNG

is generally used for light-duty vehicles being roughly 3 times denser than CNG. By the way, a cryogenic vessel is required onboard. Since cryogenic temperatures not higher than 160 K are mandatory to maintain acceptable pressure levels inside of the vessel, this fuel cannot be used in light-duty sector, in which vehicles could remain unused for a long time. Thus, compared to CNG, LNG represents the best substitute of diesel in transport sector. On the other hand, LNG requires energy intensive processes in order to be produced, increasing its global environmental impact over CNG. A comparison among the well-to-wheel life cycle GHG emissions for CNG, LNG and diesel has been made (Arteconi et al., 2010a; Arteconi et al., 2010b). It shows that, compared with Diesel, CNG reduces GHG emissions by 14% and LNG by 3% to 10%, depending on supply option. Although CNG vehicles refueling is a widely available and mature technology, several issues regarding traditional refueling stations remains. It is the case of temperature rising during vessel charge and high power required for the gas compression. Heavy-duty vehicles can be refueled at LNG refueling stations, LNG is stored in cryogenics tanks on board and finally burnt in LNG-adapted engines. The technology related with LNG refueling is already available. However, in order to achieve a wide LNG diffusion as vehicle fuel, the main obstacle to overcame is the problem of supply (Arteconi et al., 2012). In countries like Italy this is a critical aspect because it is not possible to purchase it at the regasification terminals and the liquefaction on site using pipeline natural gas is very challenging. In this context, the biomethane production from biogas of landfills and anaerobic digesters could play a significant role. It represents an alternative and renewable source of feedstock gas with several advantages: (i) the CO_2 emissions during its combustion are the same captured during biomass growth, (ii) it can reduce the dependency in natural gas and oil importations and (iii) it can be injected into the national gas grid. Biogas is a renewable energy source, which is considered carbon-neutral since the organic waste has photosynthesized carbon dioxide (Masse, et al., 2012). Produced by means of Anaerobic Digesters (AD) or in landfills, it presents methane concentrations up to 70% in volume. Remaining part of the gas is mainly composed by CO_2 (ranging from 30% to 50% in volume), H_2S (generally not higher than 4000 ppm) and water vapor (from 1% to 2% in volume). In AD, microorganisms digest organic substrates, producing biogas. Final biogas composition is related with biomass type. Biomass used in AD process are crops, manure, industrial wastes, sewage sludge and organic fraction of municipal solid wastes. Due to its raw composition, biogas cannot be directly used as vehicle fuel, thus a purification process is mandatory. Purification process consists of several passages and plants able to remove one or more than one compound at a time, saving as much methane as possible, preventing losses. Purification processes will be discussed later in chapter 4. At the end of compound removal process, obtained gas is no longer raw biogas but highly pure methane, called biomethane. Depending on purification technology, biomethane has a methane content ranging from 95% to more than 99.5% in volume. Production of biogas from organic waste has shown to be more environmentally friendly compared to other waste handling options such as landfilling, incineration and composting (Lin, et al., 2012). Biogas production can therefore be considered a favorable treatment for organic waste. Commercial biogas production has increased for at least two reasons. Firstly, biogas can be used as both vehicle fuel or in energy production. Secondly, it contributes to a lower GHG concentration when it is collected in a closed process (Santos, et al., 2013). Moreover, considering Table 1.1, by capturing methane produced during anaerobic digestion of biomass substrates, important air pollution is avoided (Butz, 2014). After H_2S and water removal, biogas could be directly used as combustion fuel in order to produce heat and electricity. By the way, from environmental impact perspective, it is recommended to enriched biogas methane content to a fuel (López, et al., 2013). Analyses have shown that purifying biogas to biomethane and using it instead of diesel, provides the best climate benefit (Arnøy, et al., 2013).

1.6. Structure of the Thesis

Environmental issues related with fuel combustion in the transport sector is the core of this thesis. Main purpose is to discuss how state-of-the-art technologies could be successfully used to evolve biofuels utilization. In particular, biogas was considered to be the best biofuel able to replace fossil fuels in the short-medium term without increasing dependency in NG importations. The present work is structured in three main section. In the first section (Chapter 2), worldwide energy policy related with transport sector are investigated. More detailed information are presented for People's Republic of China, Europe and Italy. Biogas and biomethane potentials in terms of achievable billion cubic meters (bcm) per year are also presented. A feasibility analysis regarding biogas used as vehicle fuel in both its compressed and liquefied form in the Italian country is presented as the starting point to develop the subsequent work. In the second section (Chapter 3), CNG technologies are investigated. A brief state-of-the-art is presented related with the conventional refueling stations. Since biogas is considered to be used instead of NG from national gas grid, the final product would be Compressed BioGas (CBG). A conventional refueling station configuration was selected for the work. Moreover, a novel patented refueling station configuration is presented. Purpose of this section is the evaluation of both the conventional and novel CBG refueling stations in order to compare energy consumption, compression power required as well as performances during the vehicles charging. The stations were completely modeled, thus compressor sizing and operation, storage sizing and charging process and vehicles

charging process models are presented and discussed. Analysis was conducted by means of NIST, Refprop software (NIST) for thermodynamic properties of gases. MathWorks®, Matlab software was used to simulate refueling station function as well as for defining charging logics. In the third section (Chapter 4), LNG technologies are investigated. A brief state-of-the-art is presented related with the conventional natural gas liquefaction plants. Main objective of this analysis regards the possibility of producing Liquefied BioGas (LBG) directly from raw biogas, avoiding standard purification process. The advantage of this possibility is to achieve the same result with a single plant instead of several. Therefore, state-of-the-art of purification techniques is presented, with a specific focus on hydrogen sulfide (H_2S) and carbon dioxide (CO_2) removal processes, namely desulphurization and upgrading processes respectively. A novel cryogenic separation process able to simultaneously remove CO_2 and producing LBG with liquefied carbon dioxide (L-CO_2) production and cold energy recovery is presented and detailed discussed. A second novel cryogenic separation process able to simultaneously remove H_2S and CO_2 and producing LBG with cold energy recovery is presented and detailed discussed. Finally, proposed processes are compared with the standard available technologies in LBG production. The analysis was conducted by means of AspenHYSYS®, AspenTech for the plant simulation and thermodynamic properties of several gaseous mixtures. MathWorks®, Matlab software was used for sensitivity analysis as well as for software connections, while modeFrontier®, ESTECO was implemented for plant optimizations. Eventually, obtained results and future perspectives are presented in final conclusions (Chapter 5).

1.7. References

- Arnøy, S., Møller, H., Modahl, I. S., Sørby, I., & Hanssen, O. J. (2013). Biogassproduksjon i Østfold-Analyse av klimanytte og økonomi i et verdikjedeperspektiv.Kråkerøy: Østfoldforskning.
- Arteconi A., Brandoni C., Evangelista D., Polonara F. 2010a, Life-cycle greenhouse gas analysis of LNG as a vehicle fuel in Europe, *Applied Energy* 87: 2005-2013.
- Arteconi A., Polonara F. 2012, LNG as vehicle fuel in Italy, *Proceedings of the 12th Cryogenics IIR Conference*, Dresda, Paper 041.
- Arteconi, A., Brandoni, C., Bartolini, C.M., Polonara, F., 2010b. Greenhouse Gas emissions of heavy-duty vehicles fuelled by natural gas. IANGV 2010. Roma.
- Butz, S. (2014). Energy and Agriculture: Science, Environment, and Solutions.Stamford: Cengage Learning.
- Crutzen, J.,Mosier,A.,Smith,K.,Winiwarter,W.,2007.N2O releasefromagro- biofuel productionnegatesglobalwarmingreductionbyreplacingfossilfuels. Atmos. Chem.Phys.Discuss.7,11191–11205.
- Demirel Y., (2012). Energy: production, conversion, storage, conservation, and coupling. Springer. Berlin Heidelberg. 2012. URL: http://www.springer.com/cn/book/9781447123712.
- Dincer I., Rose A. M., (1998). A Worldwide Perspective on Energy, Environment and Sustainable Development. International Journal of Energy Research. 22: 1305-1321.
- Directive 2008/98/EC on waste (Waste Framework Directive). Retrieved from: http://ec.europa.eu/environment/waste/framework/ (last accessed – 30/11/2017).
- EIA, Energy Information Administration, 2007. Biofuels in the US Transportation Sector. Published in Annual Energy Outlook 2007, February 2007.
- European Commission (EC) 2001. Green paper: towards a European strategy for the security of energy supply, Luxembourg. 105 p.
- Farrell, A., Plevin, R., Turner, B., Jones, A., O'Hare, M., Kammen, D., 2006. Ethanol can
- Hekkert, M.P., Hendriks, F.H.J.F., Faaij, A.P.C., Neelis, M.L., 2005. Natural gas as an alternative to crude oil in automotive fuel chains well-to-wheel analysis and transition strategy development, *Energy Policy* 33: 579-794.
- IEA 2009, Transport, Energy and CO_2 , International Energy Agency Report.
- IEA, International Energy Agency (2017), CO_2 emissions from fuel combustion.
- IPCC, Intergovernmental Panel on Climate Change (2012), Renewable Energy Sources and Climate Change Mitigation.
- IPCC, Intergovernmental Panel on Climate Change (2017), Global Worming Potential Values.
- Johnson, S,2007.The(food)priceofsuccess.FinanceDev.—Q. Mag.Int.Monetary Fund 44(4).
- Larson, E., 2008. Biofuels Production Technologies: Status, Prospects and Implica- tions for Trade and Development. United Nations Conference on Trade and Development.
- Lin, Y., Wang, D., Liang, J., & Li, G. (2012). Mesophilic anaerobic co - digestion of pulp and paper sludge and food waste for ethane production in a fed-batch basis. In Environmental Technology (pp. 2627-2633). Taylor and Francis.
- López, M. E., Rene, E. R., Veiga, M. C., & Kennes, C. (2013). Biogas Upgrading. In C. Kennes, & M. C. Veiga, Air Pollution Prevention and Control (pp. 293-318). Chichester: Wiley.
- Macedo, I.,Leal,M.,daSilva,J.,2004.Assessmentofgreenhousegasemissionsin the productionanduseoffuelethanolinBrazil.ReporttotheGovernmentof the StateofS~ao Paolo.
- Mercer-Blackman, V., Samiei, H., Cheng, K., 2008. Biofuel Demand Puschs Up Food Prices. International Monetary Fund Survey Magazine: IMF Research, 17.10.2008.
- Mitchell, D., 2008. A note on rising food prices. Policy Research Working Paper 4682, The World Bank, July 2008.
- OECD, 2007. Documentation of the AGLINK-COSIMO Model. Document AGR/CA/ APM(2006) 16/FINAL, March 2007.
- OECD, 2008.BiofuelSupportPolicies—An EconomicAssessment.
- OECD/FAO, 2009. Agricultural Outlook 2009–2018.

- OECD/ITF, 2008. Biofuels: Linking Support to Performance.
- Pimentel, D., Patzek, T., 2005. Ethanol production using corn, switchgrass and wood: biodiesel production using soybean and sunflower. Nat. Resour. Res. 14 (1).
- Rajagopal, Deepak; Zilberman, David. (2007). Review of Environmental, Economic and Policy Aspects of Biofuels. Policy Research Working Paper; No. 4341. World Bank, Washington, DC. © World Bank.
- Roser M., Ortiz-Ospina E., (2017), 'World Population Growth'. *Published online at OurWorldInData.org*. Retrieved from: https://ourworldindata.org/world-population-growth/ (last accessed – 30/11/2017).
- Santos, M., Grande, C., & Rodrigues, A. (2013, April 3). Dynamic Study of the Pressure Swing Adsorption Process for Biogas upgrading and Its Responses to Feed Disturbances. Industrial & Engineering Chemistry Reasearch, pp. 5445-5454.
- Schmidhuber, J., 2007. Biofuels: an emerging threat to Europe's Food Security? Impact of an increased biomass use on agricultural market, prices and food security: a longer-term perspective. Policy Paper 27, Notre Europe, May 2007.
- Sorda G., Banse M., Kemfert C., (2010). An Overview of Biofuel Policies Across the World. Energy Policy. 38: 6977-6988.
- UNCTAD, United Nations Conference on Trade and Development, 2008. Addressing the global food crisis: key trade, investment and commodity policies in ensuring sustainable food security and alleviating poverty. In: The High-Level Conference on World Food Security: The Challenges of Climate Change and Bioenergy, Rome, Italy, 3–5 June, 2008.
- Yeh, S., 2007. An empirical analysis on the adoption of alternative fuel vehicles: The case of natural gas vehicles. *Energy Policy* 35: 5865–5875.

2. BIOFUELS AND BIOGAS OVERVIEW – AN ITALIAN CASE STUDY

As briefly discussed in Chapter 1, biofuels have the potential to positively influence decarbonization with substantial consequences in GHG emission reduction. This is particularly referred to the transport sector, affecting 24% of global CO_2 production due to fuel combustion. A possible solution to this is represented by biofuels, able to significantly reduce environmental impact and air pollution during combustion. However, since biofuels production is not cost-effective compared with traditional fuels, incentives and specific governmental policies are required. In this Chapter, biofuels production and related incentives are presented from all over the world. Specific policies and incentive schemes related with biogas production and utilization as vehicle fuel will be discussed. Attention will be reserved for the Chinese and the European ones. Finally, the Italian incentive scheme for biogas production and utilization is investigated. A case study is presented in order to evaluate the feasibility of liquefied biogas (LBG) in the Italian context.

2.1. The Biofuels Market Evolution

Table 2.1. Biofuels production per region over the last 7 years (BP Statistical Review, 2017)

Years	2010	2011	2012	2013	2014	2015	2016	2016
Countries	Thousand tonnes of oil equivalent							
US	28044	31184	29808	31057	32890	33849	35779	43.50%
Canada	809	950	1017	1056	1188	1142	1160	1.40%
Mexico	14	13	15	58	58	58	58	0.10%
North America	**28866**	**32147**	**30840**	**32171**	**34137**	**35049**	**36997**	**45.00%**
Argentina	1670	2234	2295	2014	2644	2038	2828	3.40%
Brazil	16866	14403	14739	17114	18005	19332	18552	22.50%
Colombia	455	572	627	650	676	693	626	0.80%
South America	**19220**	**17519**	**17961**	**20131**	**21703**	**22442**	**22378**	**27.20%**
Austria	391	390	390	374	329	381	419	0.50%
Belgium	603	664	562	547	574	556	558	0.70%
Finland	301	208	263	330	367	445	446	0.50%
France	2353	1935	2145	2306	2541	2519	2226	2.70%
Germany	3022	2967	3031	2770	3460	3191	3198	3.90%
Italy	678	486	298	457	585	582	583	0.70%
Netherlands	391	674	1276	1495	1756	1675	1680	2.00%
Poland	439	414	652	697	750	940	898	1.10%
Portugal	284	330	276	274	301	321	298	0.40%
Spain	1312	851	620	749	1030	1122	1148	1.40%
Sweden	339	400	491	635	789	222	211	0.30%
United Kingdom	304	322	303	517	403	310	351	0.40%
Europe	**11604**	**10876**	**11734**	**12503**	**14445**	**14012**	**13777**	**16.70%**
Africa	**8**	**8**	**23**	**32**	**40**	**40**	**40**	**-**
Australia	222	223	239	202	169	157	144	0.20%
China	1584	1970	2103	2346	2609	2653	2053	2.50%
India	123	210	229	268	349	410	505	0.60%
Indonesia	723	1110	1397	1750	2547	1354	2503	3.00%
South Korea	511	309	283	321	337	385	404	0.50%
Thailand	700	765	1054	1330	1490	1603	1610	2.00%
Asia & Pacific	**4306**	**5280**	**6300**	**7450**	**9374**	**8476**	**9110**	**11.10%**
World	**64008**	**65834**	**66863**	**72293**	**79703**	**80024**	**82306**	**100.00%**

Over the last two decades, biofuels production was driven mainly by the necessity of self-sufficient energy production, fossil fuels importation reduction and development domestic agriculture (Araújo, 2017, Kovarik, 2013). More recently, minimization in GHG emissions related with transportation sector has also become a key point in biofuels production (REN21, 2016). These fuels are seen as instruments to achieve the shift to a low-carbon and

sustainable transport sector (IRENA, 2016). Since 2000, the global biofuels supply has increased dramatically representing about 4% of the global transport fuels in 2015 (REN21, 2016). Reasons of this trend is mainly due to policies such as blending mandates, which promote greater biofuels utilization, protecting them from oil price flux over time (REN21, 2016; EIA, 2017). In special transport sectors such as aviation, marine transport, and heavy freight, biofuels seem to be the only low-carbon alternative to traditional fossil fuel (IRENA, 2016). This is mainly the case of aviation sector, in which GHG emissions are foreseen to increase in a range of about 400 - 600% from 2010 to 2050 (ICAO, 2013). Considering this trend, aviation industries set target related with GHG emissions reduction (IATA, 2015). As a consequence, in 2008 the first commercial test flight using biofuels was achieved and in 2015, 22 airline companies were using successfully biofuels as combustion fuel (REN21, 2016). However, plant construction as well as biofuels production have slowed down since 2010, reflecting policy uncertainty (REN21, 2016). This is mainly due to the criticism related with food versus fuel trade-offs, GHG emissions in an LCA perspective, and land use.
In Table 2.1, regional biofuels productions from 2010 to 2016 are reported. During 2016, Brazil and the United States represented more than 66% of the world's biofuel production. Primary feedstock sources were sugarcane for the former and corn for the latter (REN21, 2016). Figure 2.1 shows regional biofuels production trends since 1990. The European Union and Asia biofuels production market has developed considerably over the last two decades. The European Union focuses on bio-diesel using waste, soy, rapeseed, and palm as biomass source (Huenteler, 2015). On the other hand, Asian biofuels production mostly involves sugarcane, corn, wheat, and cassava. Other minor biomass sources regard palm, soybean, rapeseed, and Jatropha. From 2013 to 2015, global share of ethanol fuel compared to bio-diesel fuel is of about 3 to 1 (REN21, 2016). Regarding specific biomass used during Generation 1 to produce conventional biofuels, starch, sugar, vegetable oil, and animal fat comprehend most of the supply (OECD-UN, 2016).

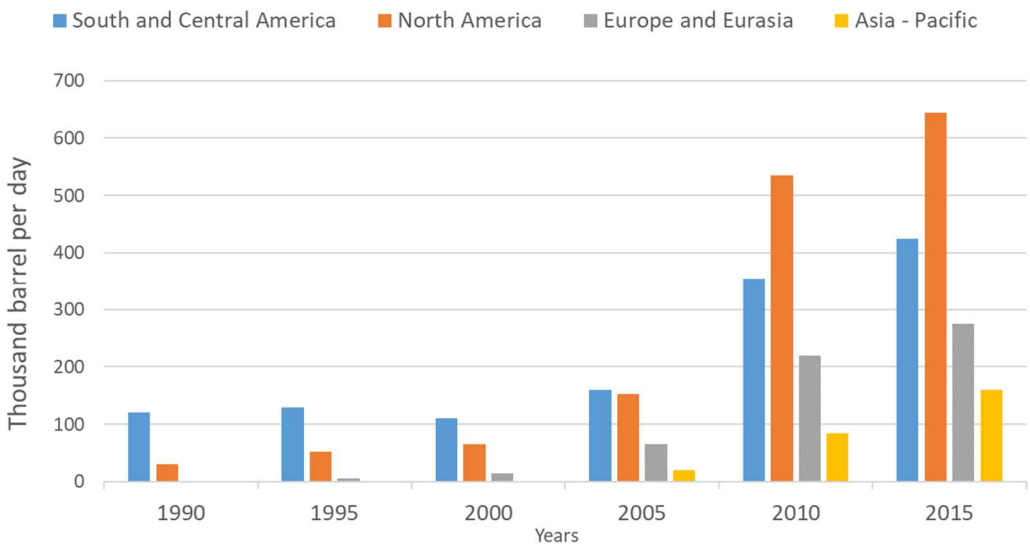

Figure 2.1. Yearly biofuel production per region

Biofuels production involves several processes and technologies able to obtain combustion fuels to substitute traditional fuels. Those processes mainly consist in hydrolysis and fermentation processes as well as esterification or trans-esterification. Table 2.2 shows brief description about feedstock and required technology for most common biofuels. As the central focus of the thesis regards biogas, this kind of fuel will be discussed more in detail in a specific section. Fermentation of sugar, such as cane or beets, allows ethanol production. Also corn or wheat starch as well as root crops are used to this purpose (EIA, 2011; Kojima, 2006; Seelke, 2007). Its higher-octane rating is higher than that of conventional gasoline, improving combustion properties. Thus, higher compression ratio could be achieved in traditional engines (Anderson, 2012). By the way, ethanol is characterized by roughly 70% as energy density as gasoline by comparison (IRENA, 2016; IRENA, 2016). As a consequence, ethanol combustion is less pollutant than traditional fuels, while granting lower autonomy. However, GHG emissions reduction could only be achieved if the productive process is environmental friendly. It is also possible to use it as an additive to gasoline, with a share of about 10% (REN21, 2016; EIA, 2011; USDA, 2016). In Brazil, common practice allows any blend of gasoline and ethanol, as well as ethanol only (Araújo, 2017). Further improvements in vehicle industries could allow a higher blending level, up to 40% of total fuel, while keeping combustion efficiency constant. At present, operating vehicles with 15% ethanol blend experiencing a considerably efficiency reduction (Theiss, 2016).

Considering biodiesel, esterification and trans-esterification of vegetable oils or animal fat allow its production for diesel blending or substitution. Although biodiesel combustion is much similar to that of traditional diesel, it presents lower carbon content ranging from 4 to almost 7 times lower than diesel. For this reason, biodiesel is cleaner during combustion, achieving GHG emissions reduction (Solomon, 2014). Biodiesel is more likely produced in EU and parts of Latin America (DOE, 2016). During Generation 2, non-food crops and residues or waste materials are strongly preferred to food-related biomass sources in order to produce advanced biofuels. Hydrolysis, fermentation (also combined with hydrolysis), pyrolysis, hydrotreating and syngas's alcohol fermentation are key processes. Biofuels obtained during Generation 2 are renewable diesel and gasoline and biobutanol. Renewable diesel and gasoline are produced from lipids or cellulosic materials. These fuels can readily replace standard fossil fuels being compatible with traditional engine and refueling stations. As a consequence, no additional investments are required in order to introduce those fuels in the market.
Hydrotreating, pyrolysis and gasification processes are commonly used to produce renewable diesel (DOE, 2016). Those processes grant less issues related with NO_X emissions, storage stability, cold properties and deposition formation, affecting mostly biofuels obtained by means of esterification process (Aatola, 2008). Regarding renewable gasoline production, fermentation of sugars is generally used as common process. Biomass fermentation is generally involved in biobutanol production. This biofuel presents an energy density lower than gasoline in a range of 10 – 20%. By the way, this value is considerably high if compared with biofuels such as biodiesel or ethanol (DOE, 2016). Comparing biofuels performances to those of traditional fossil fuel, some differences could be identified. As already mentioned, necessary octane level is generally achieved in biofuels, thus engine efficiency is not considerably affected by biofuels combustion. Another important aspect is represented by energy density. Since energy density is strictly related with vehicle's autonomy, too low values could negatively affect some biofuels diffusion. Referring to diesel performances, ethanol has an energy density reflecting a lower autonomy of about 25 – 30%, while biodiesel nearly the same. In heavy-duty engines, several studies proved biodiesel to effectively reduce GHG emissions during combustion. Although this results strongly depend on several factors such as the process used in biodiesel production, the feedstock involved in and adopted mixture (EPA, 2002), biodiesel achieves a considerably reduction in total air pollution. By completely substitute diesel with biodiesel, combustion process emits 70% less hydrocarbons and roughly 50% less particulates and carbon monoxide (CO). However, produced NO_X are increasing by 10% (EPA, 2002). As a consequence, biodiesel could grant almost 50% less air pollution if compared with standard diesel (Cowie, 2016, EPA, 2002). As for biodiesel, environmental impact of ethanol fuel is also influenced by several aspects. In particular, it depends on production process as well as on feedstock generation types. Furthermore, acetaldehyde emission during biofuels production can considerably increase air pollution. It was estimated an impact related with ethanol and biodiesel production in a range of 2-69 kg CO_2-eq/GJ and 20-49 kg CO_2-eq/GJ respectively. Thus, emission related with biofuels production still represents a challenge in a climate mitigation perspective (Cowie, 2016; EPA, 2002; Grosjean, 1990). Feedstock diversity is strongly influenced by local conditions and farms. Table 2.3 gives some insight regarding this point. Algae is related with a group of photosynthetic organisms. This feedstock is very promising for biofuels production, especially for their high oil content, limited waste streams and very low land requirements compared with other biomass sources (U.S. EPA, 2011; Dismukes, 2008). Water requirement for algae cultivations is a key point. by the way, fresh water, brackish, saline, and wastewater are allowed as water sources. However, since data related with algae to be used as feedstock source in biofuels production are still limited, environmental impact of such a biomass growth and utilization is uncertain (U.S. EPA, 2011; Dismukes, 2008; Scott, 2010). Corn represents a fundamental food source able to grow in a wide range of climates from tropical to temperate. High level of fertilizer and pesticide are associated with corn growth (Elbehri, 2013; EEA, 2006). If used as feedstock for ethanol production, water requirements are relatively low and dependent to produced ethanol (Elbehri, 2013; Aden, 2007; NRC, 2008). The United States leads the world ethanol production from corns. Jatropha is a non-food highly drought resistant crop, able to grow with a wide range of climates, soil and water conditions (Koundinya, 2008). More and more countries are investing in Jatropha as a feedstock for biofuels production. Up to now, grater producer is Guatemala which has designated 25,000 acres for its cultivation. Other major investors are represented by Mexico, Sudan, Ethiopia, and India (Lane, 2014). Lignocellulosic material derives from non-edible crops. Specific practices allow lignocellulosic materials to limit cropland expansion and related emissions (Murphy, 2015). This kind of feedstock is obtained from many different sources, such as switchgrass, trees, and agricultural crop residues. Rice straw, wheat straw, corn stover, and sugarcane bagasse are also eligible (Hadar, 2013). 2.3 billion tons of straw were available in 2011, with a potential ethanol production of about 560 million tons (Kahr, 2013). Depending on the lignocellulose feedstock, water requirements varies, however very little water is usually needed (Kumar, 2015). Incentives are disposed for biofuels production by means of this biomass type instead of common crops. The biofuel production consists in breaking down fibrous plant walls into sugars.

Table 2.2. Biofuel properties and requirements (Araujo, 2017)

	Generation 1 Ethanol	Generation 2 Ethanol	Biodiesel	Renewable diesel	Renewable gasoline	BioButanol	Biogas
Feedstock	Sugar or starches	Cellulosic materials	Vegetable oils, animal fat	Vegetable oils, animal fat	Cellulosic materials	Cellulosic materials	Vegetable, animal, industrial wastes
Technology	Fermentation, distillation, hydrolysis	Fermentation and hydrolysis	Esterification	Hydrotreating, pyrolysis, gasification	Catalytic conversion, fermentation	Fermentation,	Microorganism's digestion
Product	Gasoline additive, hydrous ethanol	Gasoline additive, hydrous ethanol	Conventional biodiesel	Renewable diesel	Bio-hydrocarbon	Gasoline additive	Rich methane gas mixture
Chemical*	C_2H_5OH	C_2H_5OH	O‖R'-C-O-R	C_nH_{2n+2}	C_6H_{14}-C_{12}-H_{26}	C_4H_9OH	CH_4, CO_2, H_2S

*(R,R'=alkyl groups)

Table 2.3. Feedstock properties and requirements (Araujo, 2017)

Feedstock (Generation)	Growing time	Growing temperature	Required water	Country
Algae (second)	Depending on environment	16 – 27 °C	Depending on environment	Emergent
Corn (first)	110 – 140 days	18 – 20 °C	500 – 800 mm	Brazil, USA, China
Jatropha (second)	90 days	16 – 21 °C	254 – 1016 mm	India, China, Indonesia
Lignocellulose (second)	Depending on source	Depending on source	Very poor requirements	Emergent
Palm (first)	5 – 6 months	27 – 28 °C	>1800 mm	Nigeria, Malaysia, Indonesia
Rapeseed (first)	85 – 110 days	3 – 12 °C	300 – 600 mm	China, India, Canada
Sorghum (second)	110 – 140 days	25 – 35 °C	450 – 650 mm	Nigeria, India, Sudan
Soybeans (first)	100 – 130 days	18 – 35 °C	450 – 700 mm	Argentina, Brazil, USA
Sugar beets (first)	140 – 200 days	20 – 25 °C	550 – 750 mm	France, USA, Russia
Sugarcane (first)	15 – 16 months	32 – 38 °C	1500 – 2500 mm	Brazil, China, India
Wheat (first)	100 – 130 days	15 – 20 °C	450 – 650 mm	Russia, China, India

Once sugars are formed, fermentation of such sugars allows the production of cellulosic ethanol. Since the process is still expansive, develop the technology in order to reduce economic impact is mandatory. Palm represents main feedstock source in biodiesel production. Grater biodiesel producers using palms are Indonesia, Malaysia, and other Southeast Asia countries (De Gorter, 2015). Oil from palm represents the largest source of vegetable oil consumed worldwide (Verheye, 2010; Rosillo-Calle, 2009; Thoenes, 2006). Palm trees requirements are linked to deep soil, a relatively constant high temperature, and continuous moisture. This feedstock mainly grows in rainy and tropical areas. Soybean is a fundamental crop in both biofuel production and food. It is responsible for 25% of global oil consumption and 65% of meal and cakes production (Thoenes, 2006). USA and Brazil are greater soybean producers (USDA, 2017). The crop could grow in temperate climates, tropical and sub-tropical areas (FAOSTAT, 2017). Sugarcane representing the second largest feedstock source to produce ethanol. Moreover, it is a basic food, growing in tropical areas. Sugarcane is grown in deep soil using fertilizers that are high in nitrogen and potassium, and low in phosphorous (FAOSTAT, 2017). Sugarcane requires high water quantity during its growing season, depending on the specific region. Moreover, deep soils and particular fertilizers are mandatory for its (FAOSTAT, 2017). Brazil is the main responsible for sugarcane production to be used as feedstock for ethanol fuel. Sweet sorghum is an annual grass crop mostly produced in the USA, Nigeria, and India (Elbehri, 2013). It can grow in tropical, sub-tropical, and temperate areas. Sweet sorghum is more versatile than sugarcane and contain higher sugar levels. It is able to grow with limited water and in poor/shallow soil (Elbehri, 2013). Compared to sugarcane and sugar beet alternatives, sweet sorghum is drought-resistant and has a much shorter growing cycle of four months (Elbehri, 2013). Due to a high-water content of about 70%, sorghum must be quickly processed (Elbehri, 2013).

2.2. Biofuels Critical Aspects

As already mentioned, biofuels production presents some critical aspects related with food prices as well as environmental impact over its LCA and overall sustainability. Regarding food criticism, Figure 2.2 shows the volatility of global agriculture prices (HLPE, 2013; Tomei, 2016). From 2006 to 2008, prices related with cereal and oilseed doubled accordingly with overall food index prices (FAO, 2017). Further increase in those prices was registered in 2011 and 2012, while corn prices experienced even greater levels in 2012 and 2013 (De Gorter, 2015). Sugar prices trend seemed to be unpredictable, with an increasing rate of about 130% from 2007 to 2011. Although food price crises already occurred in the past, such as in 1950s and 1970s, the degree of trends and phenomenon extension was quite high (HLPE, 2011). By the way, recent increasing rate in food prices indicator are not as high as that occurred during 1970s (HLPE, 2011).

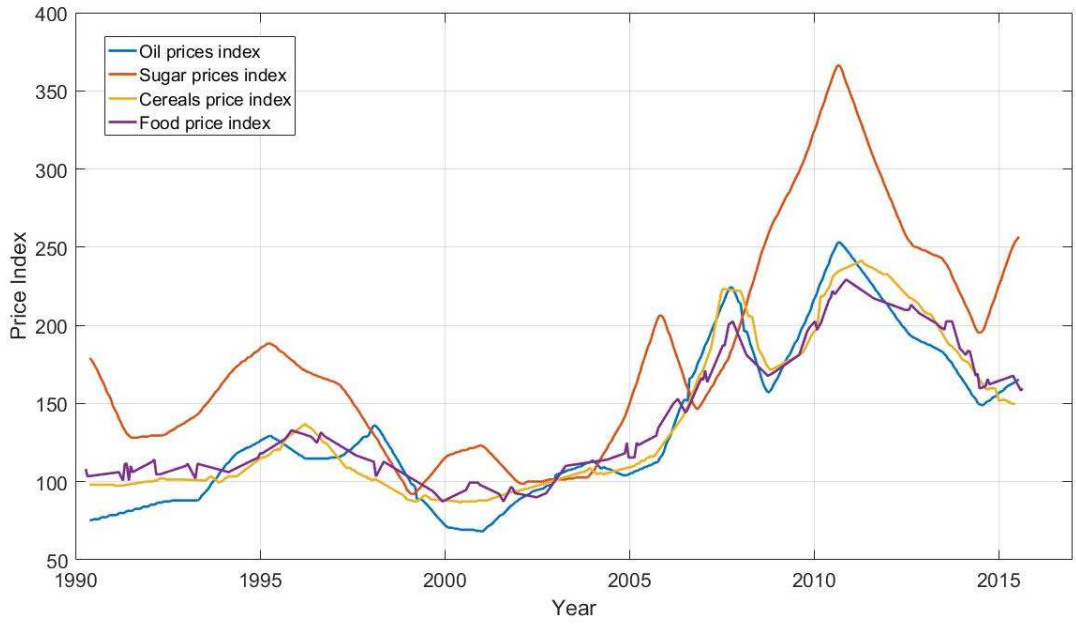

Figure 2.2. Food price index trend over the last 25 years (Araujo, 2017)

Due to intensification in biofuels production over the same period in which food prices index was rising, great attention was posed about possible connection between those aspects (De Gorter, 2015). During 2008 and 2011, G20 agendas put the basis for food prices and biofuels production linkage investigation (De Gorter, 2015). Main questions were related with biofuels production impact on food prices and land utilization to be converted from food-based to fuel-based lands (Tomei, 2016; FAO, 2016; Searchinger, 2008). At that date, any evidence was identified. By the way, several factors were introduced in order to clarify those aspects (De Gorter, 2015; HLPE, 2013; HLPE, 2011; Yang, 2013; Kahn Ribeiro, 2008). Some estimate that increased in food prices is related with biofuels production with a calculated impact ranging from 20% to 40% (Solomon, 2014). Other considerations regarding land usage are ongoing (Tomei, 2016). Up to now, social, environmental, and economic issues remain to be assessed. Meanwhile, debates continue over how to even forecast and correctly measure prices trends (De Gorter, 2015). Focusing on environmental impact, several studies were conducted in order to evaluate pollutant emissions. However, increasing interests are regarding also sustainability issues. The literature on biofuels reflects an increasing interest regarding sustainability. Some of them asses that the net GHG emissions from biofuels production and combustion can be worse than those attributed to traditional gasoline considering an LCA analysis (Searchinger, 2008; Yang, 2013; Kahn Ribeiro, 2008). On the other hand, other studies confirm that biofuels are able to efficiently reduce GHG emissions by 60%–94% if compared to fossil fuels (Holma, 2013; Highina, 2014). Concerning regional distinctions, emerging countries are responsible for higher GHG emissions than advanced nations in biofuels production (Ji, 2016). As a consequence, sustainability of biofuels is strictly dependent to several circumstances, such as differences in biofuel adoption and social context. Looking at biodiesel, it was proven to considerably reduce particulate emissions, up to 88%, compared with traditional diesel. However, depending on above mentioned factors, it can also produce grater NO_X emissions (Xue, 2011). Another sustainability key point is regarding land usage in biofuels production. The global population growth is constantly rising (UN DESA, 2015), thus lands should be able to grant food as well as city expansions and biofuels production. The United Nations' Food Agriculture Organization assesses that land utilization has increased of about 12% since 1961, meaning a net land utilization increment of almost 160 million hectares. In the same period of time, irrigated land and agricultural production have risen by a factor of 2 and from 2.5 to 3 respectively (FAO, 2011). Thanks to large use of pesticides and fertilizers, food storages were possible, mitigating such a situation (Fischer, 2002). Recent studies indicate that less than 3% of global land used for agricultural purpose are actually dedicated to biofuels production. By the way, greater concerns over land utilization for biofuels production are existing (Popp, 2014; Borras, 2012; Edenhofer, 2017). Some calculations were made in order to better understand biomass growth for biofuels production. It was found that over 13.4 billion hectares of global lands, 0.7 billion hectares are available gross lands while 0.44 billion hectares are related with technical upper limit regarding biofuels production for transport and energy sector by 2050. Approximately 80% of those lands are forecasted to concern African and South America regions (Fischer, 2006). As a consequence, such countries are going to be driving force over environmental impact and socio-economic aspects related with biofuels production. As concerns are growing regarding land utilization, the same is occurring in water consumption related with those lands cultivation. Up to now, something like 70% of global freshwater is related with agriculture while many countries are experiencing water supply issues (Fischer, 2002). And the situation is clearly forecasted to be worst in the future. Thus, biofuels production will greatly influence the available supply of water as well as the quality of the water. Considering country regions already experiencing water scarcity to be future main biofuels producers, this factors combination could easily create wide dead zones (Solomon, 2014; NRC, 2008). By the way, some biofuels production processes are able to produce positively effects on water utilization. Is the case of strategical cultivation of switchgrass, able to reduce nitrate contamination of groundwater (Bransby, 1998). Up to now, while rising energy demands is combining with water resource limitations, efforts are strongly required in order to better spatial and temporal patterns for water requirements (Scott, 2015).

Table 2.4. Biofuels thermos-physical characteristics (Araujo, 2017)

Biofuel	GHG [CO_2 ep/MJ]	Water [L/L]	Energy [MJ/L]	Net energy balance [MJ/L]
Gasoline*	94 g	2.8 – 4.6	35.4	29.3
Corn ethanol	76 g	175.4	21.3	10.1
Sugarcane ethanol	45	526	21.3	16.4
Soybean ethanol	59.19	369.2	32.7	-
Cellulosic ethanol	43	6.5	21.3	20.4 – 21.4
Biodiesel**	59.19	645.5	32.7	21.6
Algae biodiesel	-	44 - 216	32.7	-

*gasoline represents the baseline for biofuels parameter definition

**referred to rapeseed and canola biofuels

Another critical aspect related with land utilization in biofuels production processes concerns biodiversity. As a growing area is required for specific cultivations, deforestation and lands clearing practices have great negative effects over natural habitat and existing species (Cowie, 2016). Moreover, methods aimed to evaluate such aspect are still ongoing and LCA analysis are not considering this kind of environmental impact (Cowie, 2016; De Baan, 2013; De Baan, 2013). Thus, biofuels sustainability must be aligned with ecosystems conservation. At present, biodiversity is not affected in biofuels production in agricultural areas (Morgera, 2009). With advanced biofuels, greater technical potential exists in natural and anthropogenic waste recovery, which could mean, carbon emissions reduction as well as a decreased land and water utilization level. In order to achieve this result, strong investments are required, while cost reductions remain a key point for technological development to evolve into a commercial scale (Huenteler, 2015). Considering algae production, for instance, land utilization is considerably lower than that related with other biomasses in a volumetric biofuel production perspective (Dismukes, 2008). Focusing on water consumption, algae presents high water requirements. Thus, biofuel produced using such a biomass may not be suitable for water-challenged regions. Technological efforts are also needed both to reduce the costs related with the dewatering issue as well as for identifying new algal species. If one considers land use with residue-based feedstock for advanced biofuels versus that required for grain and dedicated crops in conventional biofuels, the former is more favorable since no additional land is required. Such a scenario avoids competition for land, and, in turn, has minimal impacts on food prices as well as GHG impacts (Searchinger, 2008; Grosjean, 1990) and likely water. Table 2.4 shows data related with several biofuel's properties. Looking across feedstock options, water needs are highest for algae, rapeseed, and sugarcane. Energy balances are highest for rapeseed-based fuel and cellulosic ethanol. Some estimates indicate that the energy return on investment for sugarcane ethanol relative to corn-based ethanol is 4–6 times larger (Cowie, 2016). Regarding accidents related with biofuels utilization, less dangerous effects to the environment could be found over traditional fossil fuels, since biofuels will more readily biodegrade (Cowie, 2016).

2.3. Governmental Policies

Governmental policies, incentives and penalties related with biofuels production have played major role in associated technology development as well as market penetration. Such actions mainly consist in encouraging or impeding sustainable approaches, being consequently responsible for barriers reduction. In this section, national governmental policies are discussed.

2.3.1. Canada

The Canadian Environmental Protection Act Bill C-33 established mandatory renewable content of 5% regarding gasoline and 2% regarding diesel to be achieved by 2010 and 2012 respectively. Ethanol production is mainly based on cereal grains. It was found that in 2009 ethanol output was accounting for 69%, while wheat was responsible to further 30%. On the other hand, biodiesel is mostly produced from animal fats. It was estimated that during 2009 tallow grease was responsible for 49% biodiesel feedstock, while yellow grease accounted for 37%. Canola share in biodiesel production increased considerably over the time, accounting for 14% of total production in 2009 (Dessureault,2009). Production of renewable fuels was found to have a positive impact on the Canadian economy, estimated in 2 billion $ per year (Doyletech, 2010). Moreover, direct incentive payments have been introduced since April 2008. Through the Eco ENERGY for Biofuels Program incentives related with ethanol production guaranteed 0.10 $ per liter from 2008 to the end of 2010 for manufacturers. The payment declines by 0.01 $ every year reaching its minimum in 2015 and 2016 of 0.04 $. The maximum incentive related with biodiesel was equal to 0.20 $ per liter from 2008 to 2010. As for ethanol, the incentive was decreased by 0.04 $ per year, down to 0.06 $ in 2016. In addition to the Eco ENERGY program, several fund schemes are in place to expand biofuel production by targeting an enlargement of manufacturing facilities, granting support to research clusters (Agricultural Bio-Products Innovation Program and Sustainable Development Technology Canada) and accelerating the commercialization of innovative agricultural products and services (Agri-Opportunities Program). The federal biofuel mandates and support policies were further integrated by specific legislative measures imposed and financed by individual provinces. Both Canadian federal and provincial governments are involved in defining incentive policies related with energy and biofuels production. As a consequence, biofuel supporting schemes is constantly developing, while subsidies could also overlap. Several projects are aimed at assisting the biofuels industry by means of new technology research and development, promoting its commercialization in order to achieve GHG emissions reduction. Incentives mainly consists on grants, loans, tax credits and exemptions, as well as mandates in consumptions and blending for gasoline and diesel. Mandate in consumptions is a regulation known as Renewable Fuels Standards. As present, incentives for biofuels producers are expiring or going to expire soon and no plans

were made in order to renew this kind of policy. It is the case of the Alberta Renewable Fuels Standard and the Ethanol Fuel Regulations in Saskatchewan, that are scheduled to expire in 2020 without any further indication. On the other hand, the federal Renewable Fuels Standard related with ethanol and biodiesel productions presents no expiration date. By the way, any information was released regarding minimum incentive rising. This situation represents a steady point in Canadian biofuels policies development. A critical aspect in new policies definition is related with a common view in GHG emissions reduction achievable by means of biofuels, compared with that of standard fossil fuels in a LCA basis. Although increasing concerns are related with low carbon economy, federal government only introduced voluntary guidelines sustainable biofuel production. As a consequence, the provinces have taken the lead in addressing sustainability related with biofuels production. In particular, British Columbia, Alberta, and Ontario introduced specific regulation about this point. British Columbia has introduced a Low Carbon Fuel Standard (LCFS), which assesses that fuel suppliers are required to demonstrate a 10% reduction in the carbon intensity relative to 2010 levels by 2020. The Alberta Renewable Fuels Standard assesses that GHG emissions from biofuels production processes must be at least 25% lower than those from the same quantity of fossil fuels. Finally, Ontario is not directly introducing specific regulations. However, a GHG reduction target of 15% below 1990 levels by 2020 was introduced, to become 80% GHG reduction target by 2050.

2.3.2. The United States

In July 2010, the new Renewable Fuel Standard (RFS2) regulation went into effect, based on proposals made within the context of the Energy Independence and Security Act of 2007. 36 billion gallons of renewables were set to mandatory used in transport sector by 2022. The regulation assessed that the volume of conventional biofuels should be of 15 million gallons by 2015. Cellulosic biofuels equal to 0.1 billion gallons were expected within 2010 while surge biofuels equal to 16 billion gallons were forecasted by 2022. The total contribution of advanced biofuels should at least 21 billion gallons by 2022. RFS2 also required advanced biofuels producers to achieve a life-cycle greenhouse gas (GHG) emissions reduction higher than 50%, while standard biofuels life-cycle GHG emissions should be reduced by 20%. Moreover, all renewable fuels producers must certify feedstock type used as well as complying with regulations on land utilization. The mandatory consumption of given biofuel volumes was assessed in the context of the Renewable Fuel Standards (RFS1) in the Energy Policy Act of 2005. The objective was to introduce 4 billion biofuel gallons transport sector by 2006, incrementing their share. The new regulations (RFS2) further increased such targets cy means of incentives for second generation fuels and implementing new criteria in order to effectively achieve GHG emissions reduction and sustainability. By the way, driving force in biofuel policy was related with the reduction in oil dependency. During the Energy Independence and Security Act of 2007, one of proposed objective was to decrease gasoline consumption up to 20% by the end of 2017. The Biomass Program held in 2008 had two primary targets. The first one aimed to decrease gasoline consumption up to 30% by 2030, based on 2004 levels. The second one was to produce cellulosic ethanol by means of corn utilization. US biofuel policies have always been related with ethanol industry. During 1978, the Energy Tax Act established tax credits for ethanol blenders. Several incentives were guaranteed over the decades in order to fulfill this target. At present, ethanol is mainly derived from corn cultivations. Statistics shows that 20% of total US corn supply is involved in biofuel production in order to obtain ethanol (EIA, Energy Policy Administration, 2007). In recent years, the Volumetric Ethanol Exercise Tax Credit (VEETC), enacted during 2004 by the American Jobs Creation Act, represented the main source of financial support for biofuels utilization up to 2010. It guaranteed incentives for every domestic or imported gallon of ethanol blended with other fuels, awarded without quantity limitations and gasoline price independent. Blenders can claim credits equal to 0.51 dollars per used gallon (EIA, Energy Policy Administration, 2008). The Energy Information Administration estimated that the tax credit amounted to about 2.4 billion $ in 2006. Tax credits were also guaranteed for biodiesel under the VEECT, as assessed by the American Jobs Creation Act in 2004. The tax credit was of about 1 $ per gallon of produced biodiesel from virgin oils or fats, and 0.50 $ per gallon for recycled oils feedstock. In order to protect national biofuel market from competitive foreign manufacturers, import tariffs were also introduced. There are two taxes levied against imported ethanol. The first one consists in an *ad valorem* duty of 2.5% combined with 0.54 $ per gallon tax, applied under the Most Favored Nations (MFN) scheme. The second one aimed to hinder imported to be part of the government. Being members of the North America Free Trade Agreement (NAFTA), Canada and Mexico were able to duty-free export ethanol to the US. Members of the Caribbean Basin Economic Recovery Act (CBERA) was also allowed to gain limited duty-free from exportations, since those are not higher than 7% of domestic production. Ethanol consumption is directly proportional to the engine requirements as well as to high alcohol content fuels availability. Since the 1970s every gasoline powered vehicles sold in the US can run on E10.

2.3.3. Argentina

Mandatory blending levels for gasoline and diesel were introduced in Argentina starting from 2006, thus at least 5% of blending levels is expected within 2010. The quality, technical and pricing scheme specifications for ethanol were described in 2008 within the context of the Resolution 1295/2008 and 1294/ 2008. Specifications related with biodiesel production and domestic prices were further introduced in 2010 within the context of the Resolution 6/2010 and 7/2010. biodiesel's domestic price was set up with Resolution in February 2010. Tax incentives were not available for biofuel manufacturers that export biofuels. Regarding biodiesel and ethanol sold to the internal market, financial support was guaranteed. Producers are able to choose the incentive nature, thus reimbursement of the value added tax or accelerated depreciation on capital investments were both possible. In addition, the government assures that the biofuel output will be purchased for the 15 years period that corresponds to the term of the Biofuel Law. By the way, financial incentives are reviewed year by year with governmental set prices (Rutz et al., 2009). Biodiesel production is with soybean. Recently, biodiesel output and related productive capacity have substantially increased. It was seen an increment of about 430% from 2008 to 2007 (Argentine Renewable Energies Chamber, 2009). Regarding ethanol production, which is mainly related with sugar industry, less development was registered. Up to the end of 2009, almost total biofuel production was exported. Exported biofuels are not directly incentivized, while biodiesel exporting is guaranteed for favorable export tariffs compared to its feedstock. Soybean and soy are taxed respectively at 35% and 32%, while biodiesel is taxed at 17.5%. According with the European Renewable Energy Directive of 2009, a 35% reduction in GHG emissions is expected from biofuels. Moreover, it assessed that soybean oil accounts for emissions reduction by only 31%.

2.3.4. Brazil

Brazil presents the highest developed and integrated biofuel policy structure. First policies were related with the oil crisis of the 1970s. Thus, in 1975, the National Alcohol Program Pro alcohol was introduced to the purpose of ethanol production by means of sugar cane. Main objective was the energy supply constraints limitations, providing a stable internal demand for sugar cane production surplus (Walter et al, 1999). Agreements with manufacturers were also made to allow market development for biofueled vehicles. Up to 1985, roughly 96% of sold vehicles in Brazil were fueled with ethanol (Colares, 2008). However, subsequent oil prices reduction had negative effects diffusion of such biofuel. As a consequence, sold ethanol fueled vehicles rate decreased by 1% during the 1990s. Moreover, increasing value rate of Brazilian currency, from 1994 to 1999, also determined ethanol prices to increase. Regulations were introduced in order to reduce those effects, thus 22% of ethanol content was required in gasoline, subsequently risen up to 25% in 2003. Other regulations were made in 1998 with the liberalization of hydrated alcohol prices to be used in fuels. Oil prices fluctuations related with the period 2003 – 2008, contributed to the success of ethanol biofuel, becoming again a cheap oil alternative. Another successful factor was related with flex-fuel engine technology introduction, which allows usage of gasoline as well as ethanol. Back to initial standard levels, 83% of sold vehicles were adopting such technology in 2006. As a consequence, Brazil achieved oil importation independence (Colares, 2008). This successful governmental policy is proven by sugar and ethanol production importance in Brazilian economy. Regarding this point 3.6 million jobs and 3.5% of GDP were achieved, while 50% of total sugar cane supply was related with ethanol production (de Almeida's et al., 2008). From a price point of view, ethanol produced in Brazilian was recognized to be the most competitive in the world. Some estimations assessed ethanol cost of Brazilian regions to be 0.23 $ per liter (Macedo and Nogueira, 2005). This target was achieved by means of several factors. The first one is related with sugar price, which is considerably cheap. Moreover, such feedstock is grown in highly productive lands, in regions in which irrigation is not necessary, due to ambient conditions. The second important driving force was represented by governmental policies, which strongly supports investments in technology and process development related with biofuels. At present, although ethanol production is not gaining direct subsidies, its production is still highly preferred to gasoline production. In fact, gasoline experienced high tax levels, up to 0.26 $ per liter, much higher than that related with ethanol, to be 0.01 $ per liter. Moreover, VAT related with fuels are considerable different for ethanol and gasoline. In Rio de Janeiro this difference consists on a 50% VAT related with gasoline while only 36% VAT is related with ethanol. Other states imposed VAT levels on ethanol even lower. It was estimated a total tax incentives of about 977 million $ per year related with ethanol (de Almeida's et al. 2008). Looking at the period 1970 – 1990, total support amounted to roughly 16 billion $. Considering successful policies and results related with ethanol production, new investments were made in biodiesel production. During the National Program on Biodiesel Production and Usage (PNPB) in 2005, minimum level of 2% of standard diesel was forecasted to be replaced by biodiesel from 2008 to 2012, with a further increment up to 5% from 2013 onwards (Colares, 2008). By the way, a result of 4% in biodiesel blending

was already achieved by 2009. Biodiesel production accounted for about 1.5 billion liters during 2009 (Barros, 2009). The Brazilian biodiesel production is strictly related with soybean and vegetable oil plants such as castor bean, palm tree and jatropha. Being less cost- competitive than ethanol, biodiesel requires more important incentives. Main supporters of such incentives are essentially related with governmental policies and tax exemptions. Referring to the former, the National Petroleum Agency (ANP) purchase as biodiesel as required in order to fulfill required targets. Regarding the latter, tax exemptions were introduced depending on specific production region and feedstock type. Due to these factors, tax incentives is varying from 73% to 100% (Barros, 2009).

2.3.5. Brazil biofuels annual 2017 (reference)

During the 21st Conference of the Parties (COP21) of the United Nations Framework Convention on Climate Change, the RenovaBio program was introduced. Main objective was to create a regulatory framework to develop the biofuels sector by means of energy efficiency in biofuels production processes and use. Moreover, the program recognizes different GHG emissions reduction depending on specific considered biofuel. During 2017, the government allows 600 million liters duty free enter, with a tax equal to 20% for exceeding volumes. The US represents the main ethanol supplier. The mandate regarding ethanol and biodiesel are respectively set to 27% (E27) and 8% (B8).

2.3.6. Colombia

During 2001, the government imposed at least 10% bioethanol blend in cities with a population higher than 500,000, The law went into force during 2005 (Pinzon, 2007). As a consequence, during 2009, 75% of consumed gasoline had 10% ethanol content (Rutz et al., 2009). The main target was to achieve blending level of 10% by 2010, rising this value up to 25% by 2020 (ProExport Colombia, 2008). Sugar cane represents the main feedstock in ethanol production and its prices is strictly related with this biomass, as guaranteed by the government. Moreover, tax incentives were involved in biofuels production. Main regulatory lows were Law 939 and Resolution 1289, introduced in 2004 and 2005 respectively. The latter established an obligatory blending level equal to 5% for biodiesel to be achieved within by 2008 (Pinzon, 2008). Further evolution related with such regulation fixed blending levels up to 10% and 20% by 2010 and 2012 respectively (Rutz et al., 2009). Main feedstock source in biodiesel production is palm oil which usage involves tax incentives. However, biodiesel from crops is also incentivized by specific tax regulations. Other incentives are related with industrial projects involved in biofuels production. During 2009, 60% of total sold vehicles were expected to be E85 flex-fuel type by 2012, to be further increased up to 100% within 2016 (Rutz et al., 2009). Up to now, Colombian ethanol production from sugarcane is supplied by seven plants, with a total production potential of 600 million liters. Considering standard growing sugarcane, ethanol production of about 450 million liters and 530 million liters is expected during 2017 and 2018 respectively. Importations in ethanol were of 22.8 million liters during 2016, mostly from US, representing 81,3% on total importations. In the half part of 2017, ethanol importations achieve the highest historical level of 33.5 million liter, while in the second part of the year, importations account for about 7.9 million liters per month on average.

2.3.7. The European Union

In April 2009, European Union established a minimum target of 10% for biofuels to be involved in the transport sector by 2020. Mandatory target was part of the EU Directive 2009/28/EC regarding renewable energy. Moreover, a minimum 35% reduction in GHG emissions were imposed to be achieved from biofuels utilization in a LCA perspective. Further GHG emissions reduction of at least 50% and 60% was also established from 2017 and 2018 respectively. The regulation scheme also considers sustainability criteria for land utilization. As a consequence, primary forests, highly biodiverse grassland, protected and carbon-rich areas were excluded to be available feedstock sources. The Directive 2003/30/EC set a biofuel market penetration of 5.75% to be achieved by 2010. However, this level was not mandatory, thus national action plans were allowed. By the way, a minimum share level in biofuel combustions of 2% were recommended within 2005. However, 2005 biofuels share accounted for only 1% while roughly 4.2% share was achieved in 2010. Those policies were part of an energy policies aimed to increase alternative energy. The Directive 2001/77/EC indicated a gross national consumption and renewable energy

production of respectively 12% and 22.1% within 2010. In 2008 the EC expected a share of 19% instead of initial target of 22%. However, during 2009, EU Directive on Renewable Energy established a mandatory target of 20% by 2020. Directive 2003/96/EC on Energy Taxation specified allowed incentives for biofuels promotion in order to achieve such target. Thus, EC approval is required in order to introduce national taxation incentives. In this case, incentives must be aligned with blending level, accounting raw material prices for no overcompensation. Moreover, their validity is referred to 6 years, nevertheless, extensions are allowed. Most Favored Nations (MFN) import tariffs are equal to 6.5% related with biodiesel. However, little imports of biodiesel are present as EU is global leader producer of such biofuel (UNCTAD, United Nations Conference on Trade and Development, 2006). A tariff equal to 3.2% regards vegetable oil related with crude soy oil, crude sunflower oil and crude rape oil for biodiesel related with industrial usage. Ethanol importations were of about 250 million liters during the period 2002 – 2004. Ethanol importations of about 30% were from MFN countries and classified as denatured alcohol or undenatured alcohol, with a tax equal to 0.102 € per liter and 0.192 € per liter respectively. Great importance in biofuel industry evolution is related with Common Agricultural Policy (CAP). During 1992, the Mac-Sharry CAP reform aimed to reduce cereals and oil seeds productions. Moreover, mandatory shares of non-food land usage were established. As a consequence, more than 95% non-food areas were involved in energy crops production. During 2003, a further CAP reform introduced Single Payment Schemes (SPS) that separate producer support and production decisions. An incentive of about 45 € per hectare for areas lower than 1.5 million hectares, was established for energy crop cultivation. Another reform of CAP was subsequent introduced by the Council Regulation (EC) No 73/2009, in which such incentive was suspended. During 2014, biofuels share was about 4.9%, far from proposed targets. Since such regulation scheme is going to expire within 2020, uncertainty related with EU policymakers supporting program are increasing.

2.3.8. China

China's biofuel policies mostly regard ethanol production while marginal subsidies were found for biodiesel. This is mainly due to the fact that China is vegetable oil importer. During 2001, the government introduced standards for ethanol as well as for bioethanol to be used as vehicle fuels. In 2002, the Ethanol Promotion Program was introduced to handle with maize stock-piles surplus. Similarly, bioethanol to be used as vehicle fuel was regulating by the State Scheme of Pilot Projects. In 2004 the National Development and Reform Commission (NDRC) initiated the State Scheme of Extensive Pilot Projects on Bioethanol Gasoline for Automobiles (SSEPP). Rigid controls were set on ethanol production and distribution. As a consequence, during 2006, extensive pilot projects achieved the blending target of 10% (Dong, 2007). In the very same year, the NDRC introduced a target of 6.6 billion liters of biofuel production by 2010 within the context of the 11th Five Year Plan. By the way, it was not approved due to increasing rate of food prices (Latner et al., 2007). During 2007, the National and Development Reform Commission (NDRC) introduced a Medium and Long-Term Development Plan in order to increase renewable energies, with a target of 10% and 15% share of the total primary energy production by 2010 and 2020 respectively. As a consequence, ethanol production was forecasted to increase up to 2 million tonnes and up to 10 million tonnes by 2010 and 2020 respectively. On the other hand, biodiesel consumption was forecasted to increase up to 200,000 tonnes and 2 million tonnes by 2010 and 2020 respectively (SI, Global Subsidies Initiative, 2008). However, allowed feedstocks were related with non-grain crops such as cassava, sweet sorghum and sweet potatoes. The price of fuel ethanol was controlled by the government. As a consequence, incentives were mandatory in order to allow biofuels production sustainability from an economic point of view. Such incentives in 2007 were equal to 200 $ per tonne of produced ethanol. However, during 2008, such incentive was replaced by payments based on plants performances (GSI, Global Subsidies Initiative, 2008). A tax exemption of 5% a VAT exemption of 17% were set as incentives for recognized biofuels producers. Moreover, further incentives equal to 438 $ per hectare and 394 $ per hectare were introduced for jatropha and cassava cultivations respectively. By the way, direct incentives for biofuels producers are missing.

2.3.9. India

Ambitious biofuels targets were introduced by Indian government. Approved in 2008, the National Policy on Biofuels introduced a share of 20% for both biodiesel and bioethanol within standard fossil fuels by 2017. The policy required biodiesel production to involve non-edible oil seeds, with a proper land conservation policy. Minimum Support Price (MSP) for biodiesel was continuously revised in order to achieve biofuels production development. Similarly, a Minimum Purchase Price (MPP) for bioethanol and biodiesel was also introduced

(Altenburg et al., 2009). Previously, Ethanol Blended Petrol (EBP) and the National Mission on Biodiesel (NMB) policies were introduced in 2003. Regarding EBP mandatory blending level equal to 5% for ethanol biofuel was required for 4 territories and 9 states. Further extension of such target was disposed for 20 states, starting from 2006. Blending requirements were also increased in order to achieve 10% share from 2008. However, this target was delayed due fluctuations in the sugar cane production availability, being the major ethanol feedstock. In addition, the EBP did not allow ethanol importations in order to encourage national biofuel industry (Singh, 2007; 2009). Regarding NMB program, 11.2 million hectares of jatropha cultivation using wasteland were forecasted within 2012 in order to achieve blending target equal to 10%. However, since purchasing price was set by national regulators every six months, biodiesel production costs were not sustainable enough. Thus, ambitious original targets could not be achieved (Singh, 2009). Fiscal incentives for biodiesel equal to 4% of tax exemption were introduced. By the way in several states this incentive was not adopted. Moreover, no direct tax incentives are provided for ethanol production.

2.3.10. Indonesia

In Indonesia, mandatory biofuel consumption levels were introduced in 2008. It was assessed a target in biofuel share equal to 2.5% and up to 20% within 2010 and 2025 respectively. Regarding ethanol share, it was required a blending level equal to 3% and up to 15% within 2010 and 2025 respectively (Dillon et al., 2008). The latter requirement evolved from an initial share level of 10% for biofuels within 2010 (Bromokusumo, 2007). However, feedstock prices fluctuations limited achievable blending level. Although in 2006, a blend level of 5% regarding biodiesel (B5) was achieved, further palm oil increased price affected blending to decrease down to 1% in 2009 (Bromokusumo, 2009). Nevertheless, new facilities building is ongoing in order to achieve governmental targets (Dillon et al., 2008). Incentives related with fuel prices were introduced, thus consequently equalization in biofuel and standard fuel production processes were possible, increasing ethanol and biodiesel blending share.

2.3.11. Malaysia

Being the leader in palm oil production, the Malaysian government launched the National Biofuel Policy (BNP) in 2005. A blending level equal to 5% regarding biodiesel (B5) was introduced. In 2007, the Biofuels Industries Act Legislation aimed the regulation of biofuel industry. However, initial blending share target seemed to be far to be accomplished. Biodiesel product mainly consists of two types. The first one is produced by means of a direct blending of palm oil with standard diesel, being known as envodiesel. The second one is palm methyl esters (PME) biodiesel. It is obtained by means of transesterification of palm oil, representing the largest share of biofuel production. During 2007, Malaysia exported 95,000 tonnes of such biofuel, being roughly 75% of total produced biodiesel (Lopez and Laan, 2008). Biodiesel producers may obtain incentives by means of the Pioneer Status (PS) or Incentive Tax Allowance (ITA). Both support schemes are related with the Promotion of Investment Acts of 1986 (Hoh, 2009). The PS scheme allows 5 years tax reduction higher than 70%. The ITA scheme allows 5 years incentives related with manufacturer's equipment and machinery purchasing. No export duties are existing regarding processed palm or biodiesel. By the way, standard fuels were strongly incentivized. Such incentives are related with end-users by means of a governmental-set biofuel price. Subsidies were of about 4.3 billion $ and 4.7 billion $ in 2006 and 2007 respectively. In order to reduce petroleum subsidies, biofuel shares were meant to be a possible solution. However, fluctuation in palm oil costs negatively affected biodiesel production processes, which become much expensive than that of standard diesel. As a consequence, the original target of blending level of 5% were not become into force. It was estimated an economic impact of about 675 million $ per year in the case of target to be mandatory (Lopez and Laan, 2008).

2.3.12. Thailand

Thailand successfully implemented biofuels production consuming almost 1 billion liters in 2009 (Preechajarn and Prasertsri, 2009). Incentives related with ethanol consumption, consisting in tax exemptions, allowed ethanol blends with final cost significantly cheaper than standard gasoline. Production of ethanol production is mainly obtained by means of sugar cane. A total production 12.3 million liters per day of such biofuel were registered in 2009 (Prasertsri and Kunasirirat, 2009). By blending ethanol and regular gasoline, the so-called gasohol is obtained. Being E10 blend, this biofuel significantly contributed in substitution of standard gasoline. Its consumption risen from 4.8

million liters per day up to 9.3 million liters per day in the period 2007 – 2008. As a result, related demand reached roughly 50% of the gasoline market share in 2009 (Preechajarn and Prasertsri, 2009). Tax exemption allowed gasohol price to be at least 10–15% lower than gasoline prices. In order to increase market share of biofuels, government was promoted E20 and E85 blending levels, as well as associated fuel-compatible vehicles. Final prices of such blends are significant lower than that of gasohol, being 20% and 50% lower than standard gasoline. These values depend on tax exemptions as well as price subsidy given by the State Oil Fund (Preechajarn and Prasertsri, 2009). Regarding biodiesel, the B2 (consisting in biodiesel with a 2% of methyl ester content) has substantially replaced fossil-derived diesel 2008. Consequently, demand for pure biodiesel (B100) has increased substantially, as long as government requirements related with B100 blending with traditional diesel in order to attempt required biofuel share. In order to achieve B5 diffusion over the market, incentives were introduced, in terms of price subsidy, from the State Oil Fund. As a consequence, B5 blends final price were lower than that of B2. Moreover, national production of palm oil has been further increased by means of the Committee on Biofuel Development and Promotion (CBDP) (Peerchajarn et al., 2008).

2.3.13. Australia

During 2001 the Australian government introduced a target related with biofuel production to be at least 350 million liters per year, to be achieved within 2010. Although such target was not mandatory, 10% obligatory blending level was established by the State of New South Wales, in 2006. By the way, Australia has limited biofuel production capacity. It was registered a capacity of 140 million liters 323 million liters for ethanol and biodiesel respectively. Nevertheless, national targets are aimed to increase such production capacity up to 1 billion liters for both of them (Australian Government Rural Industries Research and Development Corporation, 2007). However, in the period 2006 – 2007, total biofuel production capacity was of about 83 million liters and 77 million liters of ethanol and biodiesel respectively (Quirke et al., 2008), while a total biofuel production of about 400 million liters with 800 million liters consumption were achieved in 2014. Although its low potential capacity, Australian government strongly promote biofuels, involving incentives considerably high compared to those related with other industries. The major incentive is represented by decreased taxes related with both ethanol and biodiesel. Excise duty of 0.38143 $ per liter for ethanol and biodiesel was introduced until 2011. Tax reduction was then removed during 2011 while excise duty decreased to 0.125 $ per liter. However, Energy Grants-Cleaner Fuels Scheme introduced other payment from 0.1 $ per liter to 0.025 $ per year up to 2015. Regarding biodiesel similar incentives could be found. Excise duty decreased to 0.191 $ per liter from 2011 while incentives provided by Energy Grants-Cleaner Fuels Scheme decreased from 0.38143 $ per liter to 0.153 $ per liter in the period up to 2009, and finally disappeared in 2015. Import taxes regarding ethanol are equal to 5%.

2.4. European and Chinese Situation in Transport Sector

In this section, an overview of European and Chinese situation regarding the transport sector is presented. Specific vehicle emission levels, fleet volumes as well as ongoing policies towards GHG emission reduction associated with transportation are discussed in detail. Natural Gas Vehicles (NGVs) diffusion level and related incentives open the biogas and biomethane potential benefits. After a brief description of such biofuel as well as of involved processes, an Italian case study is proposed in order to evaluate the ongoing incentive scheme related with biomethane production and consumption. The analysis considers LBG as final product showing high potential for such biofuel thanks to the incentives scheme.

2.4.1. The European situation

In Europe, the GHG emission reduction is achieved by means of mandatory targets, set depending on the vehicle size. Up to now these targets have been set for passenger vehicles and vans. The final goal is to reduce CO_2 emissions from transport sector by roughly 60% by 2050, compared to 1990 levels, as reported in the European Commission website (EC, 2015a).

Passenger cars are responsible for about 12% of total CO_2 emissions in Europe. Law imposes that the new cars emissions do not exceed more than 130 g CO_2/km by 2015 (average limit). This emission level must be further reduced up to 95 g CO_2/km by 2021 (average limit), corresponding to 4.1 l/100 km of petrol or 3.6 l/100 km of diesel consumption respectively (EC, 2015b). Compared with the average emission level in 2007 (158.7 g/km),

these levels represent a reduction of about 18% and 40% respectively for the 2015 and 2021 targets. Since 2010, the emission level have decreased by 17 g CO_2/km (an average of 12%) and in 2014, the average emission level for a new car was 123.4 g CO_2/km, well below the 2015 target, as reported in the monitoring of CO_2 emissions provisional data (EEA, 2009).
These emission targets have been set according with a limit value curve that imposes the maximum allowable level of emissions for every year from 2012. Penalties are foreseen for those manufacturers having a fleet with an average emission level higher than such annual level. The penalty depends from the value of exceeding emissions: 5 € for the first g/km of exceedance, 15 € for the second, 25 € for the third and 95 for each subsequent g/km. From 2019 the penalty will be 95 € from the first gram exceeding the limit.
Some incentives are granted under certain circumstances: if the manufacturer equips his vehicles with innovative technologies, he can gain credits up to a maximum of 7 g/km per year for his fleet. Moreover, incentives are foreseen for those manufacturers able to produce vehicles with a very low emission level (lower than 50 g/km). The incentive will be proportional to the number of low emitting vehicles, that, depending on the year, will be enumerated as reported in Table 2.5.

Table 2.5. Incentive for those manufacturers able to produce passenger vehicles or vans with an emission level lower than 50 g/km (Source: EEA, 2009).

Passenger Vehicles (1st Stage)	**Passenger Vehicles (2nd Stage)**	**Vans**
3.5 vehicles in 2012 and 2013	2 vehicles in 2020	3.5 in 2014 and 2015
2.5 in 2014	1.67 in 2021	2.5 in 2016
1.5 in 2015	1.33 in 2022	1.5 in 2017
1 from 2016 to 2019	1 from 2023	1 from 2018 onwards

Smaller manufacturers have different targets:

- Manufacturers with a sales volume between 10’000 and 300’000 cars per year, can decide to lower their average emission level of 25% from 2012 to 2019, compared with that of 2007, and of 45% starting from 2020, compared with that of 2007;
- Manufacturers with a sales volume between 1'000 and 10'000 cars per year, can decide to set their own targets, that must be approved by the commission;
- Manufacturers with a sales volume lower than 1'000 new cars per year, or cars manufactured for a special purpose have no mandatory target to respect.

Regarding vans (light commercial vehicles), they represent about 12% of the European light-duty vehicles market and a similar regulation has been set in order to reduce the GHG emissions related with them. The targets are mandatory for those vehicles used to carry goods, weighing up to 3.5 tonnes and less than 2.61 tonnes when empty. Law imposes that the new vans emissions do not exceed more than 175 g CO_2/km by 2017 (average limit). This emission level must be further reduced down to 147 g CO_2/km by 2020 (average limit), corresponding to 5.5 l/100 km of diesel (EC, 2015c).
As for passenger vehicles, penalties are foreseen if the average CO_2 emissions of a manufacturer's fleet exceed its limit value in any year from 2014. The penalty is the same of that for the light duty vehicles.
Also for vans, credits up to a maximum of 7 g/km per year for the fleet will be granted for those manufacturers that equip their vans with innovative technologies. Moreover, if the produced vans have a very low emission level (less than 50 g/km, the same as for passenger cars), each one will be considered as reported in Table 2.5. This incentive is recognized for a maximum of 25’000 vans from 2014 to 2017.
Also in this case, smaller manufacturers have different targets:

- Manufacturers with a sales volume between 1’000 and 22’000 cars per year can decide to set their own targets that must be approved by the commission;
- Manufacturers with a sales volume lower 1’000 have no mandatory target to respect.

Moreover, manufacturers can join together to meet these targets.
Regarding Heavy-Duty Vehicles (HDVs), they represent roughly a quarter of road transport emission and about 5% of total GHG emissions in Europe with a growth of about 36% from 1990 to 2010. To meet the targets for 2050, some actions are necessary. However, up to now, accurate measures and reports from this sector are missing so it is actually not possible to define any goal. Some studies have shown that the current technology level could permit to reduce GHG emissions by at least 30% and this reduction is cost-effective (EC, 2015d). At present, the Commission has developed a simulating tool able to measure CO_2 emissions from new HDVs.
One of the target for the 2020 in Europe is about renewable sources share. By 2020, each EU member state should guarantee that in the transport sector this share would be at least 10% of the total energy used for transportation. The final target is to reduce GHG emissions from this sector by 10%, to be achieved as follows (EC, 2015e):

- 6% by means of biofuels;
- 2% by means eco-innovations;
- 2% by means of CMD credits for flaring reduction not directly linked to EU oil consumption.

As part of these targets, natural gas as vehicle fuel is supported in order to reduce GHG emissions. Biomethane is also considered as a valuable renewable source for air pollution reduction. At present, the current situation about NGV and refuelling stations in Europe is reported in Tables 2.6 and 2.7 for the main countries.

Table 2.6. NGVs situation in the main European countries (NGVA, 2014a).

Country	Total NGVs	Light Duty Vehicles	Buses	Trucks	Other	% in the country	% in the area
Italy	885.300	880.000	2.300	3.000	0	2,16%	77,04%
Ukraine	388.000	19.400	232.788	135.793	19	5,13%	33,77%
Armenia	244.000	192.000	17.300	34.700	0	55,45%	21,23%
Germany	98.172	95.708	1.735	176	553	0,20%	8,54%
Russia	90.050	65.000	10.000	15.000	50	0,25%	7,84%
Bulgaria	61.320	61.000	280	40	0	1,83%	5,34%
Sweden	46.715	43.795	755	2.163	2	0,92%	4,07%
France	13.550	10.050	2.400	1.100	0	0,04%	1,18%
Switzerland	11.640	11.278	173	129	60	0,25%	1,01%
Austria	8.323	8.100	167	54	2	0,16%	0,72%
Total (other 32 countries)	**1.899.602**	**1.427.467**	**275.716**	**195.037**	**1.382**	**0,55%**	**100,00%**

Table 2.7. Natural Gas stations situation in the main European countries (NGVA, 2014a).

Country	All stations	CNG stations	% in the area	L-CNG stations	LNG stations
Italy	1.049	1.040	31,70%	8	1
Germany	920	920	28,00%	0	0
Armenia	345	345	10,50%	0	0
Ukraine	324	324	9,90%	0	0
France	310	310	9,50%	0	0
Russia	253	252	7,70%	1	0
Sweden	213	205	6,30%	4	4
Austria	180	180	5,50%	0	0
Switzerland	141	139	4,20%	1	1
Bulgaria	110	110	3,40%	0	0
Total (other 32 countries)	**4.581**	**4.501**	**100,00%**	**43**	**37**

As it can be seen the share of NGVs in some cases is negligible and a lot of efforts are necessary in order to encourage NGV diffusion. For this reason, several policies have been adopted in Europe to promote natural gas as vehicle fuel. Efforts for NGVs in Europe can be divided in measures concerning the fuel, measures concerning the vehicles and measures concerning the infrastructure.

For the fuel, a reduced taxation was applied for both natural gas and biomethane in order to support their diffusion. In Germany, a reduced tax was set for CNG from 2006 until 2018 (from 31.8 €/MWh to 13.9 €/MWh). This causes a cost saving for NGVs of about 50% and 30%, compared with petrol and diesel. Moreover, to encourage the biomethane production, feed in tariff programmes have been introduced in countries like France and Sweden (NGVA Europe, 2014b).

Measures about vehicles produce mainly benefits for consumers. In fact, consumers can gain subsidies to purchase a new NGV or to substitute a conventional car with an NGV. In Italy, for example, this incentive is up to 1500 € for buying a new NGV or 500 € for converting a traditional car. Several countries adopted this kind of measures with considerable results, like Austria where the incentive is given to those consumers that purchase or convert a traditional car (up to 1000 €) and also to taxies and school buses (up to 3000 €). Other incentives related to the vehicle are about taxation schemes in terms of road taxes, parking fees and so on (NGVA Europe, 2014b).

Regarding the infrastructure, as already mentioned, it is of paramount importance to develop an appropriate refuelling station network. This aspect encourages both consumers' demand and manufacturers' new NGVs models offer. At present two projects are ongoing in this direction:

- The GasHighWay project;

- The LNG Blue Corridors project.

Aim of the GasHighWay project is to increase the use of natural gas as vehicle fuel and promote the upgrading of biogas in order to obtain biomethane to be used in the same way. Moreover, the project wants to create a network of refuelling stations for both natural gas and biomethane distributed on the European territory from the northern regions (Finland) to the southern ones (Italy). The project aims also at spreading the best technologies available for natural gas vehicles and refuelling stations as well as promoting knowledge transfer and support for those companies and organization interested in this field.

On the other hand, the LNG Blue Corridors project regards LNG infrastructure and diffusion. Aim of this project is to create an appropriate infrastructure in terms of "blue corridors" of LNG refuelling stations for heavy-duty vehicles running with liquefied natural gas. Core of the project is the construction of 14 LNG or L-CNG refuelling stations, located in critical points, (corresponding to 4 "blue corridors") and the realization of a fleet of about 100 HDV, running along those corridors.

2.4.2. The Chinese situation

Since the beginning of the century, especially in the last decades, the vehicle annual sales in China has been growing by an unexpected rate. More than 23 million vehicles were sold in China in 2014, making the Chinese auto-market the largest in the world (United Nations Environment Programme, 2015). Consequently, Chinese GHG emissions in transport sector have become the highest in the world, accounting for about 6% of global CO_2 emissions. These emissions are expected to increase more than 50% by 2020 from 2010 levels. Chinese government have set targets for 2020 in order to reduce and control air pollution and, to meet those targets, the emissions growth must be approximately halved.

In 2004, fuel economy standards were introduced by means of fuel consumption standards definition and dividing the vehicle market into 16 classes based on the vehicle mass. Several steps or phases were defined, also differentiating manual transmission (MT) and automated transmission (AT). At present, for the smallest weight class (MT), the consumption target for 2015 was set to be equal to 5.2l/100km. Looking at Figure 2.3 it can be seen in detail the phases targets for each weight class. After the second phase (end of 2011), the third phase began and mandatory average targets based on weight classes were set. These targets foreseen an average fuel consumption equal to 6.9l/100km. By implementing the first two phases a reduction of about 11.5% in fuel consumption were achieved. In 2009, during the second phase, started in 2008, the fuel consumption level was equal to 7.78 l/100 km (180.5 g/km). However, by 2010, this level had risen by 0.6% (7.83 l/100 km), most likely because larger engine and high fuel consuming cars increased their market share (United Nations Environment Programme, 2015). In order to facilitate the achievement of this mandatory emissions level, a fourth phase has been recently released, providing useful guidelines (Figure 2.3).

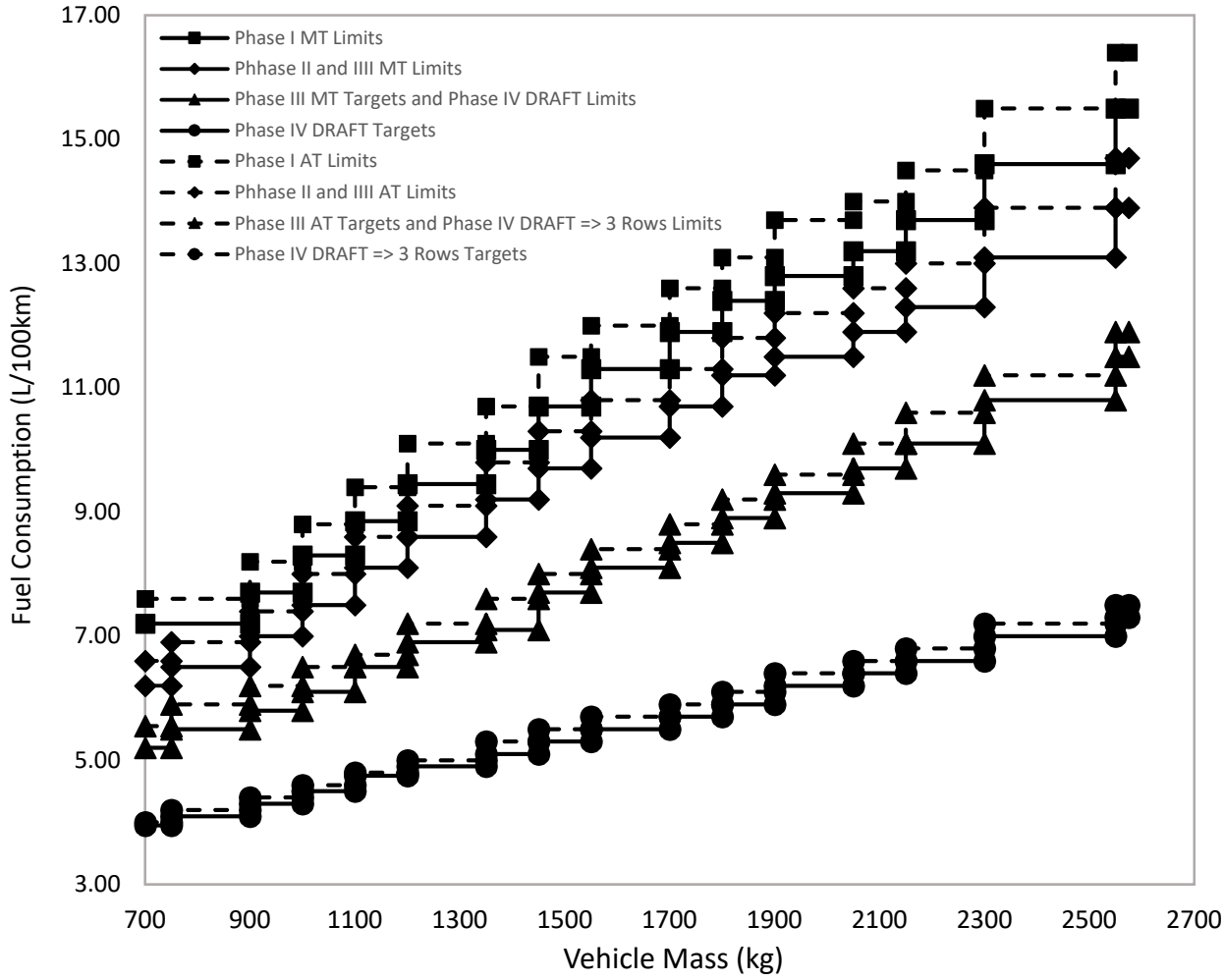

Figure 2.3. China weight-based passenger vehicle fuel consumption limits (Phases I, II and III) for automatic transmission (AT) and manual transmission (MT) vehicles (ICET, 2014).

Moreover, in 2009 gasoline and diesel excise tax was increased, from 0.2 Yuan to 1 Yuan and from 0.1 Yuan to 0.8 Yuan per litre, respectively. Due to the decreasing fuel price during 2013 and 2014, the central government increased the gasoline excise tax up to 1.52 Yuan per litre (United Nations Environment Programme, 2015). In addition, incentive and subsidies are given to consumers in order to encourage the purchase of new-energy vehicles or small engine vehicles. This subsidy is not directly given to consumers but to the manufacturers, who lowers the vehicles price. An additional subsidy is also given to those consumers who purchase a passenger vehicle (any type) with an engine capacity under 1.6 litre, consuming at least 20% less than the government standards (United Nations Environment Programme, 2015).

Table 2.8. Tax rate over the years depending on the engine displacement (United Nations Environment Programme, 2015).

Category by engine displacement (l)	Tax rate prior to 4/1/2006 (%)	Tax rate 4/1/2006 – 8/31/2008 (%)	Tax rate beginning 9/1/2008 (%)
<1.0	3	3	1
1.0 – 1.5	5	3	3
1.5 – 2.0	5	5	5
2.0 – 2.5	5	9	9
2.5 – 3.0	8	12	12
3.0 – 3.5	8	15	25
4.0 and larger	8	20	40

The Chinese law scheme includes also penalties in the form of excise taxes for manufacturers and consumers in order to promote the purchase of vehicles with smaller engines. In Table 2.8, updated excise taxes rate is reported.

It can be seen that taxation for vehicles with small engines was reduced while for vehicles with bigger engines it was increased. For engines in the category 1.5-2 litre, it remained the same.
In the transportation sector, Chinese government needs to improve energy efficiency and to optimize the energy mix by means of electric vehicles and developing the biofuel sector. Regarding natural gas, although its consumptions share represents a small fraction of the total energy consumption, in 2014 its demand has risen up to 180 billion cubic meters per annum. This quantity is about four times the quantity of 2005 and makes China the largest natural gas consumer, behind US and Russia. In 2012 transportation sector represented roughly the 9% of the natural gas consumption and the market continues to grow as a result of Chinese policies to reduce air pollution (Rory, 2015). Moreover, the government wants to reduce the coal and oil consumption in order to increase the alternative fuels share, in particular natural gas (NGVA Europe, 2015).
Natural gas as vehicle fuel has been promoted by means of several pilot projects, aimed at building and developing the infrastructure and the NGV industry. Also, private investments in this way were encouraged, as mentioned in the "Twelve Five-Year Plan". The main efforts of Chinese government consisted in reducing its dependence on natural gas importations. In 2010 this dependence was more than 15%, foreseen to be more than 35% by 2015 (12th Five-Year Plan, 2011). For this reason, in 2012, as part of the "Twelve Five-Year Plan", the National Development and Reform Commission, the Ministry of Finance, the Ministry and the National Energy Board issued the "shale gas development plan (2011-2015)". This plan aims at creating the foundation for the "Thirteen Five-Year Plan", in which a large-scale development of shale gas will take place.
In addition, the 12th Five-Year Plan has set other targets for 2015 about improving infrastructure capacity (gas pipeline length and extensiveness) and gas storage facility for supply reasons. It is foreseen that by 2015 it will be possible to supply roughly 18% of the total population, corresponding to about 250 million people (12th Five-Year Plan, 2011). The implementation mechanism is structured as follow:

- Strengthen coordination and management planning to create favourable conditions for the planning and implementation. Local governments at all levels and relevant enterprises must refine the implementation of the main objectives and priorities defined in the plan;
- Continuous adjustments are required in order to meet the goal of domestic natural gas production practice and international natural gas market. The focus is to protect the security and stability of supply and promote the healthy and the sustainable development of the natural gas industry;
- Formulate the annual implementation plan to guide the various regions and relevant enterprises to work in accordance with national strategic intention and policy and establish the evaluation and reward system to ensure the smooth implementation of planning goals and tasks.

Therefore, the plan has the effect to boost natural gas develop in every sector, included NGVs, with particular attention for HDVs. From 2009 to 2015, buses production tripled, up to 50'000 units, while truck production grew by 50% in just two years. The ENN, one of the largest companies for NGVs in China, said that by the end of 2015 the number of HDVs will rise up to 300'000 units. Also, LNG refuelling stations have been built intensively in recent years. Up to now some companies are planning to build-up more than 1'000 LNG refuelling stations in the next 5 years (NGVA Europe, 2015).
Another aspect of Chinese natural gas policies is the pricing reform. This was partially addressed in the "2007 Gas Policy" and specified more in detail in the "2012 Gas Policy". Important aspects of both documents are reported below (Blumental et al., 2013):

- 2007 Gas Policy: "deepen the pricing reform of natural gas and improve the pricing mechanism, gradually rationalize the ratio between natural gas prices and alternative fuel prices and fully utilize the role of natural gas price in adjusting supply and the demand.";
- 2012 Gas Policy: "**expedite the establishment of price linkage between natural gas price and the prices of alternative fuels, establish and improve the price linkage from upstream to downstream**, encourage the study and implementation of **differential pricing policies including seasonal price and interruptible price** in regions with large fluctuation in gas demand, provide guidance on the reasonable consumption of natural gas, **increase the utilization of natural gas** and support an innovative trading system in connection with natural gas.".

As it can be seen, the "2012 Gas Policy" explains more in detail how natural gas pricing should be reformed.
Finally, reforms in the natural gas sector in China had the consequence to boost the development of natural gas vehicles and refuelling stations. Tables 2.9-2.11 describes the current NGV vehicles and refuelling stations in China and the growth trend in this sector since 2010.

Table 2.9. Natural gas vehicles market comparison between different countries (Source: Li Y., 2015).

Ranking	Country	NGVs (10000)	Refueling stations
1	China	441.4	4455
2	Iran	400	2220
3	Pakistan	370	2997
4	Argentina	248.7	1939
5	India	180	936
6	Brazil	178	1805
7	Italy	88.5	1049
8	Colombia	50	692
9	Thailand	45.7	497
10	Uzbekistan	45	213
Total	**Other 83 countries**	**2274.6**	**26523**

Table 2.10. CNG vehicles and refuelling stations in China over the years (Source: Li Y., 2015).

Year	CNG vehicles (10000)	Annual growth (%)	CNG stations	Annual growth (%)
2010	110	22.2	1800	28.6
2011	148.5	35	2300	27.8
2012	208.5	40.4	3014	31
2013	323.5	55.2	3732	23.8
2014	441.1	36.6	4455	19.4

Table 2.11. LNG vehicles and refuelling stations in China over the years (Source: Li Y., 2015).

Year	LNG vehicles (10000)	Annual growth (%)	LNG stations	Annual growth (%)
2010	1	-	About 100	-
2011	3.8	280	About 200	100
2012	7.5	97.4	More than 600	200
2013	13	73.3	1844	207
2014	18.4	33.5	2500	35.6

As it can be seen, although the Chinese policies are not specifically oriented to natural gas vehicles production and diffusion in terms of infrastructure development, China's growth rate in this field was impressive, making China the first Country in terms of both NGVs and refuelling stations.

2.5. Biogas and Biomethane

As for ethanol and biodiesel obtained from biomass, biogas also represents a valuable biofuel (Table 2.2) which is strongly influencing biofuel market as well as energy and transport sectors. In this section, biogas production processes as well as biogas applications and involved technology are discussed in detail.

2.5.1. Introduction to Biogas

For decades, anaerobic digester systems have been involved in municipal wastewater facilities. In more recent years, AD have been used in order to dispose wastes from industrial and agricultural sectors (Burke, 2001). Main objective of such technologies is to optimize the growth of *methanogenic* bacteria, able to effectively produce CH_4 from biomasses. Looking at the global biogas production process, several sub-processes could be identified as follows:

1. **Manure collection and handling:** this step consists in finding correct amount of water and inorganic solids to be mixed with manure during collection and handling process.
2. **Pretreatment:** pretreatment is highly recommended process prior to the introduction in the anaerobic digester. This step includes screening, grit removal, mixing, and/or flow equalization. It is used in order to adjust the mixture composition in terms of manure and water to fulfill process requirements of related digestion technology. A specific tank is usually used to store manure and process water. Pretreatment

process avoid sands and rocks to be accidentally introduced into the anaerobic digester. Moreover, depending on biomass and digestion technology, it also controls and fix the mixture.

3. **Anaerobic digestion:** consisting in a specific vessel, the anaerobic digester is designed in order to avoid air infiltration, promoting methanogenic bacteria growth. Digesters designs may differ considerably. It could be a simple tank or covered lagoon as well as a tank provided with internal baffles. Its design could also include the possibility of heating or mixing biomass substrates. Type of anaerobic digesters mainly depend on manure characteristics and collection technique. Some configurations also allow reduction in H_2S production, preventing corrosion.
4. **By-product recovery and effluent use:** since gaseous substances are produce by biological digestion, a considerable amount of solid material is produced as biogas process by-product. This material could be used for cattle bedding or to be sold as a soil amendment. Regarding ruminant and hog manure solids, digestion processes usually takes place in a covered lagoon, thus no valuable by-product could be recovered.
5. **Biogas recovery:** biogas is produced during the digestion process. Biogas formation occurs in bubbles to substrate surface, thus, depending on the type of digester, it may accumulate beneath a fixed rigid top, a flexible inflatable top, or a floating cover. Generally, a specific plastic pipe is able to collect biogas to be sent to the gas handling subsystems.
6. **Biogas handling:** depending on the specific application, produced biogas is usually compressed up to the operating pressure in order to be metered. Prior to this, biogas could be processed to remove some contaminants such as H_2S and CO_2. If that is the case, then biogas becomes biomethane. Depending on applications, biogas storage may occur.

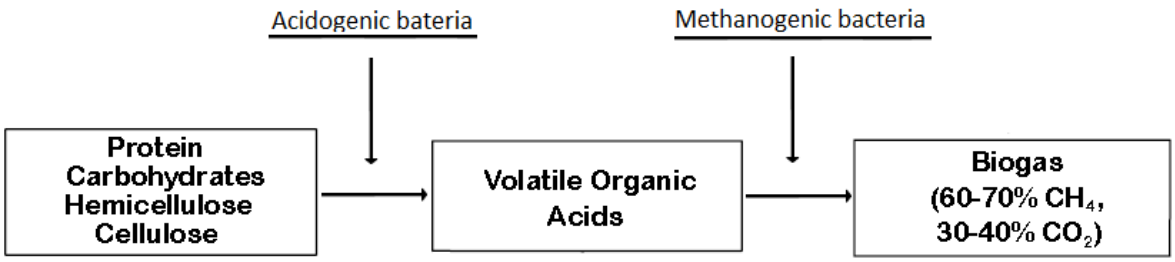

Figure 2.4. Schematic processes involved in biogas production.

Figure 2.4 schematically shows biogas production process. As it can be seen, two main stages are involved in biogas production.
The first stage, accounts for decomposition performed by acidogenic bacteria able to form acids, characterized by fast growth rate. Hydrolysis of protein, carbohydrate, cellulose, and hemicellulose contained in the manure occurs and mainly short-chain fatty acids are formed as well as CO_2 and hydrogen (H_2). Those acids, such as acetic, propionic, and butyric acids. At this stage, the decomposition products are characterized by unpleasant odors coming from produced acids, metabolic products and H_2S. During the second stage, produced acids, together with H_2, are metabolized by methanogenic bacteria. Final result of this process is production of biogas with a variable composition, generally characterized by CH_4 and CO_2 as major compounds, with a volumetric percentage as that reported in Figure 2.5. The methanogenic bacteria present a slow growth rate and temperature sensitiveness if compared with acidogenic bacteria. Typically, such bacteria require an almost constant pH higher than 6, temperatures of about 21-22 °C and something like 15 in order to effectively convert organic acids into biogas. Final biogas composition and efficiency in biomass digestion process strictly depend on adopted technology. A brief description of such processes is given below.

2.5.1.1. Covered lagoon biogas systems

This type of technology is mostly used for liquid wastes with higher organic solved loads digestion. The total solid content is limited to 5 to 7%. Commonly used substrates are liquid manure, palm oil effluents, effluents from starch or from production plants. Figure 4 illustrates a schematic view of the process.

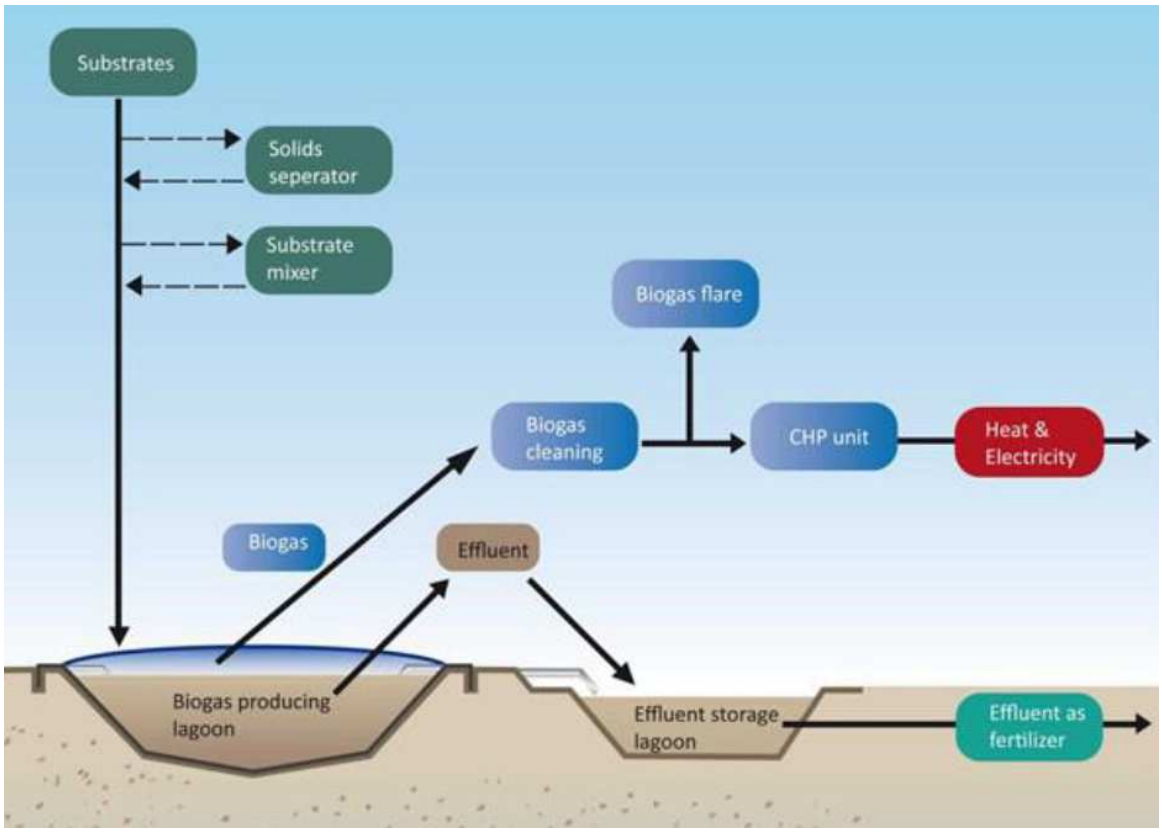

Figure 2.5. Schematic view of the covered lagoon system

Born for agricultural liquid wastes disposal in emerging countries, lagoons usage is mainly linked to high space availability. The lagoon is constructed on site, in many cases without any isolation layer at the bottom. Thus, lagoon will be filled with large quantities of effluent in an aerobic – anaerobic combined treatment. At the upper lagoon level, dissolved oxygen and microorganisms partially decompose the organic matter. Thus, through precipitation and decantation of solids, a bottom layer of organic matter will be built. Consequence of aerobic decomposition consumption of dissolved oxygen, combined with the building of a bottom layer (active settled solids), an anaerobic environment is created in which further decomposition of the organic matter occurs. Therefore, methane will be produced. In recent times, some technical components in order to improve the anaerobic digestion within the lagoon were developed (stirring installation through circulating pipes and pumps, sludge removal through suction pipeline grids, etc.). The effluent is injected into the closed and covered lagoon through a hermetic piping system. Its bottom is isolated through the use of impermeable geo-membranes and it is covered with a gas-hermetic membrane. Suction pipes are built at the bottom of the lagoon, thus the settled sludge is collected. Advantage related with this technology, is that no moving parts of equipment are needed. In case of higher developed lagoons, stirring processes is achieved by means of circulation of the substrates. At different vertical levels, suction and injection pipes allow circulation of effluent ensuring a proper mixture of new and old effluents. An extraction pipe allows the digested effluent to be sent into a secondary, smaller lagoon, where the treated water is used as fertilizer in the field. Produced biogas is conducted through pipelines to a desulphurization and drying modules in order to be burnt into CHP unit. Covered lagoon technology could be used in several climate regions. Being the process an exothermic process an intern heating system in warm regions is normally not. However, it could be required in colder regions.

2.5.1.2. Agricultural biogas plants

Initially, agricultural biogas plants were built in order to dispose liquid manure in cattle farms. At present, agricultural biogas plants are generally related with crops digestion. Considering German biogas plants, maize is commonly used as biomass feedstock due to its high growth rate as well as producible methane. In 2013, in this country, that is leader in biogas production, there existing more than 7,000 biogas plants (Source: Fachverband Biogas e.V. –German biogas association). For this reason, this technology can be considered highly mature. As for common biofuels, major issue related with agricultural biogas plant regarding the possible competition between energy and nutrition related with crops utilization. Moreover, the addition of fertilizers for energy crops cultivation

is also a factor to be considered in the environmental performances. Figure 2.6 shows a schematic view of agricultural biogas process.

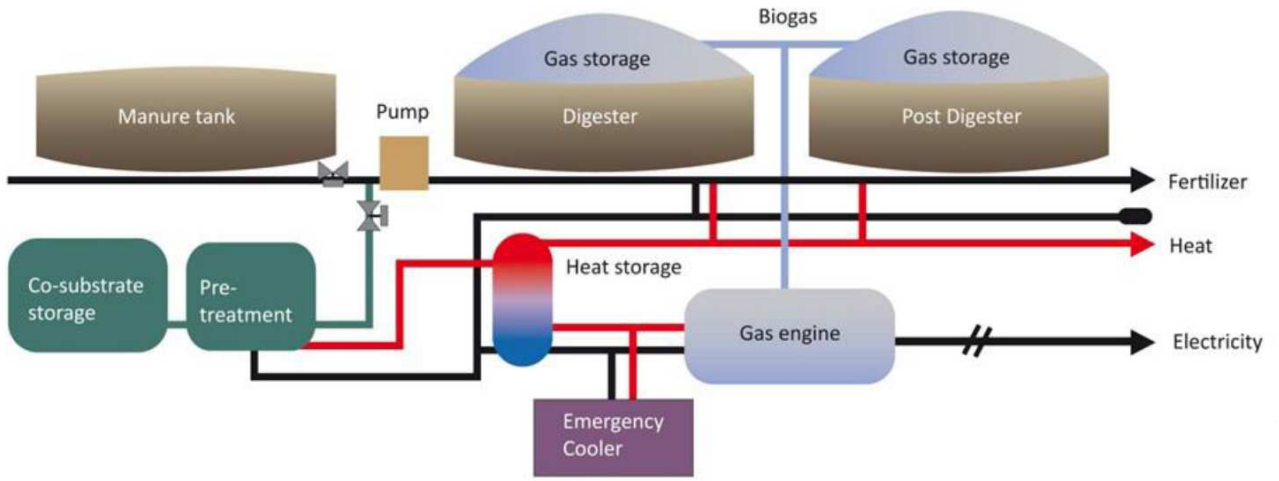

Figure 2.6. Schematic view of the agricultural biogas plant

In the first step, the substrate is pretreated in order to sterilize it, according with local hygienic regulations. During this step, temperatures up to 70°C and resting time of about one hour are required. It is common practice to sterilize only the co-substrate. The pretreatment process allows large potential to optimize the biogas plant. Pretreatment also allows the sorting of substrates in order to reduce the amount of contamination. Generally, those plants are continuously fed. Substrates is stored into a smaller feeding unit with a storage capacities of one day. This allows a constant fermentation process. Part of the heat generated is usually used to provide a comfortable temperature for the mesophilic or thermophilic bacteria. Single or two-stage processes could be found regarding this technology. In two-stage plants, main objective is to maximize the efficiency, taking into account optimal environmental conditions for the microbacterial fermentation process. This is the case of hydrolysis process, which prefers a slightly acidic environment and takes place within a few hours/days. On the other hand, methanogenesis works best in neutral conditions and anaerobic environment, requiring times measured in weeks. In single-stage biogas plants, every biochemical process occurs in the same. By the way, a second reactor for remaining biomass digestion may be required. Produced biogas is generally stored in specific storage units with a capacity of six. The storage system is the hermetic roof over the reactors. Obtained biogas is then cleaned in order to be burned in gas engines, producing electricity and heat. Otherwise, further purification processes allow biomethane production to be injected into the national natural gas grid. Some plants, depending on the substrate used require an additional step before the engine. If produced biogas is used for electricity and heat generation, then a fraction of produced heat is used in order to achieve optimum temperature for the sterilization process as well as for fermentation process. This kind of technology is usually considerably expansive. Building costs related with plant construction are generally related with engine house as well as the substrate storage and additional housing for secondary equipment. Costs are consistently varying from a country to another, thus general estimates could not be easily made. An important and basic principle for the design of biogas plants and corresponding cost estimations is to design the output of the generator sets to exactly match the available amount of substrate and its expected biogas yield, in quality as well as quantity. This makes it possible to achieve an optimum number of operating hours of around 8,000 hours per year.

2.5.1.3. Industrial biogas plants

Industrial biogas plants are represented by high standard levels, as well as used materials, equipment and technologies. It could be said that industrial biogas plants are characterized by more sophisticated control and measurement systems and equipment in order to match with quality requirements. As a consequence, investments related with such plants are generally cost intensive. Moreover, they are design in order to dispose specific wastes and substrates. In industrial biogas plants single or multi stage process are possible. Pretreatment unit is generally not mandatory, depending on waste type. Considering a multi stage, pretreatment equipped industrial biogas plant, hydrolysis, fermenting and storage tanks could be observed, similarly to agricultural processes. Basic biogas purification allows the gas to be burned in a co-generation plant in order to produce electricity as well as heat. Those kind of biogas plants also allow disposal of the environment endangering wastes, gaining additional incomes. Main

industrial biogas plants concerning breweries, alcohol manufacturers, starch from potatoes or wheat manufacturers and sugar manufacturers. At present, the increasing demand for heat and electricity combined with the increasing diversity related with wastes production causes on-site energy generation to increase considerably over other potential applications. Generally, industrial biogas plants are related with large scale plants, due to higher costs and quality standards. Focusing on costs, the pretreatment unit accounts for the major part of them, being feasible for plants with installed electrical capacity higher than 1 MW. Cheaper facilities are generally related with single stage plants.

2.5.1.4. Sludge treatment plants

In order to handle with contaminated waste water, sludge treatment is widely used technology. Mechanical, biological and chemical processes are involved in sewage treatment, with the purpose of producing harmless fluids and solids. The technology strictly requires stabilization of sludges to handle them. This stabilization process occurs in anaerobic reactors, producing a high methane content gas. On-site usage of produced biogas grants covering of consumption related with treatment itself. Consequently, overall sustainability of sewage treatment plants is increased. The first step is to reduce water content. Obtained viscous sludge stream is then stored into large hermetic reactors. After being heated at temperatures up to 38 °C, bacteria begin to grow constantly, enabling the sewage treatment. The sludge is now digested in order to produce biogas to be generally burned in CHP for electricity and heat generation. Generated heat is involved in heating digesters during treatment process. On the other hand, electricity is used in order to cover plant's consumption or to be fed into electrical grid. Criticisms in such plants are related with hydrogen sulphide and water, as well as siloxanes coming from degradation of soaps and other cosmetics. This mixture is highly dangerous being considerably corrosive with plant components, thus avoiding such compounds is mandatory.

2.5.1.5. Solid waste – dry fermentation

In dry fermentation, substrates are generally characterized by water content not higher than 30% being impossible to be pumped. It is the case of household wastes containing plastic materials. In order to allow proper bacteria growth, anaerobic digestion should be achieved with enough water content. However, in dry fermentation process total solid concentrations is usually higher than 15% and water addition is not even necessary. Several processes are available. Batch and continuous process are existing in single or double stage configuration, able to work in both mesophilic and thermophilic temperature ranges. Batch operations are stable and simple processes being independent on specific feeding facility. Moreover, batch operation prevents substrate streams to leave the reactor after short residence time. Since homogenous substrate is achieved, its structure enabling percolate infiltration, thus high digestion rate is possible. In order to activate the anaerobic process, percolate re-circulating from the bottom to the upper surface's digester by means of sprinklers is necessary practice. Batch processes are generally involved in small size unit up to 150 m3. Regarding continuous dry fermentation processes, charging and extraction system is required. Moreover, mechanical or hydraulic substrate mixing equipment is needed. This kind of process is generally involved in large scale unit, up to 2,000 m3.

2.5.1.6. Environmental Impacts of Anaerobic Digestion

The environmental impacts of anaerobic digestion processes depend on several factors. By the way, manure management system and produced biogas utilization are major items. Regarding biogas application, flaring, combustion electricity and heat generation, or biomethane production causes environmental benefits. In particular, GHG and volatile organic compound (VOC) emissions reduction, pathogen generation control and water quality improvement are linked with biogas production and overmentioned applications. However, NO_X production during biogas combustion could be a critical point, causing high air pollution. This compound is generally produced during combustion of methane gases, thus including NG. Its emission rate depends on several factors, however properly engineered flares are able to decrease its formation while rich burn piston engines are responsible for higher nitrogen oxides emissions. At present, catalytic controls as well as microturbines are able to handle with NO_X. GHG reduction by means of biogas could be achieved in two distinct ways. The first one regards manure management system. In fact, storage of manure in anaerobic conditions prevents methane losses to be released in the atmosphere,

being CH_4 highly dangerous GHG. The second one is related with traditional fossil fuel combustion reduction. Thus, replacing those fuels with biogas and biomethane, GHG emissions reduction could be achieved. Regarding the first point, as already mentioned in Chapter 1, burning biogas avoids methane releasing in the atmosphere. At present, CH_4 constitutes 22% of anthropogenic GHG emissions globally. USA methane pollution accounts for about 10% for both anthropogenic and animal manure sectors (US DOE, 1999b, pp. 6, 13-14). Since each unit of CH_4 corresponds to 28 units of CO_2, by using methane as combustion fuel 28 units of GHG are replaced by 1 unit only. This benefit will occur as long as the methane is combusted, making biogas and biomethane highly environmental friendly gases. Volatile organic compounds combined with NO_X produce ozone, that is the primary air pollutant element. Regarding biogas plants, VOCs are generated by methanogenic bacteria during manure transformation into biogas. It was seen that the more effective the methanogenic decomposition, the lower the VOCs. Those compounds are formed by means of enteric fermentation and released primarily through the cow's breath. Of course, this compound is also produced during biogas production process. By proper biogas plant designs, it is possible to heavily reduce VOCs formation, consequently increasing methane production. Moreover, remaining fraction is eliminated during biogas combustion. NO_X emissions are produces by any fuel during combustion process into engines. This is mainly related with high temperature levels. Regarding reciprocating engines, maximum formation of such gas is mainly related with slightly lean fuel mixtures. It was seen that turbines generally are responsible for less NO_X generation than reciprocating engines. In biogas production plant for electricity and heat generation, reciprocating engines are generally involved. By the way, a properly engineered flare gas system will cause lower NO_X levels than traditional reciprocating engines, thus decreasing overall GHG emissions. Moreover, lean-burn engines are able to achieve even lower nitrogen oxides emissions, therefore since enough biogas is supplied to reciprocating engine NO_X generation can be kept to very low levels. The Inland Empire Utility Agency in Chino, California uses from 0.7 to 1.4 MW engines for electricity and heat generation from biogas, producing less than 50 ppm of NO_X (Clifton, 2004). At present, several catalytic conversion technologies allow NO_X generation control, however biogas impurities substantially shorten their life. In order to avoid this issue, H_2S biogas content must be decreased as much as possible. By purifying biogas to biomethane, corrosion associated with such impurities is completely avoided and, since methane content is much higher than simple biogas, GHG emissions are further reduced. Regarding pathogens associated with substrates degradation, in AD with mesophilic and thermophilic temperature levels pathogen reduction greater than 99% could be achieved.

2.5.2. Biogas Potential in European and Chinese Context

2.5.2.1. European situation

As one of the European targets, by 2020 at least 20% of the total energy consumption must be from renewable sources. At present, biomass represents the renewable energy source mostly used in Europe and biogas has an important role. In 2014 more than 15'000 biogas plants were existing with an equivalent installed power of about 8000 MW (Stambasky, 2015). In Figure 2.7 the European biogas plants distribution is reported for 2013. Moreover, more than 300 biomethane plants exist, accounting for about 1 billion cubic meters of biomethane produced (Stambasky, 2015). Some studies indicate that the biogas potential in Europe is still largely unexploited and this sector is expected to grow more and more in next years. Table 2.12 shows the biomethane technical potential for each biomass resource.

Table 2.12. Biomass feedstock and biomethane potential in Europe (Source: Stambasky, 2015)

Biomass resource	**Potential**	**Percentage**
Woody biomass	66 billion cubic meters	43.7%
Herbaceous biomass	11 billion cubic meters	7.3%
Wet biomass residues	26 billion cubic meters	17.2%
Energy crops	48 – 143 billion cubic meters	31.8%
Total	**151 – 246 billion cubic meters**	**100%**

In future, the use of biogas is expected to grow considerably and is foreseen that by 2030 the 30% of the technical potential will be reached (15% within 2020). Moreover, biomethane share on biogas production is expected to pass from 2% in 2010 to 26% by 2020 and up to 37.5% within 2030. Consequently, the biomethane share on total natural gas will grow from 3% in 2010 to 5% by 2020 and up to 8% within 2030 (Stambasky, 2015).

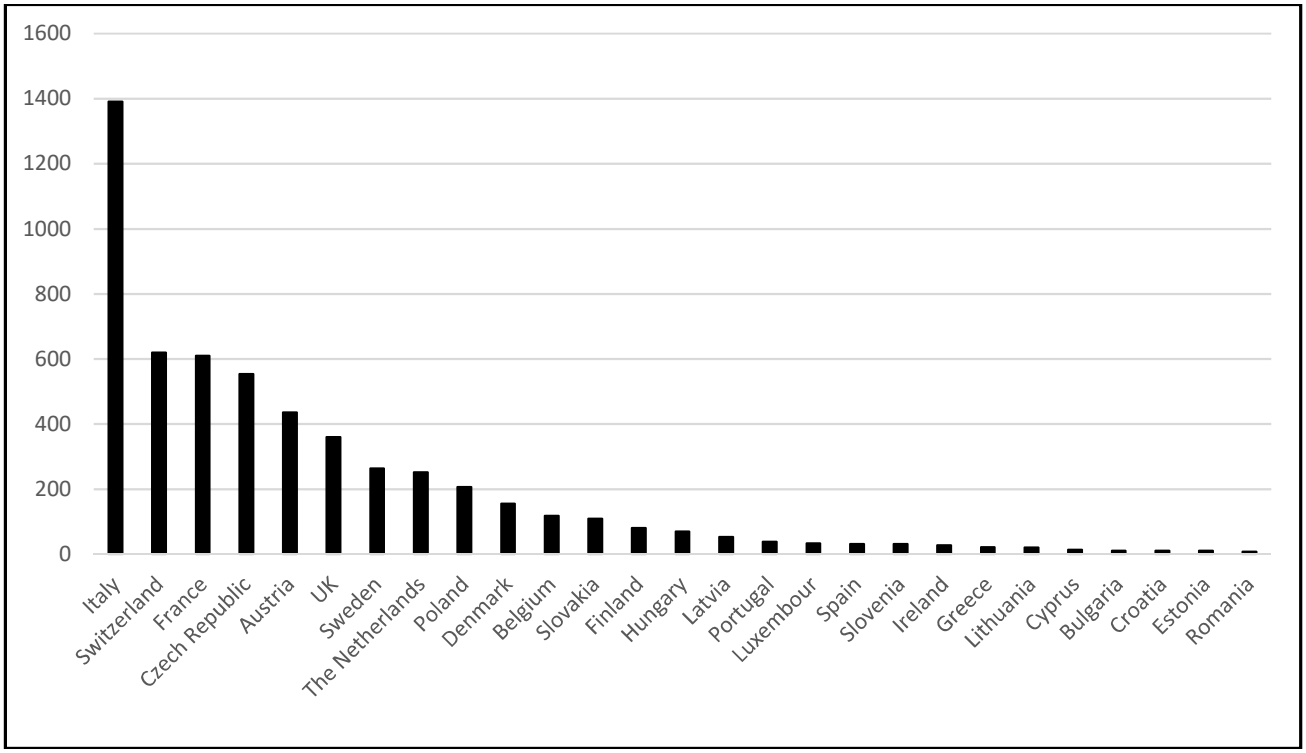

Figure 2.7. European biogas plants distribution by country. Germany has 9000 plants, not represented (Source: Stambasky, 2015)

2.5.2.2. Chinese situation

In China, as well as in Europe, biogas production represents an important sector and here the first biogas plant in the world was built at the end of the 19th century (Deublein and Steinhauser, 2008). Biogas produced from anaerobic digestion is very important and it comes also from domestic production with more than 30 million household digesters (**Jyothilakshmi and Prakash, 2015**). As part of the 12th Five-Year Plan (2011), the Chinese government is increasing its investments in this sector and biogas infrastructure is growing rapidly. One reason for that is the fact that biogas potential in China is very high. In Table 2.13 biomass feedstock and biogas production achievable are reported (Bischoff, 2014).

Table 2.13. Biomass feedstock and biogas potential in China (Source: Bischoff, 2014)

Biomass	Quantity	Biogas achievable
Agricultural straw	700 million tons (50% can be used)	100 billion cubic meters
Animal waste and wastewater	3 billion tons	108 billion cubic meters
Industrial waste and wastewater	2.7 billion tons	11 billion cubic meters
Organic municipal solid waste	77 million tons	9 billion cubic meters
Municipal sewage sludge	2.11 million tons	2 billion cubic meters

As it can be seen, biogas potential from waste material is about 230 billion cubic meters per year corresponding to a biomethane potential of about 150 billion cubic meters per year. Therefore, biomethane in China can play a significant role in both energy production and vehicle fuel market.

2.6. Biomethane from Biogas Methane Enrichment

As already said, biogas, compared to fossil fuels, is able to reduce GHG emissions using locally available sources. Moreover, by-product of biogas production process, namely digestate, is a high-value fertilizer in crop cultivations able to replace common fertilizers. Germany is the major biogas producer worldwide, with approximately 25% total installed capacity. This is mainly due to the strong development of agricultural biogas plants on farms. Up to 2014,

more than 8000 agricultural biogas production plants were operating in such country. Several other countries, such as Italy, have already developed new pathways for biogas production using biomasses and biological wastes. Many European countries have established specific incentive schemes for electricity production using biogas. Biogas represents a renewable energy source characterized by a high CH_4 levels. The composition of biogas is strictly related with carbon oxidation–reduction state of the specific biomass present in the waste and the type of anaerobic digestion process (Jonsson et al. 2003). Biogas is a complex mixture composed by several compounds. Table 2.14 shows some insight regarding this point. As it can be seen, biogas produced in landfills is substantially different compared to that of anaerobic digestion based biogas.

Table 2.14. (Jaffrin et al. 2003; Persson et al. 2006)

Constituents	**Composition [% mol]**			
	Biogas (landfills)	**Biogas (AD)**	**Biomethane**	**Wet NG**
CH_4	35-65	53-70	≥ 95	84.6
CO_2	15-50	30-47	≤ 3	≤ 5
H_2	0-3	0	0	0
H_2O	0-5	5-10	0	0
N_2	5-40	0.3	0	≤ 10
O_2	0-5	0-1	≤ 0.6	0
H_2S	0-0.01	0-1	≤ 0.4	≤ 5
NH_3	traces	Traces	0	0
Heavy Carbons	0.002-0.02	0-0.02	0	15.4
Siloxanes [mg S /m^3]	0-50	0-41	0	0
LHV [MJ/Nm^3]	**16**	**23**	**36.1**	**39**

Carbon dioxide and nitrogen represents major contaminants of biogas decreasing its lower heating value (LHV) and therefore its Wobbe index (Ryckebosch et al. 2011). O_2 contaminant in the biogas could causes explosion hazards, while too high H_2S levels, combined with H_2O contaminant, causes high corrosion risks in every associated biogas component compressors, pipelines, gas storage tanks and engines. Similarly, NH_3 and hydrocarbons generate corrosive products during combustion able to damage engines and its pipelines (Petersson and Wellinger 2009). Finally, siloxanes combustion generates silicone oxide causing deposits in biogas combustion engines and valves. As a consequence, abrasion, overheating and malfunctioning issues occur (Abatzoglou and Boivin 2009). Biogas is used in a wide range of applications. It has been mostly used as a combustion fuel in order to achieve on-site heat, steam and electricity generation in industry. Moreover, it finds application also as a substrate in fuel cells, as well as for domestic and industrial use instead of NG. Finally, injection into national natural gas grids and transport sector are emerging and growing biogas applications (Rasi 2009; Andriani et al. 2014). In Europe, biogas production accounts for more than 13.4 million tons of oil equivalent equal to 52.3 TWh of electricity and heat generation. Heat from biogas combustion is sold to district networks, accounting for more than 432 megatons of oil equivalent (EurObserv'ER 2014). Moreover, further improvements in European AD network, actually of about 14.000 plants, are foreseen with a total produced volume of about 18–20 million m3 within 2030, representing roughly 3 % of total EU gas consumption (European Biogas Association 2013). Depending on biogas final utilization, required composition may vary considerably. Onsite biogas for heat generation purposes only requires H2S removal with a final content not higher than 1000 ppmv as well as simple water removal process before combustion (Bailo´n and Hinge 2012). Combustion engines for combined heat and power generation usage, requires water, and H2S, NH3, siloxanes and halocarbons removal processes to achieve compounds content to be in a range of 200–1000 ppmv, 32–50, 5–28 and 65–100 mg m-3, respectively. Final biogas purity is strictly dependent to involved process. On the other hand, turbines and micro-turbines for CHP generation very low levels of about 0.03–0.1 ppmv for siloxane content and pressurized dew point of at least -6.7 °C for water content. By the way, such technologies allow 10,000–70,000 ppmv of hydrogen sulfide as well as 200–1500 ppmv Cl/F of halocarbon (Soreanu et al. 2011). Looking at potential application of biogas, those related with transport sector as well as injection into the national gas grid present the highest quality requirements. Biogas produced to such purposes are called biomethane. Its final composition and ranges of major compounds are reported in Table 2.14. Processes involved in biomethane production are generally more complex and cost-intensive if compared with technologies related with biogas applications abovementioned. Such techniques are commonly characterized by high energy or chemical requirements as well as complex plants and thermodynamic or chemical reactions involved in. Next section provides detailed description of major biogas contaminants, characterized by CO2, H2S, H2O and associated available removal processes. Table 2.15 and Table 2.16 provides further information relating with efficiency and operative conditions as well as operative costs.

2.6.1. H_2O removal process

At present water biogas content is removed by means of physical / chemical process, being the only available technology to this purpose (Rutledge 2005). Water adsorption process is able to achieve -40 °C dewpoint in biomethane by means of pressurized columns (6–10 bar). Adsorbent materials are generally silica, alumina, magnesium oxide or activated carbon. The process requires two columns which operates in parallel. This method allows water adsorption and materials regeneration by increasing and decreasing pressure levels. High investment costs are generally associated with the process. However, it is characterized by low operating costs. Absorption technique process is able to achieve -15 °C biomethane dewpoint by means of glycols, which require regeneration temperatures up to 200 °C. The technique also allows oil and dust removal requiring high operating and investment costs associated with temperature and pressure levels and involved materials respectively. As a consequence, high biomethane flow rate up to 500 m^3/h is required in order to make the process sustainable (Ryckebosch et al. 2011). By using hygroscopic salts instead of glycols, high efficiency can be achieved but still high associated costs were found, being such material not regenerable (Persson et al. 2006). Finally, cooling of biogas at atmospheric pressure allows subsequent water separation by condensation. The low costs associated with such process is characterized also by low efficiencies of about 0.5 °C dewpoint in order to avoid water freezing. Biomethane compression could increase efficiency down to -18 °C (Ryckebosch et al. 2011).

2.6.2 H_2S removal processes

When referring to H_2S removal processes, common name of such technologies is desulphurization processes. In this section, commonly used desulphurization technologies are briefly described.

2.6.2.1. In-Situ Precipitation Process

The in-situ precipitation desulphurization process allows H_2S control formation during anaerobic digestion of substrates. It consists in adding some specific substances directly into the digester. Those substances are $FeSO_4^2$, $FeCl_3$ and $FeCl_2$. Chemical reactions occur, thus hydrogen sulphide in biogas content is limited by means of insoluble FeS salt (Petersson and Wellinger 2009;). It is generally recommended for those plant presenting a high H_2S level, being unfeasible in a cost-efficient point of view. This is mainly due to the fact that a storage tank and appropriate pumps are necessary equipment. Moreover, costs associated with chemical reagents purchase negatively affect overall operating costs (Tomas et al. 2009).

2.6.2.2. Adsorption Process

Involving two parallel adsorbent modules, this technology operates by means of Fe_2O, ZnO, $Fe(OH)_3$, or activated carbon. The process is an adsorption-regeneration process. Main issues associated with the technology regards regeneration and material costs, thus limiting its usage to small-scale applications (Abatzoglou and Boivin 2009). Main characteristics of adsorption process are related with simplicity, high efficiency and fast oxidation (Petersson and Wellinger 2009). Residence time is ranging from 1 to 15 minutes. Due to heat generation during material regeneration, auto-ignition may occur. High operating costs of about 0.021–0.037 €/m^3 are associated with the process while investment cost of about 120 to 640 €/$(m^3/h)^{-1}$ is required. Costs related with activated carbon material purchase are of about 0.0005 – 0.0037 €/kg (Abatzoglou and Boivin 2009).

2.6.2.3. Absorption Process

In absorption process, conventional gas–liquid contactors are generally involved, using water or organic solvents. The process could be both physical or chemical depending on used substance. Water allows single pass as well as absorption – desorption processes. Regarding organic solvents, regeneration is strictly required, with high associated costs (Ryckebosch et al. 2011). Selexol is generally used as organic solvent in such

This technology is suitable for low hydrogen sulfide concentrations or combining it with carbon dioxide removal (Wellinger and Lindberg 1999). Adding scrubbing materials to the process can increase overall efficiency. Commonly used materials are NaOH, $FeCl_2$, $Fe(OH)_3$ and more complex compounds. Considering a full process using NaOH and H_2O_2, high efficiency could be achieved with an operating cost of about 0.03 €/m^3 (Miltner et al. 2012).

2.6.2.4. Membrane Separation Process

Based on the selective permeability of specific materials to H_2S, CH_4 retention is guaranteed. The process is not highly efficient, however it could be improved by means of alkaline liquids (Ryckebosch et al. 2011). Main disadvantage of the process is related with high pressure requirements, with biogas pressures ranging from 25 to 41 bar.

Table 2.15. Performances of the described desulphurization technologies

Process	H_2S final content	Removed H_2S [vol]	Costs [€/m^3]	Requirements
In-situ	100-150 ppm	-	0.024	Chemicals
Adsorption	1 ppm	95%	0.021-0.037	Material regenerations
Absorption	1-10 ppm	90-100%	0.03	High temperatures
Membrane	-	58-94%	-	Specific membranes

2.6.3. CO_2 Removal Processes

At present, several carbon dioxide removal technologies are able to efficiently enrich methane content in biogas up to biomethane levels. When talking about CO_2 removal process, common name of such technologies is upgrading processes. In this section, available and mature upgrading technique are briefly described.

2.6.3.1. Water Scrubbing Process

In those plants, water is used in order to selective absorb carbon dioxide from biogas flow, being CO_2 solubility 26 times higher than that of CH_4 in aqueous substrates (Sinnott 2005). Accounting for roughly 41% of global upgrading units, water scrubbing process is a mature technique. By involving simple water, less sensitivity to biogas impurities is guaranteed. Moreover, the process is characterized by high simplicity, allowing single-pass configurations with water pressures up to 10 bar (Tynell et al. 2007). By the way, most recent plants are generally equipped with a second stage in order to achieve water regeneration. Water requirements are strictly related with water temperature and pressure levels. Related investment costs range from 5500 €/m^3 to 2500 €/m^3 for biogas flow rate ranging from 100 Nm^3/h to 500 Nm^3/h. Operation costs are in a range of 0.11 – 0.15 €/Nm^3, mainly related with biogas and water compression and water cooling (Urban et al. 2009; Bauer et al. 2013).

2.6.3.2. Organic Solvent Scrubbing Process

The process is similar to water scrubbing process, using organic solvents instead of water. Most commonly used solvents are glycol-based solvents, such as Selexol or Genosorb, which are characterized by high CO_2 absorb capacity. Being highly affine with carbon dioxide, smaller plants footprint are achievable, thus investment costs are reduced. A first step in which water and other minor impurities are further removed is necessary, at temperatures up to 40 °C. During the second step, temperature is cooled down to 20 °C, thus absorption process take place. Main disadvantage of the technology is represented by high sensitivity to H_2S, thus a desulphurization process is highly recommended. Investment costs are in the range of 4500 €/m^3 to 2000 €/m^3 for biogas flow rate of 250 Nm^3/h to 1000 Nm^3/h respectively (Bauer et al. 2013).

2.6.3.3. Chemical Scrubbing Process

Similar to organic solvent scrubber, this technology involves alcanol amines or alkali aqueous solutions as absorbent substances (Andriani et al. 2014). Structure of the plant regards an absorption, a desorption and a reboiler units. Process configuration is generally simpler than that used in water and organic solvent scrubbing processes. Pressure levels are considerably low, ranging from 1.5 to 3 bar, giving the process to be low energy-intensive (Patterson et al. 2011). Moreover, very high efficiency levels are achieved (Ryckebosch et al. 2011; Bauer et al. 2013). At present, this technique presents a share of about 22% globally related with other upgrading systems (Thran et al. 2014). Investment costs related with this technology ranging from 3200 €/m^3 to 1500 €/m^3 for biogas flow rate from 600 Nm^3/h to 1800 Nm^3/h respectively (Bauer et al. 2013). Regarding operative requirements, main consumptions were found relating with biogas and liquid compressions as well as amine regeneration process, which accounts for the great part (Gunther 2007; Beil 2009; Bauer et al. 2013).

2.6.3.4. Pressure Swing Adsorption Process

Pressure swing adsorption, namely PSA upgrading process, accounts for a share in upgrading market equal to 21% globally (Patterson et al. 2011; Thran et al. 2014). The process involves high specific surface area materials able to effectively adsorb carbon dioxide by means of average pore diameter. Such materials are commonly activated carbon or alumina, zeolite, silica-gel and polymeric sorbents (Patterson et al. 2011; Ryckebosch et al. 2011). Several vertical columns are packed with such materials. Since adsorption process takes place in 4 steps, at least 4 columns are required. These phases consist in pressurization, feed, blowdown and purge. Pressurization column generally is characterized by pressures up to 10 bar. The removed carbon dioxide is generally vented into the atmosphere after regeneration. High efficiencies could be achieved by means of PSA, by the way the process is hydrogen sulfide sensitive, thus a pretreatment is recommended. Investment costs related with this technology ranging from 2700 €/m^3 to 1500 €/m^3 for biogas flow rate from 600 Nm^3/h to 2000 Nm^3/h respectively (Bauer et al. 2013). Associated operative consumptions are related with biogas compression and electricity (Persson 2007; Beil 2009).

2.6.3.5. Membrane Separation Process

As for desulphurization process, membrane upgrading system is able to remove carbon dioxide by means of specific materials through a selective permeation process. Membrane materials are generally polymeric materials, presenting lower costs and high-pressure resistance. High biogas pressures are generally required in order to achieve good purification level, ranging from 6 bar to 40 bar (Bauer et al. 2013). At present, it is a mature technology, with a share in upgrading market of about 10% globally (Patterson et al. 2011; Thran et al. 2014). Main advantages of this technique are related with several compounds removal ability as well as its simple configuration. During the process, CO_2, O_2, H_2O and H_2S are removed (Ryckebosch et al. 2011). Several configurations are allowed. Sigle-pass or multi stage membrane with recirculation are available configurations for gas to gas units. Regarding gas to liquid units, fluids are in a counter current mode at atmospheric pressure (Ryckebosch et al. 2011). Depending on plant configuration, materials and pressure levels, upgrading performances could vary considerably from 92% to more than 99% (Andriani et al. 2014). Investment costs related with this technology ranging from 2500 €/m^3 to 6000 €/m^3 for biogas flow rate from 400 Nm^3/h to 100 Nm^3/h respectively (Bauer et al. 2013). Associated operative consumptions are related with biogas compression and membrane replacement (Bauer et al. 2013).

2.6.3.6. Cryogenic upgrading

In common cryogenic upgrading systems, different liquefaction and solidification temperatures related with biogas compounds are considered in order to achieve impurities separation. It is not the case of those compounds having a liquefaction temperature lower than that of methane, such as oxygen and nitrogen. Biogas flow is compressed up to 10 bar and then cooled down into several steps in which specific compounds are removed. Thus, -25 °C, -55 °C and -85 °C cooling temperature allows H_2S, CO_2 and remaining CO_2 removal, respectively (Ryckebosch et al. 2011). By the way, most common cryogenic units require biogas pressure to be increased up to 80 bar by means of a multi-stage intercooled compressor (Patterson et al. 2011; Ryckebosch et al. 2011). Being high energy intensive, cryogenic upgrading technology is still in a developing phase, thus its global share is of about 0.4% globally.

Table 2.16. Performances of the described upgrading processes

Process	CH_4 [%]	Lost CH_4 [%]	Costs [€/m^3]	Requirements	Global share
Water scr.	95-96	1-2	0.11-0.15	10-20 bar	41%
Organic scr.*	96-98	2	0.14-0.18	Chemicals	5%
Chemical scr.*	99-99.9	<0.05	0.16-0.17	120-150 °C	22%
PSA	96-98	2	0.06-0.07	4-10 bar	21%
Membrane*	96-98	0.5-1	0.13-0.22	6-20 / 20-40 bar	10%
Cryogenic	97	2	0.4	80 bar / -110 °C	0.4%

*H_2S sensitive

2.7. LBG Feasibility: an Italian Case Study

In order to investigate the Italian scenario for LBG, three different business models were considered. For each case, the LBG fuel chain was analysed and every phase of LBG production was studied in detail. Such phases regard: 1) biogas production and upgrading, 2) compression and transportation (if necessary), 3) LBG production, 4) LBG vehicles refuelling. The best technological configuration was considered and the LBG production costs for every phase were evaluated. The business models considered are the following:

i. One owner for all the chain (Figure 2.8a);
ii. Two different owners, one for the biogas production and upgrading phases, another one for the LBG production and vehicles refuelling phases (Figure 2.8b);
iii. Five biogas producers that agreed to build up together a liquefaction facility, sharing investments and revenues (Figure 2.8c).

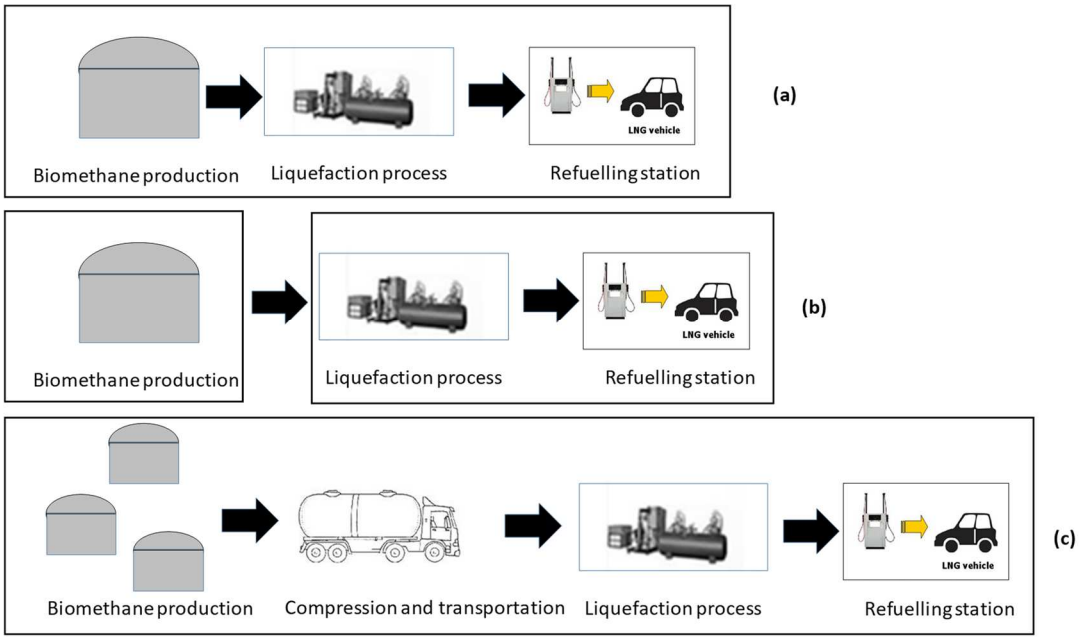

Figure 2.8. Considered business models.

The Italian incentive scheme is considered and its minimum value to make each business model economically feasible was assessed. A sensitivity analysis by varying the possible incentives value and the incidence they have on LBG production cost was also performed.

By the current Italian law regulation, the disposal of organic waste in landfills is no longer allowed. For this reason, only biogas from anaerobic digesters is taken into account in this analysis. As already mentioned, raw biogas cannot be directly used as a source of feedstock gas and an upgrading process is necessary in order to remove CO_2 and other minor components. In this work, a biogas composition of 53% CH_4 and 47% CO_2 was considered.

At present, PWS is one of the cheapest and simplest technology (Nie et al., 2013), and the most common upgrading process. Thus, it was considered in this work.

In Italy, the typical biogas plant size is 500 $Sm^3 \cdot h^{-1}$. This production rate corresponds to about 250 $Nm^3 \cdot h^{-1}$ of biomethane after the upgrading process. During this phase, a 6% volume loss during the process was taken into account (Warren, 2012).

2.7.1. Biomethane compression and transportation

This phase is present only in the third business model considered. It is necessary to compress the biomethane produced in the digester up to 20 MPa, thus it can be transported from the digesters to the liquefaction facility by means of trucks with a stack of 20 cylinders for CNG. A compression station of about 67 kW is installed at every biomethane production plant.

2.7.2. LBG production

Analysing the first two business models, the biomethane flow rate available is enough to supply a 10'000 litre/day liquefaction plant. On the other hand in the third scenario five biogas producers were considered, thus the size of the liquefaction plant is of about 60'000 litre/day. For these sizes, the capital cost of the liquefaction plant must be as low as possible (Arteconi et al., 2011). To this purpose a triple pressure Linde cycle (Walker, 1983) was considered both for its efficiency and simplicity. In Figure 2.9 a schematic of this system is shown.

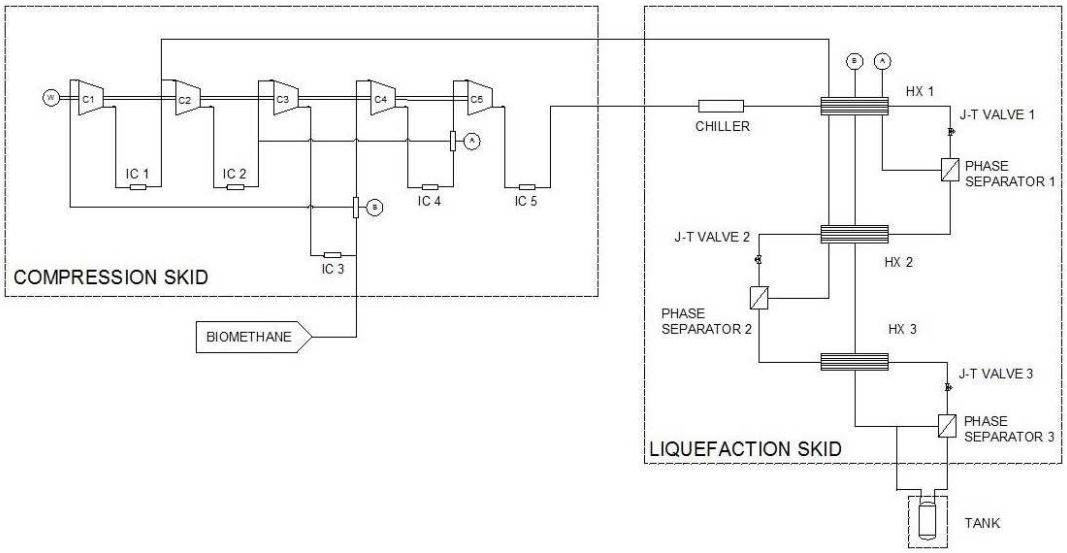

Figure 2.9. Schematic of the liquefaction cycle (Arteconi et al., 2015).

The thermodynamic analysis of the cycle was performed by means of a steady-state model simulated with the software EES (Klein, 2013). In the first two business models considered the biomethane from the PWS has an inlet pressure of 0.5 MPa, while in third scenario where it is compressed and transported an average inlet pressure of 7 MPa is assumed. In order to reach the quality requested for liquefaction, the inlet biomethane needs to be further purified by means of a molecular sieve, before entering the liquefaction plant. It is compressed up to about 20 MPa. Inter-refrigerated compression stages were considered to decrease compressed methane temperature down to 40°C. A vapour compression chiller allows to achieve a pre-cooling temperature of -25°C before the main recuperative heat exchanger. Eventually the gas is liquefied through the throttling process by means of Joule-Thomson (JT) valves in three different stages (final pressure 0.5 MPa). Further details are provided elsewhere (Arteconi et al., 2015). In Table 2.17 a summary of the energy performance and efficiency of the liquefaction cycle are reported.

Table 2.17. Energy performance of the liquefaction cycle.

Liquefaction plant components	10'000 litre/day	60'000 litre/day
Compressor power	85 kW	440 kW
Chiller electrical power	15 kW	77 kW
Air cooler max power	3 kW	15 kW
Auxiliaries	10 kW	45 kW
Mole sieve	20 kW	50 kW
Total power	133 kW	627 kW
Efficiency	0.78 kWh·kg^{-1} $_{LNG}$	0.73 kWh·kg^{-1} $_{LNG}$

2.7.3. Refuelling

For refuelling phase, a L-CNG station was considered, that allows to refuel both LNG and CNG. Depending on the business model considered, a 10'000 or 60'000 litres storage tank is necessary. The LNG is then pumped from the storage to the onboard tanks.

3.2. LNG market and incentives scheme

In order to evaluate the feasibility of liquid biomethane as vehicle fuel, a selling price for LBG on the market was assessed. In a previous study (Arteconi et al., 2012) it was estimated that it should be lower than 60% of the fuel price to be replaced (diesel). Thus, a price of 1 €·kg^{-1}of LBG (taxes excluded, i.e. 0.39 €·litre^{-1}) was considered to be the retail price.

The Italian incentive scheme for biomethane is pretty complicated and the incentive value itself depends on the following aspects: (i) the type of feedstock used in the biogas production (waste/by-products or dedicated biomass), (ii) which is the final purpose of the biomethane produced (vehicle fuel, gas injected into the grid...) and whether the plant is new or not. Moreover, for biomethane used as vehicle fuel, it is also important to know if the owner of the biogas plant is the same owner of the refuelling station. In Table 2.18 the incentive scheme for biomethane as vehicle fuel is reported. It can be seen that the incentive grows with the by-products percentage, reaching its maximum with 100% by-product biomass. The incentive lasts for 20 years and after the first 10 years there is no longer a distinction based on the ownership of the LBG refuelling station. If the biogas plant is already existing the incentive is recognized for the 70% of the correspondent value for new plants.

Table 2.18. Summary of the Italian incentives scheme for biomethane from digesters.

Feedstock composition	Number of CIC			
	New plant		Existing plant	
	Sold to others refuelling station	Own refuelling station	Sold to others refuelling station	Own refuelling station
By – products* < 70%	1	1 · 1.5 (1st÷10th year) 1 (11th÷20th year)	1 · 0.7	1 · 0.7 · 1.5 (1st÷10th year) 1 · 0.7 (11th÷20th year)
By – products* ≥ 70%	1.7	1.7 · 1.5 (1st÷10th year) 1.7 (11th÷20th year)	1.7 · 0.7	1.7 · 0.7 · 1.5 (1st÷10th year) 1.7 · 0.7 (11th÷20th year)
By – products* = 100%	2	2 · 1.5 (1st÷10th year) 2 (11th÷20th year)	2 · 0.7	2 · 0,7 · 1,5 (1st÷10th year) 2 · 0.7 (11th÷20th year)

CIC: base incentive (€/10 Gcal biofuel)

This type of incentive was introduced to promote the substitution of fossil fuels with biofuels as indicated by the EU directive that aims at replacing 20% of conventional fuel consumption with alternative fuels by the year 2020 (EC, 2001). At present, there is not a value of the base incentive (called CIC, measured in €·10^{-1} Gcal of biomethane produced). It is assumed to vary between 300 and 900 €·10^{-1} Gcal (0.25 to 0.76 €·Nm^{-3} of biomethane, considering a lower heating value for biomethane of about 35 MJ·Nm^{-3}), based on the existing market for biofuels.

2.7.4. Results

Aim of the present analysis was to assess the final production cost of LBG, thus to determine whether it is feasible for the vehicles fuel market. To this purpose three business models were evaluated. In the first case, it was assumed only one owner for all the chain, who gains incentives and revenues from LBG's sale. The owner's mark-up (10%) was also taken into account. In the second case, it was assumed one owner for the biogas and upgrading plants and a second owner for the liquefaction plant and refuelling station. In this situation, the first owner gains incentives and revenues by selling biomethane to the second one, who gains revenue from LBG's sale only. The main difference with the first scenario is in the incentive obtained (Table 2.18), because the biomethane is sold to a refuelling station with a different owner. The specific costs of each phase in first and second scenario are the same for all the chain. In the last case (third scenario) it was assumed five biogas producers that agreed to build up together a liquefaction facility, sharing investments and revenues from incentives and LBG's sale. For this scenario, the liquefaction facility is far away from every biogas plant thus the produced biomethane must be compressed on site and transported by truck. For each biogas producer electricity consumption and maintenance costs of the compression station were taken into account. The biogas and upgrading plant of each producer are the same of those considered in the first and second scenarios, so the biogas and biomethane production costs are the same. Looking at the partial map of the existing biogas plants in Italy (Figure 2.10), it is possible to notice that there are several plants close to each other and to the coast in the North-East of the country. LBG production rate in the third scenario is considerably bigger than in the other scenarios and it suits for ferries and boats refuelling. For this purpose, the liquefaction facility and refuelling station were considered to be on shore in this last case. According with the existing Italian biogas plants location (Figure 2.10), an average distance of 26 km was assumed from each biogas plant to the liquefaction facility.

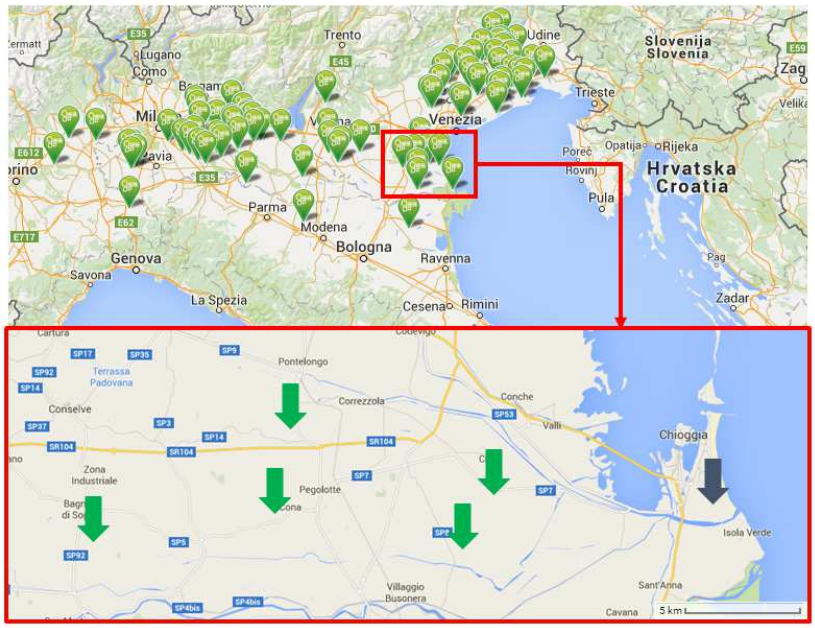

Figure 2.10. Partial map of the existing biogas plants in Italy and the related map of the 3rd business model. Green arrows stand for the existing biogas plant considered, blue arrow indicates the LBG facility location.

Regarding the incentive calculation, it was assumed that the plants are new in every scenario, while the feedstock composition to produce biogas can vary (100%, 75%, 50% by-products).
For the biogas production, some assumptions were made in order to define feedstock costs, investment and operative costs (Ragazzoni, 2013). Depending on feedstock composition the biogas production cost was estimated to be 0.32 €·Sm^{-3}, 0.33 €·Sm^{-3} and 0.35 €·Sm^{-3} of biogas, respectively for a by-product percentage of 100%, 75% and 50%. These values highlight the great influence of the feedstock composition on the biogas production cost: higher quality biomass causes a considerable increase in costs. The upgrading technology considered was PWS and the specific cost of this stage is 0.22 €·Sm^{-3} of biomethane (Warren, 2012). Then the total cost for biomethane production was found (see Table 2.19).

Table 2.19. Biogas and biomethane specific production costs

By-products	Biogas production cost	Biomethane production cost
100%	0.32 €·Sm^{-3} *biogas*	0.71 €·Sm^{-3} *biomethane*
75%	0.33 €·Sm^{-3} *biogas*	0.73 €·Sm^{-3} *biomethane*
50%	0.35 €·Sm^{-3} *biogas*	0.75 €·Sm^{-3} *biomethane*

For the liquefaction process the energy consumption was assessed, as previously specified (Table 2.17). Capital cost of the plants, the electricity consumption, operation and maintenance costs were considered, thus the economic evaluation was performed. The hypothesis assumed in the analysis are:

- capital costs were assessed on the basis of authors' knowledge (Arteconi et al, 2011);
- amortization period: 15 years;
- annual capital charge: 3% for 15 years;
- maintenance cost: 2.5% of capital investment per year;
- labour cost: 20€/h per person per 24h a day;
- working hours: 8500 h/y;
- energy price: electricity 0.17 €·kWh^{-1} (prices on the Italian market).

In Table 2.20 the specific costs, referred to LBG production, are reported. It is evident that, in any case, the LBG production cost is higher than the reference market price set previously (1 €·kg^{-1} equal to 0.39 €·$litre^{-1}$, see section 3.2) and this is due mainly to the high production cost of biomethane (almost double of pipeline gas price) and to the liquefaction process. For this reason, the incentives play a major role. It can be seen that the difference between the first and second scenario lays in the difference of ownership for the biogas plant and refuelling station, that in the second case increases the biomethane cost because of the mark-up of its producer. Instead, the LBG production cost in the third scenario is lower than in the other scenarios, thanks to the economies of scale of the liquefaction plant and refuelling station. Nevertheless, in this case a compression station and transportation via truck for each producer is necessary, thus the final difference is minimal.

The minimum value of the incentive that allows to equal the LBG production cost with the forecasted LNG market price (1 €·kg^{-1}) was assessed (Table 2.21). Every incentive higher than the minimum value contributes to gain a revenue from selling LBG as vehicle fuel. Values obtained are well within the foreseeable variation range for such incentives, as explained in section 2.7.3 (0.25 to 0.76 €·Nm^{-3} of biomethane).

Table 2.20. Specific costs for each phase of every considered scenario, referred to the LBG produced.

Business model	By-products	Biogas + Upgrading	Compression + Transport	Liquefaction costs	Station costs	Total
1st scenario	100%	0,41 €/l	-	0,13 €/l	0,02 €/l	0,56 €/l
	75%	0,43 €/l				0,58 €/l
	50%	0,44 €/l				0,59 €/l
2nd scenario	100%	0,45 €/l	-	0,13 €/l	0,02 €/l	0,60 €/l
	75%	0,47 €/l				0,62 €/l
	50%	0,48 €/l				0,63 €/l
3rd scenario	100%	0,41 €/l	0,05 €/l	0,07 €/l	0,01 €/l	0,55 €/l
	75%	0,43 €/l				0,56 €/l
	50%	0,44 €/l				0,57 €/l

Table 2.21. Minimum identified incentives for each business model. Base values (CIC) and total incentive accounting for the multipliers of the specific case.

By-products	1st scenario		2nd scenario		3rd scenario	
	base incentive	total incentive	base incentive	total incentive	base incentive	total incentive
100%	0,10 €/Sm^3	0.30 €/Sm^3	0,19 €/Sm^3	0.38 €/Sm^3	0,09 €/Sm^3	0.28 €/Sm^3
75%	0,13 €/Sm^3	0.33 €/Sm^3	0,24 €/Sm^3	0.40 €/Sm^3	0,12 €/Sm^3	0.30 €/Sm^3
50%	0,23 €/Sm^3	0.35 €/Sm^3	0,42 €/Sm^3	0.42 €/Sm^3	0,21 €/Sm^3	0.32 €/Sm^3

Comparing the minimum value of the base incentive for the different business models, it can be seen that it depends on the LBG production cost (Table 2.20) and on the corresponding incentive scheme for the considered business model (Table 2.18). In particular, for the second scenario the necessary incentive is the highest and this is due mainly to the lower multiplier in case of different owners for the biogas plant and refuelling station. On the other hand for the 1st and 3rd scenarios the minimum incentive is considerably lower, thus these options are actually more attractive. Moreover, considering several biogas producers as in the third scenario, economies of scale can be obtained by means of larger liquefaction facilities and refuelling stations, thus the minimum incentive necessary can be even lower. Especially the latter option represents an important opportunity for LBG in the Italian market.
Figures 2.11 shows the LBG production cost for the third business model, considered the most interesting to be applied, when the base incentive varies within the foreseen range (0.25 to 0.76 €·Nm^{-3} of biomethane) and the multipliers specified in Table 2.17 are applied. The obtained LBG net production cost is always lower than the forecasted threshold LNG market price and this difference can be also considerably high, making attractive the biogas source.

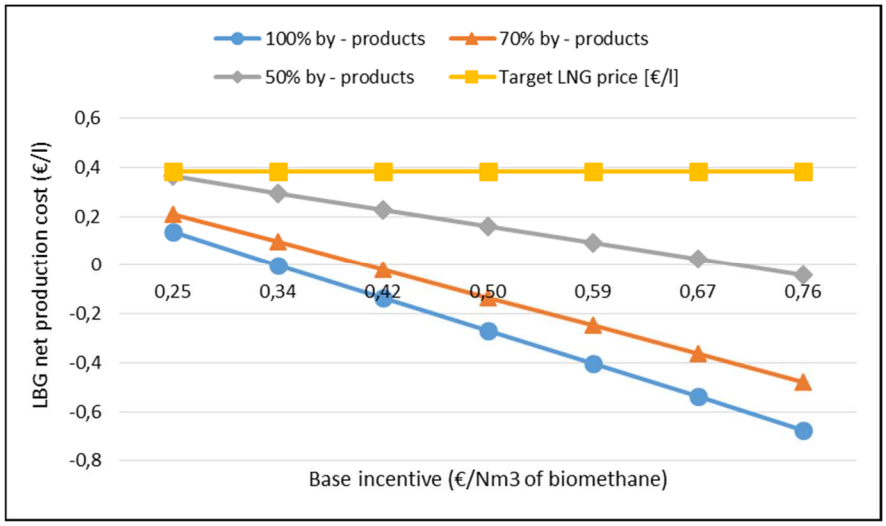

Figure 2.11. Net LBG production cost by varying the base incentive for third scenario, when revenues from incentives are accounted for.

2.8. Conclusions

In the last decade biofuels production driving force has been related mainly with governmental policies. Every country from all over the world introduced mandatory blending levels for biofuels to be introduced on the market related with standard fossil fuels. Moreover, incentives were introduced, essentially characterized by tax exemptions, import / export regulation and subsidies, allowing the fast growth of biofuels production and consumption. These policies are strictly related with national governments, since internal societal structure, economic level, land availability and achievable cultivations. Such and other aspects strongly influence proposed targets as well as biofuel market penetration and technology development. Other incentives are related with production chain support, industry support, such as investments and land utilization as well as final biofuels prices incentives. Main issue to be overcome in order to achieve global sustainability in biofuels production is related with such combustion fuels production, namely environmental impact and total GHG emitted. In order to prevent a negative impact, in recent years more specific policies were introduced and adopted globally. Those are mainly related with land utilization, feedstock typology and involved technology level in an LCA perspective. Moreover, in order to avoid food prices increasing due to mandatory targets and land usage, new regulatory schemes are ongoing mostly associated with bioethanol and biodiesel. Second-generation fuels and technologies were implemented as key point in several country's policy, especially in United States and European Union in which GHG emissions reduction is strictly required. It is the case of Germany, in which biofuel production trends are going to be quantified in a GHG reduction point of view instead of produced volumes. Nevertheless, reaching such a target worldwide will be highly challenging for policymakers. Moreover, up to now, a large number of countries and producers are not using second-generation approach, thus biofuels are still based on grains, sugar or vegetable oils. By the way, biofuels is a key point in the transport sector in a sustainability point of view. Feedstocks such as Jatropha, switchgrass, and algae could allow lower land cultivation area, having a good potential for the future biofuels production. However, more efforts are required in order to increase their economic sustainability. Since the

biofuel production sector must face those kind of obstacles, specific policies are of paramount importance. Increasing biofuel sustainability is a key factor in this sense. By the way, as part of policies involved in biofuel sector evolution and technological development, incentives are forecasted to decrease during time, to be further eliminated. Reducing fossil fuels use should be an important factor in order to increase biofuel production and consumption costs. Still, uncertainties related with needed governmental support are crucial for the sector to be independent.
Focusing on the transport sector, it accounts for about 24% of global CO_2 and it will continue to grow in the future. For this reason, it is of paramount importance to intervene with policies intended to lower and control GHG emissions. European and Chinese specific situation were described. As shown, both countries had adopted similar actions by setting limits for cars emissions, introducing taxes schemes and promoting alternative fuels usage. As a consequence, some targets have already been achieved, but a lot of work is still required. In Europe, these policies refer to passenger cars and vans and set maximum emissions, penalties and incentives to manufacturers; heavy duty vehicles have not been considered yet due to lack of information about their emission level. In China, limits in the CO_2 emissions were set as well. Moreover, other measures like tax instruments and penalties are used. Similar considerations could be made regarding biofuels policy concerning agricultural policy, blending mandates, subsidies and tax instrument referring especially to ethanol and bio-diesel fuels. Several plans were also made for natural gas as alternative fuel in transport sector but NGVs share in both Europe and China is still too low. However, despite information about China's policy were not available in detail, natural gas vehicles industry has known an impressive growth of about 300% in NGVs, more than 1700% in LNG vehicles and about 150% in refueling stations. In addition, big efforts were put inside the gas development plan as part of the "12th Five-Year Plan". An important role could be played by biomethane as vehicle fuel. With this purpose, in Europe incentive policy exists with several examples in different countries, promoting green energy and NGVs diffusions. On the other hand, in China it can be seen that there is a huge and growing market for biogas and at present there are several biogas plants producing biomethane as vehicle fuel. The 12th Five-Year Plan for Biomass Energy Development claim ambitious targets but up to now an incentive scheme for biomethane is missing. However, Chinese government is increasing its investments in biogas infrastructure. An Italian case study related with biogas and biomethane national incentive scheme was examined, showing great potential in LBG production by means of biomethane liquefaction process. A technical and economic analysis for the production of LBG was performed considering three different business models for the LBG value chain in the Italian context. Main result of this study is that, in any case, the LBG produced using biogas as feedstock is not feasible, because of the high biogas production cost. However, with a proper incentive scheme such as the Italian one for biomethane, the use of this feedstock can be attractive. The minimum incentive to make this kind of project economically interesting was calculated. Depending on the biomass composition and business model considered, the minimum value of the base incentive was estimated to vary from 0.10 €/Sm^3 to 0.42 €/Sm^3. The analysis shows that is not convenient to have more than one owner in the fuel value chain, due to the mark-up of each producer and mainly to the reduced incentive gained. On the other hand, the option with more biogas producers that contribute to supply the same liquefaction facility, sharing investment costs and revenues, is a particularly attractive one. In fact, particularly in the Italian context with a pretty high density of biogas plants, it is possible to build-up larger liquefaction facility and refueling stations in order to supply bigger customers and fleets, like ferries and boats, reducing production costs by mean of economies of scale. Eventually the biogas and biomethane potential in China is reported. It can be seen that actually there is a huge and growing market for biogas and at present there are several biogas plants producing biomethane to be used as vehicle fuel. The 12th Five-Year Plan for Biomass Energy Development claim ambitious targets but up to now an incentive scheme for biomethane is missing. However, Chinese government is increasing its investments in biogas infrastructure thus the model can be extended and future options for different business models are possible.

2.9. References

- Aatola, H.; Larmi, M.; Sarjovaara, T.; Mikkonen, S. (2008). Hydrotreated Vegetable Oil (HVO) as a Renewable Diesel Fuel: Trade-off between NOx, Particulate Emission, and Fuel Consumption of a Heavy-Duty Engine. SAE Int. J. Engines 2008, 1, 1251–1262.
- Abatzoglou N, Boivin S (2009) A review of biogas purification processes. Biofuels Bioprod Bioref 3:42–71. doi:10.1002/bbb.117.
- Aden, A.Water Usage for Current and Future Ethanol Production. Southwest Hydrol. (2007), 6, 22–23.
- Anderson, J.; DiCicco, D.; Ginder, J.; Kramer, U.; Raney-Pablo, H.; Wallington, T. High Octane Number Ethanol-Gasoline Blends. Fuel 2012, 97, 585–594.

- Andriani D., Wresta A., Atmaja T., Saepudin A., (2014). A review on optimization production and upgrading biogas through CO2 removal using various techniques. Appl Biochem Biotechnol 172:1909–1928. doi:10.1007/s12010-013-0652-x
- Araújo, K. (2017). Low Carbon Energy Transitions: Turning Points in National Policy and Innovation; Oxford University Press: New York, NY, USA, 2017.
- Argentine Renewable Energies Chamber, Ca´mara Argentina de Energı´as Renovable (CADER), 2009. State of the Argentine Biodiesel Industry — First Semester 2009 Report.
- Arteconi A., Spitoni M., Polonara F. 2015, The feasibility of liquid biogas (LBG) in Italy, *Proceedings of the 24th International Congress of Refrigeration,* Yokohama, Paper 0504.
- Arteconi, A., Brandoni, C., Santori, G., Polonara, F., 2011. Micro-scale LNG liquefaction plants, *Proceedings of the 23rd International Congress of Refrigeration*, Prague, paper 489
- Bailo´n L, Hinge J (2012) Report: biogas and bio-syngas upgrading. Danish Technological Institute.
- Barros, S., 2009. Brazil Biofuels Annual—Biodiesel Annual Report. USDA Foreign Agricultural Service, GAIN Report Number BR9009.
- Bauer F, Hulteberg C, Persson T, Tamm D (2013) Biogas upgrading—review of commercial technologies. SGC Rapport 2013:270. SGC.
- Biofuels: The Fuel of the Future, Asia. Available online: http://www.biofuel.org.uk. (last accessed on 28/11/2017).
- Blumental D., Yong X., Deemer P., Zhang S. (2013). *United States: China Issues New Natural Gas Utilization Policy*. Retrieved from http://www.mondaq.com/unitedstates/x/217828/Oil+Gas+Electricity/China+Issues+New+Natural+Gas+Utilization+Policy. (last accessed on 28/11/2017).
- Borras, S.; Franco, J. Global Land Grabbing and Trajectories of Agrarian Change: A Preliminary Analysis. J. Agrar. Chang. 2012, 12, 34–59.
- BP Statistical Review of World Energy – June 2017, (2017). Retrieved from https://www.bp.com/en/global/corporate/energy-economics/statistical-review-of-world-energy/downloads.html (last accessed on 28/11/2017)
- BP. Statistical Review of World Energy; BP: London, UK, 2016.
- Bransby, D.; McLaughlin, S.; Parrish, D. A Review of Carbon and Nitrogen Balances in Switchgrass Grown for Energy. Biomass Bioenergy 1998, 14, 379–384.
- Bromokusumo, A., 2007. Indonesia Biofuels Annual 2007. USDA Foreign Agricultural Service, GAIN Report Number ID7019, June 2007.
- Bromokusumo, A., 2009. Indonesia Biofuels Annual 2009. USDA Foreign Agricultural Service, GAIN Report Number ID9017, 01.06.2009.
- Colares, J., 2008. A breief history of Brazilian Biofuel Legislation. Syracuse J. Law Commerce 35 (2).
- Consumer Reports. Diesel vs. Biodiesel vs. Vegetable Oil. Available online: http://www.consumerreports.org/cro/2012/05/diesel-vs-biodiesel-vs-vegetable-oil/index.htm (last accessed on 28/11/2017).
- Cowie, A.; Soimakallio, S.; Brandao, M. Environmental Risks and Opportunities of Biofuels. In The Law and Policy of Biofuels; Bouthillier, Y.L., Cowie, A., Martin, P., McLeod-Kilmurray, H., Eds.; Edward Elgar: Cheltenham, UK, 2016.
- de Almeida, E. F., Bomtempo, J. V., de Souzae Silva, C. M. ,2008. The performance of Brazilian biofuels: an economic, environmental and social analysis. Published in Biofuels—Linking Supportto Performance by the OECD/ITF,pp.151–188.
- De Baan, L.; Mutel, C.; Curran, M.; Hellweg, S.; Koellner, T. Land Use in Lifecycle Assessment. Environ. Sci. Technol. 2013, 47, 9281–9290.
- De Baan, L.D.; Alkemade, R.; Koellner, T. Land Use Impacts on Biodiversity in LCA: A Global Approach. Int. J. Life Cycle Assess. 2013, 18, 1216–1230.
- De Gorter, H.; Drabik, D.; Just, D. The Economics of Biofuel Policies; Palgrave: New York, NY, USA, 2015.
- Department of Energy (DOE). Alternative Fuels Data Center. Available online: http://www.afdc.energy.gov/fuels/emerging.html (last accessed on 28 August 2016).
- Dessureault, D., 2009. Canada Biofuels Annual. USDA Foreign Agricultural Service, GAIN Report Number CA9037, approved by U.S. Embassy, 30.06.2009.
- Deublein D. & Steinhauser A. (2008). *Biogas: from Waste and Renewable Resources (An Introduction)*. WILEY-VCH Verlag GmbH & Co. KGaA.

- Dillon H. S., Laan T., Dillon H. S., 2008. Biofuels — at what cost? Government support for ethanol biodiesel in Indonesia. The Global Studies Initiative, Part of the International Institute for Sustainable Development, December 2008.
- Dismukes, G.; Carrieri, D.; Bennette, N.; Ananyev, G.; Posewitz, M. Aquatic Phototrophs: Efficient Alternatives to Land-based Crops for Biofuels. Curr. Opin. Biotechnol. 2008, 19, 235–240.
- Dong, F., 2007. Food security and biofuels development: the case of China. Briefing Paper 07-BP-52, Centre for Agricultural and Rural Development, Iowa State University, October 2007.
- Doyletech Corporation, 2010. Total economic impact assessment of biofuel plants in Canada. Prepared for the Canadian Renewable Fuels Association (CRFA), May 2010.
- EC, European Commission (2015a). *Climate Action, Reducing emissions from transport*. Retrieved from http://ec.europa.eu/clima/policies/transport/index_en.htm. (last accessed on 28/11/2017).
- EC, European Commission (2015b). *Climate Action, Reducing CO2 emissions from passenger cars*. Retrieved from http://ec.europa.eu/clima/policies/transport/vehicles/cars/index_en.htm. (last accessed on 28/11/2017).
- EC, European Commission (2015c). *Climate Action, Reducing CO2 emissions from vans*. Retrieved from http://ec.europa.eu/clima/policies/transport/vehicles/vans/index_en.htm. (last accessed on 28/11/2017).
- EC, European Commission (2015d). *Climate Action, Reducing CO2 emissions from heavy duty vehicles*. Retrieved from http://ec.europa.eu/clima/policies/transport/vehicles/heavy/index_en.htm. (last accessed on 28/11/2017).
- EC, European Commission (2015e). *Climate Action, Fuel Quality*. Retrieved from http://ec.europa.eu/clima/policies/transport/fuel/index_en.htm. (last accessed on 28/11/2017).
- Edenhofer, O.; Pichs-Madruga, R.; Sokona, Y.; Seyboth, K.; Matschoss, P.; Kadner, S.; Zwickel, T.; Eickemeier, P.; Hansen, G.; Schlomer, S.; et al. Renewable Energy Sources and Climate Change Mitigation; Special Report of the IPCC; IPCC, 2011; Available online: http://www.ipcc.ch/report/srren/ (last accessed on 28/11/2017).
- EEA, European Environment Agency (2009). *Monitoring of CO2 emissions from passenger cars – Regulation 443/2009*. Retrieved from http://www.eea.europa.eu/data-and-maps/data/co2-cars-emission-8 (last accessed on 28/11/2017).
- EIA, Energy Information Administration, 2007. Biofuels in the US Transportation Sector. Published in Annual Energy Outlook 2007, February 2007.
- EIA, Energy Information Administration, 2008. Annual Energy Outlook 2008 with Projections to 2030, Legislation and Regulations, Report No DOE/EIA- 0383(2008), June 2008.
- Elbehri, A.; Liu, A.; Segerstedt, A.; Liu, P.; Babilonia Estrada, R.; Hölldobler, B.W.; Davies, S.J.C.; Stephen Navarro, C.L.; Andrew, J.F.; Pérez, H. (2013). Biofuels and the Sustainability Challenge: A Global Assessment of Sustainability Issues, Trends and Policies for Biofuels and Related Feedstocks; FAO: Rome, Italy, 2013.
- Energy Information Administration (EIA). Available online: http://www.eia.gov/totalenergy/data/annual/index.php. (last accessed on 28/11/2017).
- EurObserv'ER (2014) Biogas barometer.
- European Environment Agency (EEA). How Much Bioenergy Can Europe Produce without Harming the Environment? EC: Copenhagen, Denmark, 2006.
- FAO. Information. Available online: http://www.fao.org/. (last accessed on 28/11/2017).
- FAO; Earthscan/Routledge. The State of the World's Land and Water Resources for Food and Agriculture; FAO and Earthscan/Routledge: Abingdon, UK, 2011.
- FAOSTAT. Information. Available online: http://faostat3.fao.org/home/E.%2019%20Aug.%202016. (last accessed on 28/11/2017).
- Farrel R., (2017). Ausrtalia, Biofuel Annual. Retrieved from https://gain.fas.usda.gov/Recent GAIN Publications/Biofuels Annual_Canberra_Australia_8-15-2017.pdf (last accessed from 28/11/2017)
- Fischer, G.; van Velthuizen, H.; Nachtergaele, F. Global Agro-Ecological Zones Assessment; Report RP 06 003; IIASA: Vienna, Austria, 2006.
- Fischer, G.; van Velthuizen, H.; Shah, M.; Nachtergaele, F. Global Agro-Ecological Assessment for Agriculture in the 21st Century; Report RR 02 02; IIASA; FAO: Laxenburg, Austria; Rome, Italy, 2002.
- Grosjean, D.; Miguel, A.H.; Tavares, T.M. Urban Air Pollution in Brazil: Acetaldehyde and other Carbonyls. Atmos. Environ. Part B Urban Atmos. 1990, 24, 101–106.

- GSI, Global Subsidies Initiative, 2008. Biofuels — at what cost? Government support for ethanol and biodiesel in China. Based on report commissioned by GSI from Energy Research Institute of the National Development and Reform Commission, November 2008.
- Hadar, Y. Sources for Lignocellulosic Raw Materials for the Production of Ethanol. In Lignocellulose Conversion; Springer: Heidelberg, Germany, 2013.
- High Level Panel of Experts of Food Security and Nutrition (HLPE), UN Committee on World Food Security. Biofuels and Food Security, Report; HLPE: Rome, Italy, 2013.
- High Level Panel of Experts of Food Security and Nutrition (HLPE), UN Committee on World Food Security. Price Volatility and Food Security, Report; HLPE, UN Committee on World Food Security: Rome, Italy, 2011.
- Highina, B.; Bugaje, I.; Umar, B. A Review of Second Generation Biofuel: A Comparison of its Carbon Footprints. Eur. J. Eng. Technol. 2014, 2, 117–125.
- Hoh, R., 2009. Malaysia Biofuels Annual. USDA Foreign Agricultural Service, GAIN Report Number MY9026, approved by D. Cottrell, 12.06.2009.
- Holma, A.; Koponen, K.; Antikainen, R.; Lardon, L.; Leskinen, P.; Roux, P. Current Limits of Life Cycle Assessment Framework in Eevaluating Environmental Sustainability—Case of Two Evolving Biofuel Technologies. J. Clean. Prod. 2013, 54, 215–228.
- Huenteler, J.; Lee, H. The Future of Low Carbon Road Transport; Rapporteur's Report; Belfer Center, Kennedy School of Government, Harvard University: Cambridge, MA, USA, 2015.
- International Air Transportation Association (IATA). 2015 Report on Alternative Fuels; International Air Transportation Association: Montreal, QC, Canada; Geneva, Switzerland, 2015.
- International Civil Aviation Organization (ICAO). 2013 Environmental Report: Destination Green; International Civil Aviation Organization: Montreal, QC, Canada, 2013.
- International Energy Agency (IEA). Biofuels for Transport; IEA/OECD: Paris, France, 2011.
- International Renewable Energy Agency (IRENA). Boosting Biofuels; International Renewable Energy Agency: Abu Dhabi, UAE, 2016.
- International Renewable Energy Agency (IRENA). Innovation Outlook: Advanced Liquid Biofuels; International Renewable Energy Agency: Abu Dhabi, UAE, 2016.
- Jaffrin A, Bentounes N, Joan AM, Makhlouf S (2003) Landfill biogas for heating greenhouses and providing carbon dioxide supplement for plant growth. Biosyst Eng 86:113–123. doi:10.1016/S1537-5110(03)00110-7.
- Ji, X.; Long, X. A Review of the Ecological and Socioeconomic Effects of Biofuel and Energy Policy Recommendations. Renew. Sustain. Energy Rev. 2016, 61, 41–52.
- Jo¨nsson O, Polman E, Jensen J, Eklund R, Schyl H, Ivarsson S (2003) Sustainable gas enters the European Gas Distribution System. In: World gas conference, Tokio.
- Jyothilakshmi R. & Prakash S. V. (2015). Production of biogas using small-scale plug flow reactor and sizing calculation for biodegradable solid waste. *Renewables, Wind, Water and Solar*. doi: 10.1186/s40807-015-0006-0.
- Kahr, H.; Wimberger, J.; Schürz, D.; Jäger, A. Evaluation of the Biomass Potential for the Production of Lignocellulosic Bioethanol from Various Agricultural Residues in Austria and Worldwide. Energy Proc. 2013, 40, 146–155.
- Klein S.A., 2013. EES - Engineering Equation Solver, F-Chart Software. (http://www.fchart.com/ees/) (last accessed – 28/11/2017).
- Kojima, M.; Johnson, T. Potential for Biofuels in Transport in Developing Countries; ESMAP Paper, Knowledge Exchange Series No 4; World Bank: Washington, DC, USA, 2006.
- Koundinya, V. Jatropha Profile; Agricultural Marketing Resource Center: Ames, IA, USA, 2008.
- Kovarik, B. History of Biofuels. In Biofuels Crops; Singh, B.P., Ed.; Center for Bioscience International (CABI): Wellington, UK, 2013.
- Kumar, G.; Bakonyi, P.; Periyasamy, S.; Kim, S.H.; Nemestóthy, N.; Bélafi-Bakó, K. Lignocellulose biohydrogen: Practical challenges and recent progress. Renew. Sustain. Energy Rev. 2015, 44, 728–737.
- Latner, K., Wagner, O., Junyang, J., 2007. People Republic of China Biofuels Annal 2007. USDA Foreign Agricultural Report Service, GAIN Report Number CH7039, approved by US Embassy, June 2007.
- Li Y. (2015). *China's Natural Gas Car Ownership Rose to First in the World, China Energy Network*. Retrieved from http://www.china5e.com/news/news-905755-0.html. (last accessed on 28/11/2017).
- Lopez, G. P., Laan, T., 2008. Biofuels — at what cost? Government support for biodiesel in Malaysia. The Global Studies Initiative, part of the International Institute for Sustainable Development, September 2008.

- Macedo I., Nogueira L., 2005. Biocombustveis. Cadernos NAE, No. 2, Nu´cleo de Assuntos Estrate´ gicos da Presidˆencia da Repu´ blica, Brası´lia.
- Miltner M, Makaruk A, Krischan J, Harasek M (2012) Chemical-oxidative scrubbing for the removal of hydrogen sulphide from raw biogas: potentials and economics. Water Sci Technol 66:1354–1360. doi:10.2166/wst.2012.329
- Morgera, E.; Kulovesi, K.; Gobena, A. Case Studies on Bioenergy Policy and Law: Options for Sustainability; FAO Legal Office: Rome, Italy, 2009.
- Murphy, C.; Kendall, A. Lifecycle Analysis of Biochemical Cellulosic Ethanol under Multiple Scenarios. GCB Bioenergy 2015, 7, 1019–1033.
- National Research Council (NRC). Water Implications of Biofuels Production in the United States; NRC: Washington, DC, USA, 2008.
- NGVA, Natural & bio Gas Vehicle Association Europe. (2014a). *European NGV Statistics*.
- NGVA, Natural & bio Gas Vehicle Association Europe. (2014b). *Catalogue of Incentives and Best Practices in Europe for NGVs*.
- NGVA, Natural & bio Gas Vehicle Association Europe. (2015). *Air Pollution Policies Spark NGV Market in China*
- Nie H., Jiang H., Chong D., Wu Q., Xu C., Zhou H. 2013, Comparison of water scrubbing and propylene carbonate absorption for biogas upgrading process, *Energy and Fuel* 27(6):3239 –3245.
- Oladosu, G.; Msangi, S. Biofuel-Food Market Interactions: A Review of Modeling Approaches and Findings. Agriculture 2013, 3, 53–71.
- Organization for Economic Cooperation and Development (OECD)-UN Food and Agriculture Organization (FAO). Agricultural Outlook 2016–2025; OECD: Paris, France, 2016.
- Patterson T, Esteves S, Dinsdale R, Guwy A (2011) An evaluation of the policy and techno-economic factors affecting the potential for biogas upgrading for transport fuel use in the UK. Energ Policy 39:1806–1816. doi: 10.1016/j.enpol.2011.01.017
- Persson M, Jo¨nsson O, Wellinger A (2006) Biogas upgrading to vehicle fuel standards and grid injection. IEA Bioenergy.
- Persson M., Wellinger A., Rehnlund B., Rahm L., (2007). Report on technological applicability of existing biogas upgrading processes. Biogasmax.
- Pinzon, L., 2009. Colmbia Biofuels Annual. USDA Foreign Agricultural Service, approved by E. Mello, 01.06.2009.
- Popp, J.; Lakner, Z.; Harangi-Rakos, M.; Fari, M. The Effect of Bioenergy Expansion: Food, Energy and Environment. Renew. Sustain. Energy Rev. 2014, 32, 559–578.
- Preechajarn, S., Prasertsri, P., Kunasirirat, M., 2007. Thailand Bio-fuels Annual 2007. USDA Foreign Agricultural Service, GAIN Report Number TH7070, approved by U.S. Embassy, 04.06.2007.
- Preecharjarn, S., Prasertsri, P., 2009. Thailand Biofuels Annual 2009. USDA Foreign Agricultural Service, GAIN Report Number TH9282, approved by G. Meyer, 01.06.2009.
- ProExport Colombia, 2008. Biofuel Industry in Colombia. Retrived in May 2010.
- Quirke D., Steenblick R., Warner B., 2008. Biofuels — at what cost? Government Support for Ethanol and Biodiesel in Australia. The Global Studies Initiative, Part of the International Institute for Sustainable Development, April 2008).
- Ragazzoni A. 2013, Analisi della redditività degli impianti per la produzione di biogas alla luce delle nuove tariffe incentivanti, Programma di sviluppo rurale dell'Emilia Romagna (Italian Reference).
- Rasi S (2009) Biogas composition and upgrading to biomethane. University of Jyva¨skyla¨, Jyva¨skyla
- Renewable Energy Network 21 (REN21). Global Status Report; REN21: Paris, France, 2016.
- Rory J. (2015). *Energy Briefing (China)*. Global Economics.
- Rosillo-Calle, F.; Pelkmans, L.; Walter, A. A Global Overview of Vegetable Oils, with Reference to Biodiesel, Task 40 IEA Bioenergy Report; IEA: Paris, France, 2009.
- Rutledge B (2005) California biogas industry assessment white paper. WestStart-CALSTART.
- Rutz, D., Thebaud, A., Janssen, R., Segura, S., Riegelhaupt, E., Ballesteros, M., Manzanares, P., St. James, C., Serafini, D., Coelho, S., Guardabassi, P., Aroca, G., Soler, L., Nadal, G., Bravo, G., 2009. Biofuel Policies and Legislation in Latin America, BioTop Project. Seventh Framework Programme, European Commis- sion, August 2009.
- Ryckebosch E., Drouillon M., Vervaeren H., (2011). Techniques for transformation of biogas to biomethane. Biomass Bioenerg 35:1633–1645. doi:10.1016/j.biombioe.2011.02.033

- Scott, C.; Sugg, Z. Global Energy Development and Climate-InducedWater Scarcity-Physical Limits, Sectoral Constraints, and Policy Imperatives. Energies 2015, 8, 8211–8225.
- Scott, S.; Davey, M.; Dennis, J.; Horst, I.; Howe, C.; Lea-Smith, D.; Smith, A. Biodiesel from Algae: Challenges and Prospects. Curr. Opin. Biotechnol. 2010, 21, 277–286.
- Searchinger, T.; Heimlich, R.; Houghton, R.A.; Dong, F.; Elobeid, A.; Fabiosa, J.; Tokgoz, S.; Hayes, D.; Yu, T.-H. Use of U.S. Croplands for Biofuels Increases Greenhouse Gases through Emissions from Land-Use Change. Science 2008, 319, 1238–1240.
- Seelke, C.; Yacobucci, B. Ethanol and Other Biofuels: Potential for U.S.-Brazil Cooperation; CRS Report RL34191, September 27, 2007, and Environmental Protection Agency (EPA), Renewable Fuel Standard Program. Available online: https://www.epa.gov/renewable-fuel-standard-program (last accessed on 28/11/2017).
- Singh, S., 2007. India Biofuels Annual, USDA Foreign Agricultural Service, GAIN Report Number IN7047, approved by U.S. Embassy in New Delhi, 06.01.2007
- Singh, S., 2009. India Biofuels Annual. USDA Foreign Agricultural Service, GAIN Report Number IN9080, approved by H. Higgins, 15.06.2009.
- Sinnott RK (2005) Chemical engineering design, vol 6, 4th edn. Elsevier Butterworth-Heinemann, Oxford
- Solomon, B.; Bailis, R. (Eds.) Sustainable Development of Biofuels in Latin America and the Caribbean; Springer: New York, NY, USA, 2014.
- Soreanu G, Be´land M, Falletta P, Edmonson K, Svoboda L, Al-Jamal M, Seto P (2011) Approaches concerning siloxane removal from biogas—a review. Can Biosyst Eng 53:8.1–8.18
- Stambasky J. (2015). Biogas & Biomethane in Europe. *Agriculture and Renewable Energy: the Biogas/Biomethane Value Chain*, promoted by the Municipality of Reggio Emilia. Italy: Loris Malaguzzi International Centre.
- Theiss, T.; Alleman, T.; Brooker, A.; Elgowainy, A.; Fioroni, G.; Han, J.; Huff, S.; Johnson, C.; Kass, M.; Leiby, P.; et al. Summary of High-Octane, Mid-Level Ethanol Blends Study; ORNL/TM-2016/42; Oak Ridge National Laboratory: Oak Ridge, TN, USA, 2016.
- Thoenes, P. Soybean International Commodity Profile, Background Paper for the Competitive Commercial Agriculture in Sub-Saharan Africa (CCAA) Study; FAO: Rome, Italy, 2006.
- Thompson, B.P. The Agricultural Ethics of Biofuels: The Food vs. Fuel Debate. Agriculture 2012, 2, 339–358.
- Thra¨n D et al. (2014) Biomethane—status and factors affecting market development and trade. IEA Task 40 and Task 37 Joint Study.
- Toma`s M, Fortuny M, Lao C, Gabriel D, Lafuente J, Gamisans X (2009) Technical and economical study of a full-scale biotrickling filter for H2S removal from biogas. Water Pract Technol 4. doi:10.2166/wpt.2009.026
- Tomei, J.; Helliwell, R. Food versus Fuel? Going Beyond Biofuels. Land Use Policy 2016, 56, 320–326.
- Tynell A ° , Bo¨rjesson G, Persson M (2007) Microbial growth on pall rings: a problem when upgrading biogas with the water-wash absorption technique. Appl Biochem Biotechnol 141:299–320. doi:10.1007/BF02729069
- U.S. Department of Agriculture (USDA). EU Biofuel Mandates by Member State; GAIN Report GM 16009; USDA:Washington, DC, USA, 2016.
- U.S. Department of Agriculture (USDA). EU Biofuels Annual 2016; GAIN Report Number NL 6021; USDA: Washington, DC, USA, 2016.
- U.S. Department of Agriculture (USDA). EU's General Court Rules Against Anti-Dumping Duty on US; GAIN Report GM E16025; USDA:Washington, DC, USA, 2016.
- U.S. Environmental Protection Agency (U.S. EPA). Biofuels and the Environment: The First Triennial Report to Congress (2011 Final Report); EPA/600/R-10/183F; U.S. Environmental Protection Agency: Washington, DC, USA, 2011.
- UN Department of Economic and Social Affairs (UN DESA), Population Division. 2015 Revision, World Population Prospects, Report; ESA/P/WP.241; United Nations: New York, NY, USA, 2015.
- UN Food and Agriculture Organization (FAO). Food Outlook, Biennial Report on Global Food Markets; FAO: Rome, Italy, 2016.
- United Nations Environment Programme (2015), *The Chinese Automotive Fuel Economy Policy*.
- Urban W, Girod K, Lohmann H (2009) Executive report: the German Market for Biomethane. Deutsche Energie-Agentur GmbH (DENA), German Energy Agency.

- USDA. Information. 2016. Available online: http://plants.usda.gov/core/profile?symbol=JACU2 (last accessed on 28/11/2017).
- Verheye, W.H. Growth and Production of Oil Palm; UNESCO-EOLSS Publishers: Belgium, Europe, 2010.
- Walker G. 1983, *Cryocoolers – Part1: Fundamentals*. Plenum Press, New York and London, 365p.
- Walter, A., Cortez, L., 1999. An historical overview of the Brazilian Bioethanol Program. Renew. Energy Dev. 11 (1).
- Warren K. 2012, A techno-economic comparison of biogas upgrading technologies in Europe, Master Thesis, University of Jyväskylä.
- Wellinger A, Lindberg A (1999) Biogas upgrading and utilization. IEA Bioenergy.
- Xue, J.; Grift, T.; Hansen, A. Effect of Biodiesel on Engine Performance and Emissions. Renew. Sustain. Energy Rev. 2011, 15, 1098–1116.
- Yang, Q.; Chen, G.Q. Greenhouse gas emissions of corn—Ethanol production in China. Ecol. Model. 2013, 252, 176–184. 64. Kahn Ribeiro, S.; Figueroa, M.; Creutzig, F.; Dubeux, C.; Hupe, J.; Kobayashi, S. 2012: Chapter 9—Energy End-Use: Transport. In Global Energy Assessment—Toward a Sustainable Future; Cambridge University Press: Cambridge, UK; New York, NY, USA; The International Institute for Applied Systems Analysis: Laxenburg, Austria, 2008; pp. 575–648.

3. COMPRESSED NATURAL GAS (CNG) REFUELING TECHNOLOGY

3.1 Introduction

CNG (Compressed Natural Gas) is a gaseous fuel consisting of a mixture of hydrocarbons, mainly methane. Looking at Table 3.1, conventional natural gas composition is presented.

Table 3.1. Typical thermos-physical property and composition ranges for NG (NAESB, 2002)

Component	**Typical composition [mole %]**	**Composition range [mole %]**
Methane	94.9	87 – 96
Ethane	2.5	1.8 – 5.1
Propane	0.2	0.1 – 1.5
iso-Butane	0.03	0.01 – 0.3
normal-Butane	0.03	0.01 – 0.3
iso-Pentane	0.01	trace – 0.14
Normal-Pentane	0.01	trace – 0.04
Hexanes plus	0.01	trace – 0.06
Nitrogen	1.6	1.3 – 5.6
Carbon Dioxide	0.7	0.1 – 1
Oxygen	0.02	0.01 – 0.1
Hydrogen	trace	trace – 0.02
Specific Gravity	0.585	0.57 – 0.62
Gross Heating Value [MJ/m^3]	37.8	36 – 40.2
Octane number	115	110 - 130

In order to be used in the transport sector as vehicle fuel in standard engines, NG compression is mandatory, thus CNG is obtained. Depending on the local legislation, such final pressure may vary in a range from 200 bar up to 250 bar. It presents no color, no odor and is less dense than air regarding physical properties, while related with human health, it is non – carcinogenic and non – toxic fuel. Ignition temperature related with NG is about 540°C, much higher than that related with gasoline, which varies between 260°C to 280°C (Setchkin, 1954). Thus, if scattered into atmosphere, a potential explosion occurs only with a concentration in air ranging from 4.4% to 15% (IUPAC, 2006). Since produced CO_2 during its combustion process is considerably lower than that of standard fossil fuels, it is commonly considered a green fuel. Moreover, since it has a very low H_2S and water content, corrosion risks are avoided. CNG presents higher-octane number and lower cetane number if compared with standard gasoline, thus it represents an excellent alternative fuel for gasoline-based engines. On the other hand, it is unsuitable as single fuel for diesel-based engines since compression energy in such engines is not high enough for ignition. In order to avoid this issue, dual-fuel technology allows NG to be used in such engines by blending it with common diesel during the combustion process. Moreover, its high-octane number prevents knocks during combustion, thus no specific additives are required. As long as NG for light-duty vehicles is in its compressed gaseous form, no explosion occurs during accidents. In fact, as already mentioned, being lighter than air and explosive only in a particular mixing range, it would burn more likely away from the ground.
Some water is generally mixed in pipeline natural gas. This compound does not affect processes involved in domestic or industrial usage, but it may be critical in CNG applications. Being compressed to very high-pressure levels, water may condense and corrosion as well as other issues may occur during CNG station operation and vehicles refueling. In order to avoid such problems, water must be removed or at least reduced. Other critical contaminants related with natural gas from the national gas grid, may be oil and particulate. Combining those impurities with water as well as oxygen or hydrogen sulfide, systemic problems may occur in CNG stations as well as in NG vehicles. Moreover, time-dependent natural gas composition related with gas grid must be considered in order to guarantee a standard refueling level for end-users in terms of actual refueled energy content of NG.

3.2. Conventional CNG Stations

Compressed Natural Gas refueling stations present strict requirements in terms of design and safety aspects. This is mainly due to the CNG infrastructure which involves high pressure natural gas. At present, four CNG refueling station designs are available on market, depending on design requirements, fueling requirements and fueled vehicles. Being in a gaseous form, NG presents several differences and critical aspects related to transportation (NG supply for the CNG station) and refueling process. Regarding the former, traditional combustion fuels such as gasoline and diesel are commonly supplied to conventional refueling station by means of trucks on public or dedicated roads. On the other hand, gaseous natural gas cannot be easily transported on road due to its low energy density, compared to the forementioned fuels. By the way, developed countries are usually characterized by a national natural gas grid in order to quickly transport NG. Therefore, conventional CNG stations are supplied by purchasing NG from such infrastructure, to be further compressed on-site. However, if the refueling station is far from the national gas grid, building up a new pipeline segment would be very expansive. If this is the case, then road transport could be achieved by means of high pressured NG vessels. By the way, this solution only allows small daily natural gas quantity while requiring high footprint compared with other stations, due to pressurized vessels storage near the CNG station. Regarding the fueling process critical aspects, they are discussed with more detail in the next sections. However, they are mainly related with vehicle refueling time and final temperature of vehicle's vessel due to refueling process.
For conventional CNG refueling stations, five principal configurations are available:

1. Cascade Fast-Filling;
2. Buffer Fast-Filling;
3. Time-Filling;
4. Liquefied – Compressed Natural Gas (L-CNG); and
5. Combination-Filling.

The last one is actually a combination of fast-filling and time-filling designs. It was developed in order to achieve higher flexibility for end-users. Safety requirements, which are the same for any kind of CNG adopted configuration, are stricter than those of standard gasoline and diesel stations. Three main requirements could be identified:

- The station must involve two emergency shutdown devices (EDS). They must be located at 3 meters and in a range from 7 to 20 meters from the dispensing area, respectively. In standard oil-based fuels stations this requirement is mandatory for just one EDS device, to be placed up to 20 meters from dispensing area;
- The compressor room must include an additional EDS in order to provide additional safety level;
- Dispensing area and compressor room must be equipped with fire extinguishers,

In this section, a brief description of conventional CNG stations is presented. Moreover, CNG and L-CNG refueling station supply options, not related with the national natural gas grid, are described. Furthermore, the fast-filling charging process is mentioned. Generally, vehicles arrive at the CNG station with a very low pressure inside of their vessels. On the other hand, the station storage presents generally a high pressure, always higher then160 bar. Thus, the vehicles could be partially or totally filled, depending on related volumes pressure level, by simply open the valve connecting vehicle vessels and station's storage. The natural gas flow takes place naturally as a consequence of the pressure difference. This process is generally known as Fast-Filling-Process (FFP), which is going to be used from now on.

3.2.1. Cascade Fast-Filling Configuration

This kind of configuration is designed in order to handle variable refueling demand. It presents a structure similar to that of conventional gasoline and diesel station.

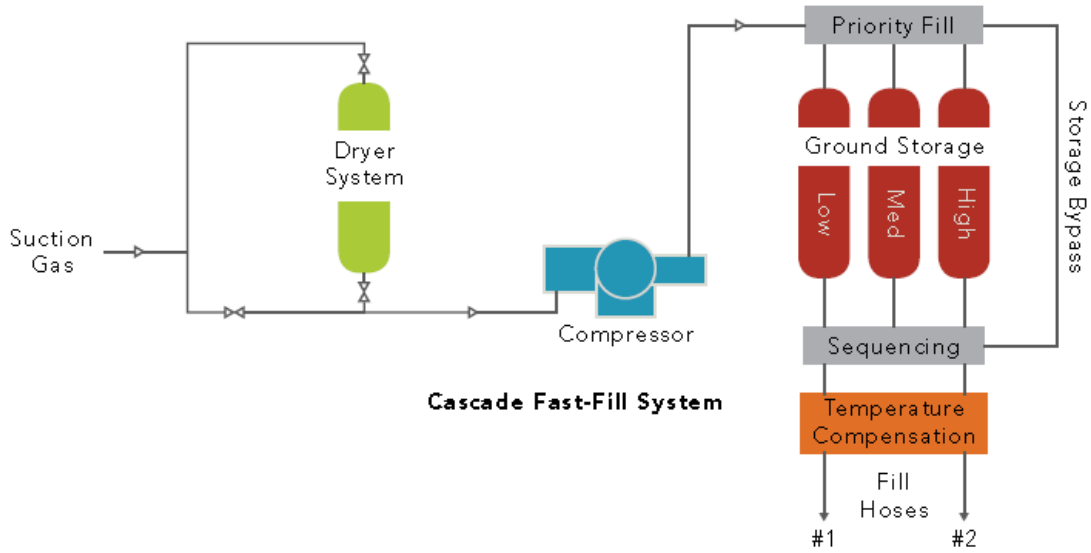

Figure 3.1. Schematic view of the Cascage Fas-Filling CNG station

To achieve quick refueling and fulfilling requirements during the day, a storage properly designed is needed for peak fuel demand. High attention in compressor sizing is mandatory in order to achieve a complete vehicle charge as well as a quick storage refueling. Some cascade fast-filling stations age equipped with a secondary compressor, thus vehicle refueling and NG supply could be easily achieved. Moreover, if a compressor unit is missing due to damage or regular maintenance, the secondary unit could still continue to operate. Figure 3.1 provides a general scheme of such CNG refueling station configuration. As it can be seen, several components can be identified. Considering the station to be supplied by means of national gas grid, the very first unit is characterized by the dryer system. In this system, potential water content or vapor content is removed in order to avoid compressor damage or corrosion issues. Thus, pre-treated natural gas is sent to the compressor unit in which NG is compressed and send into the station storage or directly to the vehicle vessel, if the storage is already fulfilled. A multistage intercooled reciprocating compressor is used to charge the storage system from the pipeline. A priority panel is responsible for vehicles onboard vessel filling sequence, depending on pressure levels. Aim of the sequencing unit is to properly select the right vehicle to be charged in order to minimize the filling time. The temperature compensation unit is responsible for the CNG adjusted temperature. As clearly described in the following section, the higher is CNG temperature, the lower is the filled mass into the vehicle vessel. For this reason, CNG temperature must be regulated, generally by means of ambient temperature cooling units. Finally, not included in Figure 3.1, a dispenser is involved in order to dispense NG into vehicle vessels (Kountz et al., 1996, Kountz et al., 1998a, Kountz et al., 1998b). In buffer CNG refueling stations, storage unit is commonly divided in three separate storages, namely low-pressure storage, medium-pressure storage and high-pressure storage. Vehicles refueling is then achieved from the lower pressure storage to the higher pressure. (Farzaneh et al. 2011). Storage pressure levels are varying between one station to another, depending on manufacturer performance standards.

3.2.2. Buffer Fast-Filling Configuration

The buffer fast-filling configuration allows highly fast vehicle refueling, one after another. For this reason, its main application is generally dedicated to buses and taxi refueling. Commonly, buffer stations are typically on-site fueling stations for a particular type of end-users, thus designed specifically for the needs of such fleet. Figure 3.2 shows a schematic of that CNG station configuration.

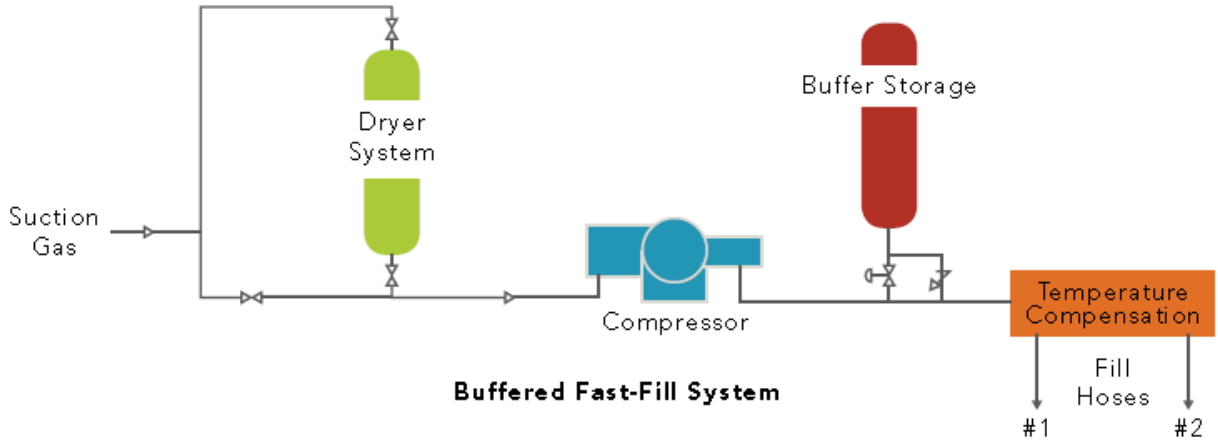

Figure 3.2. Schematic view of the Buffer Fast -Filling CNG station

As it can be seen, several components are nearly the same of those used in cascade fast-filling configuration. Main difference between this station and the previous station is related to the storage strategy. In buffer configuration, the storage is a single storage with a lower total capacity if compared with cascade configuration. Moreover, presenting a pressure level ranging from 205 bar up to 250 bar, it allows vehicle refueling from both storage and compressor. As for cascade configuration, compressors involved in buffer stations are commonly multi-stage intercooled compressors.

3.2.3. Time-Filling configuration

In the time-filling CNG refueling stations, main objectives are reducing operation costs for fleet vehicles following specific paths and always going back to a central location. This station is characterized by high refueling time and it is particular indicated for nighttime refueling. School buses and refuse trucks are generally common applications. Figure 3.3 shows a schematic of such CNG station.

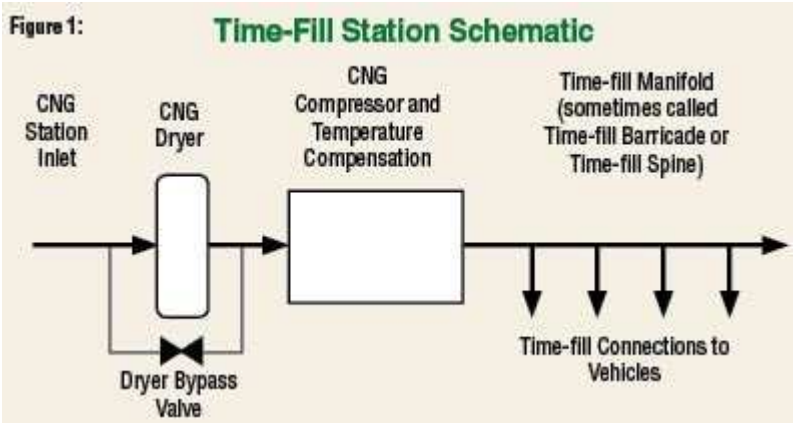

Figure 3.3. Schematic view of the Time-Filling CNG station

Giving the station scheme, main characteristic is represented by time-filling manifold, which allows parallel fuel charging. Moreover, vehicles are fueled from the compressor only, since no storage unit is present. However, specific fleet requirements may need the addition of a small storage unit as well as a fast-filling dispensing system, even if they are generally avoided in order to decrease associated investment cost.

3.2.4. L-CNG Stations

Another possible solution is represented by CNG stations using LNG instead of conventional NG from piping as a feedstock. This particular configuration presents advantages if compared with other conventional CNG refueling stations.

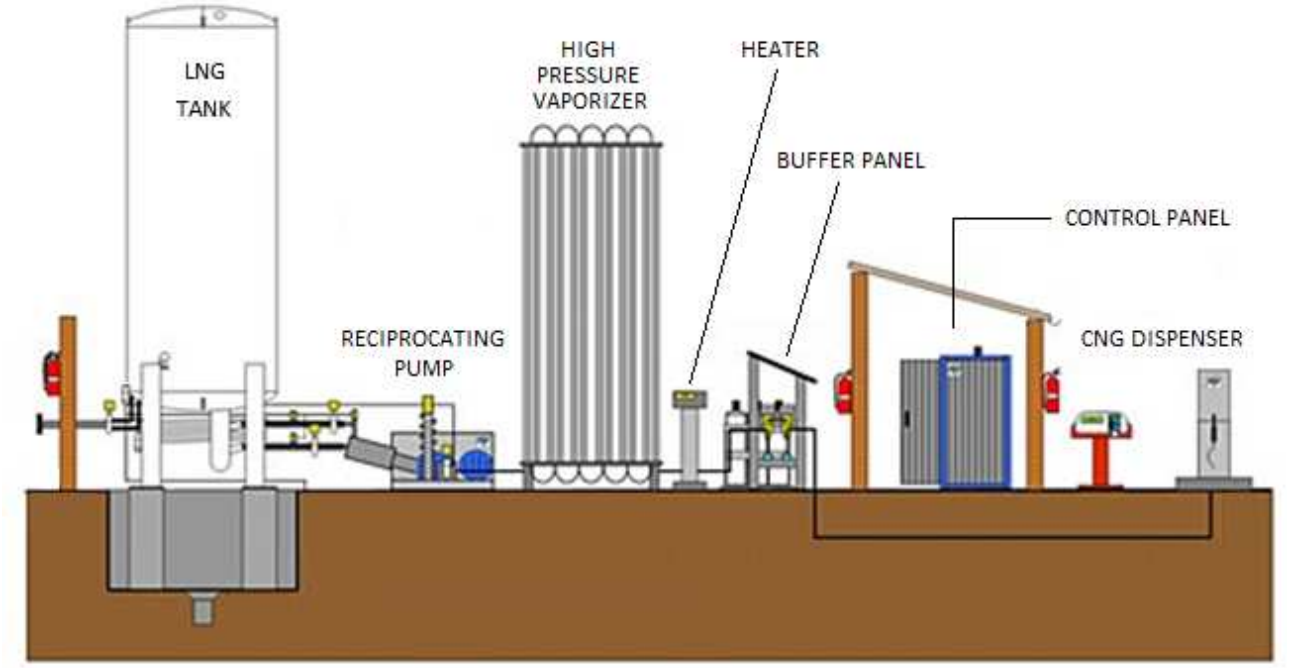

Figure 3.4. Schematic view of an L-CNG refueling station

First of all, because of cryogenic temperatures, liquefied natural gas is almost pure methane, thus, no water, hydrogen sulfide and other compounds are mixed, but only traces of nitrogen, oxygen and hydrogen. This means that no dryer unit or pretreatment is required. Moreover, corrosion, fuel lines plugging and hydrates formation processes are no longer involved. By the way, being almost a pure single compound, it is characterized by quality levels far higher than those presented by CNG. Such properties allow LNG to be successfully employed as vehicle fuel, instead of gasoline. Proper L-CNG refueling station design allows refueling of both heavy-duty and light-duty vehicles, using LNG or CNG respectively. A schematic of the L-CNG stations presented in Figure 3.4. As it can be seen, required equipment in L-CNG refueling stations are substantially different between those involved in CNG traditional refueling stations. LNG is stored in the cryogenic tank able to maintain cryogenic temperatures, avoiding fast liquid methane evaporation. Liquefied natural gas with a minimum pressure of about 2 bar are allowed for those refueling stations. In order to achieve light-vehicle refueling, LNG must be compressed up to the same pressure level as CNG traditional stations and then converted into its gaseous form. Those processes take place by means of the reciprocating pump and high-pressure vaporizer units respectively. Therefore, cryogenic pump allows LNG to be pumped up to high pressure to be sent into the high-pressure vaporizer. This unit is actually a simple heat exchanger in which LNG in constantly vaporized through ambient temperature air. A heater could be also involved in the process to make it quickly. Afterwards the process is similar to that of CNG traditional stations. Buffer and control panels account for control and regulation of several parameters. While the former is responsible for line pressure, vaporizer outlet temperature, buffer pressure and valves, the latter mainly consists of an interface able to allow communication between operators and the system. Finally, the dispenser is responsible for vehicles refueling. Involving a cryogenic pump instead of a standard multi-stage compressor unit, energy consumption related to high pressure level is drastically reduced compared to a CNG station. As a consequence of its particular configuration, very fast filling processes could be achieved, depending on manufacturer adopted technology as well as end-users vehicles. Main disadvantage of this configuration is mainly due to LNG supply.

3.2.5. The Mobile Fuel Supply

In order to achieve NGVs diffusion and NG utilization in the transport sector, infrastructure and supply issues related to natural gas must be overcome. As previously discussed, CNG refueling station supply could be achieved by means of natural gas purchase directly to the national gas grid. However, if the refueling station is far from the national pipeline, NG supply may become difficult. Moreover, with the increasing number of NGVs a constantly

rising number of CNG refueling stations are going to be built. A possible solution is the so called mobile fuel system, also known as 'mother-daughter' system.

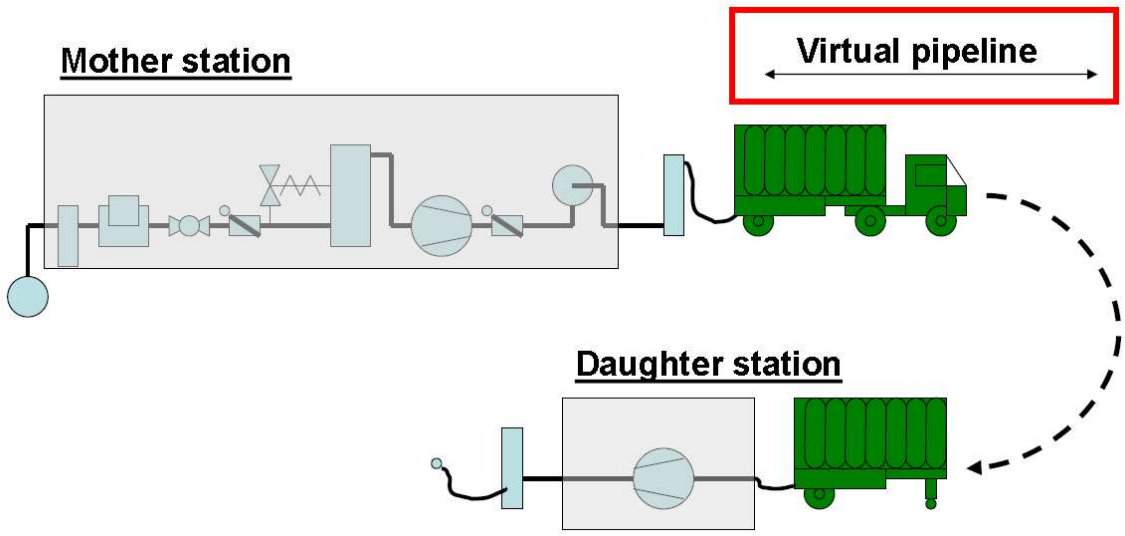

Figure 3.5. Schematic view of the mobile 'Mother-Daughter' process (Source: *Mobile Fuel & Fuelling System Safety, Gijsbrecht van Schoonhoven, at Clean Fuels Consulting Critical Issues Workshop,* CNG & LNG SAFETY: Perception & Reality, Brussels, October 2014.)

Introduced in Italy in the mid-1930s, it allows CNG refueling station supply for those stations far from the national pipeline. Figure 3.5 gives some insight of such process. The process is actually really simple. The mother station is located close to the national natural gas grid. In the station, a dryer system and a compressor system guarantee natural gas pretreatment and compression up to 250 bar. This process is nearly the same of first process discussed for CNG conventional refueling stations. Compressed natural gas from pipeline is further stored in several vessels, which are packed and transported to the daughter station by means of on-road transportation by tracks. In the daughter station, vessels are used for NG supply. Generally, since the required footprint of daughter stations should allow enough vessels to satisfy the CNG vehicle demand, such demand is usually limited, thus this operation is a daily operation. In the daughter station, a compressor unit is placed in order to achieve NGVs proper refueling (Sattari, 2007).

3.3. Alternative CNG: S.TRA.TE.G.I.E. s.r.l. Patent

The S.TRA.TE.G.I.E. s.r.l. is an Italian company founded in 2005. Its central projects are addressed to CNG and LNG innovative systems. Regarding the compressed natural gas, the company files a patent, published in 2009, in which an innovative CNG refueling station configuration was proposed.
The novel configuration is similar to the cascade configuration previously discussed. However, since the main adopted configuration in the Italian market is related with the buffer configuration, aim of the innovation is to compete with such CNG refueling station type. From now on, this novel technology is going to be called 'alternative CNG system'. In this alternative system, main innovations are related to the following aspects:

- Storage charging strategy;
- Storage cooling system.

For the former innovation, a particular charging strategy was developed in order to achieve a reduction in the installed compressor power. In Figure 3.6, a schematic of the compressor for the alternative CNG station is reported.

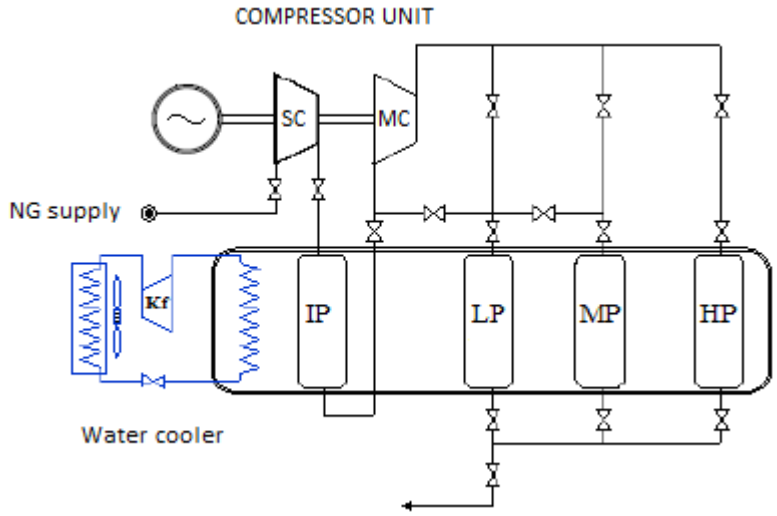

Figure 3.6. Schematic representation of the alternative CNG refueling station (S.TRA.TE.G.I.E. s.r.l. patent)

In the alternative station represented in Figure 3.6, NG coming from the pipeline enters into the main reciprocating multistage compressor unit (MC). Here it is compressed into three different storages following a specific strategy. Each storage has an associated minimum and maximum pressure level. The storages charging process takes place into three main steps. In the first step, NG is compressed into the low-pressure storage (LP) until its maximum related pressure is reached. In the second step, by valves switching, the compressor starts the middle-pressure (MP) storage charge using natural gas stored in the LP storage. Thus, MP storage is charged until one of the following situation is reached:

- LP reaches its minimum pressure level;
- MP reaches its maximum pressure level.

If the former occurs, then related valves are switched back to the first step configuration and LP is charged again. In the third step, something similar to the second step takes place. The high-pressure (HP) storage is charged by means of natural gas stored in the MP storage. During the process, the following situations may occur:

- MP reaches its minimum pressure level;
- HP reaches its maximum pressure level.

However, in any case, the charging control system must restore the configuration related with the second step. In fact, if the former is the case, MP must be refueled again in order to achieve the subsequent HP charge. On the other hand, if the latter occurs, it means that HP has been completely refueled, but MP has not. The iteration of the those three steps, finally allows the complete charge of LP, MP and HP storages. The maximum HP pressure level is 250 bar, the same as in the buffer configuration. Main advantage of this charging system is that the MC unit is charging only one pressure level at a time. This task is accomplished by one, or two at maximum, compressor stages. As a consequence, the required compressor power is drastically decreased. Moreover, the strategy allows to continuously run the MC, avoiding associated start and stop practice which may damage the electric motor, requiring high power peaks. Depending on the natural gas pressure level coming from the pipeline, a secondary compressor (SC) may be required. This compressor provides natural gas compression at an intermediate pressure (IP) level, in order to allow optimal conditions for the MC.

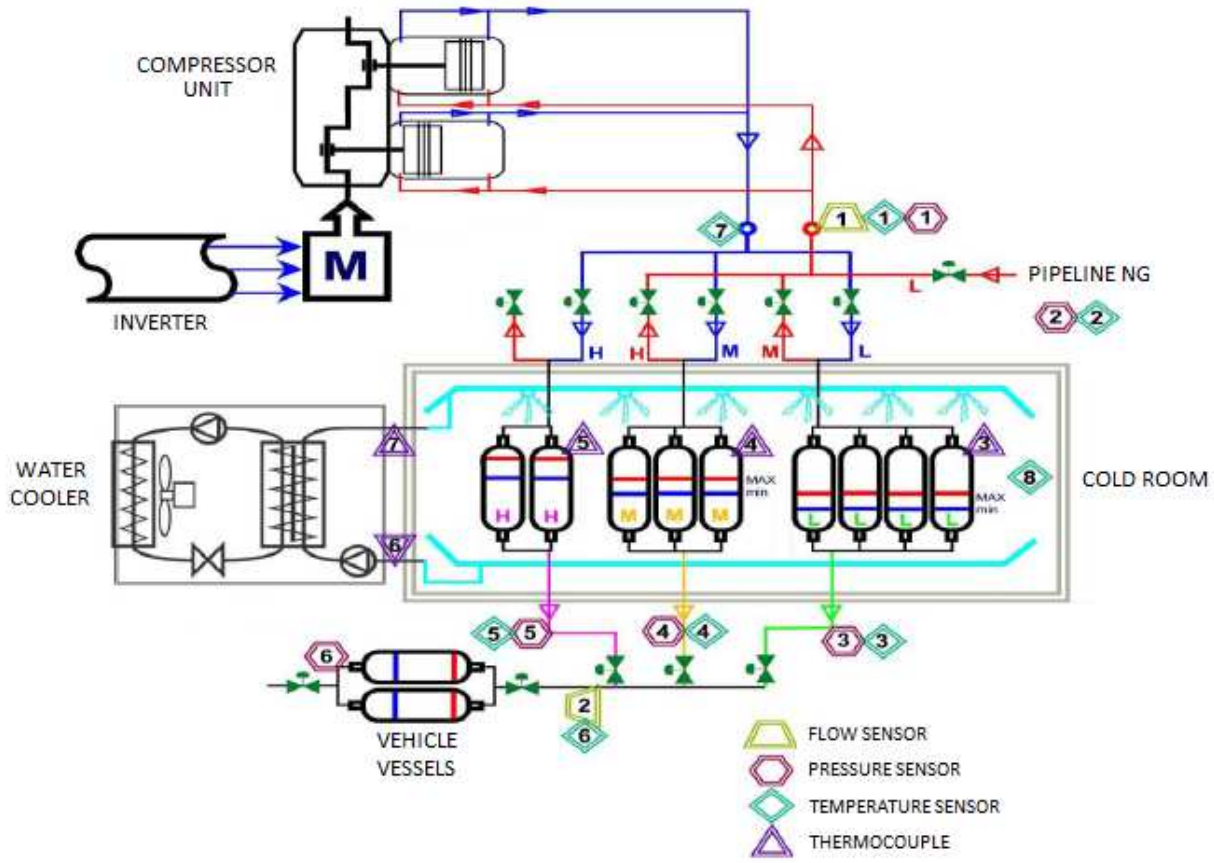

Figure 3.7. Detailed view of the alternative CNG station

The other innovative aspect of the alternative system is related to the storage cooling system. In Figure 3.7 a more detailed scheme of the alternative station is given. The cooling system consists in placing the abovementioned three storages into a cold room. This cold room is cooled down by means of a water cooler. Advantage of this system is mainly related to the limitation of the natural gas temperature increase during the compression process. This unit has two main functions:

- Replacing the air cooler unit;
- Achieve a higher storage charge efficiency.

Regarding the first point, being the main compressor a multistage compressor, generally an air intercooler system is used. However, due to the particular charging strategy adopted in the alternative system, the air cooler could be replaced by a more efficient water cooler in order to cool down both compressed natural gas and stored natural gas. The second function is related with the increasing in stored NG pressure. In fact, during the storage charging process, the gas inside of the storage in compressed to high pressure level, thus its temperature increases. As a consequence, once the maximum pressure is reached, the stored gas presents high temperature levels. However, the stored mass due to this high temperature is lower than the theoretical natural gas mass chargeable if the process runs at constant temperature. Consequently, a lower natural gas mass stored means a decreased number of total vehicles refueled. In the alternative station, in order to avoid the abovementioned critical aspect, a cold room is involved and the charging process is iterated as long as both temperature and pressure levels in the storages are aligned with previously fixed targets. Regarding the vehicle fueling process, the system acts exactly in the same way of that proposed in the cascade configuration, thus FFP occurs starting from the LP storage, followed by the MP and HP storages respectively.

3.4. The CNG Alternative Station Simulation Model

In this section, the CNG alternative refueling station is modeled taking into account every single component and process. The abovementioned alternative system is compared with a conventional CNG refueling. The considered conventional station has a buffer configuration, being the most common configuration in the Italian CNG refueling stations market. Both alternative and buffer station are intended to be on-site, thus no 'mother-daughter' system is

involved in the model. The analysis considers the vehicle refueling only by means of FFP in order to evaluate the maximum number of chargeable vehicles without using the compressor unit. Biomethane is considered to be the feedstock source for the CNG stations, thus they are actually CBG, Compressed BioGas stations.
As a consequence, pure methane is considered in the model, begin biomethane almost 100% of such gas. Thermodynamic and transport properties of methane are computed by means of NIST, Refprop. Regarding the simulation of the proposed CNG station configurations, MathWorks®, Matlab software is employed.
The comparison of the two proposed configurations is based on total power required for the compressor, storage volume, time and energy necessary for the storage charging process, total stored mass, as well as biomethane temperature and pressure conditions at the end of the storage charging process. Moreover, the time for the vehicle refueling process, final biomethane temperature and total charged mass at the end of the FFP are calculated both for alternative and buffer CBG configuration.

3.4.1. Multistage Reciprocating Compressor

One of the most important equipment involved in the CNG refueling stations is the reciprocating compressor. Reciprocating compressors are used in a wide range of industrial applications, such as refineries and power plants and refrigeration system just to mention a few. This is mainly due to their ability to operate in a wide range of pressure ratios and mass flow rates (Cierniak, 2001). In the CNG refueling stations, such compressor is generally a multistage compressor which involves 3-4 compressor stages (Farzaneh-Gord et al., 2014, Farzaneh-Gord et al., 2012). It is also the major item in investment costs as well as in operative costs due to electrical input work (Farzaneh-Gord et al., 2012). Many models for reciprocating compressors were proposed by several researchers. Such models are generally referred to as global models and differential models. In any case, the central value is the crank angle, which is the angle between the crankshaft and the piston axes (Stouffs et al., 2000). In the present analysis both design and operation conditions of the reciprocating compressor are taken into account.

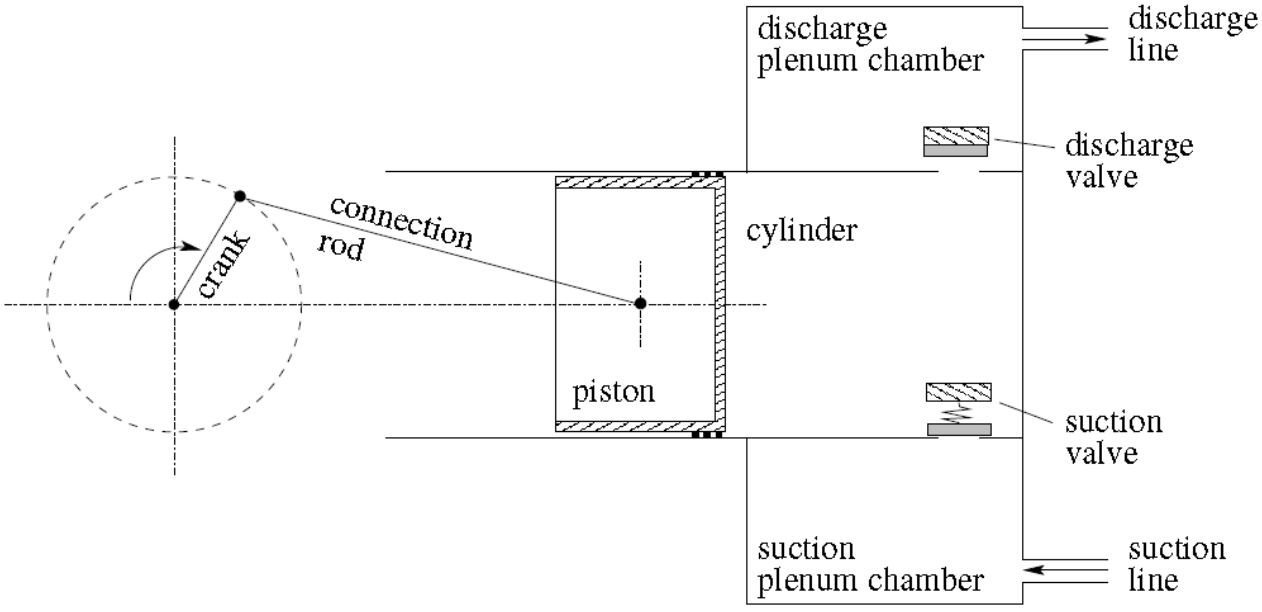

Figure 3.8. Schematic view of the compressor cylinder and its cinematic governed by the crankshaft (Habing, 2005)

Figure 3.8 shows a schematic representation of a single stage reciprocating compressor. As it can be seen, the cinematic of the compressor is completely dependent on the crankshaft motion. Its rotary motion is converted to a linear motion related with the piston, by means of a connecting rod. Such movement is followed by a periodically increasing and decreasing chamber volume. A suction valve and a discharge valve are then opened and closed alternatively in order to allow a certain gas flow into the chamber. The ideal thermodynamic cycle of a reciprocating compressor is reported in Figure 3.9, while Figure 3.10 provides a schematic view of the main phases of the compression process.

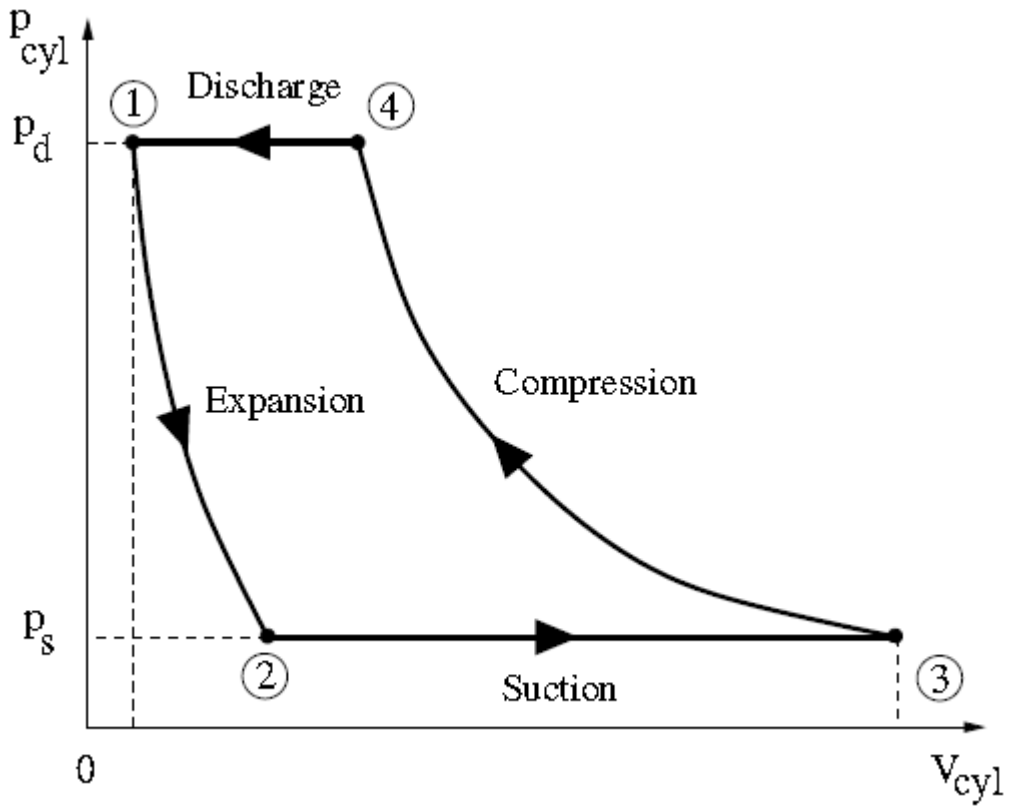

Figure 3.9. Thermodynamic ideal cycle for the single stage compressor

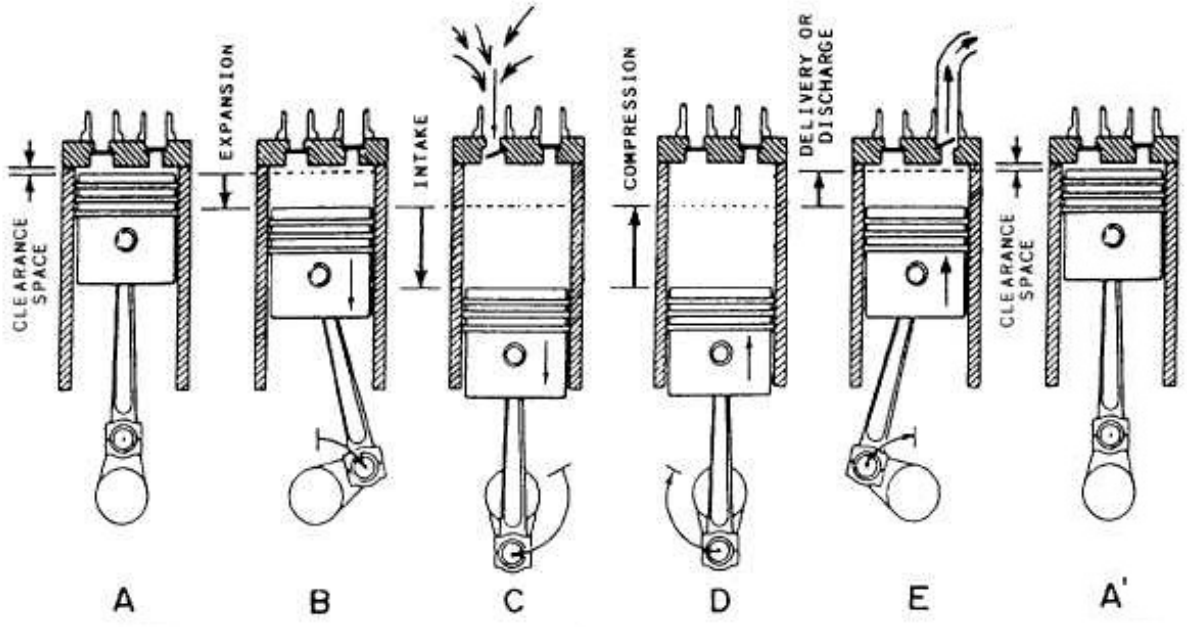

Figure 3.10. Compression stages and associated valve displacement

Point 1 in Figure 3.9 corresponds to the piston position A in Figure 3.10. The volume between the piston and the cylinder head is known as ‘clearance volume’ (CV). This configuration is called Top Dead Centre (TDC) defined as the farthest piston position from the crankshaft. As the crankshaft begins its rotation, the piston displacement allows an increasing volume inside of the cylinder. At this moment, the internal pressure is still higher than that in the suction chamber, thus gas inside the compression chamber is expanded due to the piston motion. When the

internal pressure is lower than the suction pressure, the suction valve begins to open and gas flows into the cylinder. The very beginning of this process is represented by point 2 in Figure 3.9, corresponding to the piston position B in Figure 3.10. As the crankshaft continues its rotary motion, the gas continues to flow inside the cylinder at constant pressure, reaching point 3 in Figure 3.9 and C configuration in Figure 3.10. At this moment, the pressure inside the cylinder is equal to that inside the suction chamber, thus the suction valve is closed, that is the configuration D represented in Figure 3.10. This configuration is called Bottom Dead Centre (BDC), defined as the nearest piston position from the crankshaft. Considering point 1 and point 3 in Figure 3.9, the related net volume is called compressor displacement (CD). On the other hand, the volume related to point 2 and point 3 in Figure 3.9 is the effective compressor displacement (ECD), representing the theoretical maximum gas volume to be sucked from the suction chamber and to be discharged into the discharge chamber. Thus, the crankshaft rotation speed is strictly related with the theoretical maximum gas volume flow rate. As the crankshaft continues its rotation, the gas inside the cylinder is compressed. This is due to the fact that the suction valve is now closed, being internal pressure higher than that of the suction chamber. Moreover, at this moment the internal pressure is still lower than that of the discharge chamber. When the gas pressure inside the cylinder is higher than that in the discharge chamber, the discharge valve begins to open and the gas is discharged into the discharge chamber. The very beginning of this process, corresponds to point 4 in Figure 3.9 and to piston position E in Figure 3.10. From now on, the gas is discharged at constant pressure, until the piston reaches again the TDC position, represented by point 1 and situation A' in Figures 3.9 and 3.10 respectively. At this point, the discharge valve is closed again, since internal pressure is now lower or equal to that of discharge chamber, but still higher than that in the suction chamber, thus suction valve is closed too.
Considering Figure 3.9, several considerations may be done. Referring to the cylinder volume associated with points 1, 2 and 3, an important parameter is found.

$$CD = V_1 - V_3 \qquad (1)$$

$$ECD = V_2 - V_3 \qquad (2)$$

$$\lambda = \frac{ECD}{CD} = \frac{m_s}{\rho_s * CD} \qquad (3)$$

Where CD and ECD are compressor displacement and effective compressor displacement respectively, as previously mentioned, m_s, ρ_s are the gaseous mass coming from the suction chamber and its density respectively and λ is the cylinder filling ratio. This geometric parameter represents the ratio between the volume of gas that is actually sucked by suction chamber and the theoretical volume of gas which the cylinder could suck from suction chamber. Being related with the CV, this parameter strongly influences compressor efficiency. Back to Figure 3.9, another definition of cylinder filling ration could be obtained. Since expansion and compression processes involved during the piston movement are adiabatic transformations, the following equations are obtained:

$$(P_1 * V_1)^k = (P_2 * V_2)^k \rightarrow \frac{V_2}{V_1} = \left(\frac{P_1}{P_2}\right)^{\frac{1}{k}} = \beta^{\frac{1}{k}} \qquad (4)$$

$$\lambda = 1 - \mu * \left[\left(\beta^{\frac{1}{n}}\right) - 1\right] \qquad (5)$$

$$\mu = \frac{V_3}{CD} \qquad (6)$$

Where P_1 and P_2 are the pressures associated with volumes V_1 and V_2, k is the polytrophic index of the gas related with the suction chamber temperature and pressure levels and β is the compressor pressure ratio. Considering equation (3), m_s represents the gas mass theoretically sucked and discharged at the end of a crankshaft revolution. Thus, the theoretical gas mass flow rate of the compressor is given by the following equation:

$$\dot{m}_C = m_s * \frac{60}{rpm} \qquad (7)$$

Where $\dot{m}_C$ is the theoretical mass flow rate [kg/s] of the compressor, while rpm represents rotations per minute of the crankshaft. Combining equations (3), (5) and (7), the theoretical mass flow rate of the compressor is given as a function of geometric properties and pressure ratio of the compressor.

$$\dot{m}_C = \rho_s * CD * \left\{1 - \mu * \left[\left(\beta^{\frac{1}{n}}\right) - 1\right]\right\} \quad (8)$$

Regarding the compressor displacement, another relation can be found. Figure 3.11 represents a schematic view of the piston movement related with crankshaft. Knowing the CD factor and a, representing the crank length of the compressor, the compressor bore (CB) can be easily calculated as follows:

$$CB = \sqrt{\frac{4*CD}{\pi*a}} \quad (9)$$

Relations (8) and (9) can be used in order to achieve a first sizing of a single stage reciprocating compressor.
Back to Figure 3.11, some considerations related with the piston cinematic can be made. Considering the TDC point to be in x = 0, then the associated crankshaft angle α is equal to 0 too.

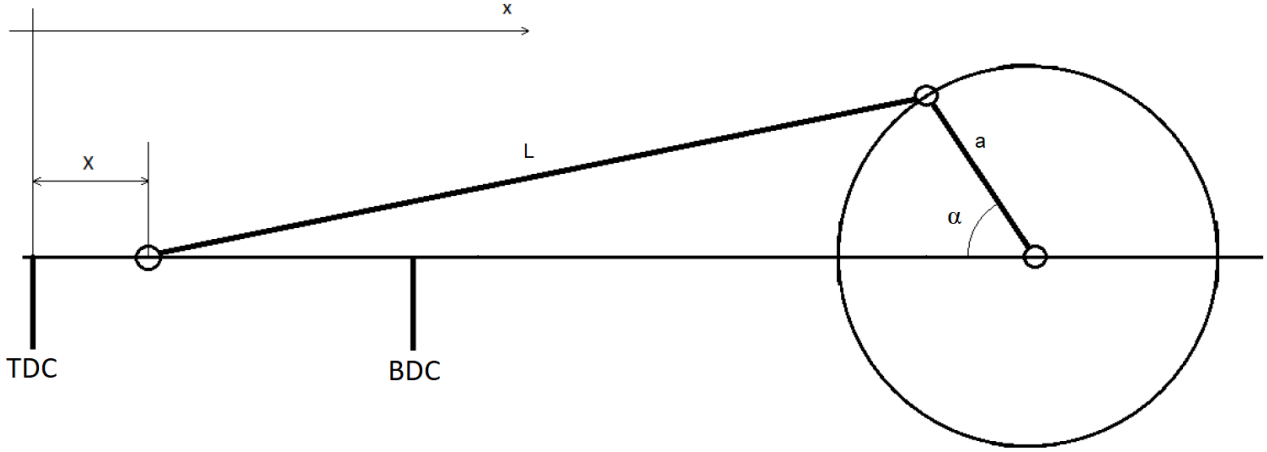

Figure 3.11.Analysis of the piston and crankshaft cinematics

The fundamental equation for the piston position x and speed v as a function of the crankshaft angle α is as follows:

$$x(\omega) = a * \left[1 - \cos\alpha + \frac{1}{r} * \left(1 - \sqrt{1 - (\mathrm{r} * \sin\alpha)^2}\right)\right] \quad (10)$$

$$v(\omega) = a * \omega \left[\sin\alpha + \frac{r*(\sin 2\alpha)}{2*\sqrt{1-(r*\sin\alpha)^2}}\right] \quad (11)$$

$$r = \frac{a}{L} \quad (12)$$

$$\omega = 2 * \pi * \frac{rpm}{60} \quad (13)$$

Where a and L, are lengths of crank and connection rod respectively, while ω represents the angular speed related with the crankshaft rotation. The crank length is also exactly half of the stroke length. By combining equations (9) and (10) the instantaneous volume of the cylinder is given according to the following equation:

$$V(\omega) = CV + \left(\pi * \frac{CB^2}{4}\right) \quad (14)$$

The abovementioned relations allow to achieve a first attempt sizing of a single stage of the compressor by means of a few number of geometric parameters and specifications. However, since the CBG station requires a multistage reciprocating compressor, a multistage model of the compressor is necessary. In Figure 3.12, a schematic view of a two-stage reciprocating compressor is presented.

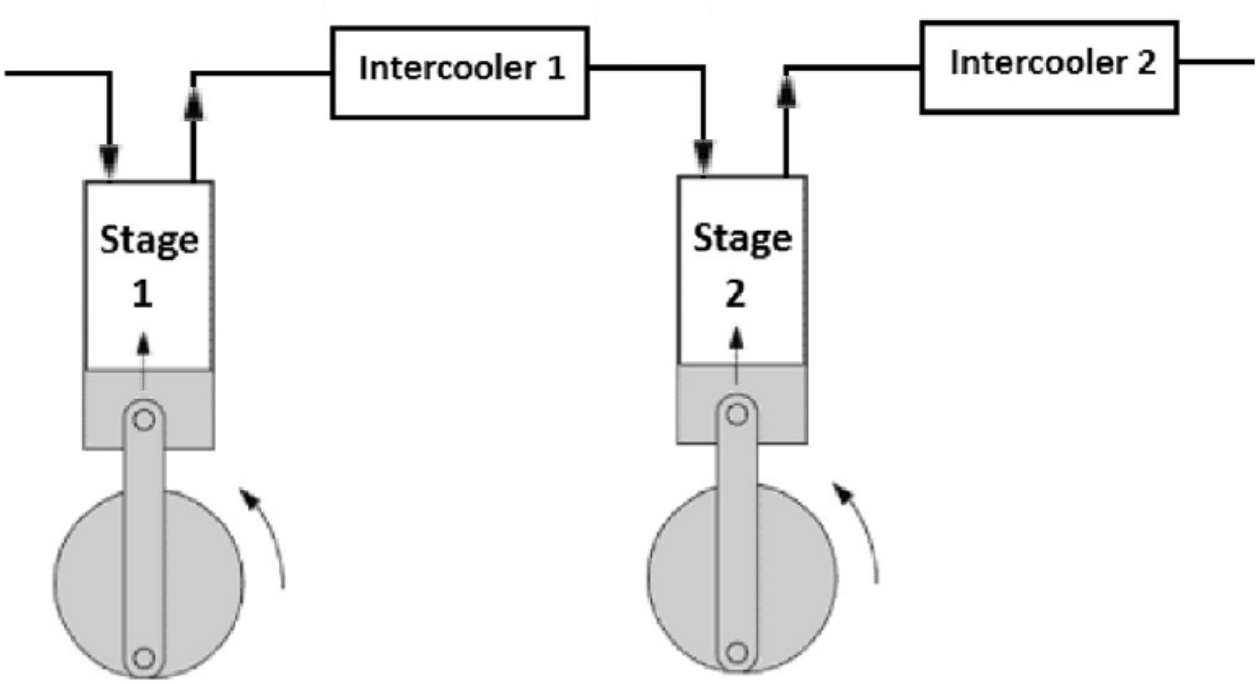

Figure 3.12. Schematic view of a multistage intercooled reciprocating compressor

The multistage reciprocating compressor is a particular compressor able to work with a high-pressure ratio. It is strictly necessary in order to achieve very high-pressure levels. A single stage compressor is unfeasible to achieve the same results for essentially two reasons:

- High-pressures means high volumes for the compression process;
- Very high related temperatures.

For the former reason, Figure 3.9 may give some information. Since the compression process (from points 3 to point 4 in the figure) is an adiabatic process, achievable maximum pressure in the compressor is strictly related with compressor displacement. As a consequence, to increase the gas pressure to very high levels, CD should be very high, thus footprint of the compressor is dramatically increased. Furthermore, by increasing the gas pressure in a close volume, assuming no heat is transferred through the cylinder and piston walls, the gas temperature would increase as a consequence. Considering the compression process in Figure 3.9 from point 3 to point 4, from the ideal gas law and the equation (4), one may conclude the follow equation:

$$\frac{T_4}{T_3} = \left(\frac{P_4}{P_3}\right)^{\frac{k-1}{k}} = \beta^{\frac{k-1}{k}} \qquad (15)$$

Thus, the higher the pressure ratio, the higher the final compressed gas temperature. In order to achieve high-pressure levels without increasing the gas temperature, an isothermal compression process should be performed. However, this kind of process is just an ideal process and a real compressor could not obtain such a result. By the way, a multistage compressor is able to approach a similar compression by means of several, intercooled stages. Thus, each compression stage is able to increase gas pressure with a certain pressure ratio. The gas is then cooled in air-cooler or water-cooler, depending on the cooling fluid. Then, a second compression stage accounts for further gas compression and subsequent cooling, until the required final pressure is reached. In Figure 3.13 the adiabatic compression process is compared with an isothermal compression process.

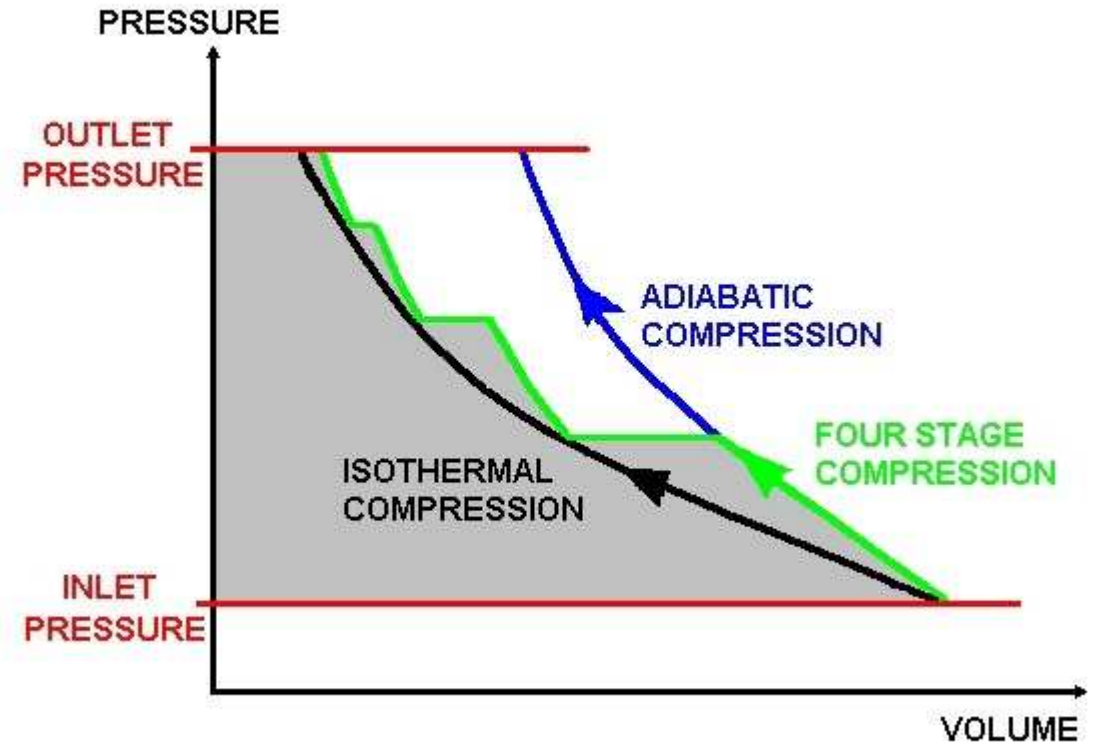

Figure 3.13. Comparison between the compression process of the single and multistage compressor

As it can be seen, the adiabatic compression by means of a single stage (blue curve in the figure), is characterized by high gas final temperature levels. On the other hand, a multi stage compression process (the green curve in the figure), is able to approach an isothermal compression (represented by the black line in the figure). As a consequence, the final gas pressure is reached with a limited gas temperature rise. The number of stages depends on the overall pressure ratio. The PR of each stage should achieve the optimal compressor performances. The following relation expresses the pressure ratio of a stage as a function of the total pressure ratio:

$$\beta_s = \sqrt[n]{\beta_T} \qquad (16)$$

Where β_s and β_T are the PR of the single storage and the overall PR of the compressor respectively. This relation achieves minimum compression work during the process. The number of stages should be enough to avoid too high stage temperatures. In order to achieve a first attempt of sizing a multi stage reciprocating compressor, the following considerations are made:

- The mass discharged in the i-th stage is the same of that entering in the i+1-th stage;
- The nominal compressor mass flow rate is related with the very first stage.

Regarding the first point, the gas mass contained into the cylinder of the i-th stage is considered as a control volume. For this control volume, the following equation may be written:

$$\frac{dm_V}{dt} = (\dot{m}_s - \dot{m}_d) \qquad (17)$$

Where $\dot{m}_s$ and $\dot{m}_d$, are suction and discharge mass flow rate respectively. The term $\frac{dm_V}{d\alpha}$ indicates the mass of the gas inside the control volume as a function of time. Considering the multistage compressor, the subsequent equation can be written:

$$\frac{dm_V}{dt}(i) = -\frac{dm_V}{dt}(i+1) \qquad (18)$$

where the index i indicates the i-th compressor stage. As previously mentioned, this relation assesses that gas mass flow rate is the same in every single compressor stage during the compression process.
Regarding the second point, it represents a fundamental relation in order to achieve a first sizing attempt of each stage. In fact, considering equation (3), the compression mass flow is related with suction conditions. Moreover, equation (18) assesses that this mass flow is the same for each stage. As a consequence, the mass flow rate of the multistage reciprocating compressor is strictly related to geometry and suction conditions (temperature and pressure) of the first stage. Once the first stage is sized, the following could be sized as well on the basis of the same considerations. This is possible because the following characteristics are the same for each stage:

- The crankshaft rotation speed;
- The stroke length.

In order to achieve a comprehensive compressor sizing, the valve motion is taken into account. A schematic view of a compressor valve is presented in Figure 3.14.

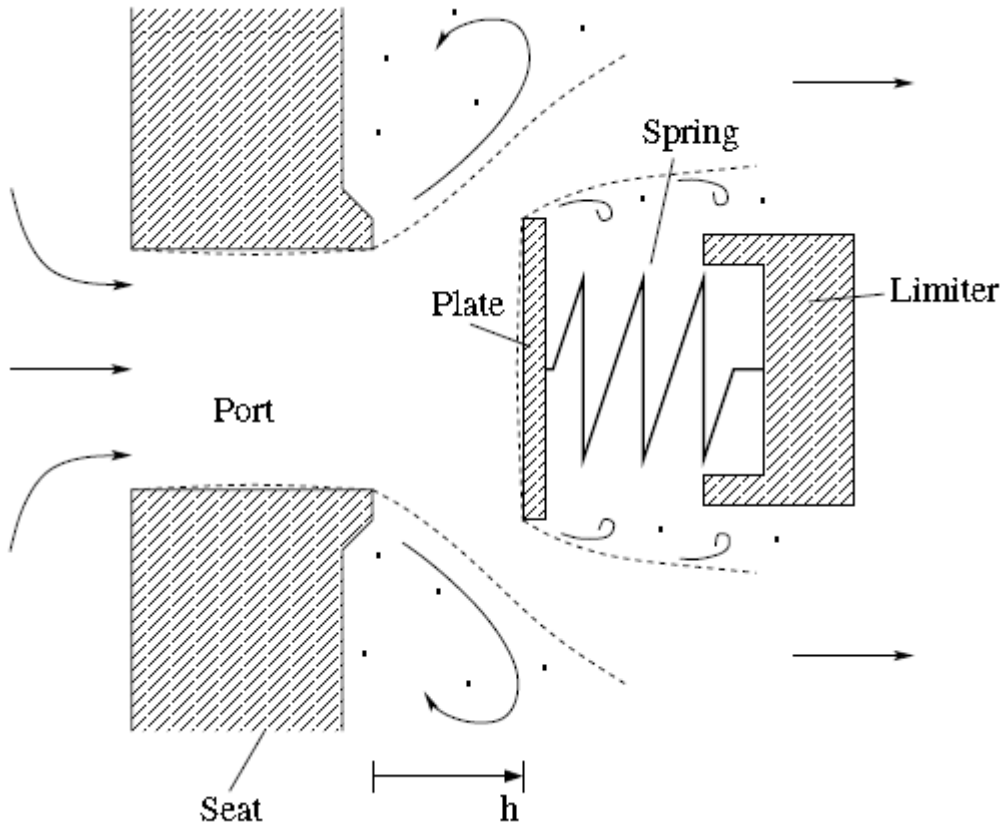

Figure 3.14. Schematic view of the plate valve movement

Figure 3.14 representes a discharge valve, but the same considerations could be made also for the suction valve. As shown, the valve comprehends several components. The port is the bore in which the mass flow takes place once the valve is open. The plate and the spring represent the key components, responsible for the opening and closing of the port. The plate and the spring could be considered as a single part. In fact, reciprocating compressors generally involve plate valves. This means that a metal plate is used as a valve. Being deformed by means of different pressures acting on its surfaces, it also acts as a spring with a certain preload force. In order to keep the plate in its right position, a seat and a limiter are provided to this purpose. In order to achieve a first sizing attempt of the compressor, several information are required. The plate valve sizing is related to:

- Port area sizing;
- Plate area and mass sizing;
- Spring sizing.

Regarding the port area sizing, the maximum achievable volume flow rate is used as a key factor. In fact, the gas flow through the port area cannot be higher than the corresponding speed of sound of the gas itself (Pandeys, 1986). Considering this aspect, the port area is given by the following equations:

$$A_s = \frac{\dot{V}_s}{M * c_s} \quad (19)$$

$$A_d = \frac{\dot{V}_d}{M * c_d} \quad (20)$$

Where A_s, A_d, $\dot{V}_s$, $\dot{V}_d$, c_s and c_d are the port area, volume gas flow and the gas speed of sound for the suction and the discharge areas respectively. M represents the maximum Mach number, according to the required specifications. The volume flow rate is a function of the gas density in the suction and discharge areas, thus:

$$\dot{V}_s = \frac{\dot{m}_s}{\rho_s(T_s, P_s)} \quad (21)$$

$$\dot{V}_d = \frac{\dot{m}_d}{\rho_d(T_d, P_d)} \quad (22)$$

Where P and T terms are pressure and temperature conditions of suction and discharge chamber, respectively. Thus, once the operative conditions of the suction and the discharge chambers are defined, a first sizing of the port area can be achieved, referring to nominal operating conditions, as a function of the gas volume flow.
Considering the valve plate, as already mentioned, this component is crucial being the main responsible for the gas flowing into and out the cylinder. The associated model of the plate valve is generally a model in which a rigid plate and a spring can be distinguished (Figure 3.14). In this model, the same assumptions are adopted. In order to define geometric ratios related to this component, a real natural gas multistage reciprocating compressor was used as a reference (FORNOVOGAS®).

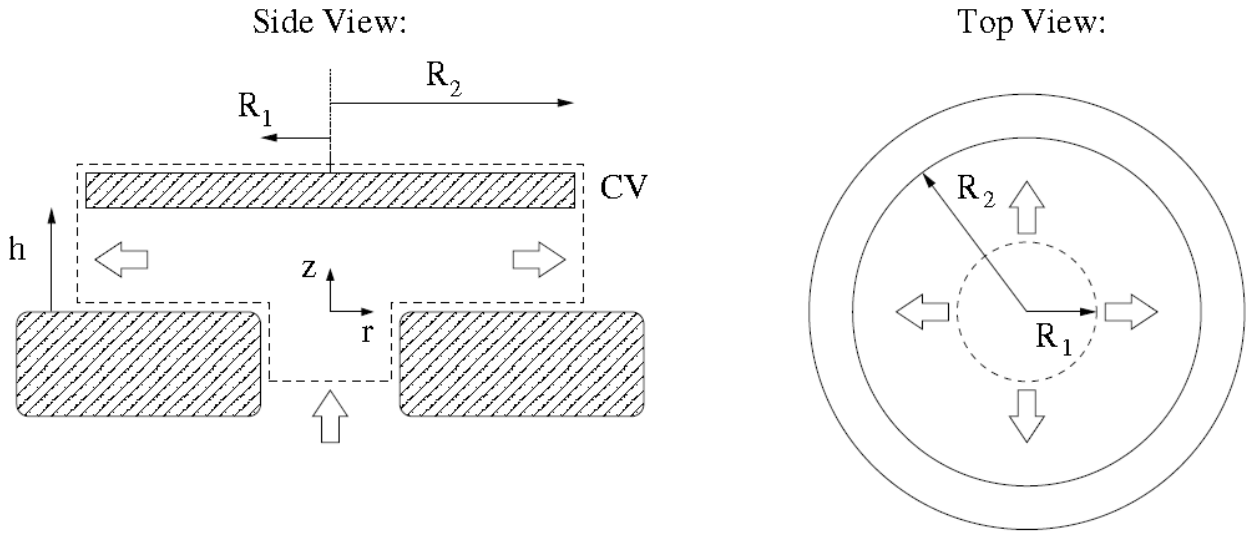

Figure 3.15. Schematic view of the plate valve model and flowing gas

The plate valve can be schematically represented as in Figure 3.15. Looking at the figure, a useful parameter can be defined as follows:

$$S_{ratio} = \frac{R_1}{2 * h_{max} * R_2} \quad (23)$$

Where R_1, R_2 and h_{max}, are the port and plate radius and maximum plate valve displacement during the gas flow respectively. This parameter, obtained by means of real reciprocating compressor data, allows a first attempt size of the plate geometry. This assumption is considered for both suction and discharge plate valves. Moreover, it was also possible to calculate the plate mass as a function of its geometry and density. To this purpose, several plate valves were analyzed in order to evaluate general geometry considerations as well as calculating characteristic density. Thus, the plate mass is obtained as follows:

$$M_p = V_p * \rho_{steel} \quad (24)$$

Where V_p and ρ_p, are the plate volume and the associated steel density.
Regarding the spring component, (Pandeys, 1986) the following relations are proposed:

$$K_s = 0.1 * \frac{P_s * A_s}{h_{s-max}} \quad (25)$$

$$K_d = 0.1 * \frac{P_d * A_d}{h_{d-max}} \quad (26)$$

Being K_s and K_d suction and discharge valve spring stiffness respectively. Back to the equations from (19) to (22) referring to the valves port area as a function of the gas volume flow. The gas volume flow is also a function of upstream density, valve opening and pressure difference between in-cylinder and external chambers. Giving these assumptions, a quasi-steady volume flow rate through the suction and discharge valves can be written as follows (Habing,):

$$\dot{V}_s = \alpha_s * \varepsilon_s(T_s, P_s) * L_s * h_s * \sqrt{\frac{2*(P_s - P_V)}{\rho_s}} \quad (27)$$

$$\dot{V}_d = \alpha_d * \varepsilon_d(T_d, P_d) * L_d * h_d * \sqrt{\frac{2*(P_V - P_d)}{\rho_d}} \quad (28)$$

Where α_s, α_d, ε_s and ε_d, are semi-empirical coefficient and compressibility factor of suction and discharge valve respectively. L_s and L_d are the total edge length of the plates, h_s and h_d represents the valves opening while P_V is the pressure of the in-cylinder chamber. While the compressibility factor is related with the gas thermodynamic properties, the semi-empirical coefficient is given as a function of the valve displacement and is generally obtained by means of experimental analysis. In Figure 3.16, the semi-empirical coefficient is represented as a function of the ratio between the actual valve displacement and its maximum displacement, according with (Habing, 2005). The estimated semi-empirical coefficient is also related to the gas flow physical properties during the suction and the discharge processes. It was seen that the viscous flow solution can only apply to very small valve openings, while the inviscid flow solution can only apply to large valve opening. Considering this aspect, also the gas force acting on the plate surface during its flow can be defined, depending on the viscous or inviscid flow assumptions. As for the suction process, the gas force is referred to the gas coming from the suction chamber, while during the discharge process, the gas force is related with that of the gas discharged from the in-cylinder chamber. Considers the Figure 3.15. Regarding the viscous flow assumption, the following equations are derived:

$$F_{g,s} = \frac{1}{\ln\left(\frac{R_{2,s}}{R_{1,s}}\right)} * (P_s - P_V) * \pi * \left(R_{2,s}^2 - R_{1,s}^2\right) \quad (29)$$

$$F_{g,d} = \frac{1}{\ln\left(\frac{R_{2,d}}{R_{1,d}}\right)} * (P_V - P_d) * \pi * \left(R_{2,d}^2 - R_{1,d}^2\right) \quad (30)$$

Where F_g is the gas force acting on the valve plate while the gas is flowing. The other terms are easily derived from the previous considerations. Regarding the inviscid flow assumption, the following equations are obtained:

$$F_{g,s} = \left[1 - \ln\left(\frac{R_{2,s}^2}{R_{1,s}^2}\right) + \frac{4}{R_{1,s}^2} * h_s^2\right] * \frac{1}{2} * \rho_s * u_{1-2,s}^2 * \pi * R_{2,s}^2 \quad (31)$$

$$F_{g,d} = \left[1 - \ln\left(\frac{R_{2,d}^2}{R_{1,d}^2}\right) + \frac{4}{R_{1,d}^2} * h_d^2\right] * \frac{1}{2} * \rho_V * u_{1-2,d}^2 * \pi * R_{2,d}^2 \quad (32)$$

Where $u_{1-2,s}^2$ and $u_{1-2,d}^2$ are the gas flow speed through the valve during the suction and discharge process.

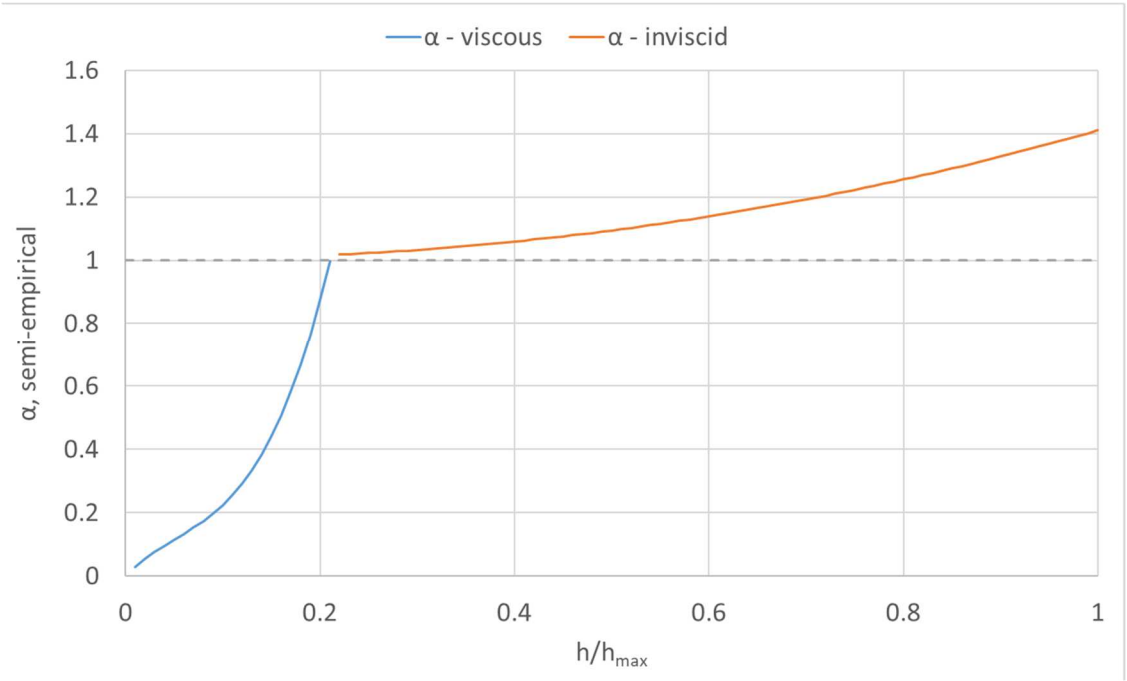

Figure 3.16. α-semiempirical coefficient as a function of the relative valve displacement

The definition of the dynamic behavior of the plate valve is of paramount importance begin this component the main responsible for gas flowing through the compressor stages. In fact, in reciprocating compressors, suction and discharge valves are not driven by the crankshaft rotation (that is the case of compressor engines), but their motion is dependent on the pressure level inside the cylinder and in the suction and discharge chambers, as it can be seen in equations (27) and (28). Several models are available in literature. (Nieter, 1984) proposed a model in which the valve motion is a function of the crankshaft angle and pressure levels. The related equations are as follows:

$$\frac{d^2x_s}{d\alpha^2} = \frac{1}{m_s*\omega^2} * \left[-k_s * \omega_s + C_{fs} * A_s * (P_s - P_V) + F_{ps}\right] \quad (33)$$

$$\frac{d^2x_d}{d\alpha^2} = \frac{1}{m_d*\omega^2} * \left[-k_d * \omega_d + C_{fd} * A_d * (P_V - P_d) + F_{pd}\right] \quad (34)$$

Where F_{ps}, F_{pd}, C_{fs} and C_{fd} are preloaded forces applied on suction and discharge valves and coefficients accounting for energy losses through the orifice, respectively. A_s and A_d are the suction and discharge valve areas respectively (Boswirth, 2000; Boswirth, 2001). While giving good results for a steady state analysis, the model seemed to be not stable when suction and discharge chamber levels are continuously changing during the time. Since the present analysis aims to model the reciprocating compressor of a CBG station during the storage charge, a model based on the forces balance is proposed for the valve plates. In the Figure 3.17, an overview of the forces acting on the plate valve during the gas flow is presented.

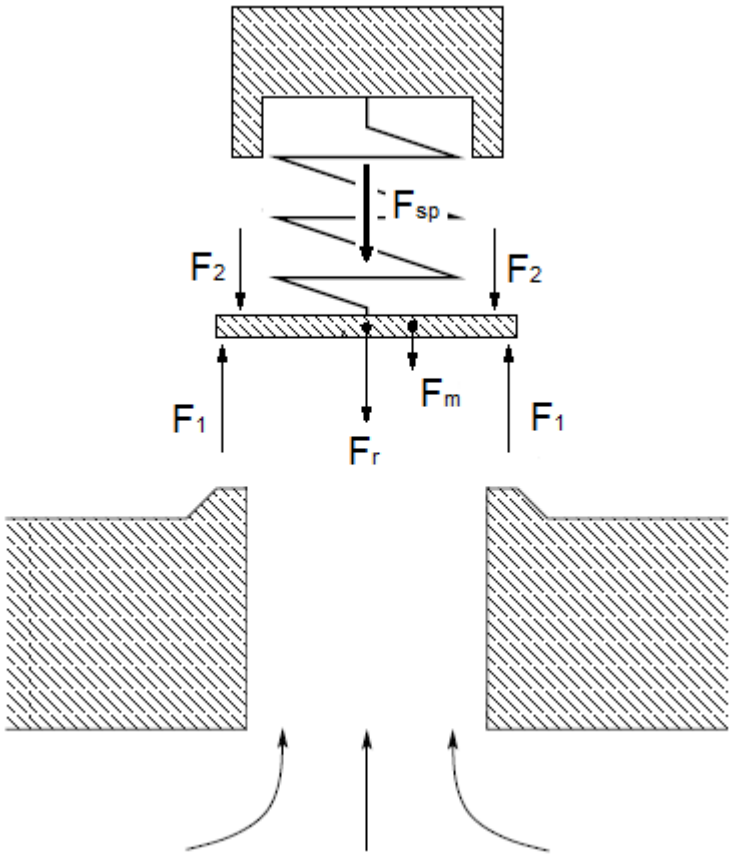

Figure 3.17. Balance of the forces and pressures acting on the valve (Habing, 2005)

Considering the proposed approach, several forces can be identified, thus an instantaneous balance can be written as follows:

$$F_r = F_1 - F_2 - F_{sp} - F_m \quad (35)$$

$$F_{sp} = K_{sp} * [x_0 - h(t)] \quad (36)$$

$$F_r = M_p * \frac{d^2h}{dt^2} \quad (37)$$

The terms in the above equations are as follows:

- F_r is the resultant force of the forces balance applied to the plate valve;
- F_1, F_2 are the forces related to the static pressures acting on the plate valve; during the suction process, they are related to the suction chamber and the in-cylinder chamber pressures respectively, while in the discharge process, they are related to the in-cylinder chamber and the discharge chamber pressures respectively;
- F_{sp} represents the force associated with the spring, therefore it is a function of the plate valve displacement;
- F_m is the force associated with the weight of the plate valve;
- X_0 is the spring compression related with its preload; it is found by considering the preload force and the spring stiffness.

Considering a quasi-steady analysis, the equation (37) can be finally used in order to find the present plate valve displacement, given by the following equations:

$$a_p(t_i) = \frac{d^2h}{dt^2} \quad (38)$$

$$u_p(t_i) = u_p(t_{i-1}) + a_p(t_i) * \Delta t \quad (39)$$

$$h(t_i) = h(t_{i-1}) + u_p(t_{i-1}) + \frac{1}{2} * a_p(t_i) * (\Delta t)^2 \quad (40)$$

where Δt is the time step adopted, given by $t_i - t_{i-1}$, while u_p is the speed of the plate valve at the given time. Main assumptions of this model are related to the quasi-steady assumption and to the simplification of the valve motion to be a uniformly accelerated motion for each time step of the compression process.
The thermodynamic properties of the fluid during the whole compression process are related to the first thermodynamic law:

$$\dot{Q}_V + \sum\left[\dot{m}_s * \left(h_s + \frac{u_s^2}{2}\right)\right] = \sum\left[\dot{m}_d * \left(h_d + \frac{u_d^2}{2}\right)\right] + \frac{d}{dt}\left[m * \left(U_S + \frac{u^2}{2}\right)\right]_V + \dot{W}_V \qquad (41)$$

Where $\dot{Q}$, $\dot{m}$, h, u, U_S and $\dot{W}$ represent heat transfer, mass flow rates, enthalpy, speed, specific internal energy and work rate, respectively. Moreover, the subscripts s, d, and V are related to the suction, discharge and in-cylinder chambers, respectively. In the equation, the potential energies are neglected. Since the compression process involves suction and discharge process, the velocity terms cannot be neglected. However, considering the compression and expansion phases associated with the in-cylinder gas with closed suction and discharge plate valves, velocity terms related to in-cylinder volume can be neglected. Writing (41) in its differential form, the following equation is found:

$$\frac{dQ_V}{dt} + \frac{dm_s}{dt} * h_s = \frac{dm_d}{dt} * h_d + \frac{d(m*U_s)_V}{dt} + \frac{dW_V}{dt} \qquad (42)$$

Regarding the work rate associated with the compression process, it can be written as follows:

$$\frac{dW_V}{dt} = P_V * \frac{dV_V}{dt} \qquad (43)$$

Where V_V is the instantaneous in-cylinder volume. Equations (42) and (43) can be combined in order to obtain the following equation:

$$\frac{dQ_V}{dt} + \frac{dm_s}{dt} * h_s = \frac{dm_d}{dt} * h_d + \frac{d(m*U_s)_V}{dt} + P_V * \frac{dV_V}{dt} \qquad (44)$$

Which allows to compute the thermodynamic evolution of both the compression and expansion processes. The instantaneous gas properties are computed by means of the Refprop software. As already mentioned, the working fluid is biomethane, which is almost 100% methane, thus pure CH_4 is considered in the analysis. The proposed model is implemented in the Matlab software and is able to achieve a first sizing of the multistage reciprocating compressor as well as a simulation of the compression process. The model is able to handle time-dependent temperature and pressure levels of the suction and discharge chambers. A validation of the proposed model was performed using experimental data (Khadem, 2015). In the experiment, the performance of a single stage reciprocating compressor for air as working fluid are measured. The proposed model was used to simulate a complete compression cycle. Figures 3.18 and 3.19 show a comparison of the predicted and the experimental results. As it can be seen, a good agreement between the experimental and predicted results was found. It must be noted that in Figure 3.18, predicted initial and final pressure are different since the first compression cycle was considered. The real compressor is an air compressor, with a nominal suction pressure of 1 bar and a discharge pressure of 9 bar with a compressor speed of 3000 rpm. Table 3.2 shows further comparison between the predicted and experimental peak pressure, volume flow rate and required power.

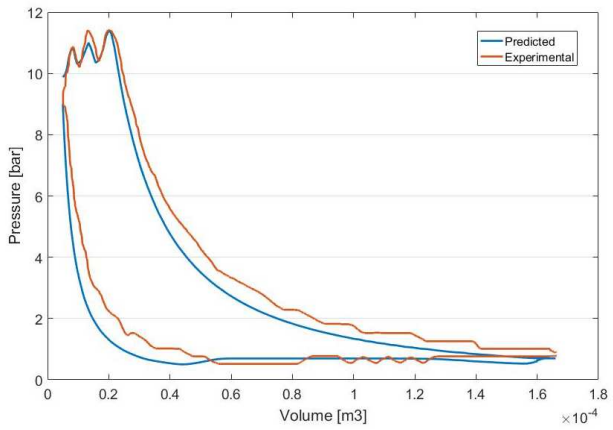

Figure 3.18. Pressure vs Temperature diagram of the

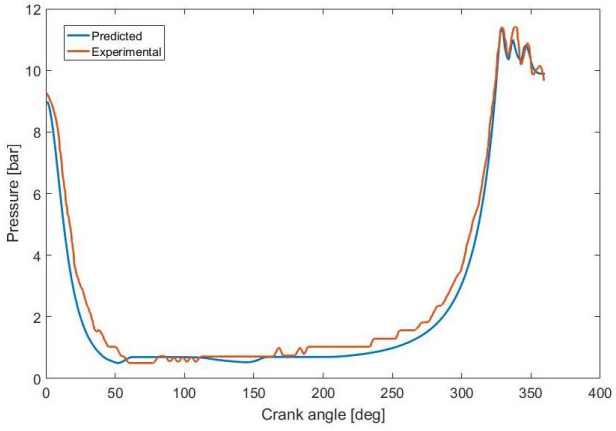

Figure 3.19. Pressure path during the compression phase

compression phase as a function of the crank angle

Table 3.2. Results of the present model compared with experimental results

Parameter	Experimental results	Predicted results	Relative error
Peak pressure [bar]	11.42	11.39	0.26
Volume flow rate [m^3/min.]	0.264	0.271	2.65
Power [W]	2542	2550.9	0.35

Considering the present analysis, the available input data are reported in Table 3.3.

Table 3.3.Initial characteristic parameters for the compressor sizing (FORNOVOGAS®)

Input parameters	
Overall P_s [bar]	15
Overall P_d [bar]	270
$T_{intercooler}$ [°C]	35
$\dot{V}_{biomethane}$ [$Nm^3\ h^{-1}$]	1500
rpm [$minute^{-1}$]	800
Stroke [m]	0.15
a/L factor	0.28
μ factor	0.15
Mack number	0.1
h_{max} [mm]	1-6
S_{ratio}	0.24
Steel density [kg m^3]	7107.44
Spring preload [%]	10
X_0 [mm]	3

The h_{max} factor is varying depending on the stage CD, by means of an empirical relation given a reciprocating compressor manufacturer (FORNOVOGAS®). Once the initial parameters are introduced in the model, the first sizing of the reciprocating compressor is achieved. The optimal stage number for the compression process was found to be three. The output data obtained from the sizing model are reported in Table 3.4.

Table 3.4.Results of the sizing algorithm for each compressor stage

Output parameters	1st compression stage	2nd compression stage	3rd compression stage
CD [m^3]	0.002641	0.000979	0.000339
CB [m]	0.149725	0.091149	0.053621
CV [m^3]	0.000396	0.000147	5.08E-05
A_s [m^2]	0.006526	0.00245	0.000856
A_d [m^2]	0.005819	0.002109	0.000648
D_s [m]	0.091152	0.055855	0.033017
D_d [m]	0.086075	0.051822	0.028723
$H_{s,max}$ [m]	0.006	0.005349	0.003933
$H_{d,max}$ [m]	0.005349	0.003933	0.001
$A_{p,s}$ [m^2]	0.026102	0.009801	0.003425
$A_{p,s}$ [m^2]	0.023276	0.008437	0.002592
$D_{p,s}$ [m]	0.182303	0.111709	0.066034
$D_{p,d}$ [m]	0.172151	0.103644	0.057446
$M_{p,s}$ [kg]	0.061027	0.022915	0.008007
$M_{p,d}$ [kg]	0.054419	0.019725	0.00606
K_s [N m^{-1}]	32627.88	32107.15	29402.85
K_d [N m^{-1}]	76250.24	72433.42	58317.15
Suction preload [N]	97.28498	96.09666	88.13
Discharge preload [N]	229.2846	217.4938	175.0109

Where D_s, D_d, $A_{p,s}$, $A_{p,d}$, $D_{p,s}$, $D_{p,d}$, $M_{p,s}$, $M_{p,d}$, are the port diameter, plate area, plate diameter and plate mass respectively. The subscripts s, d, 'p,s', 'p,d' are related to suction, discharge, suction plate and discharge plate respectively. Since the final scope is to compare the performance of the buffer configuration and the alternative

configuration, the obtained compressor was considered for both the configurations. Finally, the obtained results allow the simulation of the storage charging process.

3.4.2. The Fast-Filling Process and Connecting Pipes

During the vehicles refueling at the CBG station, the high pressure biomethane flows into the vehicle vessel by means of the pressure difference inside the volumes. This filling process is called fast-filling process. During the FFP, a valve is opened in order to connect the CBG storage with the vehicle cylinder. At this point, the biomethane begins to flow from the storage to the cylinder. The process occurs since one of the following situations occur:

- The difference between the volume pressure is no longer able to achieve FFP;
- The vessel pressure reaches the requested pressure.

During the FFP, the onboard vessel experiences an increasing temperature, up to 40°C. The increased temperature reduces the gas density, thus the filled mass inside the cylinder, as previously mentioned. The refueling process is achieved by means of a dedicated connecting pipe in which the gas flows from the storage to the vehicle. As the pressure difference of these volumes is quite high for almost the whole process, the gas speed inside this pipe is considerably high as well. Thus, pressure drops across the pipe occur, influencing the FFP.
In this section, the FFP is modeled in a quasi-steady state in order to determine the thermodynamics of the process as well as gas thermos-physical properties inside both the storage and the onboard cylinder. Moreover, a model for the connecting pipe pressure drop during the FFP is discussed. Finally, a validation of such models is proposed in order to evaluate the FFP and connection pipe pressure drops.

3.4.2.1. The FFP model

Several studies were conducted in order to evaluate such a process. The first proposed model of the FFP was developed by (Kountz, 1994). The model was based on the first law of thermodynamics. A computer program was developed in order to simulate FFP with a single storage. (Farzaneh et al., 2007) and (Farzaneh, 2008) developed a computer program as well, based on the Peng-Robinson equation of state for pure methane and single storage configuration. A first comparison between the FFP with buffer and cascade storage configurations was proposed by (Farzaneh et al., 2011). A theoretical analysis of the configurations was performed in order to compare the performance of such stations. This analysis was conducted assuming a constant pressure of storages during the FFP. In the present work, the analysis of the FFP is based on that proposed by (Farzaneh et al., 2011). The onboard cylinder is assumed to be an adiabatic system. However, the current analysis is going to consider the CBG storage pressure, temperature and biomethane stored mass to be time-dependent, due to FFP itself. The model is based on the first law of thermodynamics. Figure 3.20 provides a schematic view of the FFP.

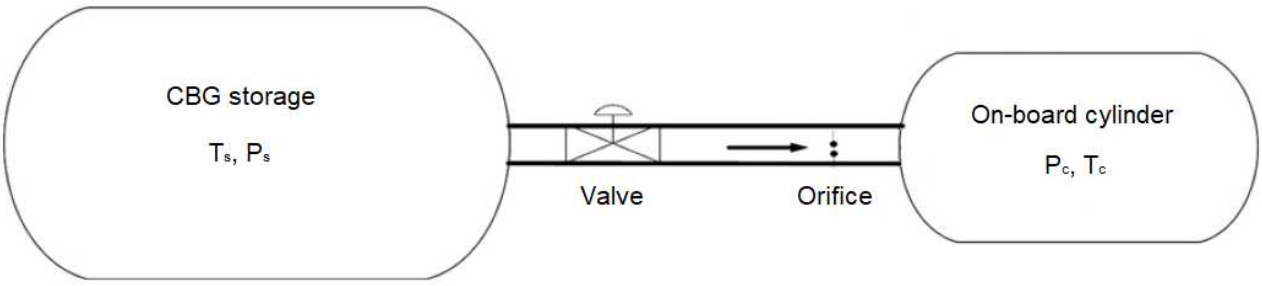

Figure 3.20. Schematic view of the storage and onboard cylinder system during the FFP.

The CBG storage and the On-board cylinder are considered as control volumes during the present analysis. Consider the equation (41). For the biomethane in the storage volume and in the onboard cylinder volume, the potential and gas speed terms may be neglected. Depending on the considered control volume, the equation could be written as follows:

$$\frac{dU_S}{dt} = \delta\dot{Q}_S - \dot{m}_e * \left(\frac{u_e^2}{2} + h_e\right) \quad (45)$$

$$\frac{dU_C}{dt} = \delta\dot{Q}_C - \dot{m}_i * \left(\frac{u_i^2}{2} + h_i\right) \quad (46)$$

Where $\dot{m}$ and h are mass flow and enthalpy respectively. The subscript S, C, e and i are related with the storage and cylinder, exiting and incoming mass, respectively. $\delta\dot{Q}$ represents the heat lost through the storage and cylinder walls due to temperature difference with the environment. Thus, the first equation belongs to the storage discharging process while the second one is related with the cylinder refueling process. Considering the term associated with the heat losses, the following equations are obtained:

$$\delta\dot{Q}_S = -H_S * A_S * (T_S - T_\infty) \quad (47)$$

$$\delta\dot{Q}_C = -H_C * A_C * (T_C - T_\infty) \quad (48)$$

Where H, A and T_∞ are the convective heat transfer coefficient, the surface area of the volume and the external temperature, respectively. Looking at the equations (45) and (46), the stagnation enthalpy is introduced, thus by equations (47) and (48):

$$\frac{d(m_S * U_{S,S})}{dt} + \frac{d(m_S * h_{R,S})}{dt} = -H_S * A_S * (T_S - T_\infty) \quad (49)$$

$$\frac{d(m_S * U_{S,C})}{dt} - \frac{d(m_C * h_{R,C})}{dt} = -H_C * A_C * (T_C - T_\infty) \quad (50)$$

Where $U_{S,S}$ and $U_{S,C}$ are the specific internal energy, while $h_{R,S}$ and $h_{R,C}$ are the stagnation enthalpy, related with the storage and the cylinder respectively. The last two equations are rearranged and then integrated from the start of the FFP to a generic time instant:

$$\int_{start}^{end} d\left[m_S * U_{S,S} + m_S * h_{r,S}\right] = -\int_0^t H_S * A_S * (T_S - T_\infty)dt \quad (51)$$

$$\int_{start}^{end} d\left[m_C * U_{S,C} - m_C * h_{r,C}\right] = -\int_0^t H_C * A_C * (T_C - T_\infty)dt \quad (52)$$

The integration of the equations (51) and (52) gives the final result:

$$\left[m_S * \left(U_{S,S} + h_{r,S}\right)\right]_t - \left[m_S * \left(U_{S,S} + h_{r,S}\right)\right]_o = -H_S * A_S * \Delta T_{AV,S} * t \quad (53)$$

$$\left[m_C * \left(U_{S,C} - h_{r,C}\right)\right]_t - \left[m_C * \left(U_{S,C} - h_{r,C}\right)\right]_o = -H_C * A_C * \Delta T_{AV,C} * t \quad (54)$$

Where ΔT_{AV} is representing the average temperature difference between the volume and the environment, while t is the time considered from the start to the end of the process. The subscript 0 and t are referred to the time instants considered (thus, 0 is the start condition while t is the final or interrupted condition). The average temperature is defined as follows:

$$\Delta T_{AV,S} = \frac{1}{t} * \int_0^t (T_S - T_\infty)\, dt \quad (55)$$

$$\Delta T_{AV,C} = \frac{1}{t} * \int_0^t (T_C - T_\infty)\, dt \quad (56)$$

Since the thermodynamic properties of the gas inside the storage as well as in the cylinder are investigated, combining equations from (53) to (55), the first law of thermodynamics for these volumes can be written in order to calculate the volume internal energy, thus:

$$\left[U_{S,S}\right]_t = -\left\{\left[h_{r,S}\right]_t + \frac{\left(H_S * A_S * \Delta T_{AV,S} * t\right) + \left[m_S * \left(U_{S,S} + h_{r,S}\right)\right]_o}{[m_S]_t}\right\} \quad (57)$$

$$\left[U_{S,C}\right]_t = \left[h_{r,C}\right]_t + \frac{\left(H_C * A_C * \Delta T_{AV,C} * t\right) + \left[m_C * \left(U_{S,C} - h_{r,C}\right)\right]_o}{[m_C]_t} \quad (58)$$

Consider now the volume to be adiabatic, this heat transfer between the volume and the environment is no longer considered. As a consequence, equations (57) and (58) can be written as follows:

$$[U_{S,S}]_t = -\left\{[h_{r,S}]_t + \frac{[m_S*(U_{S,S}+h_{r,S})]_o}{[m_S]_t}\right\} \quad (58)$$

$$[U_{S,C}]_t = [h_{r,C}]_t + \frac{[m_C*(U_{S,C}-h_{r,C})]_o}{[m_C]_t} \quad (59)$$

Equations from (57) to (59) are considered in order to simulate the FFP. Regarding the buffer CBG refueling station configuration, equations (58) and (59) are implemented for the storage, while for the alternative CBG refueling station, equations (57) and (58) are considered for each storage. This is mainly due to the fact that for the former configuration, a dedicated storage cooling system is missing, while in the alternative station, a water cooling process is used in order to control the storage temperature. By the way, both CBG considered configurations are using equations (58) and (59). This means that the heat flow between the volume and the environment is neglected.

3.4.2.2. The Connecting Pipe

As already mentioned, the connecting pipe allows the FFP by connecting the refueling station storage to the onboard cylinder. Figure 3.21 shows a schematic view of the connecting pipe.

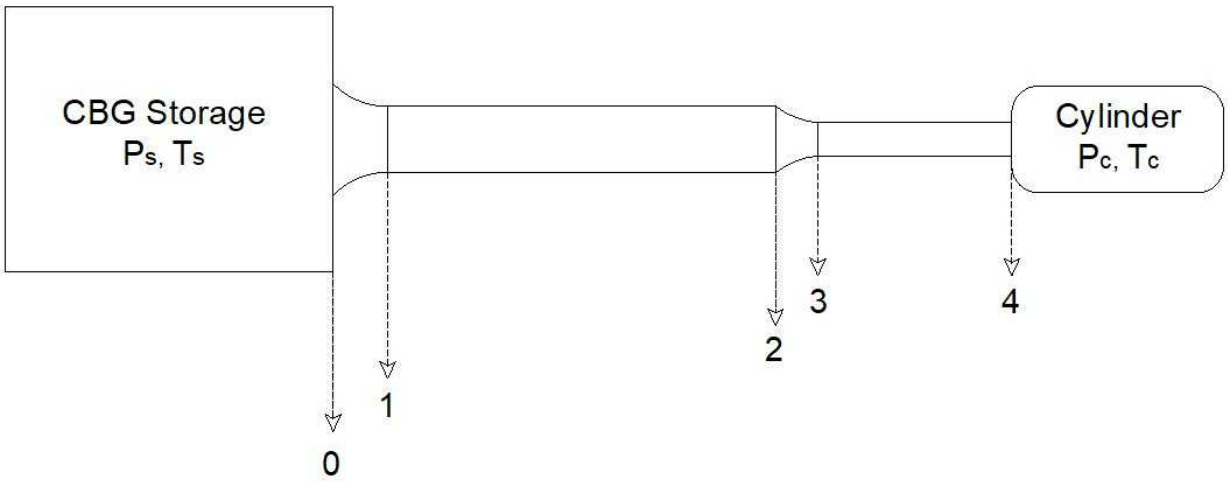

Figure 3.21. FFP process analysis and modeling

Looking at the figure, the connecting pipe may be divided into several specific sections. In general, two main sections can be distinguished:

- The pipe connecting the CBG storage to the dispenser;
- The pipe connecting the dispenser to the vehicle cylinder.

In Figure 3.21, such section is represented by the segment from 0 to 2 for the former and from 2 to 4 for the latter. (Oosthuizen, 1997) proposed a model for the connecting pipe. Such mathematical model aimed to calculate the mass flow rate of CNG during the vehicle refueling, considering the connecting pipe. The gas flow inside the pipe was modeled by means of the Fanno equations, thus the flow was considered a Fanno flow, which means an adiabatic flow through a cylindrical pipe with a constant cross-section. The same model was also proposed by (Khadem, 2015). In order to model the connecting pipe, some assumptions are necessary. First of all, the nozzles lying along the pipe are considered to be isentropic nozzle, which accounts for the gas expansion and acceleration. Such nozzles are represented in Figure 3.21 by the segments 0 – 1 and 2 – 3. The second assumption is related to the straight pipe section, in which pressure drops occur. An adiabatic flow through a constant area is assumed to create friction between the gas and the pipe itself, thus generating pressure drops. This kind of flow description is generally known as Fanno flow. The definition of this flow requires to solve several equations related with: continuity, momentum and energy. Such governing equations are as follows:

$$\frac{d(\rho*u)}{dx} = 0 \quad (60)$$

$$\frac{d(\rho*u^2)}{dx} + \frac{dP}{dx} + \frac{f}{2*d} * \rho u^2 = 0 \quad (61)$$

$$\frac{d}{dx}\left[\rho * u * \left(h + \frac{u^2}{2}\right)\right] = 0 \quad (62)$$

$$P = \rho * \frac{R}{M} * T \quad (63)$$

Where ρ, u, P, f, d, h, R, M, and T are density, velocity, pressure, the Fanning friction factor, pipe diameter, enthalpy, gas constant, molecular weight and temperature respectively. The Mach number equation and gas flow rate equations:

$$M = \frac{u}{\sqrt{k*R*T}} \quad (64)$$

$$\dot{m} = \frac{P}{R*T} * A * M * \sqrt{k * R * T} \quad (65)$$

Where M and A are Mach number along the pipeline and the cross-section of the connecting pipe, respectively. k represents the ratio of heat capacities. Equation (63) allows the definition of the gas mass flow inside the connecting pipe, as a function of the Mach number of the gas through the pipe. Combining equations from (60) to (65), the Fanno flow equations are derived:

$$\frac{f*k}{2*d} * dx = \frac{1-M^2}{M^2*\left[1+\left(M^2*\frac{k-1}{2}\right)\right]} * \frac{dM}{M} \quad (66)$$

$$\frac{dP}{P} = -\frac{1+(k+1)*M}{1+\left(\frac{k-1}{2}\right)*M^2} * \frac{dM}{M} \quad (67)$$

$$\frac{dT}{T} = -\frac{(k-1)*M}{1+\left(\frac{k-1}{2}\right)*M^2} * dM \quad (68)$$

Where d is the internal diameter of the pipe related to the associated pipe section. By means of such equations, the model of the connecting pipe is given. The mathematical modeling related with the Fanno flow, is considered to be a quasi-steady process, thus a numerical procedure was proposed by (Khadem, 2015).
Equations (66), (67) and (68) are used firstly to determine the critical pressure inside the on-board cylinder. This corresponds with a Mach number in section 4 (Figure 3.21) equal to 1. If the critical pressure is greater than that in the on-board cylinder, the flow is choked and gas mass flow rate is constant, defined by equation (65). Otherwise, the flow is not choked and the mass flow rate is defined by a trial and error iterative procedure. As a consequence, the flowing gas pressure at section 4 is determined by estimating a Mach number in such section and pressure in section 4 is calculated by means of equations from (66) to (68). The estimated pressure and the calculated one are compered in order to achieve the minimum possible discrepancy, according with the algorithm tolerance, thus the procedure is iterated if this is not the case. Once the mass flow rate is obtained, equations (58) and (59) could be solved in order to define the thermodynamics of the storage and the on-board cylinder. This procedure takes place at each time-step, until the final pressure inside the cylinder reaches the requested value. The overmentioned iterative procedure is essentially based on the ideal Fanno flow equations. This means that the gas flowing into the connecting pipe is considered an ideal gas. Looking at such equations, the ratio of heat capacity k is assumed constant through the connecting pipe. By the way, this is not true. In fact, being this coefficient highly temperature-dependent, being the gas flow thermodynamic properties quickly and strongly changing during the expansion process, assuming the ratio of heat capacity constant from section 0 to section 4 may lead to associated errors. Moreover, the iterative trial and error procedure is a complex procedure, requiring long computation time. For those reasons, another procedure is proposed, aiming to simplify the model. Moreover, the ratio of heat capacity is no longer constant. The model is based on the same assumptions of those proposed by (Khadem, 2015). Such assumptions assess that the flow is described by two isentropic expansions (in sections 0 – 1 and 2 – 3 in Figure 3.21) and two adiabatic flows (in sections 1 – 2 and 3 – 4). The pressure drops along the connecting pipes are computed as fluid dynamic losses by means of the Darcy-Weisbach relation:

$$\Delta P = f(Re) * L * \frac{\rho}{2} * \frac{u^2}{d} \quad (69)$$

Where f(Re), L and d, are friction factor (given as a function of the Reynolds number), length and internal diameter of the considered pipe section. Regarding the friction factor, the Poiseuille's law and the Karman-Prandtl relations were considered:

$$f_{laminar} = \frac{64}{Re} \tag{70}$$

$$\frac{1}{\sqrt{f_{turbolent}}} = -1.93 * \ln\left(\frac{1.9}{Re*\sqrt{f_{turbolent}}}\right) \tag{71}$$

Where $f_{laminar}$ and $f_{turbolent}$ are friction factors related to the flow condition. The latter equation assumes a smooth-pipe flow. Taking into account the pressure losses through the connecting pipe, a further assumption assesses the stagnation enthalpy conservation (from point 0 to point 4). The continuity equations are also involved. Giving those relations and assumptions, an equation system could be written and correctly solved, thus a trial and error procedure is no longer required. The equation system is generally described from the following equations:

$$h_r(T_0, P_0) = h_x(T_x, P_x) + \frac{u_x^2(T_x, P_x)}{2} \tag{72}$$

$$\rho_x(T_x, P_x) * u_x(T_x, P_x) = \rho_{x+1}(T_{x+1}, P_{x+1}) * u_{x+1}(T_{x+1}, P_{x+1}) \tag{73}$$

$$P_x - P_{x+1} = [f(Re)]_x * L_{x,x+1} * \frac{\rho_x(T_x, P_x)}{2} * \frac{u_x(T_x, P_x)^2}{d_x} \tag{74}$$

$$S_0(T_0, P_0) = S_1(T_1, P_1) \tag{75}$$

$$S_2(T_2, P_2) = S_3(T_3, P_3) \tag{76}$$

$$u_4 = c_C \tag{77}$$

Where S and c represents the entropy depending on the thermodynamic properties of the section and the gas speed of sound respectively. The subscript x and x+1 are related with a generic section of the connecting pipe (for x section ranging from 0 to 3 in Figure 3.21) and its subsequent section. Equation (77) assesses that the gas velocity in section 4 is equal to the gas speed of sound, obtained by the onboard cylinder thermodynamic conditions. This equation is used in order to understand if the flow is a critical flow or not. The equation system is then derived to be a 21*21 equation system. The algorithm act as follows. For given connecting pipe geometry and storage and cylinder temperature and pressure levels, the system is solved and the gas velocity in section 4 is computed. The biomethane speed of sound is obtained considering the cylinder thermodynamic state. If u_4 is higher than c_4, then the flow is choked, thus equation (77) enters into the equation system (in equations (72), (73) and (74)) and the flow characteristics in the connecting pipe are directly computed. Once the thermodynamic properties of the flow in section 4 are obtained, the mass flow rate is calculated, thus equations (58) and (59) can be used in order to evaluate the storage and cylinder properties. By considering a certain time step, this procedure is repeated until one of the following conditions occur:

- The pressure of the cylinder reaches the desired final pressure;
- The difference between the storage and cylinder pressures is no longer able to achieve FFP.

Given those conditions as final conditions, the FFP is modeled and evaluated taking into account the connecting pipe.

Comparison for the FFP model

A comparison of the model is proposed, based on the (Khadem, 2015) results. The model is referred to a buffer CNG configuration. Table 3.5 shows information related with the CNG refueling station properties. The same information were used in order to evaluate the model. Mass flow rate and onboard cylinder pressure were calculated as well as the FFP time, to be compared with the results obtained from the model proposed by (Khadem, 2015).

Table 3.5. CBG station information for the FFP

CNG station parameters	Value
Inside pipe diameter of section 1 – 2	0.007 m
Inside pipe diameter of section 3 – 4	0.003 m
Length of section 1 – 2	50 m
Length of section 3 – 4 [m]	1 m
Onboard cylinder capacity	101 l
Onboard cylinder initial pressure	1 bar
Storage capacity	5760 l
Storage initial pressure	220 bar

The storage was considered to be at constant pressure during the FFP process, thus the final condition is related to the final pressure level inside the onboard cylinder. The model runs until the mass flow rate through the connecting pipe is higher than 0.02 kg s^{-1}. Figure 3.22, 3.23 and Figure 3.24 show the results of the present study compared with those of the reference study. In such analysis, authors consider the gas as pure methane.

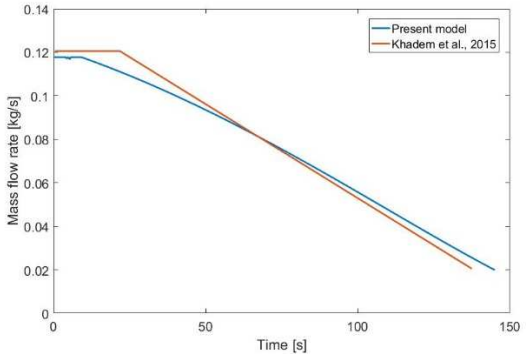

Figure 3.22. Comparison between models [Kg/s]

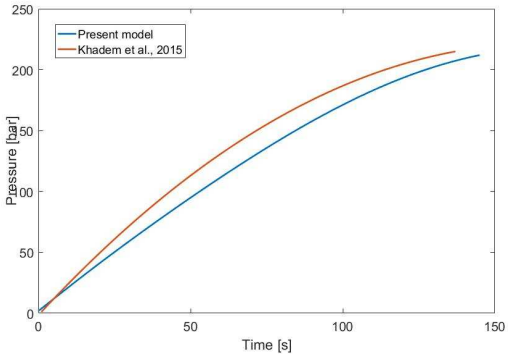

Figure 3.23. Comparison between models [bar]

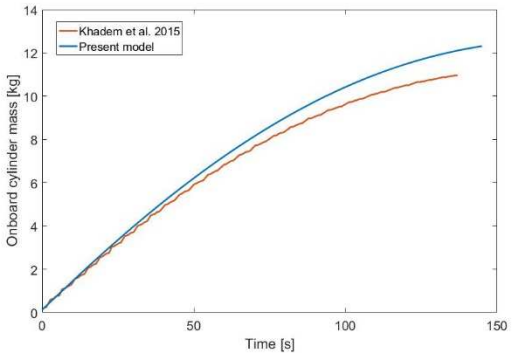

Figure 3.24. Comparison between models [kg]

Looking at the figures, some consideration may be done. The proposed model presents a higher filling time than that obtained from the reference model. The choke occurs during the first part of the FFP in both cases, but a slightly difference in the maximum achievable mass flow rate was found. The mass flow rate associated with the first part of the FFP has lower values for the proposed model if compared with the reference model. In Figure 3.24, the onboard mass charged during the FFP is reported. As it can be seen, the maximum stored biomethane is higher for the proposed model if compared with that of the reference. This is mainly due to the fact that a lower mass flow rate implies a lower increasing rate in cylinder pressure, thus the associated temperature rising is lower than that of the reference. As a consequence, the stored biomethane has a higher density, thus a higher final mass is stored inside the cylinder. Generally, the analysis showed good agreement with the reference results.

3.4.3. The Storage Cooling Process

As part of the innovation related with the alternative CBG refueling station configuration, the storages cooling process was taken into account. Figure 3.25 shows a schematic view of the CBG storages.

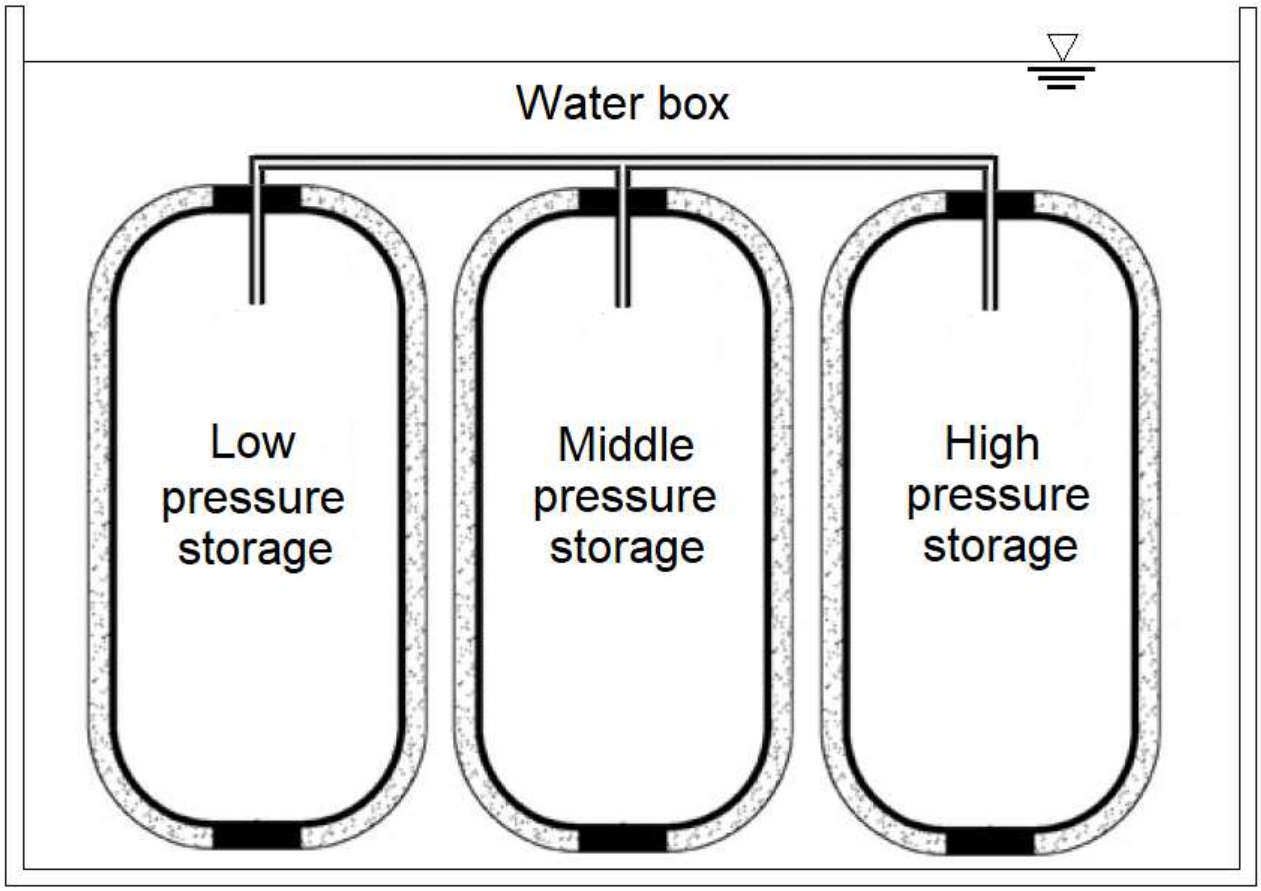

Figure 3.25. Schematic view of the cold water box providing storage refrigeration

The cooling process is considered as a transient process and it is modeled as a quasi-steady process. A condensed parameter approach is proposed for the model. This kind of model requires several assumptions in order to provide good results. Such assumptions are as follows:

- The heat capacity of the water inside the box is able to keep a constant temperature itself;
- The convective heat transfer coefficient is constant during the cooling process;
- The storage walls temperature is equal to that of the stored biomethane;
- The Biot number is << 1.

The Biot number is given by the following equation:

$$Bi = \frac{H}{\lambda_{cylinder}} * \frac{V_{cylinder}}{A_{cylinder}} \ll 1$$

Where λ, V and A are related to the conductive heat transfer capacity, volume and external surface area of the storage. For the model definition, the following equations were used (Çengel, 1998):

$$Nu = \frac{H*D}{\lambda_{water}} \quad (78)$$

$$Nu = a(Re) * Re^{b(Re)} * Pr^{\frac{1}{3}} \quad (79)$$

$$T(t) = T_{\infty} + (T_i - T_{\infty}) * e^{-\left(t*H*\left(\frac{A}{\rho*c_p*V}\right)_{cylinder}\right)} \quad (80)$$

Where T(t), T_i, ρ and c_p are the cylinder temperature at the time t, the initial cylinder temperature, the cylinder density and specific heat capacity respectively. In equation (79) the a and b coefficient are depending on the Reynolds number as well as on the cylinder geometry. For the analysis, the storage cylinders are considered to be a cylindrical body. Table 3.6 reports the cylinder specifications.

Table 3.6. Onboard cylinder geometric and material properties

Specifications	**Value**
Water temperature	15 °C
Cylinder internal diameter	0.315 m
Cylinder external diameter	0.35 m
Cylinder height	1.0265 m
Cylinder steel density	7870 kg/m^3
Cylinder steel conductive coefficient	880 J/kg*K

For the present analysis, the water Reynolds number was found to be equal to 3080, which encounters the required Bi << 1, to be of about 0.14.

3.4.4. The Algorithm Definition

For the present analysis, the NIST, Refprop software was used in order to evaluate thermodynamic and thermos-physical properties of the biomethane. The simulations were conducted by means of MathWorks®, Matlab software. The storage charging process and the vehicle fueling process strategies related with the alternative CBG refueling station, as well as those related with the buffer CBG refueling station are presented. Considering the section 3.3, the charging of the alternative CBG storages is quite complex. Figure 3.26 shows the flow chart of the charging strategy. The subscript 1st, 2nd and 3rd represent the compressor stages. At the very beginning of the storage charging process, the following assumptions were made:

- The biomethane inside the compressor stages is at ambient temperature with a pressure equal to its minimum nominal pressure, defined in the sizing step;
- The initial storage pressure inside the stages is at its minimum level, while its initial temperature is the same as the water temperature in the water box.

In the sizing process, the equation (16) was used in order to find the pressure ratio of each stage, depending on the overall pressure ratio. In the alternative CBG refueling station, the reciprocating compressor should work with one stage at a time. However, in this case the first stage is working with a too high-pressure ratio, thus the final biomethane temperature at the end of the compression process is going to rise dramatically. For this reason, while charging the LP storage, the compression process is divided into two different cases: if the LP pressure is lower than the maximum achievable pressure in the first compression stage, the LP storage is charged from the first stage only. When the pressure inside the low-pressure storage reaches a pressure level equal or higher than this value, then the first and second compression stages work together in order to fill the storage to its maximum pressure. When the LP storage reaches this condition, then it becomes the suction chamber of the MP storage, which is charged by means of the second compression stage. If during this process the LP reaches its minimum level, the MP charge is stopped and the compressor charges again the LP storage. The process continues until the pressure in LP and MP storages reaches their maximum levels, thus the HP storage is charged from the MP storage and so on. At the end of the process, LP, MP and HP storages are charged up to their maximum pressure levels. However, due to the rising temperature associated with the compression process, the temperature inside the storages may be high. For this reason, the storages are cooled down by means of a water box, as previously described, and temperature and pressure levels inside the storages are decreased, thus a further test is required in order to verify the actual pressure levels. If such pressure levels are still at their maximum, the charging process ends. Otherwise it is iterated until such condition is reached. By the way, since the compression process provides a certain temperature increase, this process may continue without reaching the target condition, with storages pressure levels which tend towards their maximum level. For this reason, the nominal maximum pressure inside the storages is slightly increased, while the final test compares the actual pressure levels with the nominal pressure levels. This is possible because the compressor is sized to reach a pressure higher than then maximum HP storage pressure (270 bar vs 250 bar). In this way, the problem is avoided and the full charge of the alternative CBG storages is obtained. During the cooling phase, the compressor does not work, until the nominal final temperature of the storages is reached.
The onboard cylinder is filled by means of the MP storage. Applying the same criteria as those used for the LP storage, the process ends and the HP continues the filling process until the vessel maximum pressure is reached.

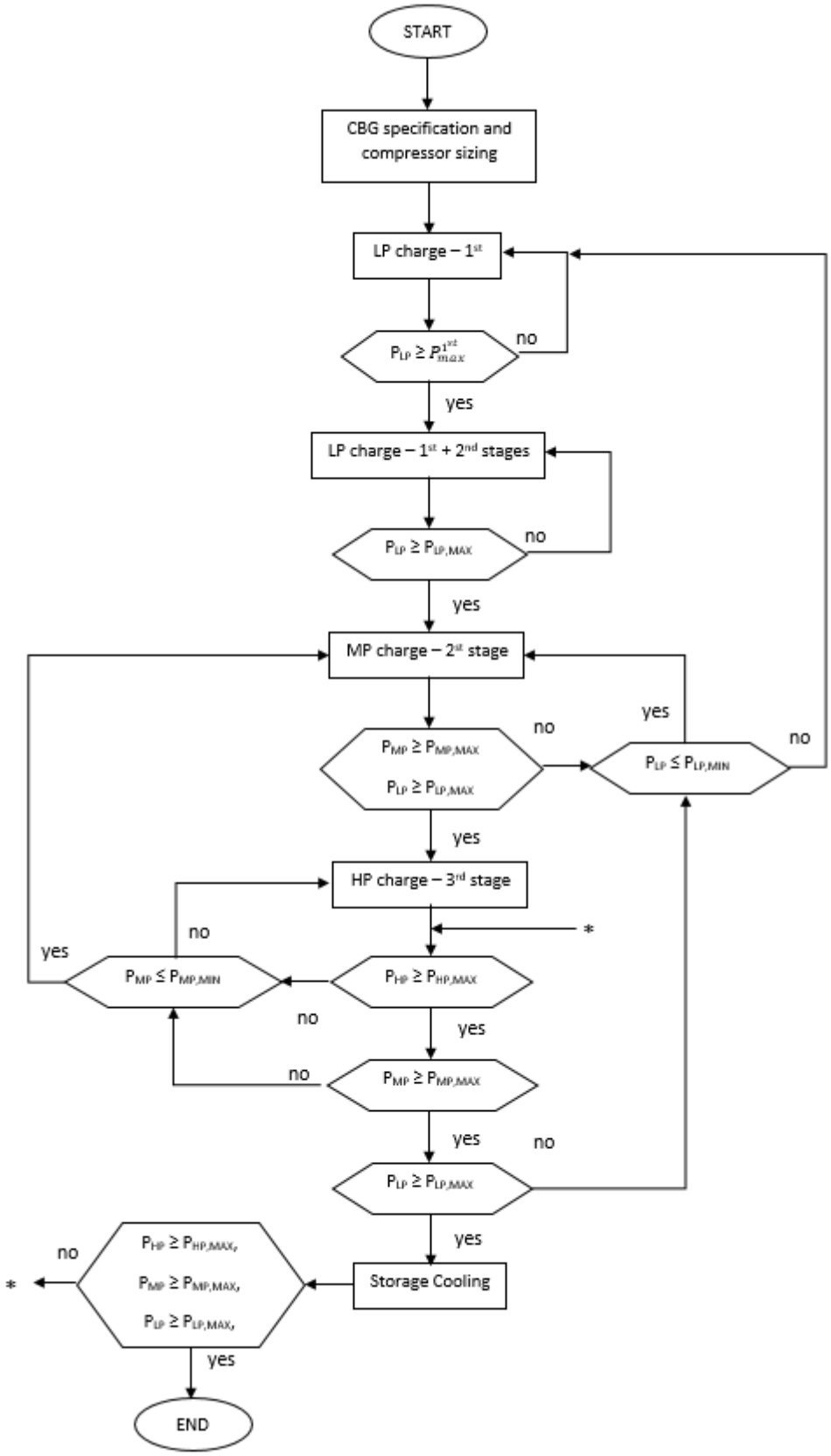

Figure 3.26. Algorithm definition and implementation on MathWorks®. Matlab software

Regarding the vehicle refueling from the alternative CBG refueling station, the onboard cylinder is filled by means of a FFP from each of the station storage. The vehicles are supposed to have a low pressure inside their cylinders, thus the filling process begins with the LP storage. Connecting these volumes, the biomethane flows by means of a pressure difference. When this pressure difference is lower than a certain fixed value, the process is interrupted. By the way, if during the filling process the high-pressure level storage reaches its minimum value, FFP could no longer occur.
Referring to the storage charge and vehicle refueling processes associated with the buffer CBG refueling configuration, the algorithm definition is quite simpler. In fact, only one pressure level is associated with the CBG station. The same assumptions related with biomethane inside the compressor stages were done. The storage initial pressure is its minimum pressure level, while its temperature is equal to the ambient temperature. The compressor stages operate now simultaneously, since the biomethane must be compressed from the lower pressure to high pressure levels, directly. Regarding the FFP associated with such configuration, the onboard cylinder is charged directly from the high-pressure storage until the vehicle vessel is filled or until the storage reaches its minimum pressure level.

3.5. Results and Discussion

In order to compare the two CBG refueling station configurations, some considerations must be done. First of all, the reciprocating compressor is exactly the same for both configurations, since its sizing only depends on external common factors such as the overall pressure ratio and the nominal mass flow rate. Moreover, the storage capacity for the two stations are intended to store the same theoretical biomethane mass, from their initial (minimum) pressure level to their filled state. Two different analysis were conducted. The first one regards the alternative station which presents a storage configuration equal to that reported in the patent. The second one regards the alternative station which presents a storage configuration intended to maximize the number of refueled vehicles. Regarding the sized reciprocating compressor, Table 3.4 reports the calculated parameters. Table 3.7 reports the storage capacity and pressure levels for the alternative CBG station.

Table 3.7. Storage geometric parameters and specifications

	Alternative / Alternative_1 CBG station			**Buffer CNG station**
Parameters	**Low-pressure**	**Middle-pressure**	**High-pressure**	**Single storage**
Cylinder number	26 / 15	32 / 18	18 / 33	98
Cylinder volume	80 l	60 l	60 l	60 l
Overall volume	2.08 / 0.88m^3	1.92 / 1.08 m^3	1.08 / 3.72 m^3	5.88 m^3
Minimum pressure	37 bar	87 bar	230 bar	230 bar
Maximum pressure	55 bar	105 bar	250 bar	250 bar

These parameters were taken equal to those proposed in the alternative station patent. Based on these characteristics, the buffer storage was defined as already mentioned.

Table 3.8. Results of the comparative analysis between proposed CBG configurations

Parameters	**Buffer**	**Alternative**	**Altenrative_1**
Time for the storage charge [s]	523.6	5384.1	13360.3
Time for the stage cooling [s]	-	3266	10478
Time for the compression [s]	523.6	2118.1	2882.3
Required compressor Power [kW]	266.7	109	95.24
Energy consumption [MJ]	29.76	56.15	100.2
Stored Mass [kg]	22.23	83.73	113.94
Number of filled vehicles	5	2	8
Average time for the FFP [s]	189	311	237
Average mass stored in the cylinder [kg]	9.41	8.38	8.25
Average temperature rise [°C]	53.45	53.48	52.78

At the beginning of the FFP, pressure and temperature of the vehicle are 30 bar and ambient temperature respectively. The volume of the onboard cylinder is equal to 90 l. Vehicles are filled one at a time and the time between one vehicle and the subsequent is 60 seconds. The target pressure for the onboard cylinder is 220 bar. The water temperature and the ambient temperature are 15°C and 35°C respectively. The quasi-steady analysis for the

compression process is based on an angle step of the compressor crankshaft of 0.15 degree, corresponding to a time step of $3.125 * 10^{-5}$ seconds. The time step related with the FFP is 0.01 seconds. A first simulation of the whole process was performed. Table 3.8 shows the related results.
The required time for the complete storage charging process is due to the charging strategy. As a consequence, the time required for the alternative station is 10.28 times than that requested for the buffer station. Considering the time while the compressor is in use in the alternative station, still the required time for the storage charge is 4.04 times that of the buffer station. On the other hand, the power required for the compression process in the alternative station is 59.13% lower than that required for the buffer station. However, due to the high time for the charging process, the final consumption energy is 88.67% higher than in the buffer station. This is the consequence of the adopted charging strategy. In fact, the pressure inside the alternative station during the compression, is constantly rising and decreasing due to the cooling system. Figure 3.27 shows the pressure trend during the charge of the alternative storages.

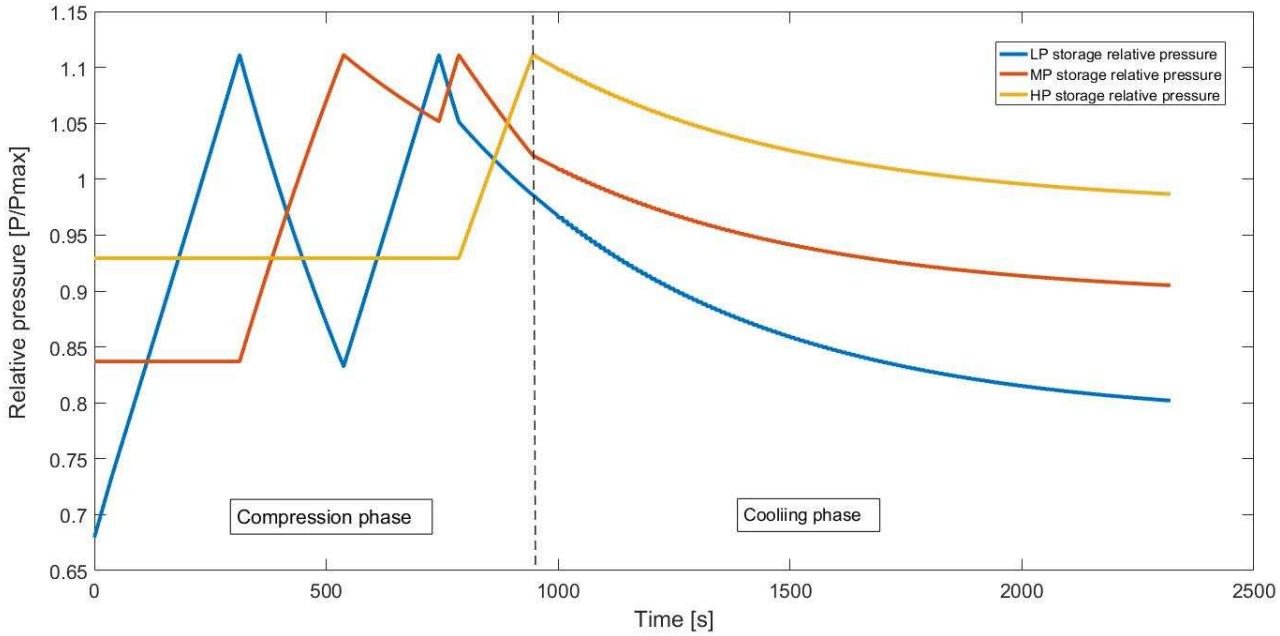

Figure 3.27. Pressure profile inside of the three storages of the alternative CBG refueling station

Looking at the figure related with the compression and cooling phases: the pressure in the figure is a relative pressure, thus it represents the pressure inside the storage at the generic time over the nominal maximum pressure of the storage itself. As it can be seen, as the compression process begins the pressure inside the LP storage is constantly increasing. When its maximum pressure is reached, the compressor begins to charge the MP storage, thus the latter is decreasing while the former is increasing. Once the pressure inside of the MP reaches its maximum level, the compressor switch on the LP storage, charging it up to its maximum pressure. Once both the LP and MP storage are at maximum pressure, the HP is then charged from the MP. When HP is filled, the compressor is no longer working. This is due to the fact that, because of the water box, an increased maximum pressure value was imposed in order to achieve a full charging of the storages with a reasonable number of charging iterations. In Figure 3.28 the compression process regarding the buffer CBG configuration is represented.

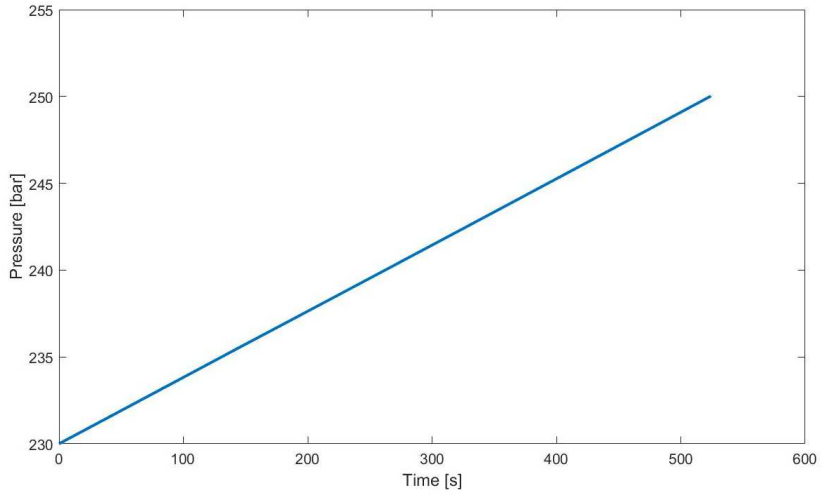

Figure 3.28. Pressure profile inside of the storage of the buffer CBG refueling station

As it can be seen, the storage is filled without any variation, up to the storage maximum level, in a single step. Regarding the alternative CBG station, the number of required compression-cooling phases to achieve the storages complete charge was found to be 3.
Once the storage of both alternative and buffer configurations is filled, the vehicle onboard cylinder can be refueled by means of a FFP. The information related to the CBG refueling station and FFP is reported in Table 3.5. In Table 3.8, results indicate that the FFP for the alternative station requires 64.55% more time than that of the buffer station, in order to fill the onboard cylinder. Moreover, the number of refueled vehicles is 5 for the buffer station, while only 2 vehicles were completely filled by the alternative station. Considering the alternative stations, the temperature, pressure and onboard cylinder mass are represented, related with the mass flow rate in figures from 3.29 to 3.31.

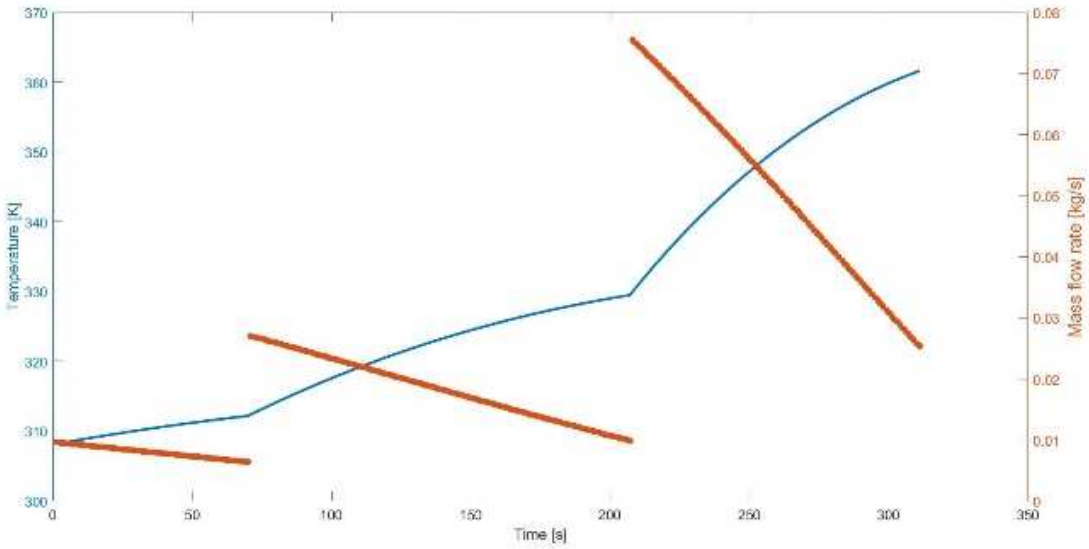

Figure 3.29. Figure 3.29. Temperature vs Mass Flow Rate in onboard cylinder during FFP in alternative station

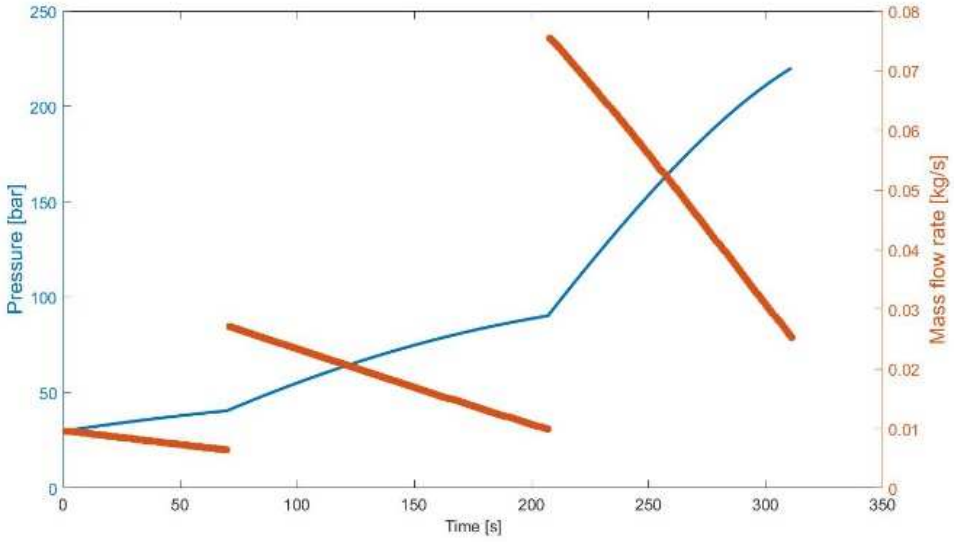

Figure 3.30. Pressure vs Mass Flow Rate in onboard cylinder during FFP in alternative station

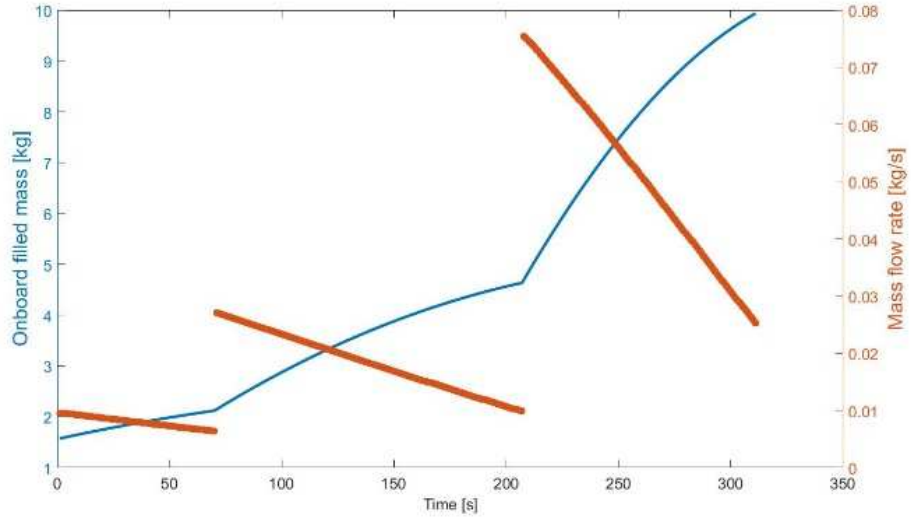

Figure 3.31. Filled Mass vs Pressure in onboard cylinder during FFP in alternative station

In the Figure from 3.29 to 3.31, the fueling strategy is shown. The mass flow rate strongly depends on the pressure difference between the storage and the onboard cylinder. As it can be seen, during the fueling from LP, that is the first storage to be used to this purpose, the mass flow rate is quite low and continue to decrease with the time due to the increasing pressure inside of the onboard vessel. As the pressure difference continue to decrease, the process is stopped in order to continue the FFP by means of the MP storage and subsequently the HP storage. The temperature, pressure and filled mass trends present this particular profile due to this filling strategy, being strictly connected with the mass flow rate. The temperature rise was found to be of about 59.4°C. Regarding Figure 3.31, the stored mass is shown to be more related to the HP storage rather than to LP or MP storages. As a consequence, the high-pressure storage seems to considerably influence the FFP.
Regarding the buffer station, the temperature, pressure and onboard cylinder mass are represented, related to the mass flow rate, in figures 3.32 to 3.34.

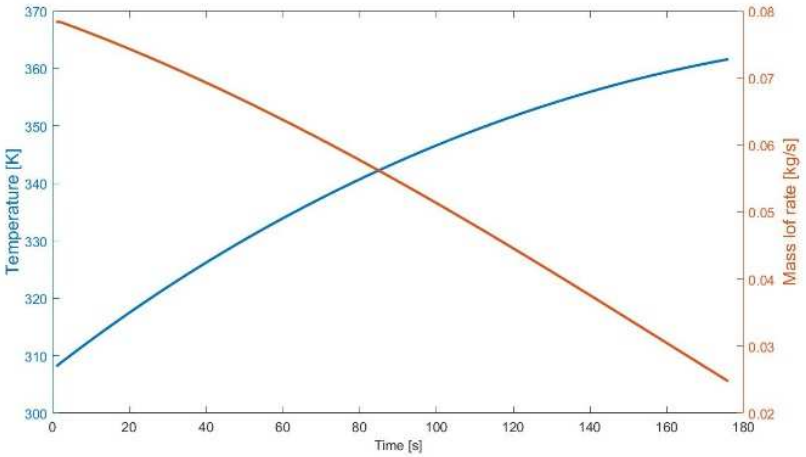

Figure 3.32. Temp. vs Mass Flow Rate in onboard cylinder for the buffer CBG

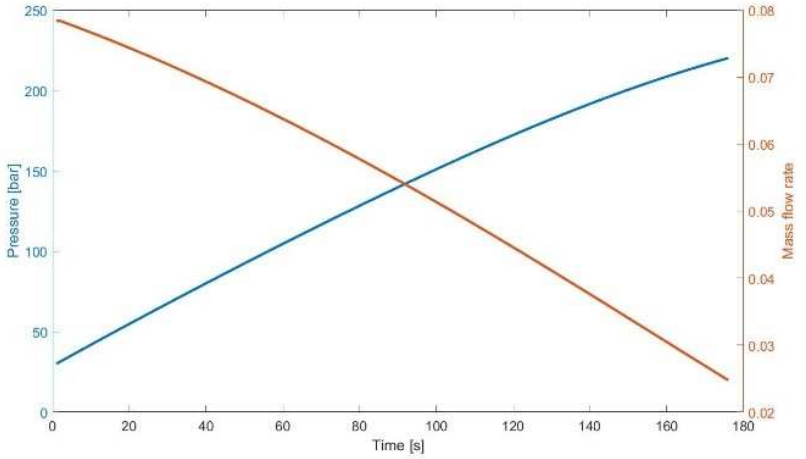

Figure 3.33. Press. vs Mass Flow Rate in onboard cylinder for the buffer CBG

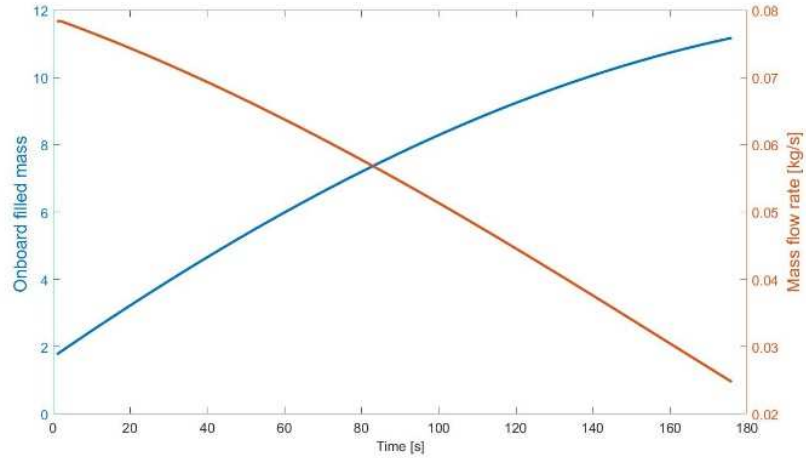

Figure 3.34. Filled Mass vs Mass Flow Rate in onboard cylinder for the buffer CBG

In this case the single storage is entirely at high-pressure, thus the vehicle is filled by means of a single step. The associated mass flow rate presents a tiny choke region, at the very beginning of the process. Being the pressure difference between the storage and the cylinder very high for a great part of the FFP, means that the process itself is faster than that of the alternative process. In Figures 3.35 and 3.36 a comparison between the mass flow rate and pressure trends of the onboard cylinder in the case of alternative and buffer processes are presented.

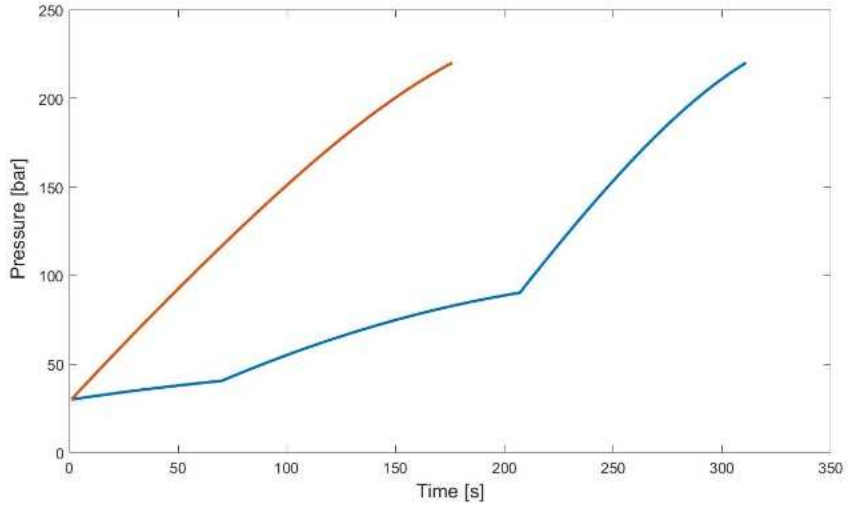

Figure 3.35. Pressure comparison between CBG systems

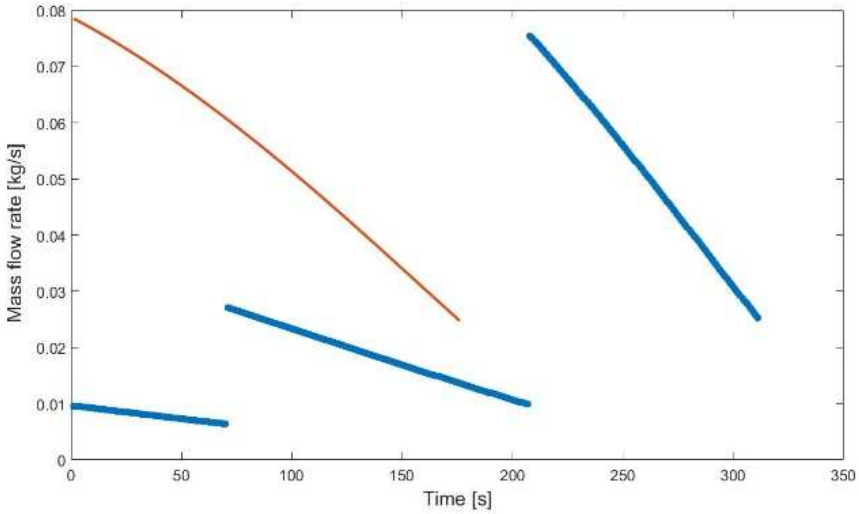

Figure 3.36 Mass Flow Rate comparison between CBG systems

As it can be seen, the rise in onboard cylinder pressure in the case of buffer CBG station is considerably higher than that related with the alternative station, due to the higher-pressure difference between the storage and the vehicle cylinder. As a consequence, the associated mass flow rate is higher as well. During the FFP, in the buffer station the pressure difference drives the biomethane flow at high speed through the connecting pipe and at the very beginning of the process the low is choked. On the other hand, in the alternative station the pressure difference between the vehicle vessel and the LP and MP storages does not allow such situation and the mass flow rate is considerably lower. However, the HP storage accounts for higher values of the mass flow rate, thus one can conclude that the pressure levels inside the alternative storages could be optimized in order to achieve better results, decreasing the FFP time.
The number of refueled vehicles of the alternative station is less than half of those refueled by the buffer station. Nevertheless, the biomethane mass charged inside the storages in the alternative station is 276.65% higher than that charged in the buffer station. This is a consequence of the storages sizing of the alternative station. For the present analysis, the size of such storages was referred to data in the alternative station patent. However, as already mentioned, the HP storage accounts for a high mass flow rate if compared with MP and LP. As a result, the HP is the first storage to reach its minimum pressure, thus interrupting the FFP. Figure 3.37 shows a comparison of the relative pressure levels inside the alternative station and the buffer station.

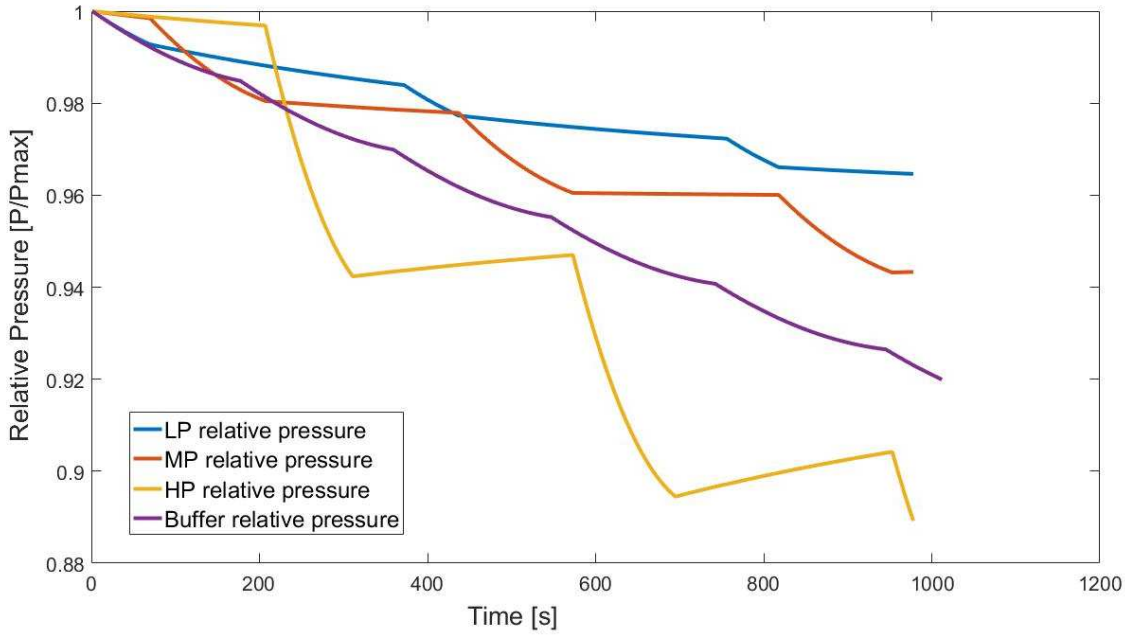

Figure 3.37. Comparison between the relative pressure levels inside the alternative station and the buffer station.

As it can be seen, the HP pressure decreases considerably if compared with the MP and LP storages. The increasing segments are related to the cooling system. In fact, also during the vehicles refueling process the water cooling system is working. The temperature of the biomethane inside the storages at the beginning of the FFP is almost the same of the cooling water. Thus, since the gas is expanding inside the cylinder, its temperature continues to decrease. When the biomethane inside the tank reaches this condition, the biomethane is colder than water used for cooling the storage. In a similar situation, the water cooling system is no longer a cooler, but behaves like a heater. On the other hand, the pressure related to the buffer system is constantly decreasing, until its minimum pressure is reached. Table 3.9 reports some information related with the final results.

Table 3.9. Pressure inside of the alternative station storages at the end of the FFP

Parameter	**Alternative Station**	**Alternative_1**
Final LP pressure vs. minimum pressure [bar]	49.02 / 37	44.62 / 37
Final MP pressure vs. minimum pressure [bar]	96.36 / 87	87 / 87
Final HP pressure vs. minimum pressure [bar]	229.86 / 230	229.97 / 230
Final buffer pressure vs. minimum pressure [bar]	229.98 / 230	229.98 / 230

As it can be seen, the pressure inside the LP and MP storages is far from its minimum allowable value. This is a consequence of the abovementioned phenomenon. On the other hand, HP storage is working as it should. In order to prevent these interruptions, the storages should be correctly sized, as well as for the minimum and maximum allowable pressure levels. Regarding the buffer system, it is not affected by such issues, making it a more robust system.

As previously discussed, storages sizing is an essential part in cascade refueling stations. The best possible combination to optimize the vehicles refueling should be that one in which the minimum pressure level is reached in each storage at the same time at the end of the process. In fact, considering Table 3.9, the refueling process is forced to stop by the high-pressure storage, while the low and middle-pressure storages are still far from their minimum values. This basically means that part of the energy used in the compression process is wasted in storing biomethane which is not used in the refueling process. For this reason, another analysis was performed in order to evaluate the impact of the storage sizing in the alternative CBG station. Consider Table 3.7. The storage configuration was that proposed in the patent for the alternative CBG station. By keeping a constant temperature, given the minimum and maximum pressure levels of each storage (low, middle and high-pressure storages), the theoretical biomethane mass stored is obtained. The theoretical mass calculated was used to size the storage of the buffer CBG station. In this second analysis, the theoretical biomethane mass is now considered to size another configuration for the alternative CBG station. However, in order to properly size the storages, the final pressure inside of each storage at the end of the refueling process should be at its minimum value. A rough storage sizing could be done by consider the biomethane mass coming from the low-pressure, the middle-pressure and the high-

pressure storages. A new configuration is then obtained for the alternative CBG station. Since the sizing criteria is to keep the theoretical stored mass constant, no changes were necessary for the buffer station. Table 3.7 shows the results of the storage sizing (Alternative_1). As for the first analysis, pressure and temperature levels of the on-board cylinders at the beginning of the refueling process are 30 bar and ambient temperature respectively. The time between one vehicle and the subsequent is 60 seconds. Target pressure for the end of the refueling process is 220 bar. The water temperature and the ambient temperature are 15°C and 35°C respectively. The same timestep for compressor operation and FFP simulations is considered to be the same of the first analysis. Table 3.8 shows the related results (Alternative_1).
As it can be seen, the required overall time for the complete storage charge is still high compared with the buffer station. However, the second analysis presents a overall charging time much higher than that of the first analysis. In fact, time for compression and storage cooling are 36% and 220.8% higher than that of the first analysis. The required time for the storage cooling is so much higher due to the fact that the high-pressure storage is higher as well. In fact, considering the alternative station charging strategy, this means a larger number of complete charging cycles, thus a longer cooling time. Increasing the high-pressure storage, the total charged mass is consequently higher, about 36% by respect with the first case. Energy consumption increases as well due to the longer compressor usage, about 78.45%, while required compressor power is slightly lower, about 12.6%. Such results are related with the stages usage during the compression operation. By the way, the main differences regard the refueling process. The alternative CBG station with optimal storage configuration is able to refuel 8 vehicles while the first configuration was able to refuel only 2. This is due to the fact that the storages are now better balanced during the refueling process. This can be observed in Table 3.9 (Alternative_1). As it can be seen, the final storages pressure compared with the minimum pressure is now closer. However, looking at the low-pressure storage, the final pressure is still much higher than the minimum, thus a better storage sizing could provide higher refueling performances. Another interesting difference between the alternative CBG station and the optimal one is the required time for the vehicle refueling. In the optimal one, the time is 23.8% lower. This reduced time is dependent to the high-pressure size compared with the others. In fact, in the optimal case during the refueling process, the pressure inside of the low and middle-pressure storages decrease quickly compared with the first analysis, since the relative volume is considerably lower. This means that to refuel a vehicle, the high-pressure storage is the now more used and the required time is lower because of the higher-pressure difference between this storage level and the on-board cylinder. Figure 3.38 shows a comparison of the relative pressure levels inside the optimal alternative station and the buffer station.

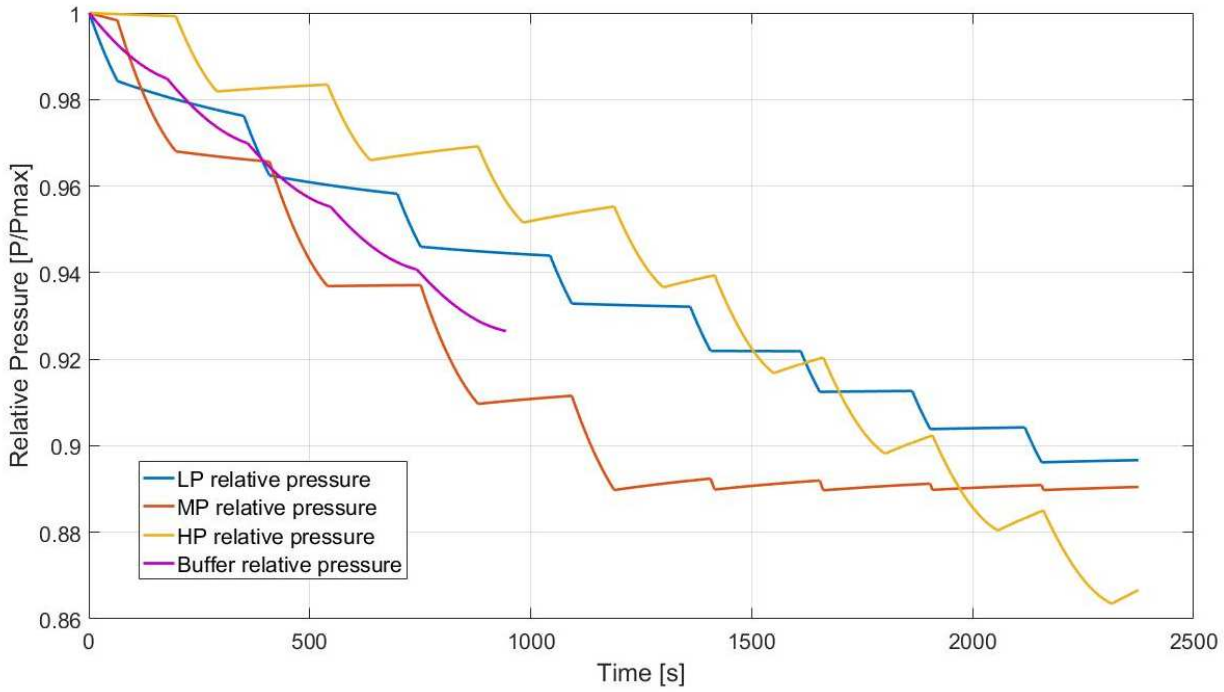

Figure 3.38. Comparison between the relative pressure levels inside the optimal alternative station and the buffer station.

Figure 3.8 shows some details regarding the refueling process. As it can be seen, the pressure inside of the middle-pressure storage reached its minimum value after the 4th refueled vehicle. Since the temperature inside of the storage

is lower than that of the water due to the refueling process, the water itself warm up the storage, thus an increasing pressure profile could be seen at the end of the 3rd refueled vehicle. The figure shows also that, although the minimum pressure value is reached in the MP storage, the refueling process is still operating. This because the pressure inside of the HP storage is still high, then the vehicle could still be refueled up to 220 bar. However, LP storage at the end of the refueling process is 20.73% higher than its minimum value, while pressure inside of the MP storage reaches such level after four refueled vehicles. This means that a more accurate sizing procedure should be developed in order to achieve minimum pressure inside of each storage at the end of refueling process. Nevertheless, results indicate that a rough storage sizing was still able to dramatically increase the number of refueled vehicles.

3.6. Conclusions

In the present analysis, an overview on the traditional CNG refueling stations is shown. A patented alternative CNG refueling station is discussed in detail. Considering the present diffusion of biogas plant on the Italian market, a comparison between two refueling station configurations is proposed, considering biogas as a feedstock source. These kind of refueling stations are known as CBG stations. The gas involved is biomethane and, in the present analysis, it is considered as pure methane, which is a realistic assumption. The CBG station is intended to be an on-site CBG station, thus no 'mother-daughter' configuration is involved. A model for both the alternative CBG station and a buffer station is proposed in order to compare the performance of such refueling stations. The buffer configuration is selected being the most common refueling station in Italy. The proposed model aims to achieve a first sizing of the reciprocating compressor, as well as the definition of the thermodynamic properties of the gas during the FFP, considering the connecting pipes. Moreover, a model for the heat transfer from the storages and the water is considered specifically for the alternative station. A validation of the proposed models is achieved through literature data, showing good accordance. The results indicate advantages and disadvantages regarding the alternative refueling station. The storages charging strategy, as well as the cooling process, allow the CBG alternative station to store a high biomethane quantity. However, the approach seems to be quite complex and requires continuous operation of the compressor unit. As a consequence, the time required from the charging process is dramatically higher for the alternative pressure, if compared to that of the buffer system. On the other hand, the alternative station presents a considerably decrease in the required electric power. The adopted storage configuration for the alternative station is related to data on the patent. The results shown critical aspects of the alternative station. These are mainly related to time for charging process, increased energy consumption and time for the FFP of the vehicles. Moreover, the number of the filled vehicles is found to be strictly connected to the station configuration. In fact, by reaching the minimum pressure condition for one of the three storages, the FFP is interrupted. In order to optimize the process, further analysis is required to better evaluate the relation between the LP, MP and HP storages, as well as their minimum and maximum pressure levels. Although the alternative CBG refueling station is able to decrease investment costs, by means of a smaller electric motor for the compression process, its performance compared with those of the buffer system, are quite poor. On the other hand, the sizing procedure for the alternative CBG station is a key factor to improve such performances. A rough storage size was performed to evaluate its influence in FFP. The analysis showed that the HP storage volume is increased considerably if compared with LP and MP storages. As a consequence, time for the complete storages charge is dramatically increased, as well as energy consumption. By the way, average time for the FFP is considerably reduced and the number of refueled vehicle is increased from 2 to 8. Results also indicate that a fine storage sizing could further increase this value. However, it must be said that the present analysis is limited by considering vehicles coming at the station at the same minimum pressure of 30 bar and the same on-board cylinder volume of 90 liters. Actually, considering a real case, vehicles are coming with random pressure levels and on-board cylinders, thus a correct storage sizing procedure should consider this aspect. By the way, this uncertainty does considerably affect the alternative CBG station performance. On the other hand, the buffer station is no longer influenced by this aspect since only one storage is operating.

3.7. References

- Boswirth, L., (2000), Stromung und Ventilplattenbewegung in Kolbenverdichterventilen, Eigenverlag, Vienna.
- Boswirth, L., (2001), Olklebe-Effekte in Kolbenverdichterventilen, *Proc. EFRC Conf., Den Haag* pp. 33. 43.
- Çengel A. Y., (1998). Thermodynamics and Heat Exchange

- Cierniak, S., (2001). Life-Cycle-Costs von Kolben- und Turbokompressoren. *Erd¨ol Erdgas Kohle* 11, 511.517.
- Farzaneh G. M., Dashtebayaz D. M., Rahbari R. H., (2011). Studying Effects of Storage Types on Performance of CNG Filling Stations. Journal of Natural Gas Science and Engineering. 3:334-340.
- Farzaneh G. M., Nahavandi N.A.P. N., (2013). Numerical Simulation of Filling Process of Natural Gas Onboard Vehicle Cylinder. J Braz. Soc. Mech. Sci. Eng.. 35: 247-256.
- Farzaneh-Gord, M., Rahbari, H.R., (2012). Numerical procedures for natural gas accurate thermodynamics properties calculation. J. Eng. Thermophys. 21 (4), 213e234.
- Farzaneh-Gord, M., Rahbari, H.R., Deymi-Dashtebayaz, M., (2014). Effects of natural Gas compositions on CNG fast filling process for buffer storage system. Oil Gas Sci. Technol. e Rev. IFP Energies nouv. 69 (2), 319e330.
- Habing A.R., (2005), Flow and Plate Motion in Compressor Valves. PhD Thesis, Universiteit Twente.
- IUPAC. Compendium of Chemical Terminology, 2nd ed. (the "Gold Book"). Compiled by A. D. McNaught and A. Wilkinson. Blackwell Scientific Publications, Oxford (1997). XML on-line corrected version: http://goldbook.iupac.org (2006-) created by M. Nic, J. Jirat, B. Kosata; updates compiled by A. Jenkins. ISBN 0-9678550-9-8. http://goldbook.iupac.org/.
- Khadem J., Saadat T. M., Farzaneh G. M., (2015). Mathematical Modeling of a Fast Filling Process at CNG Refueling Stations Considering Connecting Pipes. Journal of Natural Gas Science and Engineering. 26: 176-184.
- Lountz J. K., Blazek F. C., (1996). Apparatus and Methods for Controlling the Charging of NGV Cylinders from Natural Gas Refueling Stations. United State Patent. Patent Number: 5551490.
- Lountz J. K., Liss E. W. , Blazek F. C., (1998a). Automated Process and System for Dispending Compressed Natural Gas. United State Patent. Patent Number: 5810058.
- Lountz J. K., Liss E. W. , Blazek F. C., (1998b). Method and Apparatus for Dispensing Compressed Natural Gas. United State Patent. Patent Number: 5752552.
- NAESB, (2002). North American Energy Standard Board. Retrieved from https://www.naesb.org/pdf2/wgq_bps100605w2.pdf. (last accessed on 28/11/2017).
- Nieter, J. J. and Singh, R., (1984). A computer simulation study of compressor tuning phenomena. *J. Sound Vibr.* 97, 475.488.
- Oosthuizen, P. H., Carscallen, W. E., (1997) . Compressible Fluid Flow. McGraw-Hill.
- Pandeys N. P., (1986). A Simplified Procedure for Designing Hermetic Compressor. Proceedings of the International Compressor Engineering Conference. Paper n. 542.
- Sattari S., Roshandel R., (2007). System Analysis of Mobile CNG Transport as a way to Supply Temporary Energy end-users. Proceedings of the WSEAS international Conference on Energy Planning, Energy Saving, Environmental Education, Arcachon, France, October 14-16 2007. 127-135.
- Setchkin P., N., (1954). Self-Ignition of Combustible Liquids. Journal of Research of the National Bureau of Standards. 53: 49-66.
- Stouffs, P., Tazerout, M., Wauters, P., (2000). Thermodynamic analysis of reciprocating compressors. Int. J. Thermodyn. Sci. 40, 52e66.

4. LIQUEFIED NATURAL GAS AND BIOGAS

4.1 Introduction

As widely discussed in Chapter 2, natural gas represents a clean energy source widely used for countless applications worldwide. Production and consumption of such fuel is constantly growing. Its production experienced a rising trend from 1960 to 2010, representing 11% and 22% of the total primary energy consumption, respectively [3]. Moreover, it was estimated a global rising demand for NG of about 47% from 2011 to 2035 [4]. One of its applications is related with transport sector, to be used as vehicle fuel. In particular, Liquefied Natural Gas (LNG) is considered a valuable substitute for diesel fuel for heavy duty vehicles. In fact, thanks to the high energy density, it makes natural gas suitable also when space and weight are critical criteria for the onboard fuel tank. However, the main obstacle for LNG diffusion as vehicle fuel is related to its supply (Arteconi *et al.,* 2012). At present the solutions to this problem are to purchase it at LNG terminals or liquefying it directly from pipelines (Arteconi and Polonara, 2012). However, another possible option is to use biogas as a feedstock gas. This last possibility is getting more and more interest, especially in Europe where some regions have hundreds (and, in some cases, even thousands) of biogas plants. It is the case of Germany and Italy regions, as reported in Figure 2.7. Nevertheless, since biogas cannot be directly used for this purpose, it needs to be purified in order to obtain biomethane, and then liquefied as well as normal NG. The final result is LBG (Liquefied Bio-Gas). At present, this procedure requires several processes, as already discussed in section 2.6. By the way, in order to produce LBG, the liquefaction process represents a key factor. Since the biomethane composition is more than 95% pure methane (Table 2.14), the associated technology for its production is the same as that used for NG liquefaction. Such process, and those process associated with cryogenic applications, is highly energy-intensive. For this reason, LNG technologies are normally associated with large-scale liquefied natural gas production, in order to achieve higher process efficiencies. At present, the small-scale LNG production technology is gaining more and more interest, but its feasibility still remains challenging. It is the case of biomethane liquefaction. Since the LBG production is related to biogas plant and their capacity, such technologies are actually small, or more commonly micro scale plants. Moreover, in order to achieve biomethane liquefaction, impurities from biogas must be removed with specific processes and apparatus. Combining these aspects, although LBG represents an interesting solution for LNG supply, its production is actually challenging. A possible solution in order to reduce LBG production costs and overall energy consumption is represented by the cryogenic separation technology. In fact, if the final scope is to produce LBG, the liquefaction process and one, or even more than one, purification process could be combined together. The cryogenic technology for the biogas purification is actually existing, but still in a developing phase. Main reason is due to the fact that such process is unfeasible if limited to biogas purification (**production of liquid biogas LBG with cryogenic and conventional upgrading technology - reference**).
In the first section of this chapter, main LNG technologies are briefly presented as well as the state of the art of LBG production technologies. In the further sections of the chapter, cryogenic separation technology is presented and discussed in detail by means of three specific case studies. Firstly cryogenic separation technology intended to remove biogas carbon dioxide impurity is analysed. A cryogenic plant is proposed for such purpose and a simulation is performed by means of Aspen HYSYS ®, AspenTech software. The proposed plant is further improved in order to achieve lower energy consumption. Secondly, an optimization procedure is developed to obtain the best operational configuration. The optimization procedure involves modeFrontier®, ESTECO software, MathWorks®, Matlab software and Aspen HYSYS®, AspenTech software. Thirdly, the proposed cryogenic separation process is improved in order to achieve the combined carbon dioxide and hydrogen sulphide removal from biogas. Related simulations are performed by means of Aspen HYSYS®, AspenTech software. For each plant configuration, obtained results are compared with the state of the art conventional LBG production processes, in which upgrading and liquefaction processes are performed separately.

4.2. LNG and LBG technologies

As mentioned in the introduction of this chapter, LNG is generally produced in large-scale liquefaction plants, which means a production capacity of at least 2 MTPA (Million Tonnes Per Year). Figure 4.1 shows the typical NG cooling curve profile.

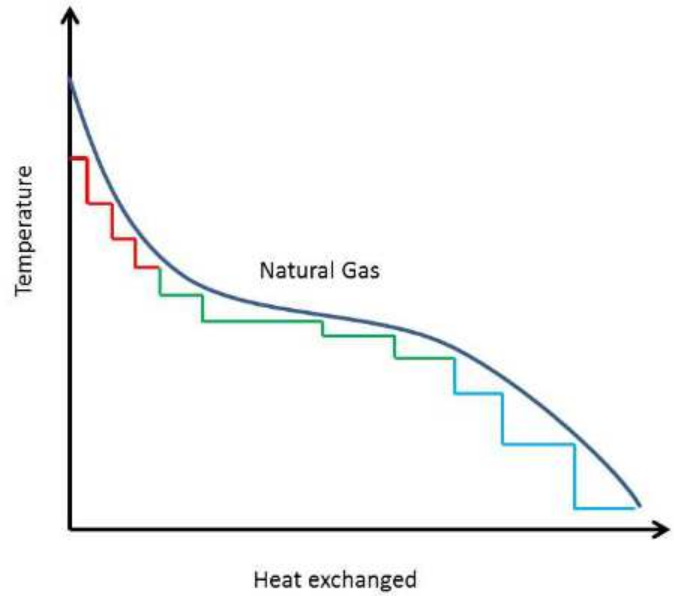

Figure 4.1. Generic cooling curve for NG refrigeration and liquefaction

Depending on NG composition, the curve changes its path. During the cooling phase, the refrigerant temperature profile should approach at NG cooling curve in order to obtain minimum energy consumption during the process (Triglio, 2012). Consequently, LNG plants processes involve refrigeration techniques able to approach such curve as much as possible. To this purpose, the most efficient natural gas liquefaction process is that based on mixed refrigerant process (MR). In this process, the natural gas temperature is decreased by means of heat exchanges with different type of refrigerants. Ethylene, propane and methane but also nitrogen refrigerants are commonly used in this kind of processes. However, the technology as well as plant components involved in those plants are very expensive, thus their application is feasible only for large scale in which the operative cost is more important than investment cost. At present several plant configurations exist, depending on LNG producers and plant manufacturers. The main available configurations are as follows:

4.2.1. Propane Pre-Cooled Mixed Refrigerant Process (C3MR)

The process is characterized by two refrigeration phases. The first one is a pre-cooling phase using propane. The second one is a mixed refrigerant refrigeration, in which a mixture of refrigerants is used. The mixture involves nitrogen, methane, ethane, ethylene and propane. Figure 4.2 shows a schematic view of the process.

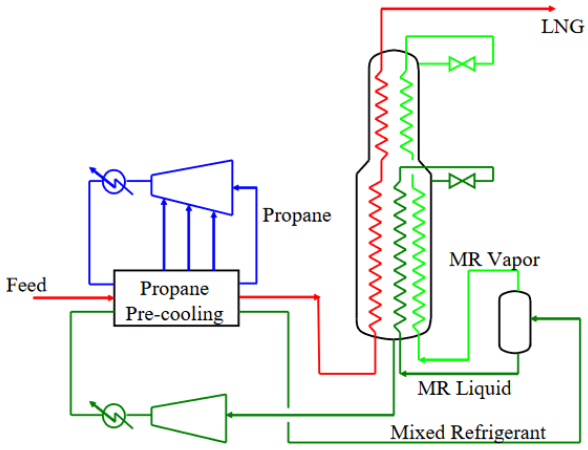

Figure 4.2. Schematic view of the C3MR system

The propane pre-cooling cycle is responsible for the mixed refrigerant cooling down to -35 °C. Subsequently, the MR flow is expanded though several J-T valves, decreasing its temperature in order to approach the methane cooling

curve. During the process, heavier fraction of the MR is condensed and sent back to the compressor unit, while the cold volatile part is responsible for the NG liquefaction.

4.2.2. ConocoPhillips Optimized Cascade®

In this technology, the MR flow is composed by propane, ethylene and methane. A cascade refrigeration process is achieved by means of several cooling and liquefaction phases. A schematic view of the process is represented in Figure 4.3.

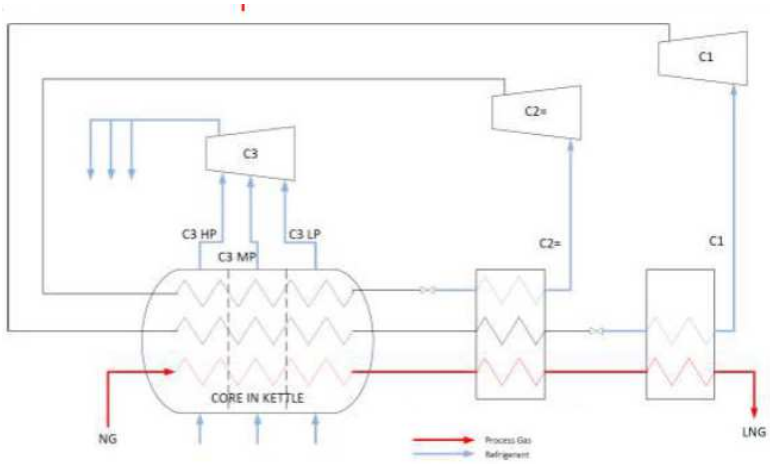

Figure 4.3. Schematic view of the ConocoPhillips system

Air or water cooling are responsible for propane liquefaction. The liquefied propane is then used for ethylene cooling and refrigeration, which accounts for methane refrigeration. Methane liquefaction is achieved by means of several J-T valves. The process is similar with C3MR process, but in this case refrigerants are separated one to each other. Thus, each refrigerant cycle presents a characteristic pressure level. Optimization of this process is possible by changing those pressure levels.

4.2.3. Statoil / Linde Mixed Fluid Cascade Process (MFCP)

Statoil and Linde developed a technology which combines MR and cascade processes. Figure 4.4 shows this LNG technology.

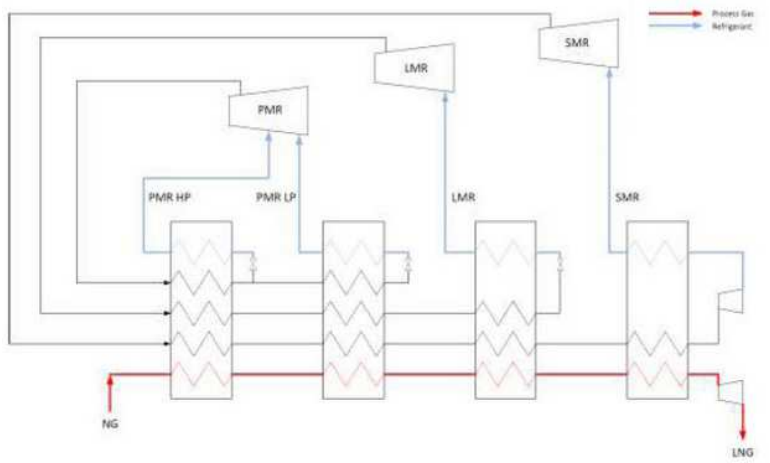

Figure 4.4.Schematic view of the MFCP

Three separate mixed refrigerant cycles were used in the process. The first one is a pre-cooling cycle, the second one is a liquefaction cycle while the third one is a sub-cooling cycle. By combining those MR systems, the natural gas is continuously cooled down. As in the previous system, three cycles were used with different pressure levels, in order to minimize energy consumption.

4.2.4. Shell DMR Process

This cycle is a dual mixed refrigerant cycle. It is based on the C3MR cycle in which the propane cycle is replaced with heavier mixed refrigerant cycle. Moreover, the heat exchanger is replaced with a spiral-wound heat exchanger. In Figure 4.5 the liquefied natural gas technology is schematically represented.

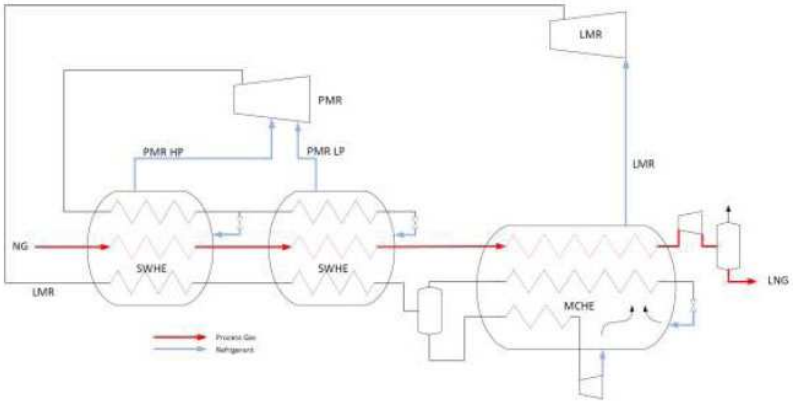

Figure 4.5. Schematic view of the Shell DMR Process

The heavy mixed refrigerant, namely PMR in the figure, accounts for the pre-cooling process. The gas is then further cooled and liquefied by means of the lighter part of the MR (LMR), in a process similar to that of the C3MR. The technology was introduced in order to achieve LNG production in regions where the ambient temperature is varying considerably during the year. To avoid energy efficiency losses due to this aspect, the technology allows the PMR adjustment to create heavier or lighter MR. Heavier MR is suited for high ambient temperatures, while lighter MR is best suited for colder air temperatures.

The abovementioned liquefaction technologies are usually used for large-scale LNG production. In fact, although such processes are presenting high energy efficiency, at the small-scale they are not feasible due to associated high investment costs. Biogas from anaerobic digestion is produced in plants that could be classified as micro-scale, according with the achievable biomethane production. By the way, some attempts to produce LBG from AD plant by means of MR technology were proposed by Wärtsilä group. The process was based on the C3MR configuration. Main objective was to decrease the investment cost associated with the technology. However, the process is not able to purify the incoming biogas, thus biomethane must be previously obtained by means of standard purification technologies. Generally, in order to produce LBG, biogas is upgraded by means of standard technologies to be further liquefied with a liquefaction facility. However, some technologies able to purify and liquefy biogas at the same time are also available in literature, but with limited description and still in a developing phase. Sometimes, such processes allow the production of liquid carbon dioxide (L-CO_2), which is a valuable by-product used in several applications, for example in the food industry. The available cryogenic technologies aimed to remove biogas impurities (mainly CO_2) liquefying it are briefly described.

4.2.5. Scandinavian GtS

The Scandinavian GtS (SGtS), is a Swedish company which is working in the field of biogas, in order to produce LBG. The prosed technology is equipped with four subsequent modules where biogas impurities are removed and biomethane liquefied. Figure 4.6 shows a schematic view of this technology.

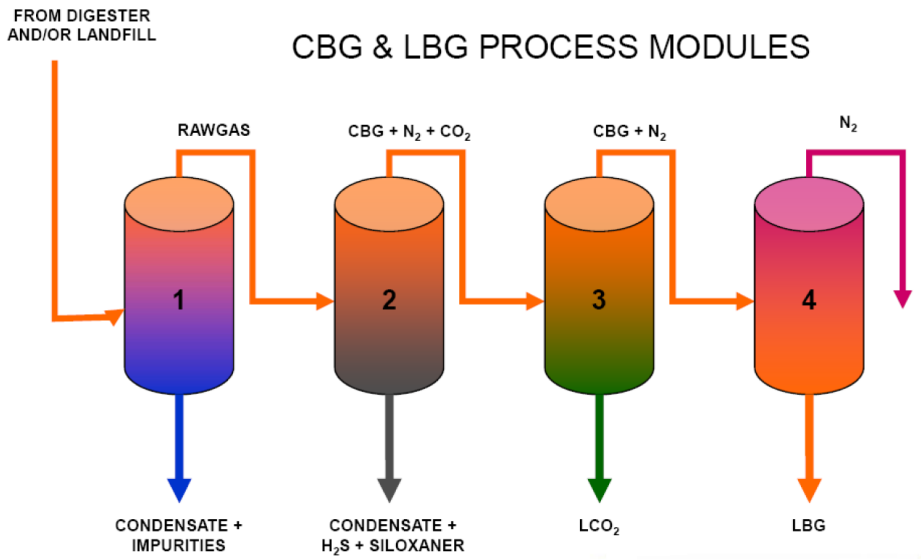

Figure 4.6. Schematic view of the Scandinavian GtS system

The technology aims to produce LBG from landfills or AD plants. At the beginning of the process, the inlet biogas is cooled down to 6°C. In this module, some impurities are condensed and removed from the gaseous flow. The second module performs hydrogen sulphide and siloxanes removal. The cleaned gas is then cooled down to -25°C in order to remove remaining water and siloxanes. The process cannot achieve the complete removal of siloxanes as well as hydrogen sulphide, thus a further purification is needed provided using an adsorber based on a catalytic process. In the third module, CO_2 is removed by cooling the gas down to -78 °C. At such temperatures, carbon dioxide is removed as L-CO_2, to be used for cooling the incoming biogas or to be sold as by-product. The gas coming from the third module is highly pure methane, approximately 99% (Johansson, 2008). At this stage, the biomethane could be compressed to CBG or liquefied to LBG. In the latter case, the gas is cooled down to -190°C in order to produce LBG. However, the liquefaction process was not provided by the company and up to now no existing plants using this process are found.

4.2.6. Acrion Technologies / Terracastus Technologies

The Acrion Technologies is an American company which is working in the field of gases presenting CO_2 concentrations higher than 10%. The proposed process is obtained by combining cryogenic and conventional technologies. Figure 4.7 provides some insight of the process.

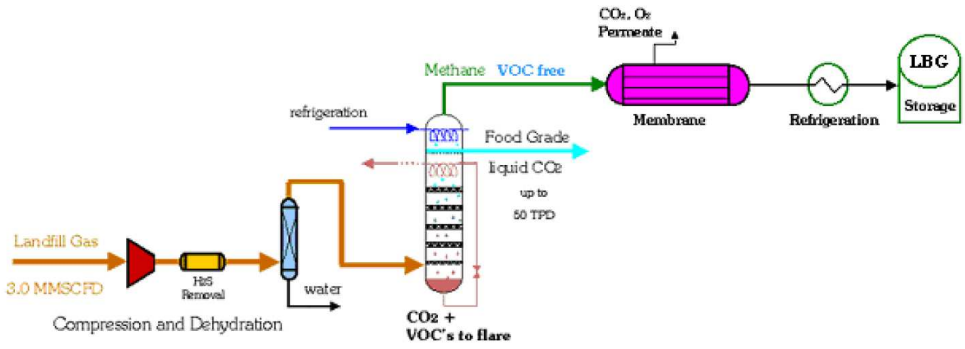

Figure 4.7. Schematic view of the Terracastus system

In the process, a distillation column is used to remove CO_2 and produce LBG. In the column, a cooling unit is responsible for the CO_2 removal. A fraction of the removed CO_2 is then condensed and removed at the top of the column as LCO_2. The remaining fraction is used to absorb other contaminants such as siloxanes and VOCs. The CO_2 flow used to this purpose is then sent to the flare, while the cleaned biogas still contains something like 25% of carbon dioxide. After the column, biogas is sent to the membrane unit, in which two membranes are responsible for the final upgrading. The obtained biomethane is 98 to 99% pure methane (Johansson, 2008). Further purification

is provided by a molecular sieve unit in order to satisfy the required purity level for the liquefaction. Such gas is then cooled down to LBG to be stored. As in the previous technology, a description of the liquefaction phase is not available.

4.2.7. Prometheus – Energy

Prometheus – Energy is an American company that produces LNG. Their project aims to produce LBG by means of commercial technologies to achieve liquefied biogas with methane content higher than 97%. The schematic view of the process is not available, since the company did not disseminate it. The process is divided into several modules. During the first phase, the gas is compressed and impurities such as water and H_2S are removed. In the second phase, the biogas upgrading to biomethane occurs by means of a cryogenic process, which is a proprietary process. In the process, CO_2 is vented and LBG is obtained by means of a closed nitrogen Brayton-Joule cycle. A pilot plant using biogas from landfills produced LBG with a purity level up to 99% (Johansson, 2008).
As previously mentioned, another possibility to produce LBG is to upgrade it by means of traditional purification technologies (section 2.6) and then liquefy it to obtain LBG. Available small-scale liquefaction technologies could be distinguished in three main categories, based on a: closed cycle and open cycle.

4.2.8. Nitrogen / Bryton-Joule cycle (closed cycle)

In this cycle, N_2 is the refrigeration fluid responsible for the biomethane refrigeration. In Figure 4.8, the schematic view of the cycle is presented.

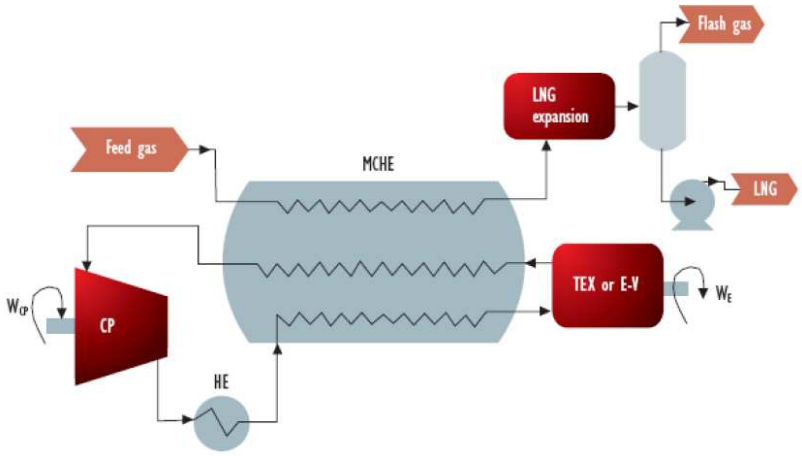

Figure 4.8. Closed cycle, nitrogen Brayton/Joule reverse cycle

During the process, the refrigerant is compressed and cooled by means of a chiller. After this initial refrigeration, it flows into the main heat exchanger in order to be further cooled down. After this step, it is sent to the turboexpander (in this case energy production will also occur) or to a J-T valve in order to quickly decrease its temperature. At this point, by entering again in the main heat exchanger, it provides cold energy for the pre-cooling phase and for the biomethane, which is liquefied to LBG. At the end of the process, nitrogen is sent back to the compressor and the cycle is closed.

4.2.9. Claude Cycle (open cycle)

The technology related with this open cycle is quite simple, and it is represented by Figure 4.9. In this process, the biomethane is compressed up to high pressures and then cooled down.

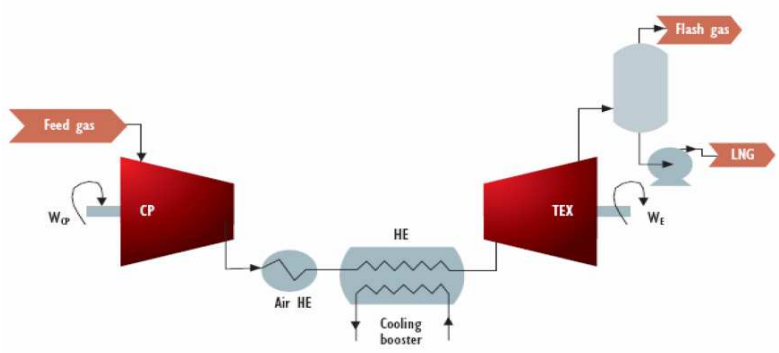

Figure 4.9. Open cycle, Claude cycle

After being cooled, the cold, compressed biomethane is sent to the turboexpander, which is a cryogenic turboexpander in order to simultaneously move the compressor and achieve high temperature decrease. A further expansion in a J-T valve could be necessary in order to avoid liquid formation inside of the turboexpander. A flash unit allows nitrogen removal. Produced LBG is then pumped and stored (Johansson, 2008).

4.2.10. Linde cycle (open cycle)

The liquefaction process based on the Linde cycle is able to achieve gas liquefaction by means of a self-cooling process. Figure 4.10 shows a schematic cycle related with this technology applied for an LNG plant.

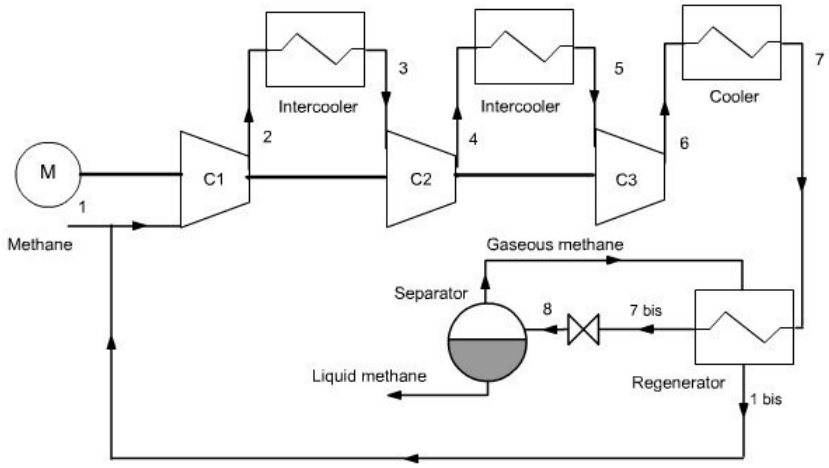

Figure 4.10. Schematic view of the Linde cycle

In the cycle, inlet biomethane is compressed into several compression stages by means of a multistage intercooled reciprocating compressor. At the end of the compression process, the biomethane flows through the main heat exchanger in which its temperature is decreased. Thus, cold and compressed biomethane is sent to a J-T valve in order to quickly decrease its temperature by means of an isenthalpic process. After the expansion, a fraction of the biomethane is condensed to LBG while the remaining part is sent back in the gaseous state. Since biomethane gaseous fraction is at very low temperature (saturated vapor), it is used to provide cold energy to the main heat exchanger, thus the biomethane is responsible for its own cooling. Flowing out of the main heat exchanger, gaseous biomethane flows back to the compressor, mixing with inlet biomethane. As it can be seen, the process requires a certain biomethane fraction to be re-circulated inside the plant. The recycled biomethane depends on the cycle efficiency.
In the next section, a cryogenic separation process to liquefy directly biogas (and not biomethane as previously seen in the above mentioned technologies) based on the Nitrogen / Bryton-Joule cycle is proposed and discussed in detail. In this process, the CO_2 removal process is obtained by means of a deposition process in which CO_2 is frozen inside of a specific heat exchanger, to be further removed.

4.3. The Cryogenic Separation Technology – CO_2 removal

Main interest related to biogas production and liquefaction concerns its usage in the transport sector as vehicle fuel. However, biogas cannot be directly used for this purpose. Nevertheless, LBG cannot be directly produced from biogas due to the presence of several impurities. Therefore, biogas needs to be purified in order to obtain biomethane, to be further liquefied as well as normal NG. At present, this procedure requires several processes. Main impurities to be removed are H_2S and CO_2. Focusing on carbon dioxide removal, an upgrading process is involved in the biomethane production. If the finale scope is to produce LBG, a liquefaction process is also required. At present those processes are generally separated. Purpose of the present work is to explore the possibility of producing LBG directly from biogas with a single plant. In this work, a particular cryogenic plant is proposed in order to obtain LBG as well as pure CO_2. Energy consumption and a roughly economic analysis are also performed. The plant is based on a specific configuration in which the final LBG is produced at high pressure if compared with the standard technology, providing several advantages. Obtained PLNG can be used in the transport sector as vehicle fuel (Economic Commission for Europe, 2013). The simulations are carried out by means of AspenHYSYS®, AspenTech.

4.3.1. Thermodynamic Bases

One of the major issue of natural gas liquefaction plants is surely the presence of CO_2. In fact, due to the high temperature difference in their boiling points, liquefying natural gas cause the carbon dioxide to freeze. Thus, plugging problems easily occurs if CO_2 concentration is too high. In the conventional LNG plants, CO_2 and other minor undesired compounds are removed by means of molecular separation unit in order to prevent these problems.

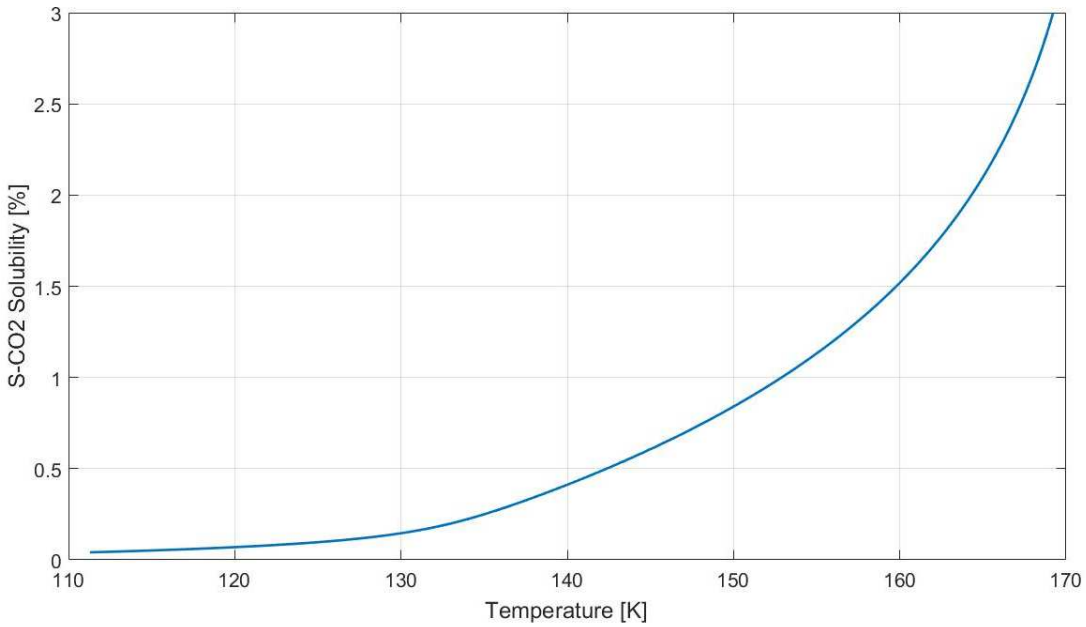

Figure 4.11. CO_2 solubility in LNG diagram

In this work, a cryogenic upgrading process is presented in which pure solid CO_2 is removed and biogas is simultaneously liquefied. To make this possible the final LBG must have a CO_2 content less than the corresponding solubility of CO_2 in liquid methane at the final temperature. In Figure 4.11 the CO_2 solubility in LNG is reported. Considering a standard liquefaction plant in which the final pressure and temperature are usually around 1 bar and 111 K respectively, the corresponding solubility is about 0.02%. Consequently, the final CO_2 content should be less than 0.01%, taking into account a safety margin. Since liquefaction processes are energy intensive, it is not convenient to have a final pressure this low because the corresponding final temperature would be consequently low. However, it should be not too high in order to avoid liquid CO_2 formation during the initial cooling phase. This is evident in Figure 4.12 in which the phase CH_4 - CO_2 binary system diagram is represented. Considering the biogas typical composition, in the diagram the 50%, 40%, 30%, and 0.1% of CO_2 content are reported. Due to the fact that liquid CO_2 should be avoided during the cooling phase, the maximum allowable pressure is about 10 bar. Thus, 7 bar was chosen as the operative pressure. At this pressure, the corresponding temperature is of about 144 K with a

solubility of about 0.55%. Thus, a final CO_2 concentration of 0.1% was chosen in order to prevent any kind of plugging issues.

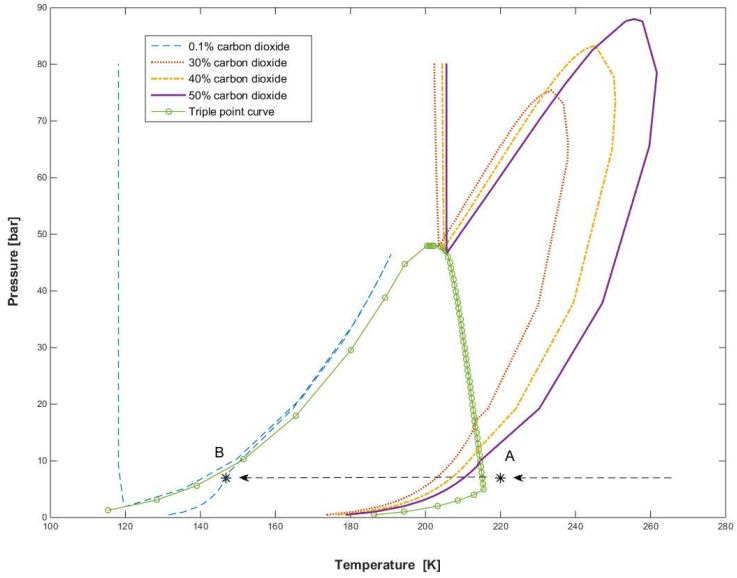

Figure 4.12. Phase diagram of CH_4 – CO_2 binary system

According with the variable biogas composition, different concentrations were considered and analysed using this operative pressure and final CO_2 concentration. The solid carbon dioxide is separated by means of a gas – solid separation unit.

4.3.2. The Cryogenic Process

The process proposed in this work is based on the PLNG (Pressurized Liquefied Natural Gas) technology. Introduced in 1998, it allows to liquefy natural gas at higher pressure by comparison with conventional LNG plants. Due to the increased final pressure, the final temperature is higher as well, requiring much less power for the liquefaction. Since the introduction of this technology, several studies were made regarding both the containment system (Fairchild et al., 2005) and the thermodynamic optimization of the process (Bowen et al., 2005; Walid M., 2015). It was found that the optimal final pressure for PLNG technology is 17 bar (Hveding A. H., 2010). Thus, this value will be used in this work.

The proposed process is schematically represented in Figure 4.13 and it is based on the PLNG process previously presented by (Xiong et al., 2015) who introduced this novel technology aimed at footprint reduction in offshore LNG plants. In order to simplify the analysis, the plant is fed by biogas composed only by CH_4 and CO_2, thus a pre-treatment unit for minor compounds removal is not taken into account. As shown in the Figure 4.13, biogas is firstly compressed to rise its pressure from atmospheric pressure (exiting from the biogas plant) up to 7 bar, as it is the operative pressure.

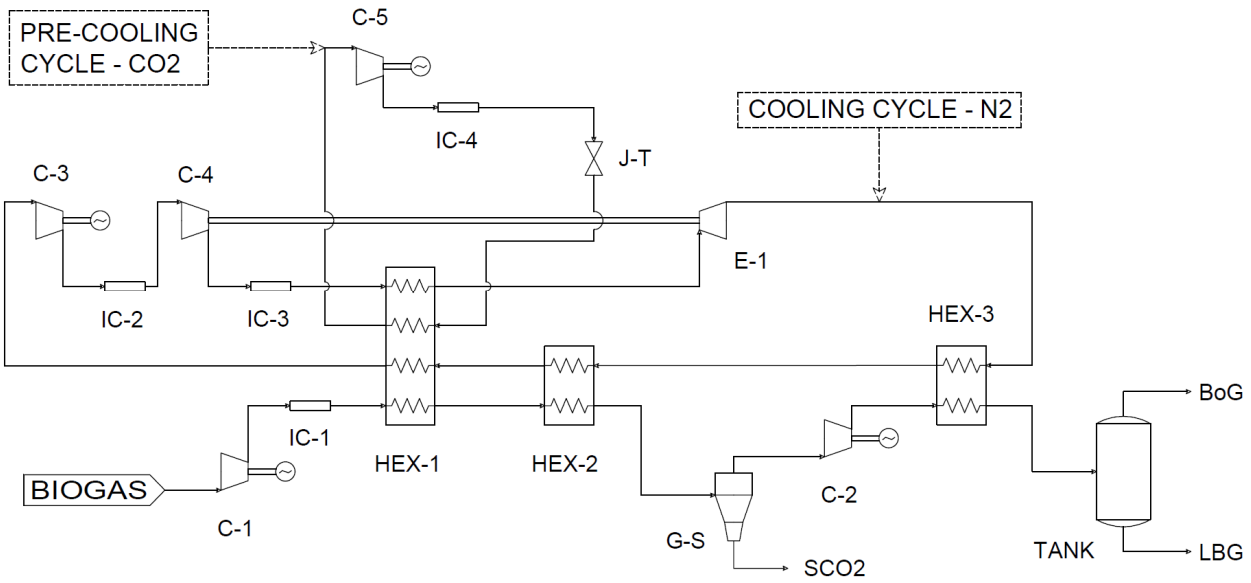

Figure 4.13. Schematic view of the proposed plant.

After this, it is cooled down by means of heat exchangers HEX-1 and HEX-2 (B point in Figure 4.12). At this point the biogas is sent to the gas – solid separation unit (G-S) in which solid CO_2 (SCO2) is removed. The gas stream is then compressed up to 17 bar by means of a cryogenic compressor. Thus, it is cooled in HEX-3 in order to obtain pressurized liquid biogas to be stored in a cryogenic tank. Refrigeration is obtained by means of two cycles, namely the pre-cooling and cooling cycle. The former is a CO_2 refrigeration cycle in which the gas is firstly compressed and cooled in an intercooler (IC-4). Thus, it is expanded in a J-T valve to be sent in the HEX-1. Regarding the cooling cycle, it is a N_2 refrigeration cycle, similar to the pre-cooling one. However, in this case the expansion takes place in an expander (E-1), in which the energy recovered is used to compress the gas (C-4).

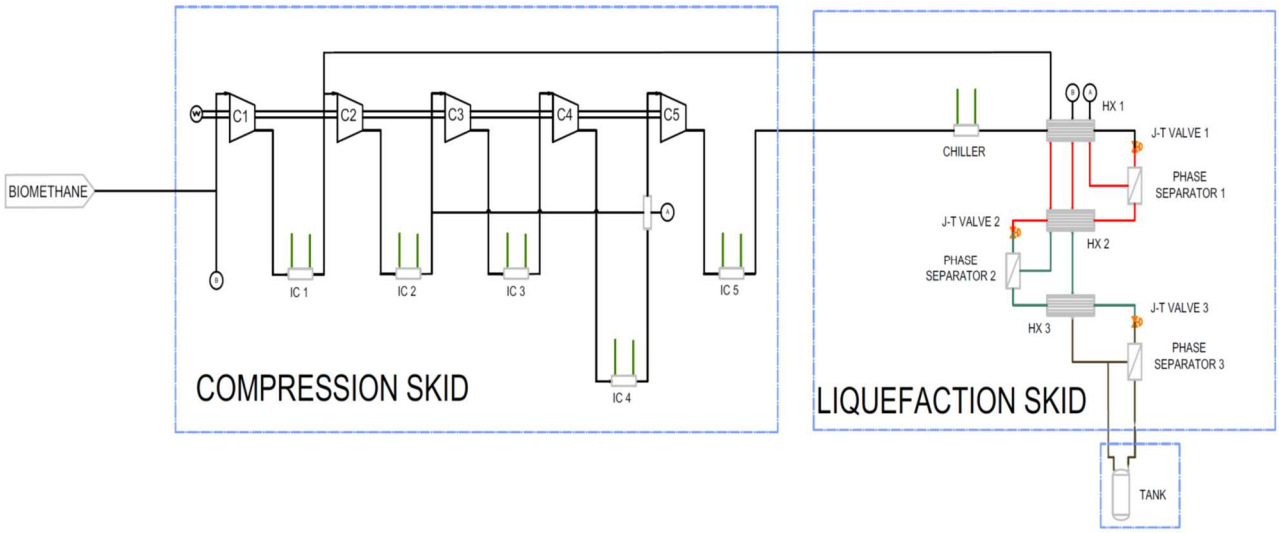

Figure 4.14. Schematic view of the triple pressure Linde cycle (Arteconi et al., 2015).

The thermodynamic analysis was performed by means of a steady-state simulation in HYSYS environment. The fluid properties were determined using the Peng-Robinson equation of state fluid package and the cycle was analysed by means of the sequential search algorithm with which the selected key parameters are optimized according to some constraints. In this work, the only constraint is the minimum approach temperature in the heat exchangers. Moreover, the stream exiting from HEX-3 must be liquid. Finally, the specific energy consumption is calculated for different biogas composition and compared with a conventional plant in which biogas is firstly upgraded and then liquefied. The upgrading technology considered for the conventional plant is the water scrubbing technology that is the cheapest and simplest one (Nie et al., 2013). Regarding the liquefaction technology, a triple pressure Linde cycle was considered, as schematically represented in Figure 4.14. This plant was analysed in a

steady – state mode, by means of EES (Klein, 2013). Since the 500 $Sm^3 \cdot h^{-1}$ is the typical Italian biogas production rate, this size was considered for the analysis.

4.3.3. Results and Discussion

Aim of the present work was to evaluate the PLNG technology as a possible candidate for biogas upgrading and liquefaction. For this purpose, a particular cycle, previously studied for another goal, was selected and analysed, and the specific energy consumption was calculated. In order to make a comparison between this technology and the standard existing technology, a conventional upgrading and liquefaction plants were considered. The selected upgrading plant is the water scrubbing while the liquefaction plant is a triple pressure Linde cycle. For the former one, operative costs were taken from Warren (2012). The biogas processed is considered to have a composition of 53% CH_4 and 47% of CO_2.
It was found that the specific cost for the water scrubbing upgrading process and liquefaction process is of about 1.77 $c€ \cdot kWh^{-1}$ and 0.36 $c€ \cdot kWh^{-1}$ of produced biogas, respectively. Thus, the specific cost of the conventional upgrading and liquefaction technology is then 2.13 $c€ \cdot kWh^{-1}$ of biogas produced. By comparison, the proposed PLNG technology, with a final CO_2 concentration of 0.1%, presents a specific cost equal to 1.64 $c€ \cdot kWh^{-1}$, 1.39 $c€ \cdot kWh^{-1}$ and 1.23 $c€ \cdot kWh^{-1}$ of produced biogas for an inlet CO_2 concentration respectively of 30%, 40% and 50% (Figure 4.15).

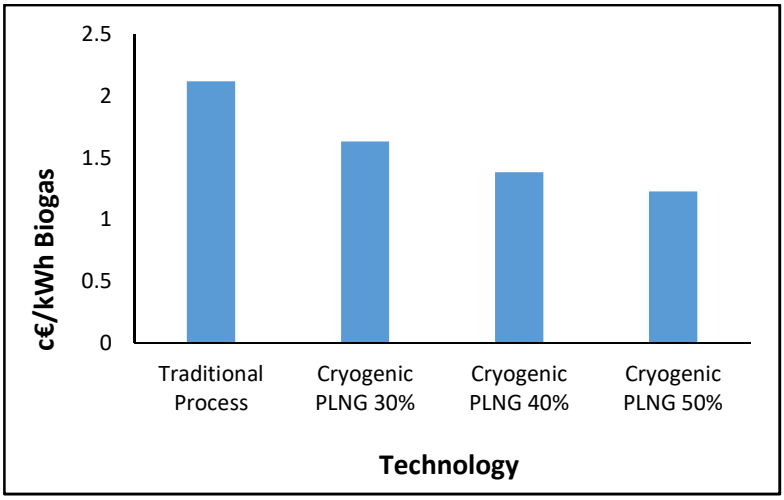

Figure 4.15. Specific cost comparison between the traditional upgrading plus liquefaction process and PLNG technology.

As it can be seen, the specific cost for the PLNG technology decreases as the CO_2 inlet biogas concentration increases. This is due to the fact that carbon dioxide has a higher density and it exchanges heat more efficiently than methane, thus minor power is requested for its liquefaction. On the other hand, a higher CO_2 concentration means a lower methane content. Consequently, the specific energy consumption, expressed as the energy consumed to obtain 1 kg of LBG, decreases as the carbon dioxide inlet content decreases, as reported in Table 4.1. Looking at this table, it is possible to note that PLNG technology is energy intensive process, with considerably higher specific energy consumption than the conventional one. However, the former allows to obtain LBG directly from biogas, with a final methane concentration included between 99.5% and 99.9%, and no molecular separation unit is required. Moreover, a considerably amount of pure CO_2 could be recovered and sold as a by-product (Table 4.1).

Table 4.1. Energy performance of the proposed liquefaction plants.

Parameter	Triple pressure Linde	PLNG (30% of CO_2)	PLNG (40% of CO_2)	PLNG (50% of CO_2)	Unit
Compressor power	100.1	529.5	448.7	389.4	kW
Chiller power	37.71	-	-	-	kW
Mole sieve	20	-	-	-	kW
Total power	157.81	529.5	448.7	389.4	kW
Specific energy consumption	0.9	1.532	1.688	1.982	$kWh \cdot kg^{-1}$ *LBG*
CO_2 recovered	-	404.4	484.2	549	$Kg \cdot h^{-1}$

Since the inlet biogas composition influences the specific energy consumption for the liquefaction process, the same happens for the final CO_2 content in LBG produced. In order to evaluate this aspect, a sensitivity analysis was performed by varying the final LBG composition. Looking at Figure 4.12, increasing the final CO_2 content means to increase its final temperature, as the B point moves to the right. Thus, the liquefaction process requires less cooling energy in HEX-2 and HEX-3. Figure 4.16 shows the results of the analysis.

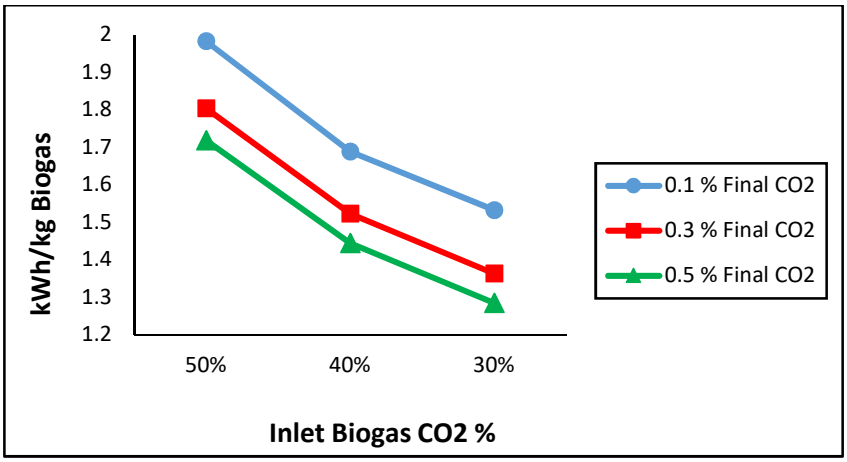

Figure 4.16. Influence of final CO_2 concentration on the specific energy consumption.

As it can be seen, the specific energy consumption decreases when the CO_2 concentration in inlet biogas decreases. These results show that, depending on the biogas inlet composition and on the carbon dioxide content of the final LBG, the specific energy consumption can vary from 1.982 $kWh \cdot kg^{-1}$ to 1.284 $kWh \cdot kg^{-1}$ of produced LBG, respectively for the worst and the best scenario. Moreover, by increasing the final CO_2 content in LBG, inlet biogas could be compressed at a higher pressure (Figure 4.12), increasing the heat exchanger efficiency and reducing the specific energy consumption.

4.3.4. Conclusions

In this work, a cryogenic upgrading process was proposed and evaluated. The final scope was to make a comparison between this technology and the conventional upgrading and liquefaction technology. It was shown that the PLNG technology has a lower specific energy consumption. Consequently, it has a lower specific cost of 1.64 $c€ \cdot kWh^{-1}$, 1.39 $c€ \cdot kWh^{-1}$ and 1.23 $c€ \cdot kWh^{-1}$, depending on the biogas composition, while the conventional process accounts for 2.13 $c€ \cdot kWh^{-1}$. In order to evaluate the dependency on the final LBG composition, a sensitivity analysis was also performed. The results show that the specific energy consumption could be considerably reduced from 1.982 $kWh \cdot kg^{-1}$ (worst scenario) to 1.284 $kWh \cdot kg^{-1}$ (best scenario) of produced LBG.
The analysis shows that PLNG technology is a valid solution for the cryogenic upgrading of biogas. Effectively, it allows liquefying it directly without conventional upgrading process or molecular separation unit. Moreover, a

considerably amount of pure CO_2 could be recovered. Finally, the plant can produce LBG with the final requested CO_2 content independently from the inlet biogas composition.

4.4. The Cryogenic Separation Optimization – CO_2 removal

As shown in the previous section, cryogenic separation technology could represent a promising solution in order to achieve LBG. It could achieve impurities removal and methane liquefaction with high purity by means of a single plant. Moreover, removed impurities allow cold energy recovery and could be sold as by-products. In this work, a modification of the cryogenic separation process able to achieve biogas purification and liquefaction is presented. In this plant, carbon dioxide (CO_2) and cold energy recovery processes are involved in order to decrease specific energy consumption while increasing the total revenue. The proposed plant is further optimized and a sensitivity analysis is also performed. The energy consumption and operative costs are compared with those of standard technologies, considering the influence of CO_2 as byproduct. Plant simulations were performed by means of AspenHYSYS®, AspenTech software. Optimization analysis were performed by means of an integration of modeFRONTIER®, ESTECO, MathWorks®, Matlab and AspenHYSYS®, AspenTech environments. Results indicate that the proposed plant represent a valid option in LBG production. It allows the replacement of two different plants, achieving carbon dioxide removal and sale as well as biomethane liquefaction. Aim of this analysis is to evaluate and optimize the proposed cryogenic separation technology. As for the previous work, a comparison between this technology and the traditional technologies is presented. The analysis also considers a traditional cryogenic upgrading technology for the comparison (Hagen et al. 2001). Finally, a sensitivity analysis was performed, based on the optimization results. Again, the considered plant size is related with the Italian biogas plant market, to be equal to 500 $Nm^3\ h^{-1}$.

4.4.1. The Liquefaction Process

The cryogenic upgrading plant proposed in this work is based on the pressurized liquefied natural gas (PLNG) that has been already discussed in the previous section. Figure 4.17 shows a schematic representation of the proposed plant.

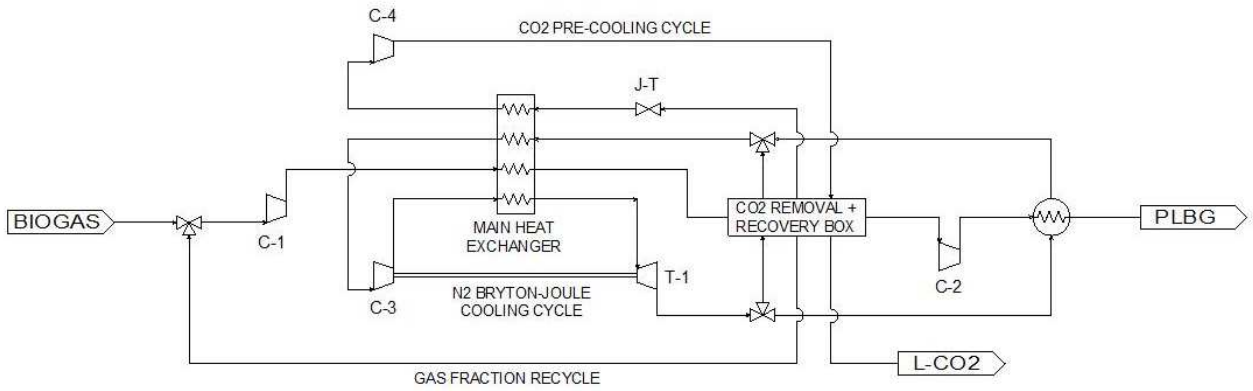

Figure 4.17. Schematic view of the cryogenic separation plant

After dehumidification and desulfurization processes, biogas is sent to the plant an initial pressure of 1 bar. Depending on its composition, it is compressed through C-1 at the appropriate operative pressure. After that, compressed biogas is sent to the main heat exchanger in which temperature is decreased down to point A represented in Figure 4.12. Then, it flows into the CO_2 removal and recovery box. Here, biogas is further cooled down to the final cooling temperature, depending on operative pressure. During the cooling process, deposition of CO_2 occurs and thus highly pure biomethane is obtained after this step. On the other hand, CO_2 removal and recovery box allows also cooling load recovery and L-CO_2 production. More details regarding CO_2 removal and recovery box are presented in next section. Biomethane produced at this level (point B in Figure 4.12) is then further compressed up to its final pressure and cooled down to subcooled PLBG ready to be stored. The cooling process is composed of two main cycles. The first one is the precooling cycle. Working fluid of the precooling cycle is carbon dioxide. After being compressed it enters into the CO_2 removal and recovery box in which its temperature is decreased. After that, it is expanded into a Joule-Thompson valve thus cooling energy is provided to main heat exchanger. The second

one is the cooling cycle based on the reversed N_2 Bryton-Joule cycle. Nitrogen is firstly compressed and sent to the main heat exchanger in which its temperature is decreased. Refrigerant is then sent to the turbo-expander in which a considerable amount of energy is recovered. After that the flow is divided into two secondary flows. The first one is responsible for the entire deposition process. The second one is responsible for biomethane final liquefaction. Eventually, the two secondary flows are mixed together and sent back to the main heat exchanger. Here, remaining cooling load is used in order to cool down both inlet compressed biogas and nitrogen. Considering Figure 4.17, compressor unit C-1, C-3 and C-4 are meant to be multi-stage air-cooled reciprocating compressors.
During the deposition process, biogas cooling and CH_4 enrichment are meant to happen simultaneously. This means that solid carbon dioxide is produced and temporally stored inside the heat exchanger. As biogas flowing through the heat exchanger is cooled down, S-CO_2 is produced on the cold surface of the heat exchanger. Thus, a growing distributive frost layer is formed. Obviously, this kind of process cannot be achieved during continuous operation due to the reduction of the heat exchanger cross-section. In order to overcome this issue, making the process continuous, a secondary heat exchanger can be introduced. Moreover, as the used pre-cooling cycle refrigerant is CO_2, this cycle can be used to achieve both cold load and S-CO_2 recovery. Figure 4.19 provides more information regarding this point. Pre-cooled biogas, coming from the main heat exchanger, is firstly sent to the primary heat exchanger counter current with cold nitrogen coming from the turbo-expander. Thus, deposition process occurs and biomethane with high purity level is produced while pure S-CO_2 is collected as a frost layer inside the primary HEX. A flow sensor (FE in the figure) is responsible for the flow measurement so as the flow decreases under a certain acceptable level means that the process cannot continue. At this point, pre-cooled biogas as well as cold nitrogen are sent to the secondary HEX by means of three-way valves TW-1, TW-2, TW-3 and TW-4. This operation allows the continuation of deposition process and biomethane production. While secondary HEX is operating, primary HEX needs to be cleaned and S-CO_2 removed. In this moment, primary HEX is filled with solid carbon dioxide and enriched biogas in gaseous phase. Through three-way valves TW-6 and TW-7, a vacuum pump removes remaining gaseous biogas to be re-circulated to the inlet biogas. Remaining mass is foreseen to be very low, thus this procedure does not affect inlet biogas composition. The vacuum pump is stopped when the flow is close to zero. At this point, primary HEX is connected with the pre-cooling cycle for cold load and S-CO_2 recovery. Using TW-5, a conveniently amount of pressurized CO_2 flows through primary HEX, directly on the frozen layer. Due to the high pressure, S-CO_2 is warmed up, changing its state to the liquid form.

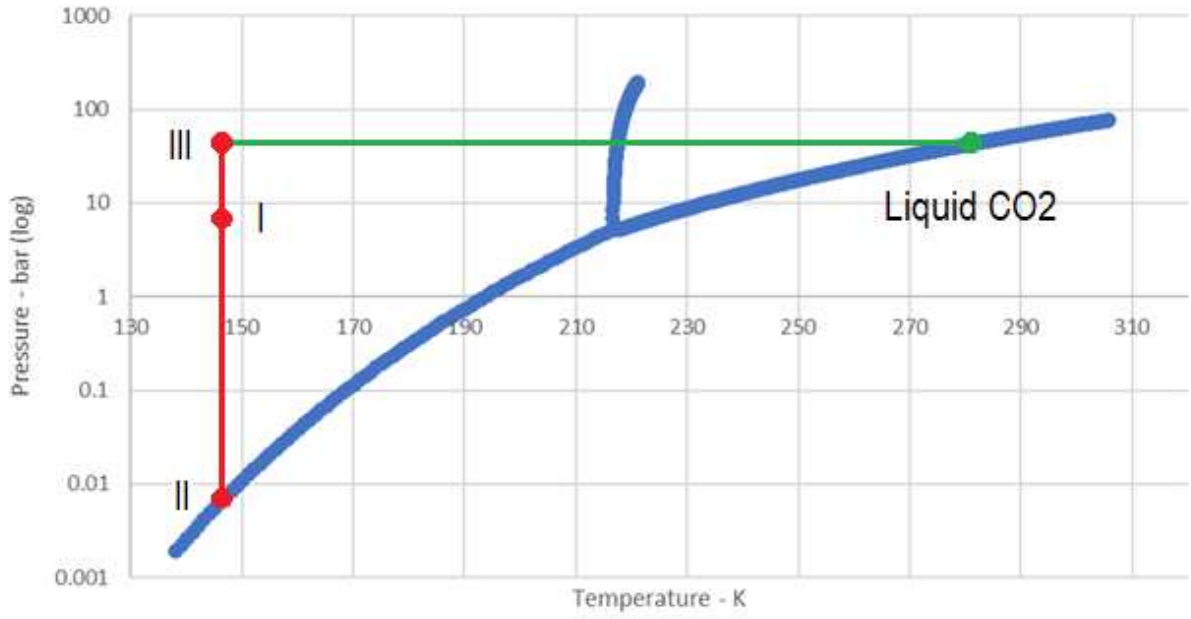

Figure 4.18. CO_2 phase diagram

Considering Figure 4.18 it is possible to better understand this passage. S-CO_2 collected on the primary HEX surface is represented by point I in the diagram. By removing remaining biogas inside of the heat exchanger, pressure is quickly decreased, thus frozen carbon dioxide begins to sublimate. Suppose the solid CO_2 temperature constant, point II in the diagram is reached. Having such a condition means that the vacuum pump flow rates is close to zero. The key point is to completely remove CH_4. The vacuum pump is then stopped and CO_2 from the pre-cooling cycle

quickly increases the pressure inside the primary HEX. Thus, point III is reached, looking at the diagram. Now, S-CO_2 cools the gaseous CO_2. The frozen layer is warmed up and liquid formation occurs. Produced L-CO_2 flow is then splitted into two flows. The first one is re-circulated to the pre-cooling cycle. The second one is pumped to higher pressure and stored in vessels, ready to be sold as by-product. As previously mentioned, produced L-CO_2 is 100% pure, allowing it to be sold for alimentary purposes. Once S-CO_2 has been removed, TW-5 is closed and primary HEX is connected with the vacuum pump. Thus, remaining carbon dioxide is re-circulated to pre-cooling cycle. At the end of the process, TW-1, TW-2, TW-3 and TW-4 restore the original situation. Thus S-CO_2 in secondary HEX is removed as well. By correctly sizing primary and secondary HEX it is possible to grant the necessary exchanging area in order to make the process continuous.

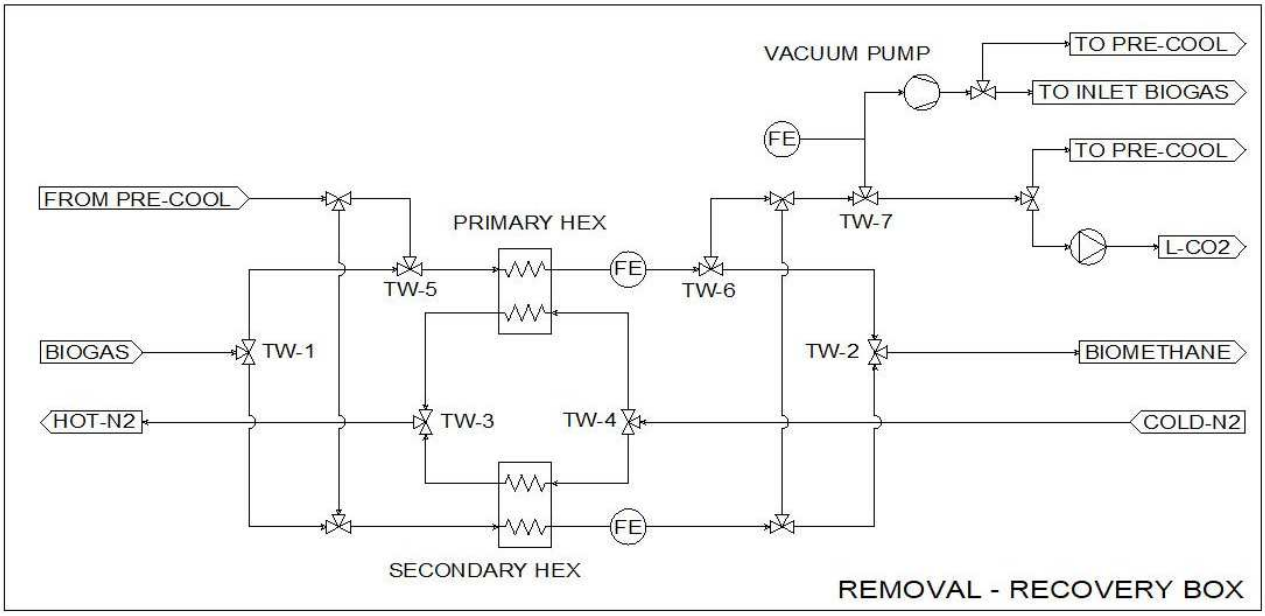

Figure 4.19. Schematic view of the L-CO_2 and cold recovery unit

As described in the previous section, the proposed process seems to be discontinuous in time. However, it can be considered a continuous process as for the flow rate in a reciprocating compressor. Thus, a steady-state analysis of the plant is possible in order to evaluate and optimize energy consumption. AspenHYSYS®, AspenTech environment was found to be the right software for such analysis. In Peng-Robinson equation of state were found to successfully predict CH_4 – CO_2 behaviour, thus this EoS package was used in this work. Considering the deposition process as represented in Figure 4.12. From point A to point B deposition of CO_2 occurs whereas temperature decreases. This process results in the formation of a frozen layer inside of the heat exchanger. This layer, accordingly with Figure 4.12, is characterized by a temperature gradient. Thus S-CO_2 formed at the very beginning of the heat exchanger has a higher temperature than that at its final cross-section. When carbon dioxide from pre-cooling cycle is sent through the heat exchanger, it encounters cooler and cooler frozen layers. Therefore, the process can be simulated in AspenHYSYS®, AspenTech as a simple counter-current heat exchanger followed by a mixer. Since the process is supposed to be continuous, S-CO_2 is considered as a stream flow. Figure 20a schematically represents what is supposed to happen during the cold and S-CO_2 recovery inside the heat exchanger. Figure 4.20b represents the process as it was implemented in the AspenHYSYS®, AspenTech software.

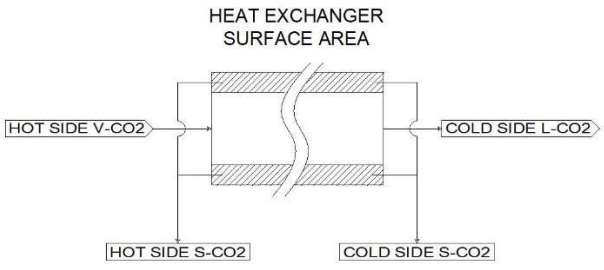

Figure 4.20a. Detail of the L-CO_2 recovery

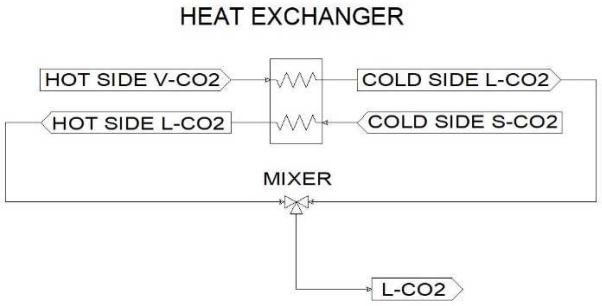

Figure 4.20b. Simulation scheme of recovery process

As already mentioned, purpose of the present work is to evaluate a novel cryogenic separation plant to simultaneously upgrade biogas and produce PLBG. Moreover, cold load as well as liquefied carbon dioxide

recovery systems were integrated in the plant. In order to evaluate the technology, a comparison with standard technologies is presented. Nowadays, interests toward cryogenic upgrading processes are growing but still the technique is not commercial, being highly energy intensive. Therefore, biogas producers interested in LBG production, to be sold as vehicle fuel, are using commercial technologies. Raw biogas, after dehumidification and desulfurization, is characterized by high CO_2 content. Standard upgrading processes allow biogas purification to biomethane with a methane content always higher than 96%. Linde cycle based liquefaction plants are the best choice to produce LBG to this scale. In such plants, several Joule-Thompson valves are used to quickly decrease gas temperature. This kind of valves are generally affected by plug issues, thus very high methane purity level is mandatory. Standard methane quality for those plants is of about 50 ppm of CO_2 at maximum (Coyle et al.). Therefore, a further purification process is necessary in order to fulfill this requirement. Molecular separation modules are generally used to this purpose. After this unit, biomethane is almost 100 % pure methane, thus LBG can be produced. Standard upgrading technologies have already been discussed in section 2.6. Regarding standard liquefaction process, Figure 4.21 shows a schematic representation of a triple expansion Linde cycle. This process was shown to be the cheapest and simples technology for this size (Nie et al., 2013)

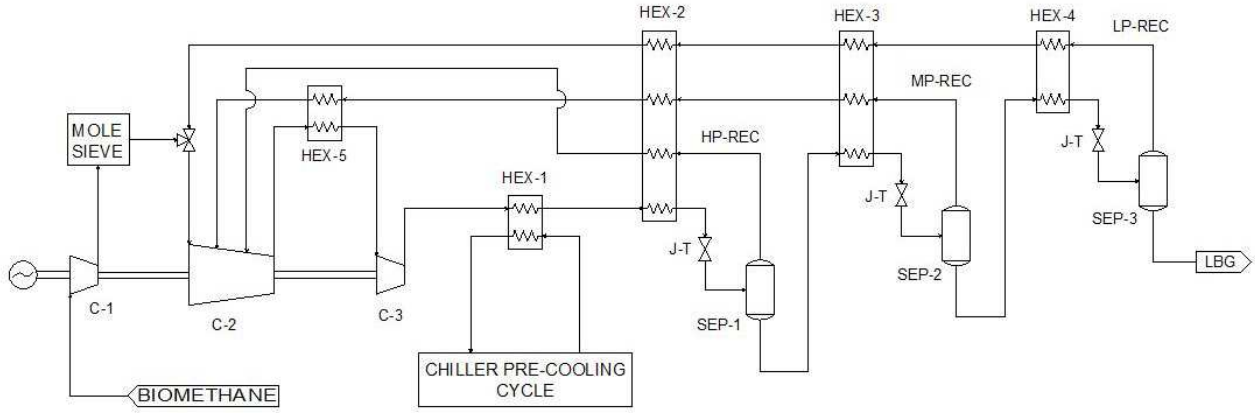

Figure 4.21. Schematic view of the triple expansion Linde cycle

Produced biomethane coming from the upgrading facility at pressure equal to 1 bar is firstly compressed in C-1 up to the low pressure recycle (LP-REC). After being compressed, it enters into the molecular separation unit for further purification. Downstream of the mole sieve module, highly pure biomethane is mixed with low pressure recycle and then compressed into several stages through C-2. Here, some cold energy load is recovered by means of HEX-5 using medium pressure recycle ad then C-3 provides final compression up to 200 bar. Compressed biomethane is pre-cooled in HEX-1 using a commercial chiller unit able to cool the stream down to -35 °C. From here on, biomethane is expanded through several Joule-Thompson valves (J-T) in which the temperature is quickly decreased. After each expansion, a certain amount of liquid is produced in the phase separator (SEP-1, SEP-2, SEP-3). Thus, the flow is splitted into two flows, namely a vapor and a liquid flow. The vapor flow is recirculated (HP-REC, MP-REC, LP-REC) in order to provide cooling load to the primary stream. The liquid flow is further cooled down and expanded. At the end of the process, in SEP-3, the final LBG is produced and stored. LBG final pressure is generally not higher than 10 bar. In fact, although increasing final LBG pressure ensures lower energy consumption due to biogas compression, final LBG temperature is increased. As a consequence, cooling load from the recycled streams decreases, thus increasing required recirculated flow. Eventually, increasing the final LBG pressure causes lower cycle efficiency. For this reason, a final LBG pressure of 8 bar was considered. In the present work, each standard upgrading biogas technology is evaluated and compared with the proposed cryogenic separation process. Specific energy consumption as well as specific LBG cost are key parameters.

4.4.2. The Optimization Process

Nowadays, optimization has begun a key point in most scientific field. By correctly defining a problem, it is possible to identify one or more than one objective functions. Those functions depend on some specific parameters under specific constraints. Defining a problem to be optimized means to identify such parameters and related constraints in order to obtain feasible results. Thus, optimizations like energy consumption minimization as well as profit maximization, just to mention a few, become possible. In process engineering the main purpose remains minimum resources consumption and maximum energy efficiency. However, time spent to achieve optimal results also

represent an important resource, thus optimization should be achieved in a reasonable time. At present, several software have been developed in order to fulfill this requirement. In this work, modeFrontier®, ESTECO optimization software was chosen for the analysis. The platform has intuitive interface, allowing coupling with third part engineering tools. Moreover, it provides several referred single and multi-objective optimization algorithms. Once the problem is defined, the software requires a Design of Experiment (DOE) matrix and an optimization algorithm in order to achieve optimization. The DOE matrix is obtained considering the following information:

- input variable ranges;
- input variable step;
- the DOE algorithm.

The input variables and ranges are user-defined. By combining such parameters, one could imagine that the optimal plant configuration related with such variables is somewhere inside of a 'design space', that is generated from the input variables. Such space is limited by the user-defined constraints. In order to find the best configuration, the software requires some information about the design space. Such information are obtained by defining the DOE algorithm. This algorithm chooses some points inside of the design space, in which each point is corresponding with a possible input variable set. This is necessary in order to give to the optimization algorithm some insight regarding the variable space. A certain number of DOE is set from the user and one or more than one DOE algorithms are chosen. Once the DOE matrix is defined, the optimization algorithm investigates the design space in these DOE configurations. The objective function of this optimization analysis is the specific energy consumption. As a consequence, for each DOE a solution is found, which means that for a specific input variable set, a related specific energy consumption is computed. Based on the collected data, the algorithm is finally able to find the preferable path, which is probably related to the best final plant configuration. The optimization analysis consisted of the following phases:

1. Selection and definition of the DOE algorithm/s;
2. DOE matrix generation;
3. Selection of the optimization algorithm;
4. Launch the optimization procedure;
5. Repeat points 1 to 4 for n times;
6. Collect the output results;
7. Select the best group of variable input set for each launch;
8. Consider those set as DOE to define another DOE matrix;
9. Launch the optimization procedure.

Once the last phase is completed, the best result from optimization procedure is obtained. The number on optimization procedure iteration was n = 3 (based on the author knowledge). Table 4.2 shows the selected algorithms and related setting values.

Table 4.2. DOE matrix definition parameters and algorithms

Algorithms	**Number of DOE / Number of iterations**
Random	50
Sobol	100
Incremental Space Filler (ISF)	350
Evolutionary Strategy (ES)	1499 - 3499

The selected algorithms are described as follows:

- **Random:** the random sequence selects a user-defined number of point in the design space using a mathematical algorithm based on the theory of random number generation;
- **Sobol:** a deterministic algorithm aiming to uniformly select points in the design space, based on a preexisting DOE matrix. The algorithm is a quasi-random algorithm;
- **Incremental Space Filler:** it is an augmenting algorithm based on a preexisting DOE matrix, able to generate a uniform distribution of the point into di design space. It implements the maxmin criterion, thus new points are added where the minimum distance between the existing point is maximized;
- **Evolutionary Strategy:** the optimization algorithm is based on the concept of 'adaption and evolution'. The optimization phases of the algorithm are: generate a population, evaluate the individuals, select the best ones, recombining them, adding mutation, evaluate new individuals. The procedure is iterated until the convergence is reached (Rechenberg, I. 1973; Hans-Paul Schwefel, 1995; Beyer et al., 2002).

While the Random algorithm can generate DOE matrixes itself, the Sobol and ISF algorithm cannot. Thus, the DOE matrix is defined by creating an initial DOE based on the Random algorithm. Subsequently, the Sobol and then the

ISF algorithms are launched, thus the final DOE is obtained. By combining those algorithms, one could be sure that two DOE generated by means of such procedure are not going to be the same. Moreover, the generated DOE is highly uniformly defined. In process engineering, minimization of energy consumption and maximization of overall efficiency are major items. To this purpose, it is useful to define specific parameters in order to effectively evaluate such characteristics. Thus, in the present work the final scope is the minimization of specific energy consumption. The parameter identifies the required energy in kWh to produce 1 kg of final product, in this case PLBG. In the proposed cryogenic separation technology, specific energy consumption is affected by several parameters, which are generally defined during the project phase. Purpose of the optimization analysis is to find the best initial configuration to minimize specific energy consumption. Information regarding chosen key parameters as well as problem constraints are presented in Table 4.3.

Table 4.3. Input parameter of the cryogenic cycle

Parameters	**Lower bound**	**Upper bound**	**Step size**
N_2 high pressure	5 bar	80 bar	0.25 bar
N_2 low pressure	1 bar	36 bar	0.25 bar
CO_2 high pressure	10 bar	57 bar	0.25 bar
CO_2 low pressure	6 bar	20 bar	0.25 bar
PLBG final pressure	15 bar	20 bar	0.125 bar
CO_2 biogas content	30% [mol]	50% [mol]	0.25% [mol]
CO_2 biomethane	0.1 % [mol]	0.5 % [mol]	0.1% [mol]

Parameters in Table 4.3 are those key parameters that actively influence specific energy consumption. CO_2 biogas content is considered as key parameter too. In fact, carbon dioxide concentration in inlet biogas strongly affects plant operative conditions as well as its efficiency. Biogas composition is a consequence of the anaerobic digestion process. More specifically, it mainly depends on biomass type and operative temperature. Thus, carbon dioxide contained in produced biogas can be controlled. Since the proposed plant also integrates cold energy recovery, to maximize CH_4 biogas content could not necessarily result in a decreased specific energy consumption. For this reason, CO_2 inlet biogas composition was selected as a key parameter. By changing inlet biogas composition, the deposition process operative pressure changes as well. In order to avoid unfeasible designs, some constraints have been introduced. Table 4.4 provides information about the constraints.

Table 4.4. Considered constraints

Constraint name	**Condition**
N_2 cooling cycle	N_2 high pressure > N_2 low pressure
CO_2 pre-cooling cycle	CO_2 high pressure > CO_2 low pressure
Deposition process pressure	PLBG final pressure > Deposition operative pressure

As already mentioned, the software used for the optimization analysis was modeFrontier®, ESTECO. On the other hand, the software used for plant simulation was AspenHYSYS®, AspenTech. In modeFrontier®, ESTECO environment, the coupling with several third part engineering tools are available. By the way, AspenHYSYS®, AspenTech cannot actually be directly coupled with modeFrontier®, ESTECO, thus in order to let those software communicate a MathWorks®, Matlab script was used.

4.4.3. Results and Discussion

Aim of the present work is to evaluate a novel cryogenic separation plant able to remove CO_2 while producing PLBG. Cold load recovery as well as L-CO_2 recovery systems are integrated in the plant. An optimization analysis is performed in order to find optimum parameters for the plant. The cryogenic separation technology is then compared with the state of the art technologies to produce LBG. Eventually, the final configuration was evaluated under variable inlet biogas compositions, which reflects a real condition of biogas plants. The optimization procedure follows the abovementioned phases in order to explore the design space. Finally, considering the optimized plant, a sensitive analysis is also performed in order to evaluate specific energy consumption variation by changing inlet biogas composition. Table 4.5 shows the results of the optimization procedure.

Table 4.5. Optimization procedure and results

Algorithm	**Evolutionary Strategy**			
File name	ES_010	ES_011	ES_012	ES_FINAL
Simulation time	7h:1m	30h:58m	8h:45m:52s	3h:59m:02s
Iteration number	1499	3499	1999	1779
Feasible results	1417	3249	1903	1736
Unfeasible results	82	250	96	43
Results with sp. en. cons. ≤ 1.2	19	421	33	11
Lower sp. en. cons. [kWh/kg]	1.154	1.153	1.151	1.092

Three optimization procedures were launched with different initial DOE matrix and iterations number. Once the data were obtained and collected, the best ones are selected in order to achieve a further optimization. The selected maximum value, based on the calculation performed, regards a specific energy consumption of 1.2 kWh/kg. The plant configuration related with such best points were considered as a new DOE, thus Sobol and ISF algorithms were applied on it and a new initial DOE matrix was generated. The final optimization provided the final best configuration, based on that procedure. Table 4.6 shows the plant parameters related with the optimal configuration.

Table 4.6. Optimum input variable set

Parameters	**Optimal values**
N_2 high pressure	45.25 bar
N_2 low pressure	16.25 bar
CO_2 high pressure	11 bar
CO_2 low pressure	6.5 bar
PLBG final pressure	16 bar
CO_2 biogas content	30% [mol]
CO_2 biomethane	0.4% [mol]
Produced LBG	252.1
Produced L-CO_2	287.9
Required power	275.3
Specific Energy Consumption [kWh/kg]	1.093

The obtained plant configuration results were compared with those of the conventional upgrading + liquefaction technologies. Table 4.7 provides information regarding such comparison.

Table 4.7. Comparison with traditional technologies

Technology	CH_4 loss [% mol]	LBG [kg/h]	Sp. cost [€/kg]	Sp. cons. [kWh/kg]
Water scrubber	2	247.94	0.23	1.424
Organic scrubber	2	247.94	0.24	1.459
Chemical scrubber	1	250.47	0.37	2.277
PSA	2	247.94	0.23	1.424
Membrane	2	245.41	0.26	1.591
Tr. Cryogenic	0.3	247.94	0.53	3.282
Novel cryogenic	0	252.1	0.18	1.093

The proposed technology presents a specific energy consumption of about 1.093 kWh kg^{-1} of produced LBG. This value is lower than any other available technology. Compared with water scrubber or pressure swing adsorption, which represent the best available traditional technologies, the energy consumption and associated costs for 1 kg of produced LBG are 23.24% and 21.74% lower, respectively. This is mainly due to the fact that traditional technologies present electric and heat requirements as well as involved materials and chemicals, which are continuously consumed. Figure 4.22 shows the comparative analysis between such technology. Moreover, assuming an electric energy cost of 0.1592 € kWh^{-1} (Italian market), an LBG market price of 1 € kg^{-1} and an L-CO_2 market price of 0.5 € kg^{-1} (for food industries – Italian market), a cost-revenue analysis was performed (Figure 4.23).

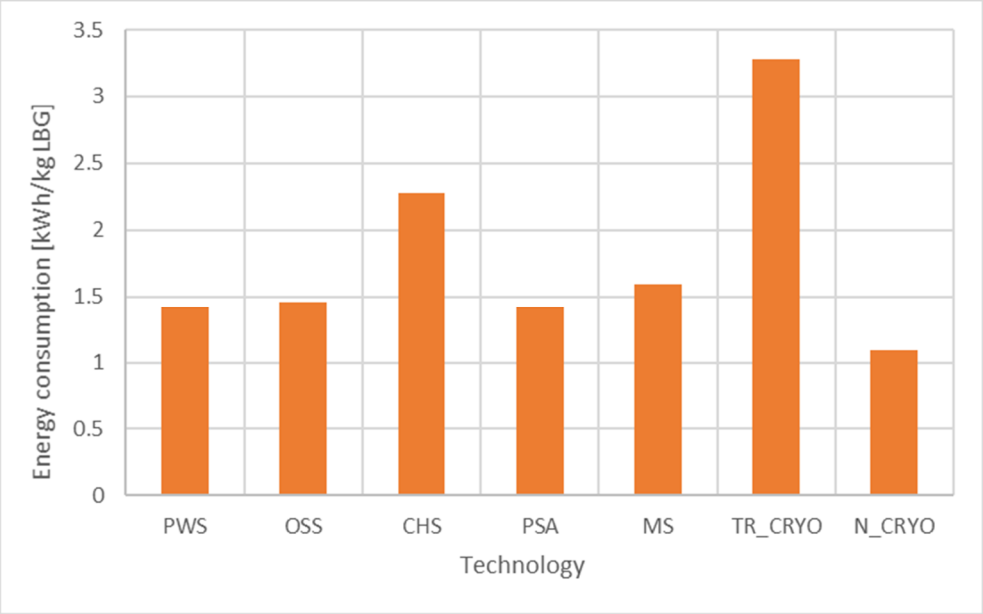

Figure 4.22. Comparison between technologies in a specific energy consumption point of view

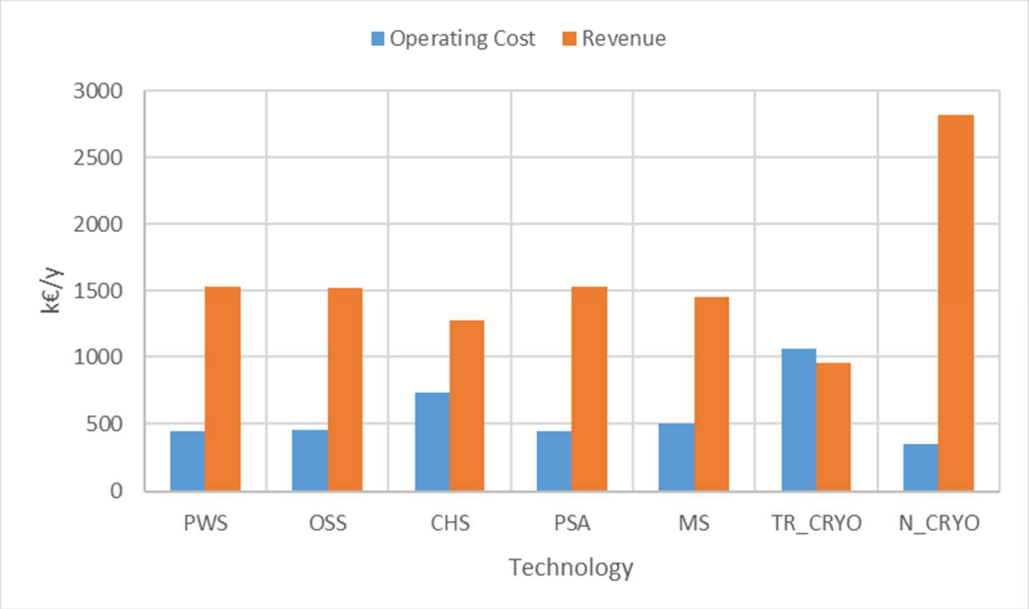

Figure 4.23. Yearly revenue and costs associated with the various technologies

Where the y-axis is reporting the considered technologies. The Figure is actually showing the total cost and revenue of the purification and liquefaction process. The acronym are as follows:

- PWS: pressurized water scrubber;
- OSS: organic solvent scrubber;
- CHS: chemical scrubber
- PSA: pressure swing adsorption;
- MS: membrane separation;
- TR_CRYO: traditional cryogenic upgrading;
- N_CRYO: novel cryogenic separation.

As it can be seen, considering the abovementioned specific prices, the novel cryogenic separation process allows the highest revenue / operative costs. This is mainly due to the fact that a large amount of L-CO_2 is produced together with LBG. In fact, during the cryogenic separation process, an L-CO_2 mass flow rate of 287 kg h^{-1} is produced. Since the liquid carbon dioxide is 100% pure component, it could be sold to the food industry for a price of at least 0.5 € kg^{-1}. Given the LBG and L-CO_2 prices as P_{LBG} and P_{LCO2}, a 'virtual' LBG mass flow rate (VLBG) could be defined as follows:

$$VLBG = \frac{R_{TOT}}{P_{LBG}} = \dot{M}_{LBG} + \frac{P_{LCO2}}{P_{LBG}} * \dot{M}_{LCO2} \quad (81)$$

Where R_{TOT}, $\dot{M}_{LBG}$ and $\dot{M}_{LCO2}$ are the total revenue, the LBG flow rate and the L-CO_2 flow rate, respectively. Thus, in this case, the VLBG is 50% higher than LBG, and so the total revenue. The VLBG results to be equal to 395.6 kg h^{-1}.

4.4.4. Variables correlation analysis

In optimization analysis, an important evaluation regards the correlation analysis. In fact, in order to better understand the problem behavior, it is necessary to evaluate how uncertainties in input variables affect the final result. To this purpose, several analyses allow to define a correlation between each input variable with the objective function. The modeFrontier®, ESTECO, environment provides some instruments to this point. In Figure 4.24, the parallel coordinate chart is given. As it can be seen, each variable is represented by a vertical axis (coordinates), while the last one on the right side is associated with the objective function.

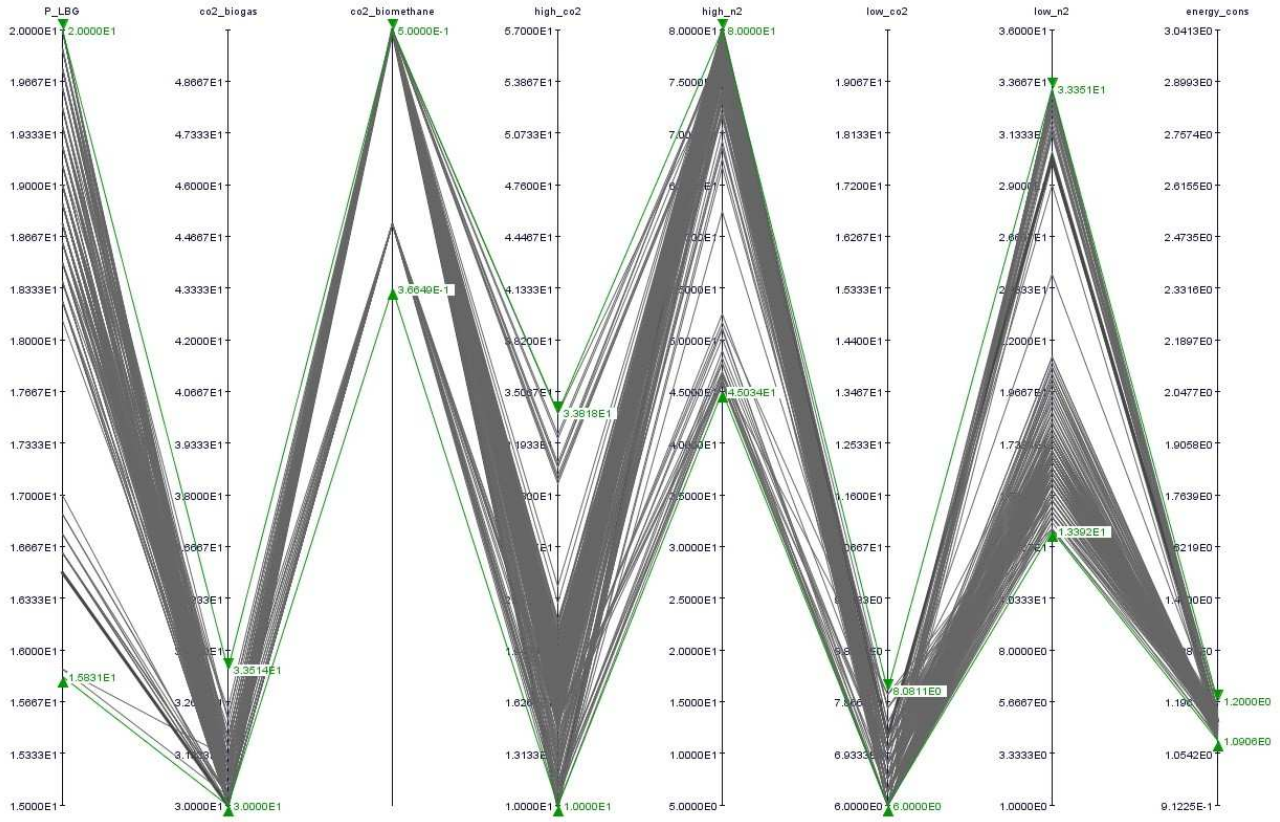

Figure 4.24. Parallel coordinates chart. Each grey line represents a considered plant configuration.

Each line is representing a specific set of input variables with the corresponding specific energy consumption. The chart allows to better understand which is the variable range which actually gives the best final results. In Table 4.8 such restricted variable ranges are reported in order to achieve a final specific energy consumption not higher than 1.2 kWh/kg (being the value previously used to sharpen the optimization procedure). Results of this analysis show that limited uncertainties in such input variable ranges still allows to achieve a final specific energy consumption between 1.093 and 1.2 kWh/kg.

Table 4.8. Input variable ranges from parallel coordinates chart analysis.

Parameters	Optimal ranges
N_2 high pressure	(45 – 80) bar
N_2 low pressure	(13.4 – 33.35) bar
CO_2 high pressure	(10 – 33.8) bar
CO_2 low pressure	(6 – 8) bar
PLBG final pressure	(16.4 – 20) bar
CO_2 biogas content	(30 – 33.5) % [mol]
CO_2 biomethane	(0.4 – 0.5) % [mol]
Specific Energy Consumption	(1.093 – 1.2) kWh/kg

In order to evaluate how much every single variable uncertainty affects the objective function, the Pearson correlation coefficient was considered. Such coefficient expresses the relationship between input variables and objective function. The coefficient is a dimensionless number ranging from -1 to 1, in which a positive value means that if associated variable increases, the objective function increases as well, while decreasing for negative values. If the coefficient is close to 0 it means that no significant correlation is found. In Figure 4.25, result of such evaluation is reported.

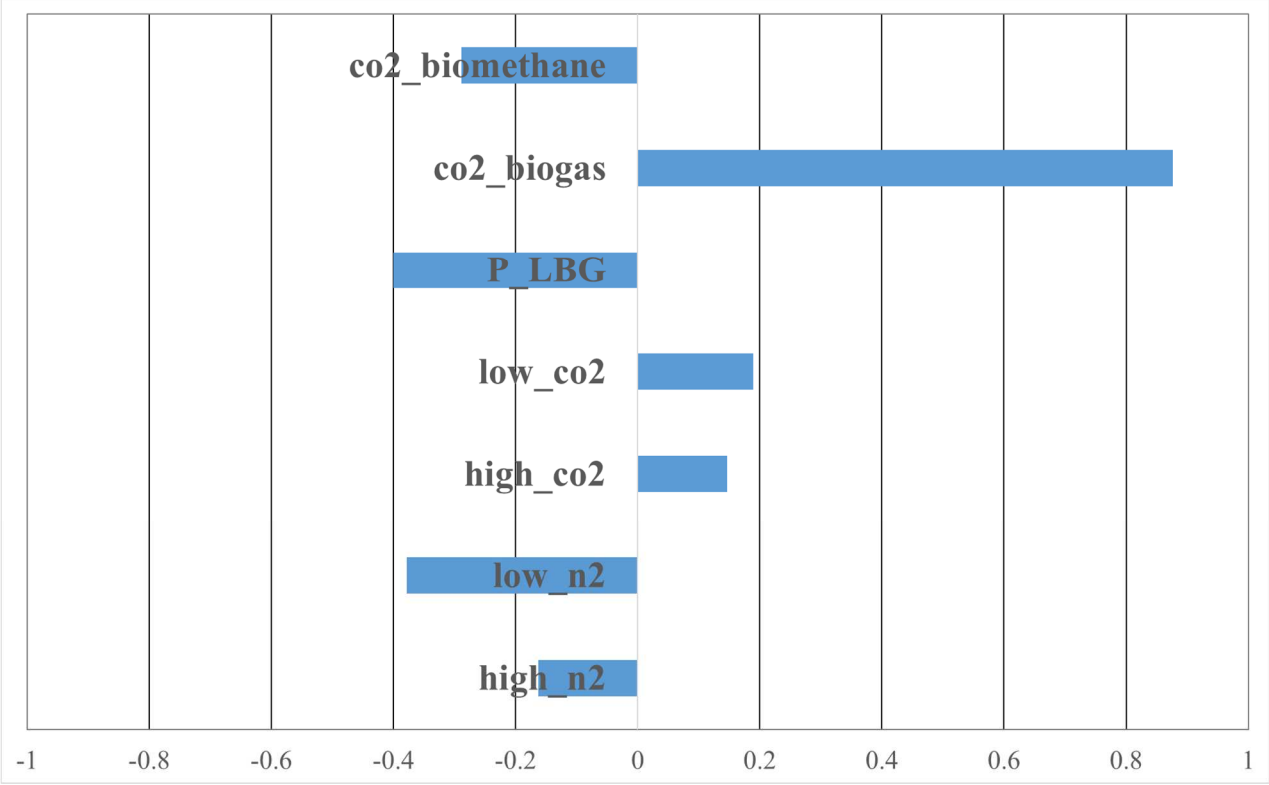

Figure 4.25. Pearson correlation coefficient analysis.

As it can be seen, inlet biogas composition and final PLBG composition and pressure have great influence in the specific energy consumption of the proposed plant. By the way, this was expected since those parameters are directly linked with energy consumption. Considering inlet biogas composition, if inlet CO_2 increases, specific energy consumption increases as well. This is mainly due to the fact that CH_4 decreases. Thus, being specific energy consumption related with produced PLBG, this value is increased. Considering final CO_2 content in biomethane, it was found that by increasing its value causes a reduced specific energy consumption. The reason is linked with the deposition process. In fact, if final carbon dioxide in produced biomethane is high, the final temperature involved in the deposition process is increased, thus reducing required cold load. Similarly, by increasing final PLBG pressure, specific energy consumption is increased because liquid formation occurs at higher temperatures, thus required cold load is reduced. The other important input variable is the nitrogen pressure in the low-pressure section of the reversed Brayton-Joule. This is a consequence of the expansion process through the cryogenic turbine. In fact, if the turbine discharging pressure is low, expanded nitrogen will be at low temperature as well, providing much cold energy load to heat exchangers. Regarding the CO_2 pre-cooling cycle, it seems to have no great effect on final specific energy consumption being mainly responsible for the biogas pre-cooling and S-CO_2 recovery. The

Parson correlation coefficient is able to evaluate the influence of each input variable on the final objective function result. However, this analysis is mainly suitable for linear problems, thus it may give insufficient information in this application. Considering such aspect, a factor analysis gives more details about the input/output correlations. In Figure 4.26 the chart of such analysis is shown.

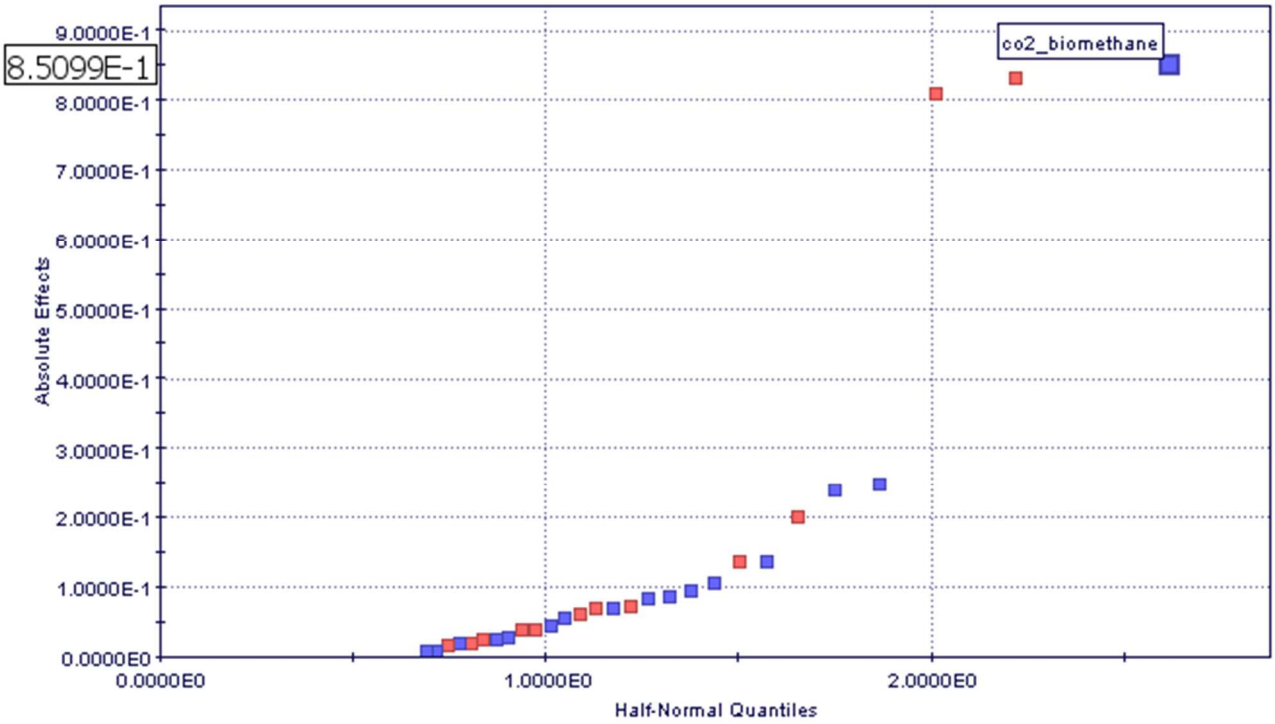

Figure 4.26. Chart of the factor analysis. The higher the absolute effect associated with the variable, the higher its effect on the objective function.

The factor analysis provides also information about the combination of input variables, instead of their single effect only. As it can be seen, specific energy consumption is mainly influenced by the final CO_2 content in biomethane after the deposition process. The second most influencing variable is the CO_2 content in inlet biogas, while the third one is the combination of these two variables. Table 4.9 provides more details about factor analysis results associated with the most relevant factors (with absolute effect higher than 0.2).

Table 4.9. Effects of factors on the specific energy consumption. Factors are intended to be variables and their combinations.

Factors	**Effect**
co2_biomethane	-0.850994912
co2_biogas	0.832653943
co2_biogas * co2_biomethane	0.810000136
P_LBG	-0.249809809
P_LBG * co2_biomethane	-0.239199729
P_LBG * co2_biogas	0.200631018

4.4.5. Sensitivity analysis

A sensitivity analysis was also performed in order to evaluate the optimized plant as a function of the inlet biogas composition. Thus, considering Table 4.6, the only variable that is changing is CO_2 percentage in inlet biogas, which is supposed to vary from a minimum value of 30% up to 50%. Figures from 4.27 to 4.29 show the analysis results related to specific consumption, operative biogas pressure, produced LBG and L-CO_2 as well as cost-revenue analysis in € h^{-1}.

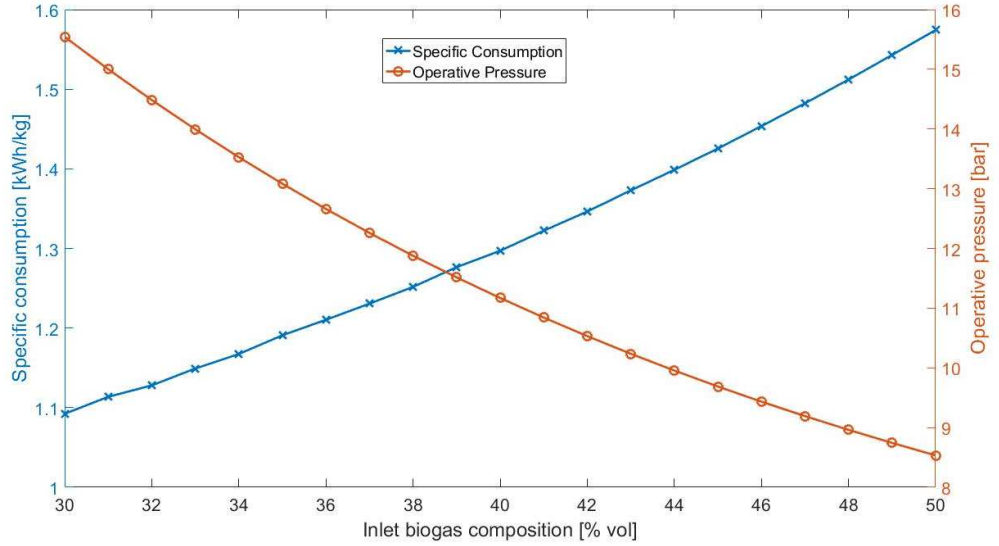

Figure 4.27. Specific consumption vs Operative pressure as function of the inlet biogas composition

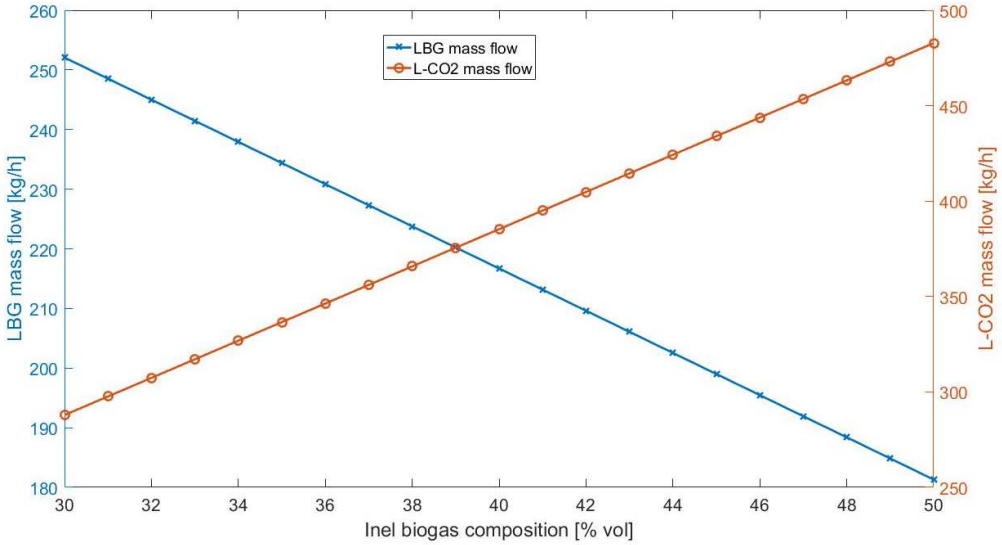

Figure 4.28. LBG and L-CO_2 mass flow produced as function of the inlet biogas composition

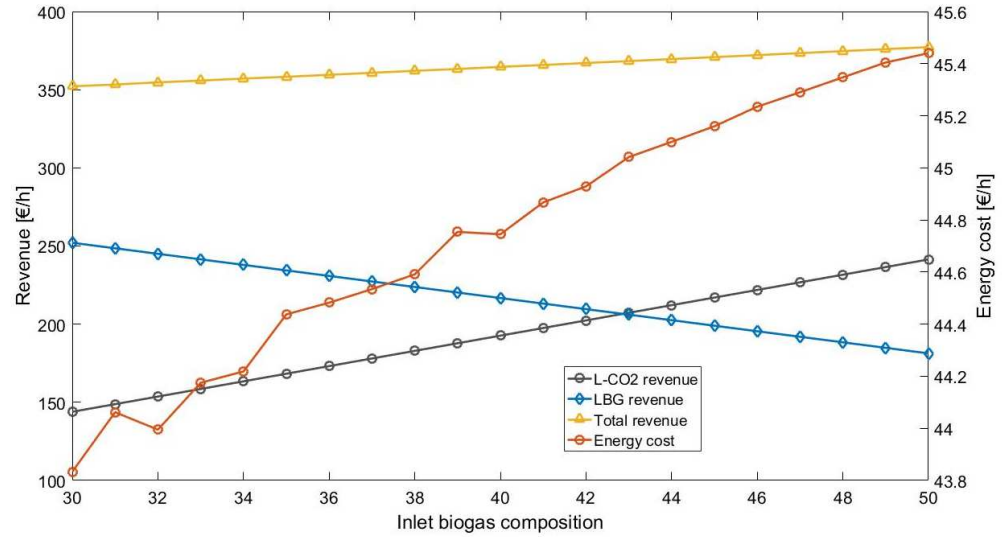

Figure 4.29. Hourly cost and revenue as a function of the inlet biogas composition

As expected, specific energy consumption increases with the increased biogas CO_2 content. This is mainly due to the fact that by increasing the carbon dioxide biogas content, the total methane content is decreased. Since this specific parameter is related with produced LBG, the specific cost is increasing. On the other hand, the operative biogas pressure during the deposition process decreases when CO_2 increases. Looking at Figure 4.12, it can be seen that highest achievable operative pressure is a function of the carbon dioxide biogas content. The maximum allowable operative pressure is important in order to achieve liquid formation inside the main heat exchanger and to achieve higher heat transfer efficiency. Regarding LBG and L-CO_2 production, several considerations may be explored from an economic point of view. In fact, looking at Figure 4.29, although specific energy consumption is increased considerably, of about 44.13%, the total hourly revenue is increased of about 7.12%. This result is linked to the hourly mass flow rate of LBG and L-CO_2 respectively.

Table 4.10. Results of the sensitivity analysis

Biogas CO_2 [% vol]	P_Opera [bar]	L-CO_2 [kg/h]	LBG [kg/h]	Sp. cons. [kWh/kg]
30	15.54301444	287.8900092	252.072517	1.092284673
31	15.00125227	297.6263885	248.533974	1.113613299
32	14.48546997	307.3635645	244.997044	1.127974441
33	13.99459114	317.1015485	241.459958	1.149178457
34	13.52756356	326.840352	237.922712	1.167415131
35	13.08335926	336.5799863	234.385302	1.190902579
36	12.66097446	346.3204628	230.847724	1.210372393
37	12.2594296	356.0617929	227.309973	1.230651151
38	11.87776934	365.803988	223.772046	1.251697185
39	11.51506254	375.5470595	220.233938	1.276460039
40	11.17040228	385.2910189	216.695645	1.297030691
41	10.84290586	395.0358775	213.157164	1.322170597
42	10.53171478	404.7816468	209.61849	1.346331334
43	10.23599477	414.5283382	206.079619	1.372882286
44	9.954935743	424.2759633	202.540546	1.398683269
45	9.687751858	434.0245334	199.001269	1.425450204
46	9.43368147	443.77406	195.461782	1.453676713
47	9.19198715	453.5245546	191.922081	1.482301583
48	8.961955683	463.2760286	188.382163	1.512060263
49	8.742898067	473.0284937	184.842024	1.542957274
50	8.534149512	482.7819611	181.301658	1.574330409

In fact, while the mass flow rate of methane is decreased by 28.07%, the mass flow rate of carbon dioxide is increased by 67.7%. The difference in the mass flow rate is ascribable to the difference in gas densities. Since CO_2 is much denser than CH_4, the mass flow variations are quite different. Table 4.10 provides final results related with the sensitive analysis.

4.4.6. Conclusions

Purpose of the present work was to evaluate a novel cryogenic separation technology able to recover liquefied carbon dioxide, producing liquefied biogas at the same time. The proposed process was evaluated and further optimized by means of a connection between modeFrontier®, ESTECO, MathWorks®, Matlab and AspenHYSYS®, AspenTech software. The optimization procedure was performed and the final optimum configuration was found. A comparison between the novel technology and the state of the art technologies was presented in order to understand the feasibility of the process. The energy consumption and associated costs for 1 kg of produced LBG was found to be 23.24% and 21.74% lower than the best available alternative, respectively. Moreover, the importance of L-CO_2 recovery as a valuable by-product was evaluated. A sensitivity analysis showed that carbon dioxide concentration in inlet biogas strongly influences the overall performances, by increasing specific energy consumption by 31.17%. However, since the liquefied carbon dioxide could be sold as a by-product for the food industry, being its density quite higher than that of CH_4, it was found that total revenue increases of 5.23% with increased CO_2 in inlet biogas.

4.5. The Cryogenic Separation Technology – CO_2 and H_2S removal

Aim of the present work is to evaluate, and compare with the state of the art upgrading techniques, a cryogenic upgrading process able to simultaneously remove H_2S and CO_2, producing LBG. Indeed, landfills biomass degradation and anaerobic digestion (AD) processes allow the production of biogas. Changes in biomass used in the process (as manure, wastes and so on), result in a different biogas composition. In order to obtain LBG for the transport sector a purification process is required. This process mainly consists of a H_2S removal unit (desulphurization) and a CO_2 removal unit (upgrading). In this section, state of the art of H_2S and CO_2 removal processes, thermodynamic description of the biogas, assumptions and operative conditions theoretically required for the cryogenic upgrading process are presented. Finally, the cryogenic upgrading and biomethane liquefaction plants are described and the proposed technology is compared with traditional technologies.

4.5.1. Thermodynamic Considerations

In this work, biogas was considered as a gas with a composition shown in Table 4.11. Main objective of this study was the definition of required operative conditions for the deposition. Moreover, liquid formation of CO2 and H2S should be avoided in order to prevent methane losses. The main obstacle at this stage was the lack of experimental data of gas behaviour at cryogenic temperatures (Langé et al., 2015). Therefore, assumptions were necessary in order to define first attempt operating conditions.

Table 4.11. Typical composition of biogas from AD, landfills and NG

Parameter	Considered Biogas	Biogas (AD)	Landfills	Natural gas
Methane (vol-%)	60	60 – 70	35 – 65	85 – 92
Other hydro carbons (vol-%)	0	0	0	9
Hydrogen (vol-%)	0	0	0 – 3	0
Carbon dioxide (vol-%)	40	30 – 40	15 – 40	0.2 – 1.5
Water (vol-%)	0	1 – 5	1 – 5	0
Nitrogen (vol-%)	0	0.2	15	0.3
Oxygen (vol-%)	0	0	1	0
Hydrogen sulphide (ppm)	4000	0 – 4000	0 – 100	1.1 – 5.9
Ammonia (ppm)	0	100	5	0
LHV (kWh/Nm^3)	6	6.39	4.44	10.83

The first assumption consists in obtaining operative conditions for cryogenic removal considering the behaviour of binary mixtures CH4 – CO2 and CH4 – H2S separately. The second assumption is to not consider the binary mixture CO2 – H2S. Those assumptions were possible due to the very low concentration of H2S in biogas. Moreover, during the gas deposition, CO2 percentage decrease rapidly with temperature, thus its influence in H2S behaviour is neglected compared with that of methane.

4.5.2. The CH_4 – CO_2 and CH_4 – H_2S Binary Systems

When analysing the biogas cryogenic upgrade, liquid and solid formation of impurities must be taken into account. The main constraints are (i) avoiding liquid formation during the deposition and (ii) grant the solid impurities solubility into final LBG. Regarding the first point, experimental data of CH_4 – CO_2 and CH_4 – H_2S binary systems were analysed (Donnelly and Katz, 1953, Khon and Kurata, 1958). Figure 4.30 illustrates the phase diagram of the considered binary systems. The process should allow the deposition of impurities, thus operating pressure must be lower than the lowest triple point. Therefore, a maximum pressure of 4 bar was considered to prevent CH_4 – H_2S liquid formation. Deposition process should take place all at once, thus an initial temperature of 210 K was considered. For determining the deposition process final temperature, phase concentration diagrams for the CH_4 – H_2S binary system at various temperatures were analysed. Optimal final conditions should achieve pure vapour methane and pure solid hydrogen sulphide. Langé et al. in 2016 widely discussed the CH_4 – H_2S binary system behaviour both at constant temperature and pressure. It was found that for this system, solid-vapour region is allowed for temperatures below 188 K. By decreasing the temperature under 186 K, solid and vapour begin to

coexist. However, at this temperature, solidification of H_2S is not possible due to its low concentration in the considered gas mixture. On the other hand, decreasing too much the temperature results in too high energy consumption for the cold load required. Moreover, since final CO_2 concentration should be lower than 1% (considering a safety margin), final temperature must be lower than 162 K (AspenHYSYS®, AspenTech calculation). Considering this, a temperature of 140 K was found to be the optimal value. In fact, H_2S is completely removed with a negligible CH_4 loss. At this final temperature, CO_2 final concentration in biomethane is of about 0.04% (Figure 4.30). It was seen that, for the selected operative pressure, a pure vapour methane and highly pure solid H_2S are obtained, thus that temperature was selected as final deposition process temperature. Since solid CO_2 and H_2S are removed together, the final mixture no longer can be considered as a by-product.

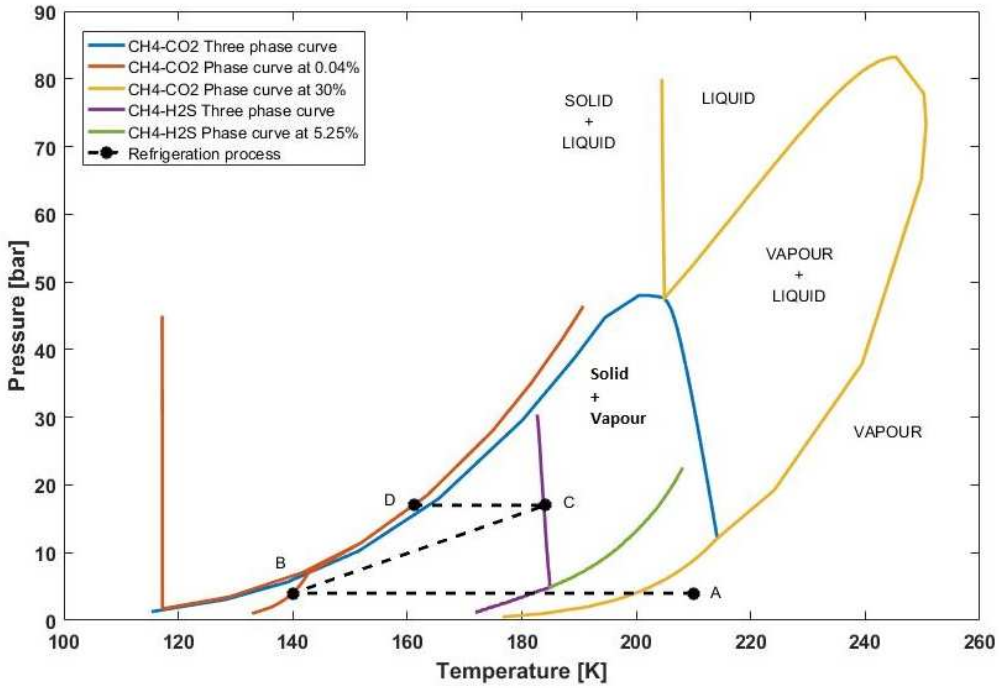

Figure 4.30. P vs T for CH_4-CO_2 and CH_4-H_2S binary systems

Considering the operating conditions for deposition previously described, biogas is firstly compressed up to 4 bar and cooled down to the starting separation process temperature (HEX-1). In HEX-2 biogas is further cooled to 140 K. In the gas – solid separation unit (G-S), vapour impurities (V-INPs) are removed and used in order to recover cold load (HEX-6). Produced biomethane is now further compressed up to 17 bar, liquefied and stored as LBG.
As far as the conventional LBG production plants are concerned, a desulphurization unit, an upgrading unit and a liquefaction unit are required. Moreover, in conventional liquefaction facilities, a molecular sieve is necessary in order to prevent plugging issues. The liquefaction technology considered is a triple pressure Linde cycle, which was demonstrated to be the best solution for small scale applications (Arteconi et al., 2011). More details about this plant can be found in a previous work in which a cryogenic process for CO_2 removal and biomethane liquefaction was proposed (Spitoni et al., 2016b).

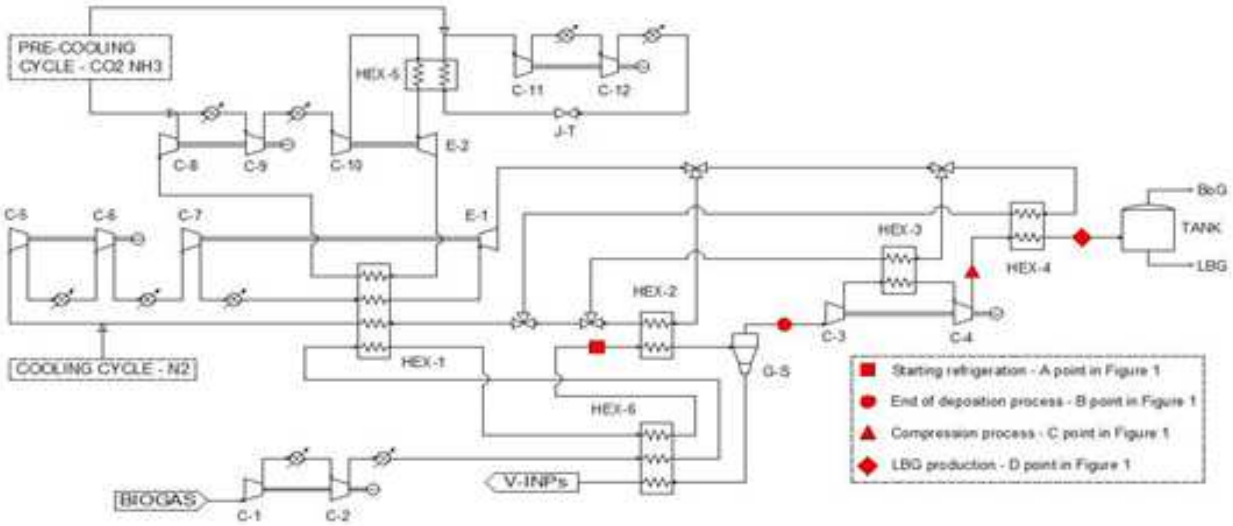

Figure 4.31. Schematic view of the cryogenic separation process for the CO_2 and H_2S compounds

A biogas flow rate of 350 $Nm^3 \cdot h^{-1}$ was assumed. Simulations were performed by means of AspenHYSYS®, AspenTech software, in the steady – state mode. Peng – Robinson equation of state package was used (Zhang et al., 2011).

4.5.3 Results and Discussion

In the present work, a comparative analysis between a novel cryogenic upgrading-liquefaction process and existing biogas liquefaction technologies was performed (Brendeløkken, 2016) and their specific energy consumption was evaluated. The existing biogas liquefaction technologies consist of a desulphurization process, an upgrading process and a liquefaction process itself. For the first one, an adsorption technique is adopted. For the last one, a triple pressure Linde cycle is considered. For the upgrading, every existing technique is evaluated (amine, membrane, PSW, PSA and cryogenic upgrading, i. e. CO_2 removal without biomethane liquefaction). Table 4.12 shows results of this analysis.

Table 4.12. Results of the simulation

Type of Technology	Novel Cryogenic	Desulphurization + Upgrading + Liquefaction				
		Amine	Membrane	PWS	PSA	Traditional Cryogenic
Total Power [kW]	288.67	168.36	213.86	217.36	205.11	332.66
Methane Losses [% - v/v]	0%	0.1%	0.43%	1%	2.12%	0.3%
CO_2 in final LNG [% - v/v]	0.04%	1%	1%	1%	1%	3%
Produced LBG [kg/h]	149.86	149.47	149.1	148.19	146.52	149.5
Specific Consumption [kWh/kg]	1.526	1.126	1.434	1.467	1.399	2.225
Operating Costs [€/kg]	0.259	0.281	0.321	0.318	0.309	0.454

The proposed technology presents a specific energy consumption of 1.526 $kWh \cdot kg^{-1}$ of LBG, higher than existing technologies but traditional cryogenic process. In particular, specific energy consumption of proposed plant is 35.5% higher than biogas liquefaction using amine process for upgrading. By the way, energy analysis does not take into account material consumption (amine, activated carbon and water) and desulphurization costs (which does not present energy consumption). The latter presents a specific cost of 0.07 $€ \cdot kg^{-1}$ of LBG while material costs depend on the considered technology. Finally, it was found that the novel technology presents the lowest specific cost of 0.259 $€ \cdot kg^{-1}$: 7.8% lower than amine, 16.2% lower than PSA, 18.5% lower than PSW and 19.3% lower than membrane process. This is due to the fact that a desulphurization process is not required and any material is consumed but compression energy. Moreover, the novel technology presents no methane losses and 0.04% of CO_2 in the final product, giving a high quality LBG. In Figure 4.32, specific costs of the considered technologies are shown.

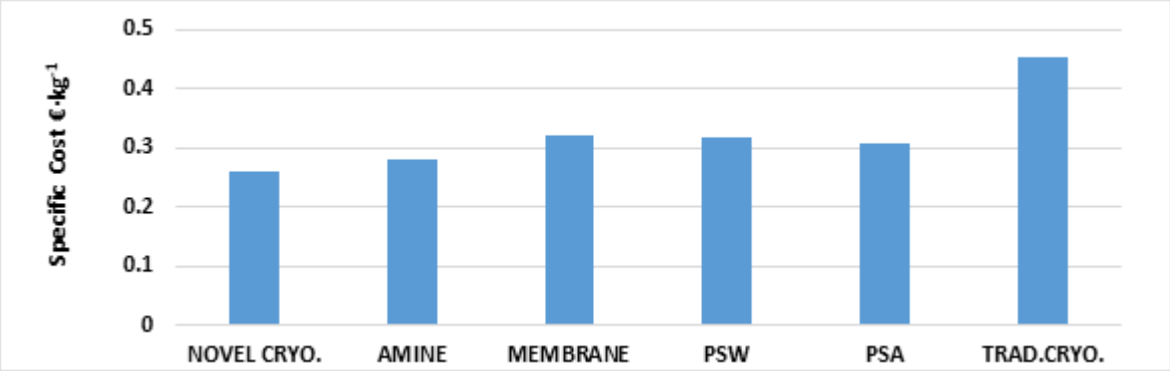

Figure 4.32. Specific energy consumption comparison

4.5.4. Conclusions

Aim of the present work was to explore the possibility to simultaneously purify and liquefy biogas from anaerobic digestion by means of a single plant. Thus, a novel cryogenic technology was proposed and evaluated and subsequently compared with state-of-the-art technologies. Results indicate a specific energy consumption of 1.526 kWh/kg, that is sensibly higher than existing technologies (but conventional cryogenic upgrading). This is mainly due to the fact that, in order to completely avoid H_2S in final LBG, final deposition temperature must be very low. However, energy analysis does not take into account consumed matter and desulphurization process costs. Thus, an economic evaluation was performed in order to better understand operating costs. Results indicate that the proposed technology has the lowest operating cost, equal to 0.259 €/kg. The analysis shows an all-in-one cryogenic upgrading and liquefaction process is possible and competitive. LBG could be produced by means of a single plant. By the way, efforts are necessary in order to have a better thermodynamic comprehension of the mixture at cryogenic temperatures and low pressures.

4.6. Final Conclusions

In this chapter, a briefly introduction about the importance on LBG as vehicle fuel opens the discussion regarding the actual available technology able to produce such a fuel. The technology associated with LBG production is generally the same as in LNG production. It was found that the most common LNG technology is the mixed refrigerant technology, which is also the most efficient technology for LNG production. However, although some efforts were spent to use this kind of processes in LBG production, MR remains mostly unfeasible for the production of liquid biogas, due to the biogas plant scale. Nowadays, when the focus is on LBG production, major practice is to purify it by means of standard purification technologies, and further liquefy it using a cryogenic liquefaction process which is feasible for the small and micro-scale applications. Given those assumptions the work was centered on the possibility to achieve biogas purification and liquefaction by means of a single plant in a feasible way. The proposed process is based on the reversed Bryton-Joule cycle and on the Pressurized Liquefied Natural Gas, which is able to allow relatively high solid CO_2 in LBG.
In the first work, the cryogenic removal of carbon dioxide with the simultaneous biomethane liquefaction was evaluated and compared with state of the art traditional technologies. It was shown that the PLNG technology has a lower specific energy consumption if compared with such traditional technologies. Consequently, it has a lower specific cost of 1.64 c€·kWh^{-1}, 1.39 c€·kWh^{-1} and 1.23 c€·kWh^{-1}, depending on the biogas composition, while the conventional process accounts for 2.13 c€·kWh^{-1}. In order to evaluate the dependency on the final LBG composition, a sensitivity analysis was also performed. The results show that the specific energy consumption could be considerably reduced from 1.982 kWh·kg^{-1} (worst scenario) to 1.284 kWh·kg^{-1} (best scenario) of produced LBG. The analysis shows that PLNG technology is a valid solution for the cryogenic upgrading of biogas. Effectively, it allows liquefying it directly without conventional upgrading process or molecular separation unit. Moreover, a considerably amount of pure CO_2 could be recovered. Finally, the plant can produce LBG with the final requested CO_2 content independently from the inlet biogas composition.
In the second work, the same cryogenic separation technology was further improved in order to achieve cold energy recovery, liquid carbon dioxide recovery as well as LBG production. The proposed configuration was subsequently optimized by means of modeFrontier®, ESTECO software and the optimal configuration which minimizes specific energy consumption was found. The technology was then compared with state of the art technologies in order to

evaluate its competitiveness. A sensitivity analysis was also performed while changing biogas composition in the optimized configuration. Results shown that the energy consumption and associated costs for 1 kg of produced LBG was found to be 23.24% and 21.74% lower than the best available alternative, respectively. Moreover, the importance of L-CO_2 recovery as a valuable by-product was evaluated. The sensitivity analysis shown that carbon dioxide concentration in inlet biogas strongly influences the overall performances, by increasing specific energy consumption by 31.17%. However, since the liquefied carbon dioxide could be sold as a by-product for the food industry, being its density quite higher than that of CH_4, finally it was found that total revenue is increased by 5.23% with increased CO_2 in inlet biogas.
In the third work, the cryogenic separation plant was rearranged in order to handle with both carbon dioxide and hydrogen sulphide removal. Thermodynamic studies were conducted in order to evaluate the feasibility of the process. It was found that the relation between CO_2 and H_2S is weak if compared with that of the CO_2 – CH_4 and H_2S – CH_4 binary systems. Finally, carbon dioxide and hydrogen sulphide does not influence considerably their own freezing behaviour. By means of this consideration, operative conditions were found in order to achieve the target of biogas purification and liquefaction. Once the plant was defined, a comparison with the state of the art traditional technologies was performed. Results indicate a specific energy consumption of 1.526 kWh/kg, that is sensibly higher than existing technologies (but conventional cryogenic upgrading). This is mainly due to the fact that, in order to completely avoid H_2S in final LBG, final deposition temperature must be very low. However, energy analysis does not take into account consumed matter and desulphurization process costs. Thus, an economic evaluation was performed in order to better understand operating costs. Results indicate that the proposed technology has the lowest operating cost, equal to 0.259 €/kg. The analysis shows an all-in-one cryogenic upgrading and liquefaction process is possible and competitive. LBG could be produced by means of a single plant. By the way, efforts are necessary in order to have a better thermodynamic comprehension of the mixture in at cryogenic temperatures and low pressures.

4.7. References

- Arteconi A., Brandoni C., Evangelista D., Polonara F. (2010). Life-cycle greenhouse gas analysis of LNG as a vehicle fuel in Europe, *Applied Energy* 87: 2005-2013.
- Arteconi A., Polonara F. (2012). LNG as vehicle fuel in Italy, *Proceedings of the 12th Cryogenics IIR Conference*, Dresda, Paper 041.
- Arteconi A., Spitoni M., Polonara F. (2015). The Feasibility of Liquid Biomethane (LBG) in Italy. *Proceedings of the 24th IIR International Congress of Refrigeration ICR2015*. Yokohama, Japan.
- Arteconi A., Spitoni M., Polonara F., Spigarelli F. (2015). The Feasibility of Liquid Biomethane as Alternative Fuel: European and Chinese Markets Comparison. *International Journal of Ambient Energy.*
- Arteconi A., Brandoni C., Santori G., Polonara F., 2011. Micro-scale LNG liquefaction plants. *Proceedings of the 23rd International Congress of Refrigeration.* Prague, Czech Republic, IIF/IIR, 2003-2009.
- Bowen R. R., Gentry M. C., Nelson E. D., Papka S. D., Leger A. T., 2005. Pressurized Liquefied Natural Gas (PLNG): A New Gas Transportation Technology. *Proceedings of the GasTech 2005, Bilbao, Spain*.
- Brendeløkken H. W., 2016. Upgrading Technologies for Biogas Production Plants – Overview and Life Cycle Cost Analysis of Available Technologies. *Master thesis, The Arctic University of Norway*.
- Coyle D., de la Vega F. F., Durr C., KBR. Natural Gas Specification Challenges in the LNG Induestry. Paper PS4-7.
- Donnelly H. G., Katz D. L., 1953. *Phase Equilibria in the Carbon Dioxide-Methane System.* Industrial & Engineering Chemistry Research, 46:511-517.
- Fairchild P., Smith P., Biery N., Farah A., Lilling D., Jackson T., et al., (2005). Protorype Container Fabrication. *Proceedings of the Fifteenth International Offshore and Polar Engineering Conference, Seoul, Korea*.
- Hagen M., Polman E., Jensen J. K., Myker A., Jönsson O., Dahl A., 2001. *Adding gas from Biomass to the Gas Grid.* Report SGC 118.
- Harold G. D., Donald L. K., (1954). Phase Equilibria in the Carbon Dioxide-Methane System. *Industrial and Engineering Chemistry 46: 511-517.*

- Hveding A. H., 2010. Production, Liquefaction and Transport of Low-Processed Natural Gas. *Master thesis, Norwegian University of Science and Technology*.
- Johansson N., (2008). Production of Liquid Biogas, LBG, with Cryogenic and Conventional Upgrading Technology. Institutionen för Teknik och Samhälle. Master Thesis.
- Klein S.A., 2013. EES - Engineering Equation Solver, F-Chart Software. (http://www.fchart.com/ees/) (last accessed – 03/2016).
- Kohn J. P., Kurata F., 1958. *Heterogeneous Phase Equilibria of the Methane-Hydrogen Sulfide Syste.* AlChE Journal, 4:211-217.
- Langé S., Campestrini M., Stringari P., 2016. *Phase Behavior of System Methane+Hydrogen Sulpfide.* AlChE Journal 62:4090-4108.
- Langé S., Pellegrini L. A., Stringari P., Coquelet C., 2015. Experimental Determination of the Solid-Liquid-Vapor Locus for the CH_4-CO_2-H_2S System and Application to the Design of a New Low-Temperature Distillation Process for the Purification of Natural Gas. *94th GPA Convention, San Antonio, United States*.
- Mezzadri M., 2014. *Come si Ottiene il Biometano Raffinando il Biogas.* Informatore Agrario (http://www.informatoreagrario.it/ita/riviste/index.asp).
- Muñoz R., Meier L., Diaz I., Jeison D., 2015. *A Review on the state-of-the-art of Physical/Chemical and Biological Technologies for Biogas Upgrading.* Springer Science+Business Media Dordrecht, 14:727-759.
- Nie H., Jiang H., Chong D., Wu Q., Xu C., Zhou H. 2013, Comparison of water scrubbing and propylene carbonate absorption for biogas upgrading process, *Energy and Fuel* 27(6):3239 –3245.
- Shen T., Lin W., 2011. *Calculation of Carbon Dioxide Solubility in Liquefied Natural Gas.* International Journal of Chemical Engineering and Applications, 2:366-371.
- Spitoni M., Polonara F., Arteconi A., 2016a. The Feasibility of Liquefied Methane as an Alternative Fuel in Europe and China. In: Spigarelli F., Curran L., Arteconi A. *China and Europe's Partnership for a more Sustainable World: Challenges and Opportunities,* Emerald Publishing, Bingley: 209-231.
- Spitoni M., Xiong X., Arteconi A., Polonara F., Lin W., 2016b. Biogas Purification and Liquefaction by means of a Cryogenic Upgrading Process. *Proceedings of the 1st International Conference IIR of Cryogenics and Refrigeration Technology*. Bucharest, Romania, IIF/IIR, 107-115.
- Triglio A., Bouza A., Di Scipio S., Modelling and simulation of Natural Gas Liquefaction Process. Advanced in Natural Gas Technology. 213-234.
- Walid M., (2015). Proposed Method for Dealing with Boil-off Gas on Board LNG Carriers During Loaded Passage, *International Journal of Multidisciplinary and Current Research 3: 508-512*.
- Warren K. (2012). A techno-economic comparison of biogas upgrading technologies in Europe, *Master Thesis, University of Jyväskylä*.
- Xiong X., Lin W., Gu A., (2015). Integration of CO_2 Cruogenic Removal with a Natural Gas Pressurized Liquefaction Process Using Gas Expansion Refrigeration, *Energy 93: 1-9*.
- Yeh S., 2007. An empirical analysis on the adoption of alternative fuel vehicles: The case of natural gas vehicles. *Energy Policy* 35: 5865–5875.
- Zhang L., Burdass R., Chaopy A., Tohidi B., Solbraa E., 2011. *Measurement and Modeling of CO_2 Frost Points in the CO_2-Methane Systems.* Journal of Chemical & Engineering Data, 56:2971-2975.
- Economic Commission for Europe, (2013). Working Party on the Transporte of Dangerous Goods. Genevra, 4-8 November 2013.
- Rechenberg, I. (1973) "Evolutionsstrategie: Optimierung technischer Systeme nach Prinzipien der biologischen Evolution", Stuttgart: Fromman-Holzboog.
- Hans-Paul Schwefel: Evolution and Optimum Seeking: New York: Wiley and Sons 1995.
- Beyer, H.-G. and Schwefel, H.-P. (2002). Evolution Strategies: A Comprehensive Introduction. In Natural Computing , 1(1):3-52.

5. CONCLUSIONS

The focus of this thesis is the evaluation of innovative Compressed and Liquefied Natural Gas (CNG – LNG) technologies using biomethane as a feedstock source in the field of transport sector. The work is divided into three main sections, which are actually connected one to each other.
The first section gives an overview on the environmental impact of human activities linked to energy utilization, production and consumption. The environmental impact is estimated by means of Green House Gas (GHG) emissions. Results show that China and North America account for the greatest part of such emissions, which are mainly produced by the electricity and heat production sector. The second most emitting sector is the transport sector, which is responsible for 24% of global GHG emissions. For the transport sector, it was estimated an increasing trend in energy utilization and GHG emissions of about 50% by 2030 and 80% by 2050. The Intergovernmental Panel on Climate Change. (IPCC) assesses that GHG emission level must be reduce by at least 50% within 2030. This means to reduce fossil fuel utilization by replace them with alternative and renewable fuels. Driven by different forces (may be environmental or linked with the internal economy), several countries decided to invest on such field. Incentives and penalties governmental policies were established to this purpose. At present, each county has been involved in an international scheme or developed their own scheme for the reduction of fossil fuel utilization. The best solution is represented by introducing mandatory blending levels. Moreover, incentives were introduced, essentially characterized by tax exemptions, import / export regulation and subsidies, allowing the fast growth of biofuels production and consumption. These policies are strictly related to national government, which are referred to internal societal structure, economic level, land availability and achievable cultivations. The majority of those policies, generally refers to biofuels such bioethanol and biodiesel. However, biogas is gaining more and more interests. This biofuel is strictly related to natural gas utilization, thus associated incentives were found in those regions in which its usage as vehicle fuel is developed. In Europe, countries like Germany, France, Sweden and Italy have adopted incentive policies in order to increase its usage. The main incentive is an indirect incentive consisting in tax exemptions. In Italy, an incentive scheme, specific for biogas and biomethane usage in the transport sector was introduced in 2013. It provides direct incentives for biogas upgrading. Moreover, the incentive is increased if biomethane is used in the transport sector as CBG or LBG. An Italian case study aimed to evaluate LBG feasibility by means of such scheme is presented. A technical and economic analysis for the production of LBG was performed considering three different business models for the LBG value chain in the Italian context. The minimum incentive to make this kind of project economically interesting was calculated. Depending on the biomass composition and business model considered, the minimum value of the base incentive was estimated to vary from 0.10 €/Sm^3 to 0.42 €/Sm^3. The analysis shows that it is not convenient to have more than one owner in the fuel value chain, due to the mark-up of each producer and mainly to the reduced incentive gained. On the other hand, the option with more biogas producers that contribute to supply the same liquefaction facility, sharing investment costs and revenues, is a particularly attractive one.
In the second section, the CNG technology was investigated. Considering the present diffusion of biogas plant on the Italian market, a comparison between two refueling station configurations was proposed, considering biogas as a feedstock source. These kind of refueling stations are known as CBG stations. The CBG station was intended to be an on-site CBG station. An innovative and alternative refueling station is compared with a traditional buffer refueling station. a model for the complete simulation of the CBG station is developed for both configurations. The proposed model aims to achieve a first attempt sizing of the reciprocating compressor, as well as the definition of the thermodynamic properties of the gas during the FFP, considering the connecting pipes. Moreover, a model for the heat transfer from the storages and the water was considered specifically for the alternative station. A validation and comparison of the proposed models was achieved, showing good agreement. The MathWorks®, Matlab, software is used to perform the CBG simulation. Results indicates critical aspects of the alternative station which are mainly related with the time for the charging process, the increased energy consumption and time for the Fast Filling Process of the vehicles. In the alternative CBG station the charged mass is 276.65% higher than that of the buffer station. The power required from the alternative CBG station is 59.13% lower than in the buffer storage. On the other hand, the final energy consumption in the alternative station system is 88.67% higher. Moreover, the number of the filled vehicles was found to be strictly connected with the station configuration. The buffer station could refuel 5 vehicles, while the alternative station could refuel only 2 vehicles. This effect is due to the storages sizing, which represents another critical aspect of the latter station. Again, the vehicle refueling at the alternative station is 64.55% higher than that of buffer system. In order to optimize the process and make the alternative station more competitive, further analysis will be required in order to better evaluate the ration between the LP, MP and HP storages, as well as their minimum and maximum pressure levels. Although the alternative CBG refueling station

is able to decrease investment costs, by means of a smaller electric motor for the compression process, its performance compared with those of the buffer system, are quite poor.
In the third section, the LNG technology was investigated. The technology associated with LBG production is generally that of the LNG production, which is adapted to the scope. Nowadays, when the focus is on LBG production, major practice is to purify it by means of standard purification technologies, and further liquefy it using a cryogenic liquefaction process which is feasible for the small and micro-scale applications. Given those assumptions the work was centered on the possibility to achieve biogas purification and liquefaction by means of a single plant in a feasible way. The proposed process is based on the reversed Bryton-Joule cycle and on the Pressurized Liquefied Natural Gas, which is able to allow relatively high solid CO_2 in LBG. The cryogenic removal of carbon dioxide with the simultaneous biomethane liquefaction was evaluated and compared with state of the art traditional technologies. It was shown that the PLNG technology has a lower specific energy consumption if compared with such traditional technologies. Consequently, it has a lower specific cost of 1.64 c€·kWh^{-1}, 1.39 c€·kWh^{-1} and 1.23 c€·kWh^{-1}, depending on the biogas composition, while the conventional process accounts for 2.13 c€·kWh^{-1}. In order to evaluate the dependency on the final LBG composition, a sensitivity analysis was also performed. The results show that the specific energy consumption could be considerably reduced from 1.982 kWh·kg^{-1} (worst scenario) to 1.284 kWh·kg^{-1} (best scenario) of produced LBG. The analysis shows that PLNG technology is a valid solution for the cryogenic upgrading of biogas. Effectively, it allows liquefying it directly without conventional upgrading process or molecular separation unit. Moreover, a considerably amount of pure CO_2 could be recovered. Finally, the plant can produce LBG with the final requested CO_2 content independently from the inlet biogas composition. This proposed technology is then further improved in order to achieve cold energy recovery, liquid carbon dioxide recovery as well as LBG production. The proposed configuration was subsequently optimized by means of modeFrontier®, ESTECO software and the optimal configuration which minimizes specific energy consumption was found. The technology was then compared with state of the art technologies in order to evaluate its competitiveness. A sensitivity analysis was also performed while changing biogas composition in the optimized configuration. A specific energy consumption of 1093 kWh kg^{-1} was found to be the best result. Results shown that the energy consumption and associated costs for 1 kg of produced LBG was found to be 23.24% and 21.74% lower than the best available alternative, respectively. Moreover, the importance of L-CO_2 recovery as a valuable by-product was evaluated. The sensitivity analysis shown that carbon dioxide concentration in inlet biogas strongly influences the overall performances, by increasing specific energy consumption by 31.17%. However, since the liquefied carbon dioxide could be sold as a by-product for the food industry, being its density quite higher than that of CH_4, finally it was found that total revenue is increased by 5.23% with increased CO_2 in inlet biogas. Finally, the possibility to achieve carbon dioxide and hydrogen sulphide removal, is evaluated. Thermodynamic studies were conducted in order to evaluate the feasibility of the process. It was found that the relation between CO_2 and H_2S is weak if compared with that of the CO_2 – CH_4 and H_2S – CH_4 binary systems. Finally, carbon dioxide and hydrogen sulphide does not influence considerably their own freezing behaviour. By means of this consideration, operative conditions were found in order to achieve the target of biogas purification and liquefaction. Once the plant was defined, a comparison with the state of the art traditional technologies was performed. Results indicate a specific energy consumption of 1.526 kWh/kg, that is sensibly higher than existing technologies (but conventional cryogenic upgrading). This is mainly due to the fact that, in order to completely avoid H_2S in final LBG, final deposition temperature must be very low. However, energy analysis does not take into account consumed matter and desulphurization process costs. Thus, an economic evaluation was performed in order to better understand operating costs. Results indicate that the proposed technology has the lowest operating cost, equal to 0.259 €/kg. The analysis shows an all-in-one cryogenic upgrading and liquefaction process is possible and competitive. LBG could be produced by means of a single plant. By the way, efforts are necessary in order to have a better thermodynamic comprehension of the mixture in at cryogenic temperatures and low pressures.

Further works concerning CBG refuelling station may be related with the optimization of the alternative station. Thus, storages volume as well as minimum and maximum pressure levels are central parameter to be optimize in order to make the station more flexible and to fasten charging and refuelling processes.
Considering the LBG technology process, a more detailed definition of the ternary system of CH_4 – CO_2 – H_2S is fundamental for defining finer allowable operating conditions. Moreover, such plant may be optimized using the proposed optimization procedure, to reach minimum specific energy consumption.
For the optimized cryogenic separation process with cold and L-CO_2 recovery, further works concerns the dynamic evaluation of the optimum variable set. Thus, the sustainability of the process could be obtained together with a first sizing of the heat exchanger in which the deposition process occurs. Finally, investment costs should be evaluated to be compared with other traditional LBG technologies.